

รายงานวิจัยฉบับสมบูรณ์

# โครงการ

"การศึกษาวิธีการสังเคราะห์ และการประยุกต์สารไทเทเนียมไดออกไซด์-ซิลิกอนไดออกไซด์เพื่อใช้เป็นเมมเบรนที่มีสมบัติพิเศษในการแยกสาร"

โดย นางสุจิตรา วงศ์เกษมจิตต์และคณะ

# สัญญาเลขที่ BRG4680013

รายงานวิจัยฉบับสมบูรณ์



# โครงการ

"การศึกษาวิธีการสังเคราะห์ และการประยุกต์สารไทเทเนียมไดออกไซด์-ซิลิกอนไดออกไซด์ เพื่อใช้เป็นเมมเบรนที่มีสมบัติพิเศษในการแยกสาร"

# คณะผู้วิจัย

- 1. นางสุจิตรา วงศ์เกษมจิตต์
- 2. นางสาวนพวรรณ พรธรรมชัย
- 3. นางสาวเมธิรา กฤษณะเศรณี

## สังกัด

วิทยาลัยปิโตรเลียมและปิโตรเคมี วิทยาลัยปิโตรเลียมและปิโตรเคมี วิทยาลัยปิโตรเลียมและปิโตรเคมี

สนับสนุนโดยสำนักงานกองทุนสนับสนุนการวิจัย (ความเห็นในรายงานนี้เป็นของผู้วิจัย สกวไม่จำเป็นต้องเห็นด้วยเสมอไป)

# กิตติกรรมประกาศ

ผู้วิจัยขอขอบพระคุณสำนักงานกองทุนสนับสนุนการวิจัย ที่ได้ให้การสนับสนุนโครงการวิจัยนี้ ด้วยดีตลอดทั้งโครงการ

# บทคัดย่อ

**รหัสโครงการ** :BRG4680013

ชื่อโครงการ: "การศึกษาวิธีการสังเคราะห์ และการประยุกต์สารไทเหเนียมไดออกไซด์-

ชิลิกอนไดออกไซด์เพื่อใช้เป็นเมมเบรนที่มีสมบัติพิเศษในการแยกสาร"

ชื่อนักวิจัย: นางสุจิตรา วงศ์เกษมจิตต์

วิทยาลัยปิโตรเลียมและปิโตรเคมี จุฬาลงกรณ์มหาวิทยาลัย

E-mail Address : caujitra@chula.ac.th

ระยะเวลาโครงการ : 3 ปี

งานวิจัยนี้ได้มีการสังเคราะห์สารประกอบโลหะจัลคอกไซด์คือ สารไททาเนียมไกลโดเลตและ สารไททาเนียมไตรไอโซโพรพาในลามีนจากวัตถุดิบที่หาง่ายและราคาถูก ด้วยกระบวนการสังเคราะห์ สารประกอบออกไซด์ขั้นตอนเดียวที่เรียกกันว่า Oxide One Pot Synthesis (OOPS) โดยสารที่ สังเคราะห์ได้มีสมบัติที่เป็นเอกลักษณ์ที่มีความสำคัญมากในกระบวนการโซล-เจล จากการวิเคราะห์ สารตัวอย่างด้วยเครื่อง XRD พบว่า สารที่ผ่านการเผาด้วยอุณหภูมิสูงจะมีการเปลี่ยนแปลงของ โครงสร้างผลึกจากชนิดอนาเทส (anatase) เป็นรูไทด์ (rutile) ที่อุณหภูมิสูง ขณะที่อุณหภูมิ 300 องศา เชลเชียส สารไม่ก่อตัวเป็นโครงสร้างผลิก ในกระบวนการผลิตสารไททาเนียมที่มีผลึกระดับนาโนและมี รูพรุนขนาดกลางโดยกระบวนการโซล-เจลนั้น สารตั้งต้นที่ใช้เป็นไททาเนียมไกลโคเลตในสภาวะที่มี องค์ประกอบเป็นน้ำและกรด ผลการวิเคราะห์จากเครื่อง XRD พบโครงสร้างผลึกชนิดอนาเทสที่ อุณหภูมิการเผาสารในช่วง 600-800 องศาเซลเซียส และมีพื้นที่ผิวสูงถึง 125 ตารางเมตรต่อกรัม ที่ อัตราส่วนโดยปริมาตรระหว่างกรดไฮโดรคลอริกและน้ำเท่ากับ 0.28 ถ้าสารไททาเนียมที่เผาที่อุณหภูมิ ผลึกไททาเนียมไดคคกด์จะมีลักษณะเป็นทรงกลมที่มีขนาดเล็กประมาณ คงศาเพลเพียส จากการศึกษาทางด้านรีโอโลจีของสารไททาเนียมไกลโคเลตโดยวิธีการของวินเทคร์พบว่า เวลาในการเกิดเจลนั้น ขึ้นอยู่กับอัตราส่วนของกรดไฮโดรคลอริกและน้ำ ความแข็งแรงของเจลนั้น เพิ่มขึ้นเมื่ออัตราสวนของกรดและน้ำสูงขึ้น ดังนั้น สามารถกล่าวได้ว่า การเพิ่มความเป็นกรดจะส่งผล ให้ความแข็งแรงของโครงสร้างเพิ่มขึ้นและไม่ก่อให้เกิดการยุบตัว จากการศึกษารีโอโลจีของไททาเนียม ไกลโคเลตเจลที่อัตราส่วนโดยโมลของกรดไฮโดรคลอริกและสารอัลคอกไซด์เท่ากับ 0.8 0.9 1.0 และ 1.1 พบว่า เวลาในการเกิดเจลแปรผันตามอัตราส่วนโดยโมลของกรดและสารอัลคอกไซด์ รวมทั้งความ แข็งแรงของเจลที่เตรียมได้ขึ้นอยู่กับอัตราส่วนของกรดเช่นกัน

ในงานวิจัยนี้ ยังได้ประสบความสำเร็จในการสังเคราะห์สารซีโอไลต์ชนิดทีเอส-วัน (TS-1) ที่ มีปริมาณไททาเนียมในโครงสร้างของซีโอไลต์สูงโดยใช้วัสดุที่เสถียรต่อโมเลกุลของน้ำในอากาศ ได้แก่ สารไททาเนียมไกลโคเลตและไซลาเทรน และใช้คลื่นไมโครเวฟเป็นแหล่งให้ความร้อนในการทำ
ปฏิกิริยา งานวิจัยนี้ได้มีการศึกษาผลกระทบจากปัจจัยที่ใช้ในการสังเคราะห์สาร ได้แก ปริมาณ TPA
โซเคียมไฮดรอกไซด์ และน้ำ รวมทั้งสภาวะต่างๆ เช่น เวลาในการเกิดปฏิกิริยา อุณหภูมิในการทำ
ปฏิกิริยา และเวลาที่ตั้งสารไว้ที่อุณหภูมิห้อง จากการศึกษาพบว่า ไททาเนียมสามารถเข้าทำปฏิกิริยา
และเป็นองค์ประกอบในโครงสร้างของสารซีโอไลต์ได้ด้วยปริมาณสูง โดยมีปริมาณไททาเนียมส่วนน้อย
ที่แยกตัวออกจากโครงสร้างของสารซีโอไลต์ ซึ่งพบในตัวอย่างที่มีอัตราส่วนของซิลิกอน/ไททาเนียม
เท่ากับ 5.0 จากการทดสอบความสามารถในการแตกสลายสาร4-ในโตรพีนอลโดยใช้สารทีเอส-วันเป็น
ตัวเร่งปฏิกิริยาพบว่า ความสามารถในการแตกสลายสาร4-ในโตรพีนอลสูงขึ้นตามปริมาณของไททา
เนียมในโครงสร้างซีโอไลต์

นอกจากนั้น ได้มีการศึกษาการแตกสลายของสาร 4-ในโตรฟืนอลโดยการเตรียมเป็นเยื่อ เลือกผ่าน โดยมีสารไททาเนียมไดออกไซด์ที่มีฟื้นที่ผิวสูงกระจายอยู่ในพอลิเมอร์ชนิดต่างๆ ได้แก่ เซลลูโลสอะซิเตด โพลีอะคลีโลไนไตร และโพลีไวนิลแอลกอฮอล์ สารไททาเนียมไดออกไซด์ที่ใช้เป็น ตัวเร่งปฏิกิริยานั้นเตรียมจากสารอัลคอกไซด์ชนิดไททาเนียมไตรไอโซโพพาโนลามีน จากการศึกษา พบว่า เยื่อเลือกผ่านที่เตรียมจากโพลีอะคลิโลไนไตรนั้นเสถียรที่สุดและมีอัตราการไหลของสารผ่านพื่น ที่ผิวเยื่อเลือกผ่านน้อยที่สุดด้วย การศึกษาความเสถียรและความสามารถในการเร่งปฏิกิริยาของสาร ไททาเนียมในเยื่อเลือกผ่านและทดสอบกับปฏิกิริยาการแตกสลายของ4-ในโตรฟืนอลพบว่า ที่ปริมาณ การใส่สารไททาเนียมมากขึ้นส่งผลให้ความสามารถในการเร่งปฏิกิริยามากขึ้นด้วย

ผลงานวิจัยทั้งหมดนี้ ได้จดสิทธิบัตรภายในประเทศ 1 ฉบับ ตีพิมพ์ในวารสารนานาชาติ จำนวน 3 ฉบับคือ Journal of Mesoporous and Microporous Materials, Journal of Materials Chemistry and Physics และ Applied Organometallic Chemistry และตีพิมพ์ในวารสาร ภายในประเทศจำนวน 1 ฉบับ นอกจากนี้ ยังมีผลงานวิจัยที่ได้ไปเสนอในที่ประชุมวิชาการ ณ ประเทศ อิตาลีอีก 1 เรื่อง

**คำหลัก** : ไททาเนียมไกลโคเลต, ไททาเนียมไตรไอโซโพรพานอลามีน, TS-1, การสลายตัวด้วยแสง, รีโอโลยี

#### Abstract

Project Code: BRG4680013

Project Title: "Study of a synthetic method and application of TiO2-SiO2 as mixed matrix

membrane"

Investigator: Ms. Sujitra Wongkasemjit

The Petroleum and Petrochemical College, Chulalongkorn University

E-mail Address: dsujitra@chula.ac.th

Project Period: 3 Years

A much milder, simpler and more straightforward reaction to titanium glycolate and titanium triisopropanolamine products is successfully investigated using low cost starting materials via the oxide one pot synthesis (OOPS) process. XRD patterns of pyrolyzed products show the morphology change from anatase to rutile as increasing calcination temperature from 500° to 1100°C, while at 300°C totally amorphous phase is formed. The mesoporous nanocrystalline titanium dioxide was prepared via the sol-gel technique using titanium glycolate as precursor in 1M HCl solution at various HCl:H2O ratios. XRD analysis indicates the anatase phase forms at calcination temperatures in the range 600°-800°C. The highest specific surface area (BET) obtained is 125 m²/g at the HCI:H2O ratio of 0.28. The material calcined at 800°C is found to be consist primarily of spherical particles with diameters smaller than 1  $\mu$ m. Application of the Winter rheological criteria for the gel point indicates that the gelation time increases with an increase of the HCI:H2O volume ratio. The fractal dimension of the critical gel cluster decreases with acid ratio, whereas the gel strength increases with acid ratio. Thus, the increase of acidity leads to a less dense but stronger network structure. From the rheological study of different titania gelling systems using HCI:alkoxide molar ratios of 0.8, 0.9, 1.0 and 1.1, the viscoelastic properties are investigated. As evaluated by Winter et al., the gelation time increases as increasing HCl:alkoxide molar ratio. The gel strength increases as a function of acid ratio and the fractal dimension determined from the frequency scaling exponent of the modulus at the gel point indicates a tight structure at low acid ratio.

TS-1 with high Ti loading is successfully synthesized using moisture-stable precursors, viz. titanium glycolate and silatrane. The microwave instrument is used as a heating source for the synthesis. The effects of the compositions (TPA<sup>+</sup>, NaOH, H<sub>2</sub>O) and conditions (aging time, reaction temperature, reaction time) are studied. The Si:Ti molar ratio and the ability of Ti incorporated into the zeolite framework are also studied. Small amount of extra-framework titanium dioxide is identified at 5.0 Si:Ti molar ratio. Photocatalytic decomposition (PCD) of 4-NP is used to test the activity of TS-1 samples and the results of all samples show high efficiency in PCD.

In addition, photocatalytic membranes are successfully prepared using an efficient, high surface area  ${\rm TiO_2}$  catalyst, dispersed into different polymeric matrices, viz. cellulose acetate, polyacrylonitrile and polyvinyl acetate. The catalyst is directly synthesized using titanium triisopropanolamine as the precursor. We find that polyacrylonitrile provides the most effective matrix, showing the highest stability and the lowest permeate flux. The amount of  ${\rm TiO_2}$  loaded in the membrane was varied between 1, 3 and 5 wt% to explore the activity and stability of membranes in the photocatalytic reaction of 4-NP. As expected, the higher the  ${\rm TiO_2}$  loading, the higher the resulting catalytic activity.

All the works described above have been nationally patented and published in three international journals, viz. Journal of Mesoporous and Microporous Materials, Journal of Materials Chemistry and Physics and Applied Organometallic Chemistry Journal, and one national journal. Moreover, there is also one proceeding presented in an international conference in Italy.

**Key words:** Titanium glycolate, Titanium triisopropanolamine, TS-1, Photocatalytic decomposition, Rheology

# **Executive Summary**

#### 1. Research Title

(English): "Study of a synthetic method and application of TiO<sub>2</sub>-SiO<sub>2</sub> as mixed matrix membrane"

(Thai): "การศึกษาวิธีการสังเคราะห์ และการประยุกต์สารไทเทเนียมไดออกไซด์-ซิลิกอนไดออกไซด์เพื่อใช้:ปืนเมมเบรนที่มีสมบัติพิเศษในการแยกสาร"

# 2. Objectives

- Study of a method for synthesizing and characterizing titanium glycolate and titanium triisopropanolamine precursors.
- 2. Study of the sol-gel process and viscoelastic property of titanium glycolate.
- 3. Study of the sol-gel process of mixed titanium glycolate and silatrane precursors.
- Preparation of a mixed matrix membrane to study its photo-catalytic property, selectivity and permeability.

## 3. Project Output

## National Patent

1. สุจิตรา วงศ์เกษมจิตต์ และนพวรรณ พรธรรมชัย เรื่อง "<u>เยื่อแผ่นสำหรับย่อยสลายสารพิษและ</u> เชื้อโรคด้วยแสง" เลขที่คำขอ 103423 เมื่อวันที่ 19 สิงหาคม พ.ศ. 2548

## International Publications

- N. Phonthammachai, E. Gulari, A.M. Jamieson and S. Wongkasemjit\*,
   "Photocatalytic Membrane of a Novel High Surface Area TiO<sub>2</sub> Synthesized from Titanium Triisopropanolamine Precursor", Appl. Organometal. Chem., In press (IF = 1.385)
- N. Phonthammachai, M. Krissanasaeranee, E. Gulari, A. Jamieson and S. Wongkasemjit\*, "Crystallization and Catalytic Activity of High Titanium Loaded TS-1 Zeolite", Materials Chemistry and Physics, 97, 458-467 (2006) (IF = 1.183).
- N. Phonthammachai, T. Chairassameewong, E. Gulari, A. Jamieson and S.
   Wongkasemjit\*, "Structural and Rheological Aspect of Mesoporous Nanocrystalline

 $TiO_2$  via Sol-Gel Process and Its Rheological Study", Mesoporous and Microporous. Mater., 66/2-3, pp. 261-271 (2003). (IF = 3.355)

## **National Publication**

 N. Phonthammachai, T. Chairassameewong, E. Gulari, A. Jamieson and S. Wongkasemjit\*, "Oxide One Pot Synthesis of a Novel Titanium Glycolate and Its Pyrolysis", J.Metals, Minerals and Materials, Chulalongkorn University, 12(1), 23-28 (2002).

# International Proceeding

 N. Phonthammachai, M. Krissanasaeranee, E. Gulari, A. Jamieson and S. Wongkasemjit, "High Surface Area and Thermally Stable TiO<sub>2</sub> Synthesized Directly from Titanium Triisopropanolamine Precursor", Micro- and Mesoporous Mineral Phases Meeting, December 6-7, 2004, Rome, Italy

# **Table Content**

		Page		
Ti+	do nago	ii		
	tle page			
	cknowledgement iii			
	ostract (Thai)	iV .		
	ostract (English)	Vİ		
	secutive Summary	viii		
	able Content	X		
CH	HAPTER			
į	INTRODUCTION	1		
11	LITERATURE REVIEW	4		
	2.1 Synthesis of Metal Alkoxides	4		
	2.2 Sol-gel Process of Metal Alkoxides	6		
	2.3 Rheological Study of Metal Alkoxides	8		
	2.4 Synthesis of TS-1 Zeolite .	10		
	2.5 Photoctalytic Membrane Reactor	12		
	References	15		
III OBJECTIVES				
IV	OXIDE ONE POT SYNTHESIS OF A NOVEL TITANIUM GLYCOLATE			
	AND ITS PYROLYSIS	19		
	Abstract	19		
	Introduction	20		
	Experimental	22		
	Results and Discussion	23		
	Conclusions	26		
	References	26		
٧	STRUCTURAL AND RHEOLOGICAL ASPECT	OF MESOPOROUS		
	NANOCRYSTALLINE TIO <sub>2</sub> SYNTHESIZED VIA SOL-GEL PROCESS			
	Abstract	27		

# Page

Intro	duction	28			
Expe	rimental	29			
Resu	lts and discussion	31			
Cond	clusions	42			
Refe	rences	42			
VI STRL	ICTURAL AND CRYSTALLIZATION OF HIGH TI- LOADE	O TS-1 ZEOLITE 44			
Abst	ract	44			
Intro	duction	45			
Expe	rimental	46			
Resu	ilts and Discussion	48			
Cond	clusions	59			
Refe	rences	60			
VII PHO	/II PHOTOCATALYTIC MEMBRANE REACTOR OF A NOVEL62				
Abst	ract	62			
Intro	duction	63			
Expe	erimental	64			
Resu	ilts and discussion	68			
Cond	clusions	77			
Refe	rences	77			
VIII COI	NCLUSIONS	80			
APPENI	DIX PROJECT OUTPUTS	82			
A. National Patent: สุจิตรา วงศ์เกษมจิตต์ และนพวรรณ พรธรรมชัย		ามชัย			
	เรื่อง "เยื่อแผ่นสำหรับย่อยสลายสารพิษและเชื้อโรคด้วยแสง"				
	เลขที่คำขอ 103423 เมื่อวันที่ 19 สิงหาคม พ.ศ. 2548	83			
B.	N. Phonthammachai, E. Gulari, A.M. Jamieson and S. W.	/ongkasemjit,			
	"Photocatalytic Membrane of a Novel High Surface Area	a TiO <sub>2</sub>			
	Synthesized from Titanium Triisopropanolamine Precurs	sor",			
	Appl. Organometal. Chem., In press	95			

C.	N. Phonthammachai, M. Krissanasaeranee, E. Gulari, A. Jamieson		
	and S. Wongkasemjit, "Crystallization and Catalytic Activity of High		
	Titanium Loaded TS-1 Zeolite", Materials Chemistry and Physics, 97,		
	458-467 (2006)102		
D.	N. Phonthammachai, T. Chairassameewong, E. Gulari, A. Jamieson		
	and S. Wongkasemjit, "Structural and Rheological Aspect of		
	Mesoporous Nanocrystalline TiO <sub>2</sub> via Sol-Gel Process and Its		
	Rheological Study", Mesoporous and Microporous. Mater., 66/2-3,		
	261-271 (2003)113		
E.	N. Phonthammachai, T. Chairassameewong, E. Gulari, A. Jamieson		
	and S. Wongkasemjit, "Oxide One Pot Synthesis of a Novel Titanium		
	Glycolate and Its Pyrolysis", J.Metals, Minerals and Materials,		
	Chulalongkorn University, 12(1), 23-28 (2002)125		
F.	N. Phonthammachai, M. Krissanasaeranee, E. Gulari, A. Jamieson		
	and S. Wongkasemjit, "High Surface Area and Thermally Stable TiO <sub>2</sub>		
	Synthesized Directly from Titanium Triisopropanolamine Precursor",		
	Micro- and Mesoporous Mineral Phases Meeting, December 6-7, 2004,		
	Rome, Italy133		

# CHAPTER I INTRODUCTION

Titanium dioxide (TiO<sub>2</sub>) is widely used in the field of catalysis, as filters or adsorbents or membrane to remove organics from wastewaters (catalytic wet oxidation) and structural and electronic promoters to improve the activity, selectivity and thermal stability of catalysts. Transitional metal substituted zeolite frameworks have received considerable attention in recent years due to their catalytic activity in a number of important industrial processes. The titanium doped TS-1 zeolite with the MFI type framework is a well-known catalyst for the selective oxidation of many organic and inorganic compounds with H<sub>2</sub>O<sub>2</sub> in mild conditions. The reaction is of interest since water is detrimental to conventional titania-silica catalysts and no environmentally undesirable side products are formed from hydrogen peroxide reactions.

Nowadays, industrial wastewater becomes more and more important problem due to increasing trend of many industries. With the same intention, many researchers have been studying to obtain the efficient wastewater treatment to mineralize all the toxic species present in the wastewater without leaving behind any hazardous residues and with low cost. There are many technologies developed for the wastewater treatment, such as, air stripping, granular activated carbon, biological degradation, chemical oxidation and heterogeneous photocatalysis, having been found to be effective for complete mineralization of many toxic, bacteria and bio-resistant organic compounds in wastewaters at such a milder experimental condition. TiO<sub>2</sub> is one of the famous catalysts for photocatalytic degradation due to its effective activity, chemical stability and non-toxic properties. A practical utilization of photocatalysis process generates the main drawback, involving expensive liquid-solid separation process due to the formation of milky dispersions after mixing the powder catalyst in water

Currently, this drawback has been solved by the use of highly dispersed fine particles in a porous material using  $TiO_2$  membrane. Titania membranes attract a great attention in recent years due to their unique characteristics, such as high water flux, semiconducting properties, photocatalysis and chemical resistances over other membrane materials, such as silica and  $\gamma$ -alumina. Many different types of existing membranes consist of a variety of materials, such as, polymers, metals, mixed solid

oxides and porous inorganic materials. However, mixed matrix membrane (MMM), a microencapsulated membrane, becomes more interesting because of its high selectivity combined with an outstanding separation performance of the catalysts, the processing capabilities and low cost of polymers used as matrix.

The important factor to produce titania with good properties is the purity of metal alkoxide precursors. The titanium dioxide has most often been carried out using the titanium alkoxide, however, the synthesis of metal alkoxides is greatly challenging to scientists due to their extreme moisture sensitivity because they contain an unsaturated Ti<sup>IV</sup> center which is highly reactive to air and moisture, therefore the reaction must be carried out under inert gas. Another reason is that they used very expensive starting materials

From that worthy knowledge, it brings up an idea to study how to improve the special features, such as, its redox/oxidation properties and its high oxygen mobility. Key point is how to increase specific surface area with homogeneous distribution of pore size. Sol-gel processing has become one of the most successful techniques for preparing nanocrystalline metallic oxide materials. In general, this method involves the hydrolysis and polycondensation of a metal alkoxide, to ultimately yield hydroxide or oxide under well-specified reaction conditions. A gel is defined as a two- or multicomponent system of semisolid nature, rich in liquid and consisting of continuous solid and fluid phases of colloidal dimensions. It contains a stable cross-linked or entangled network structure infiltrated with liquid. The network structure is formed using chemical or physical gelation processes. Chemical gelation produces branched structures based on covalent bonds between the molecules and the network subunits, whereas the physical gelation is determined by forces (Van der Waals, electrostatic, hydrogen bonding) that generate reversible intermolecular associations. The key advantage of preparing metallic oxides by the sol-gel method is the possibility to control their microstructure and homogeneity. Furthermore, the product after sol-gel processing and sintering is easy to be prepared in different forms, such as, powder, monoliths, thin film and membranes. To obtain homogeneous nanoscale macromolecular oxide networks via sol-gel processing, control of hydrolysis is essential. The properties and nature of the product are controlled by the particular alkoxide used, the presence of acidic or basic additives, the solvent and various other processing conditions (e.g. temperature). The calcination temperature is also a key factor, too low a temperature

results in incomplete combustion and too high a temperature causes phase transformation.

Although much of the work done to characterize the sol-to-gel transition has used spectroscopic techniques, most of these techniques do not provide information about molecular weights. However, a precise experimental determination of the exact transition point is rather difficult because of its divergent nature. On the other hand, rheological measurements are sensitive to the structural and textural evolution of gels and are complementary to spectroscopic experiments. Oscillatory measurement has received great attention among researchers around the world because of its ability to assess and provide important information on the physical structure and rheological properties of materials without disturbing the material configuration. Knowledge of the evolution in rheological properties during sol-gel processing is a useful guide to the manufacturer when formulating dispersion to optimize the physical properties required in the final product. The shear rheology is an ideal tool for detecting the gel point, using the self-similarity of the structure, which implies that both linear viscoelastic moduli G' and G" follow the same power law with frequency. It is generally accepted that polymeric materials as well as many dispersed particles are viscoelastic. Therefore, the steady shear measurement alone could not fully characterize the rheological behavior of these materials. Consequently, there is a growing need to carry out the rheological dynamic measurement, which can fully characterize both the viscous and the elastic components of the dispersions.

In this work titanium glycolate (Ti(OCH<sub>2</sub>CH<sub>2</sub>O)<sub>2</sub>) and titanium triisopropanol amine (Ti(OCHCH<sub>3</sub>CH<sub>2</sub>)<sub>2</sub>N(CH<sub>2</sub>CHCH<sub>3</sub>OH))<sub>2</sub> were synthesized using the Oxide One Pot Synthesis (OOPS) method and low cost starting materials. Ti(OCH<sub>2</sub>CH<sub>2</sub>O)<sub>2</sub> is a novel crystalline complex with infinite one-dimensional chains and exhibits outstanding high stability not only in alcohol but also in water. The high surface area TiO<sub>2</sub> was prepared from the synthesized precursor using the sol-gel process followed by calcinations. The rheological properties of titania were measured at different conditions to study the gelation time and gel strength. The microwave treatment of titanium glycolate and silatrane precursors in basic solution was studied to prepare TS-1 zeolite with high percentage of titanium incorporated in the zeolite framework. The application of titania as a photocatalytic membrane reactor was studied by varying the types of polymer membrane and the amount of titanium loading.

# CHAPTER II LITERATURE SURVEY

# 2.1 Synthesis of Metal Alkoxides

The metal alkoxide precursors for catalyst synthesis are of interest to study because of their remarkable ability as precursor for electroceramic materials. Apparently, the synthesis of new metal alkoxides possessing unique structures and properties is of great significance for the investigation of sol-gel process as well as the evolution of metal alkoxide chemistry. However, there are some disadvantages of metal alkoxides that make it difficult to study their structures and properties thoroughly, such as, the extreme moisture sensitivity and the tendency to form mixtures of structurally complex species upon hydrolysis. From these reasons, many literatures tried to improve the properties of metal alkoxide, such as, the synthesis of anionic titanium tris(glycolate) complex from reaction of titanium dioxide or titanium isopropoxide with glycol in the presence of alkali metal hydroxide, as shown in scheme 2.1.

$$Ti(O^{i}Pr)_{4}$$
 + 2MOH +  $x$ 's  $C_{2}H_{4}(OH)_{2}$   $-H_{2}O$   $-H_{2}O$   $-H_{2}O$   $-H_{2}O$   $-H_{2}O$   $-H_{2}O$   $-H_{2}O$   $-H_{2}O$   $-H_{2}O$ 

Scheme 2.1 The preparation of synthesized anionic titanium tris(glycolate) complex.

The hydrothermal reaction of titanium tetraethoxide, n-butylamine and glycol to obtain titanium glycolate complex was successful after the reaction at 160°-180°C for 5 days. The product exhibited outstanding high stability not only in alcohol, but also in water (scheme 2.2)<sup>2</sup>.

$$Ti(OC_2H_5)_4$$
 + x's  $HOCH_2CH_2OH$  +  $CH_3(CH_2)_3NH_2$   $O$ 

Scheme 2.2 The preparation of titanium glycolate complex by reacting titanium tetraethoxide with glycol.

The silatrane complex was synthesized by direct reaction of SiO<sub>2</sub> and triisopropanolamines. The precursor exhibited the outstanding high stability not only in alcohol but also in water and was synthesized from inexpensive starting materials as scheme 2.3<sup>3</sup>.

 $SiO_2 + N(CH_2CHCH_3OH)_3 + H_2NCH_2(CH_2NHCH_2)_2CH_2NH_2 + HOCH_2CH_2OH$ 

Scheme 2.3 The preparation of silatrane complexes by Wongasemjit's method.

The oxide one pot synthesis (OOPS) process was used to investigate a straightforward and low-cost route to produce alkoxide precursors by direct reactions of a stoichiometric mixture of silica and group I metal hydroxide with ethylene glycol, as shown in scheme 2.4<sup>4</sup>.

Scheme 2.4 The preparation of siloxane complex by the reaction of SiO<sub>2</sub> and glycol.

The synthesis of titanium tetraethoxide (Ti(OEt)<sub>4</sub>) and titanium tetrapropoxide (Ti(OPr<sup>n</sup>)<sub>4</sub>) was studied by the reaction of hydrous titanium dioxide (TiO<sub>2</sub>.nH<sub>2</sub>O, n=0.15-1.23) and dialkyl carbonates using various alkali-metal hydroxide catalysts (LiOH, NaOH, KOH and CsOH) as scheme 2.5. The reaction was carried out in autoclave at a heating rate of 90 Kh<sup>-1</sup>. It was reported that use of sodium hydroxide gave the highest yield compared to the others<sup>5</sup>.

$$TiO_2.nH_2O + (2+n)R'OC(=O)OR' \longrightarrow Ti(OR')_4 + (2+n)CO_2 + 2nR'OH$$
(when R' = Et, Pr<sup>n</sup>)

Scheme 2.5 The preparation of titanium tetraethoxide (Ti(OEt)<sub>4</sub>) and titanium tetrapropoxide (Ti(OPr)<sub>4</sub>).

# 2.2 Sol-gel Process of Metal alkoxides

Sol-gel technique has been extensively used to prepare amorphous and crystalline materials. In general, the sol-gel process is the synthesis of an inorganic network at low temperatures by a chemical reaction in solution. This technique involves the transition characterized by a relatively rapid change from a liquid (solution or colloidal solution) into a solid (gel-like state).

Generally, the precursor is dissolved in a suitable organic solvent in order to form a solution. The solvent must be carefully selected so that a solution with high concentration of the required component can be obtained. Metal oxide network formation involves the following steps:

- 1. precursor formation
- 2. hydrolysis to form solution (sol)
- 3. polycondensation
- 4. film and gel formation
- 5. organic pyrolysis by heat treatment
- 6. densification and crystallization by annealing process

There are two important reactions in polymeric gel formation. These reactions are partial hydrolysis, followed by condensation polymerization. Polymerization steps via hydrolysis and condensation reaction are illustrated, as follows<sup>6</sup>:

Hydrolysis 
$$M(OR)_n + H_2O \implies M(OR)_{n-1}(OH) + ROH$$
 (2.1)

Condensation 
$$M(OR)_n + M(OR)_{n-1}(OH) \longrightarrow M_2O(OR)_{2n-2} + ROH$$
 (2.2)

$$M(OR)_{n-1}(OH) + M(OR)_{n-1}(OH) \longrightarrow M_2O(OR)_{2n-2} + H_2O$$
 (2.3)

The M-O-M network product is formed by polycondensation reactions, as shown in Reactions 2.2 and 2.3 in which alcohol and water are produced as the byproducts. These reactions lead to a degree of gelation regarding to the appropriate amount of water. Other critical parameters usually considered are viscosity of the solutions. Therefore, many applications of controlled hydrolysis to obtain a desired molecular structure and appropriate viscosity of the solution are employed to improve spin ability and coating ability. In addition, solution concentration, viscosity, surface tension of the solution and the deposition technique determine the film thickness and uniformity.

In general, the sol-gel process gives high surface area, pore structure, homogeneous property of the products, and moreover, it is a low-temperature method for converting metal alkoxide to metal oxide. There are many works investigated the sol-gel process using various types of precursors for certain properties.

Previously, the mesoporous nanocrystalline TiO<sub>2</sub> was prepared by a sol-gel technique using butanediol mixed with tetrapropylorthotitanate and aged in ambient temperature for 1-8 weeks. The highest surface area of 97 m<sup>2</sup>/g with diameter of 10 nm was obtained after calcination at 400°C for 2h. The aging time and calcination temperature influence the phase transformation of nanophase titanium dioxide which the phase transition of anatase to rutile began at 630°C and was complete at 730°C<sup>7</sup>.

The forced hydrolysis of boiling reflux method of Ti(SO<sub>4</sub>)<sub>2</sub> solution in the presence of a small amount of H<sub>2</sub>SO<sub>4</sub> was used to prepare nanodispersed spherical TiO<sub>2</sub>. The particle size distribution was over 100 nm. The inhibition of H<sub>2</sub>SO<sub>4</sub> to phase transformation causes the nucleation rate to slow down. When the concentration of H<sub>2</sub>SO<sub>4</sub> continues to rise, the particle size increases and the production of TiO<sub>2</sub> powder is reduced dramatically<sup>8</sup>.

The MOCVD (molecular chemical vapor deposition) technology was used to synthesize nanosized anatase titania. The titanium tetrabutoxide was pyrolyzed in an oxygen-containing atmosphere and the average grain size ranging from 7.4 to 15.2 nm was observed. The preparation temperatures not only accelerate the nucleation rate, but also the particle growth rate. The smallest average grain size 7.4 nm and the highest surface area 180 m<sup>2</sup>/g were obtained at 700°C. The anatase-rutile transformation temperatures were about 700°-1000°C.

The hydrolysis of titanium tetraisopropoxide (TTIP) in the aqueous cores of water/NP-5/cyclohexane microemulsion was used to synthesize ultrafine titania particles. With increasing calcination temperature from 300° to 700°C, the specific

surface area of the TiO<sub>2</sub> particles decreased from 325.6 to 5.9 m<sup>2</sup>/g, whereas the average pore radius increased from 1.4 to 25.1 nm. The particles calcined up to 300°C indicated that they are amorphous and upon increasing the temperature to 650°C, the rutile peaks appeared<sup>10</sup>.

The sol-hydrothermal method using titanium n-butoxide (TNB) precursor in various acidic media (HCl, HNO<sub>3</sub>,  $H_2SO_4$  and  $CH_3COOH$ ) was used to synthesize nanocrystalline titanium dioxide. The nanocrystals of pure rutile with size < 10 nm were obtained at higher HCl concentrations under mild conditions. The propensity of acidic medium for rutile formation is shown as follows:  $HCl > HNO_3 > H_2SO_4 > HAc^{11}$ .

The mesoporous spherical titania particles were prepared via hydrolysis of pure titanium tetra-isopropoxide in n-heptane solution. Calcination of hydrolyzed product produced pure anatase at 400°-600°C and rutile at 800°C. The highest specific surface area of 132 m²/g and pore size of 10 nm were obtained at 400°C which are higher than that of material calcined at 600°C (58.5 m²/g) and much higher than that of the material calcined at 800°C (5.0 m²/g)<sup>12</sup>.

Nanosized titanium (IV) oxide in the anatase form was synthesized by hydrolysis of titanium n-butoxide in toluene with water at high temperature (150°-300°C). The crystalline size of the anatase was gradually increased with reaction temperature and reaction time. The surface area of 71 m<sup>2</sup>/g was received after calcination at 700 °C and the transformation temperature from anatase to rutile was at around 1000°C<sup>13</sup>.

# 2.3 Rheological Study of Metal Alkoxides

Chambon and Winter<sup>14</sup> proposed a constitutive equation for linear viscoelasticity of incipient gels, which they called the gel equation.

$$\delta(t) = S \int_{-\infty}^{t} (t - t')^{-n} \gamma(t') dt' \qquad (2.4)$$

where  $\delta$  is the shear stress,  $\gamma$  is the rate of deformation tensor, n is the relaxation exponent and S is the gel strength parameter (with dimensions Pa.s<sup>n</sup>), which depends on the cross-linking density and the molecular chain flexibility. A more general version of

this model has been developed, where the model proposed by Winter and Chambon<sup>14</sup> constitutes a special case.

The storage modulus G' and the loss modulus G" at the gel point both will follow similar power laws in frequency,

$$G' = G''/\tan \delta = S \omega^n \Gamma(1-n) \cos \delta \qquad (2.5)$$

where  $\Gamma(1-n)$  is the gamma function. The phase angle between stress ( $\delta$ ) and strain is independent of frequency but proportional to the relaxation exponent,

$$\delta = n \pi/2 \tag{2.6}$$

This result suggests that the power law behavior of the dynamic moduli can be expressed as

$$G'(\omega) \sim G''(\omega) \sim \omega^n$$
 (2.7)

Theoretical models have been elaborated to rationalize values of the relaxation exponent in the physical accessible range 0 < n < 1. In the theoretical advances, based on the fractal concept, the dynamic exponent n is associated with information about the molecular structure and connectivity of the incipient gel.

The structure may be described by a fractal dimension  $d_f$ , which is defined by  $R^d_f \sim M$ , where R is the radius of gyration and M is the mass of a molecular cluster. On the basis of the percolation approach, the Rouse model, which assumes no hydrodynamic interaction between polymeric clusters, predicts  $n = d/(d_f + 2)$  and with d = 3 (the space dimension) and  $d_f = 2.5$  (percolation statistics) n assumes a value of 0.67. In the electrical analogy, a suggested isomorphism between the complex modulus and the electrical conductivity of a percolation network with randomly distributed resistors and capacitors yields a value of n = 0.72.

If we consider a situation where the strand length between cross-linking points of the incipient gel varies, one may anticipate that increasing strand length should enhance the excluded volume effect. In order to take this into account, Muthukumar<sup>15</sup> suggested that if the excluded volume interaction is fully screened, the scaling exponent can be expressed as

$$n = d(d+2-2d_f)/2(d+2-d_f)$$
 (2.8)

Quite recently, the relation between the viscoelastic and structural properties of systems of cross-linking polymers near the gel point was considered in the framework of a mechanical ladder model, which predicts a scaling law for the complex shear modulus with an exponent  $0 \le n \le 0.5$ . It was shown that the parameter n is related to the spectral dimension  $d_s \ge 1$  of the fractal through the relationship.

$$n = 1 - d_s/2 (2.9)$$

## 2.4 Synthesis of TS-1 Zeolite

Since Taramasso et al<sup>16</sup> discovered the TS-1 zeolite, there are many researchers tried to synthesize TS-1 with improving the Ti containing in the zeolite framework by different methods and materials because of the high efficiency and molecular selectivity in oxidation reactions employing H<sub>2</sub>O<sub>2</sub>, such as the conversion of ammonia to hydroxylamine, secondary alcohols to ketones, secondary amines to dialklyhydroxylamines, or reactions, such as the hydroxylation, the olefin epoxidation, or the cyclohexanone ammoximation<sup>17</sup>.

The effect of organic amine to the formation of TS-1 zeolite was studied with various types of amine which are n-butylamine, TEAOH, TBAOH, 1,6-hexanediamine, ethylenediamine, diethylamine and triethanolamine. To decrease the cost, TPABr was used as a template instead of TPAOH. The Ti(OC<sub>4</sub>H<sub>9</sub>)<sub>4</sub> was used as the titanium source with the ratio of Si/Ti = 33. They found that the organic amine cannot act as a template in the presence of TPA<sup>+</sup>. It can only regulate the basicity of the gel. The order of the template effect of different templates is as follows: TPA<sup>+</sup>>TBA<sup>+</sup>>TEA<sup>+</sup>>>organic amine<sup>2</sup>.

The synthesis of TS-1 in fluoride medium was prepared by two different methods, mixed alkoxide and wetness-impregnation. The preparation of a sol or a gel containing Si-O-Ti bonds prior to fluoride addition is the key step of the synthesis. The mixed alkoxide method used TPAOH+HF and the wetness-impregnation used TPABr+NH<sub>4</sub>F and the mixture after addition of fluoride was transferred to Teflon-lined autoclave at 170°C for 5 days. DR-UV result of mixed alkoxide method showed that the samples at the Si/Ti ratio of 42 showed only the band at 220 nm, indicating that all the

titanium is in the zeolite framework. For the wetness-impregnation method, the sample with the Si/Ti ratio of 90 exhibited only a strong band at 220 nm<sup>18</sup>.

Titanium silicate-1 (TS-1) was synthesized in the presence of small amount of TPAOH, as nonionic surfactant. The mixture was crystallized at 140°C for 18h under autogeneous pressure at the Si/Ti ratio of 33. The result from DR-UV showed a charge transfer band at 220 nm, which is a characteristic of isolated framework of Ti<sup>4+</sup>. The sample prepared without the use of surfactant, on the other hand, showed the band at 330 nm, which suggest the presence of extra framework of TiO<sub>2</sub><sup>19</sup>.

The crystallization kinetics of TS-1 zeolite using quaternary ammonium halides (TEACl+TBACl) as template was studied. TEOS and TBOT were used as sources of silica and titanium and the crystallization was carried out statically at 160°C for 6-10 days. From the kinetics study of crystallization, as increasing the temperature of crystallization the induction period decreased and the crystallization rate increased. With the increase of the Si/Ti ratio in the reaction mixture, the crystallization rate increased and the mean crystal size decreased gradually. The crystallization rate was also depended on the (TEA+TBA)/Si ratio. Increasing the (TEA+TBA)/Si ratio leads to the increase of crystallization rate, indicating that more template molecules are advantageous to the crystallization of TS-1. The dilution of the sol mixture with water decreased the rate of crystallization and increased the average crystal size. When increasing the NH<sub>3</sub>/Si ratio, both the rate of crystallization and the crystallinity of the final product were increased<sup>20</sup>.

Microwave-assisted synthesis of molecular sieves is a relatively new area of research. It offers many distinct advantages over conventional synthesis. They include rapid heating, resulting in homogeneous nucleation, fast supersaturation by the rapid dissolution of precipitated gels, and eventually a shorter crystallization time compared to those of conventional autoclave heating. Furthermore, it is energy-efficient and economical<sup>21</sup>. It has been postulated that the major mechanism of microwave heating is due to dipole orientation and ionic conduction. However, if one is pressed to explain the mechanism of microwave heating for a given compound, one cannot clearly explain it with the kind of motion of polar molecules and/or ions<sup>22</sup>.

Aluminophosphate molecular sieves (AlPO<sub>4</sub>'s) were prepared by microwave heating without using organic template reagent. The microwave enhanced the

crystallization of aluminophosphate gels, and AlPO<sub>4</sub> were successfully obtained as single phase in a relatively short reaction time<sup>23</sup>.

Aggromerated uniformly sized zeolite Y was prepared in a microwave oven in 10 min, whereas 10-15 h was required for the conventional heating technique, depending on the lattice Si/Al ratio. Relatively high Sj/Al ratio, up to 5, could be obtained from hydrogels containing low aluminum contents without crystallization of undesired phases. ZSM-5 could also be synthesized in 30 min at 140°C by this technique<sup>24</sup>.

Effect of the variation in alkoxide precursor ratio and templating agent concentration on the production of titanium silicate (TS-1) was investigated through analysis techniques. Across the range of compositions studied, x-ray diffraction indicated that all the samples have the MFI crystalline structure, and Raman demonstrated incorporation of titanium in the zeolite framework. Energy dispersive X-ray analysis showed that samples produced using an ultra-low alkali metal content templating agent generally resulted in a higher degree of titanium incorporation in the zeolite framework. IR spectra showed the characteristic of TS-1 at 960 cm<sup>-1</sup> and DR-UV at 210 nm which is attributed to tetra-coordinted titanium<sup>2</sup>.

## 2.5 Photocatalytic membrane reactor

The nanostructured mixed matrix membranes were synthesized using the method based on interfacial crosslinking or copolymerization. To prepare the capsules, an AB-type block copolymer surfactant, consisting of ten methylmethacrylate and eight methacrylic acid units (MMA<sub>10</sub>MAA<sub>8</sub>) was employed. At high pH, MMA<sub>10</sub>MAA<sub>8</sub> is soluble in water and stabilizes w/o emulsions. Capsules were prepared by crosslinking the MAA group of neighbouring surfactants with hexanediamine. The membrane was formed using polymerization of capsules containing monomers of 70%MMA and 30%MAA combined with the interfacial crosslinking encapsulation method. The polymerization reaction was initiated by photo-initiator DMPA in combination with UV-light. The capsules containing films were prepared by dispersing the dry MMA<sub>10</sub>MAA<sub>8</sub> capsules in the MMA/MAA mixture<sup>26</sup>.

The accessible pore system of polymeric ultrafiltration membranes was modified by titanium dioxide and treated further with palladium acetate to yield catalytically active, porous nanofiltration membrane. To overcome the drawback of low thermal stability of common polymeric membranes, the inorganic filler was added to the membrane casting solution. Polyacrylonitrile (PAN), polyetherimide (PEI) and polyamideimide (PAI) were chosen as polymer matrix. The pore system of membranes was modified by two-step procedure to produce catalytically active membranes for heterogeneous catalysis in gas or liquid phase. In the first step, the pore system was narrowed by creating an inorganic titanium oxide layer on the inner surface of the pores by dipping into a solution of 3.5 wt.% tetraethyl titanate in n-hexane. The second step produced an active layer of palladium on the top of these inorganic modified pores of the membrane. The introduction of the catalyst was performed by treating the titanium dioxide modified membrane with a solution of 3 wt.% palladium acetate in methyl ethyl ketone (MEK)<sup>27</sup>.

Random copolymers of 2-hydroxyethyl acrylate (HEA) and methyl acrylate (MA) and homopolymer PHEA were prepared by free radical polymerization. The hydroxyl groups of PHEA were reacted with 3-(triethoxysilyl)propyl isocyanate to introduce triethoxysilyl (TREOS) groups. Co-hydrolysis and condensation of the TEOS groups with titanium tetrabutoxide yielded polymer/SiO<sub>2</sub>/TiO<sub>2</sub> hybrid materials. At TiO<sub>2</sub> less than or equal to 7.4%, the hybrid membranes produced were transparent. Tispecific imaging demonstrated that the TiO<sub>2</sub> phase was nano-sized and distributed uniformly inside the polymer matrix. Water vapor permeability across such hybrid membranes could be changed by varying the PHEA content and was very high for PHEA/SiO<sub>2</sub> membranes. The incorporation of MA into the hybrid allowed to reduce membrane swelling by water at no cost to membrane brittleness<sup>28</sup>.

Mixed matrix membranes of 6FDA-6FpDA-DABA, a glassy polyimide and modified zeolites (ZSM-2) were fabricated. The ZSM-2 zeolites were functionalized with amine groups by reacting them with aminopropyltrimethoxysilane in toluene. The amine-ethered zeolites interacted through secondary forces with the carboxylic groups along the polymer backbone, as documented by FTIR. Band shifts associated with hydrogen bonding of the carbonyl and amine groups were observed in the spectra. These interactions promoted adhesion between the two components. The solubility coefficient for each gas (CO<sub>2</sub>, O<sub>2</sub>, N<sub>2</sub>, He and CH<sub>4</sub>) increased, except for N<sub>2</sub>, which was largely unchanged. The changes in permeability for each gas correlated well with the

change in the diffusion coefficient. The permeabilities of He, CO<sub>2</sub> and CH<sub>4</sub> all decreased, while O<sub>2</sub> and N<sub>2</sub> increased<sup>29</sup>.

The photocatalytic membrane reactors for degradation of organic pollutants in water were prepared by using 4-nitrophenol (4NP) as a probe polluting agent and titanium dioxide in suspension was used as catalyst. The commercial membranes were; NTR7410 and NTR7450 (Nitto enko), N30F and NF-PES-010 (Hoechst), MPCB0000R98 (SEPAREM). The measured permeate flux was in the range of 5-30 l/h m<sup>2</sup> at 4 bar and all membranes showed both a rejection and capacity to adsorb the pollutant with a transitory phase varing from 80 to 400 min at 4 bar. Three factors, viz. rejection, photocatalytic degradation and adsorption, were able to maintain 4NP concentration in the permeate at very low values<sup>30</sup>.

The purification of bilge water by a combination of ultrafiltration and photocatalytic process was studied. The separation of oil from bilge water was performed on a laboratory-scale ultrafiltration pilot plant with tubular membranes made from poly(vinyl chloride) (PVC), polyacrylonitrile (PAN) and polyvinylidene fluoride (PVDF). The examined membranes with MWCO 70 kD for PVC and PAN and 100 kD fo PVDF produced a permeate with an oil content less than 15 ppm. The photocatalytic process was carried out using titanium dioxide based catalyst. The complete decomposition of oil was achieved after 2h for UV illumination using a K-TiO<sub>2</sub> photocatalyst with content amount of 0.8 g/dm<sup>3</sup>, and after 3h of UV illumination using 0.8g/dm<sup>3</sup> of KOH/TiO<sub>2</sub> photocatalyst<sup>31</sup>.

The preparation of polycrystalline TiO<sub>2</sub> samples impregnated with a modified Cu(II)-phthalocyanine (TiO<sub>2</sub>-CuPc) was reported along with an investigation on the photocatalytic behavior of this system compared with bare TiO<sub>2</sub> (both in the anatanse and rutile forms) and with TiO<sub>2</sub> samples impregnated with not functionalized commercial phthalocyanine (TiO<sub>2</sub>-CuPc) or with metal free phthalocyanine (TiO<sub>2</sub>-Pc). The photocatalytic degradation of 4-nitrophenol was studied as a probe reaction. The presence of modified CuPc showed to be beneficial only for TiO<sub>2</sub> (anatase) while the commercial not functionalized CuPc also slightly showed for both TiO<sub>2</sub> (anatase) and TiO<sub>2</sub> (rutile). The metal free Pc did not show any beneficial influence on the photoactivity. A tentative explanation of the beneficial effect due to the presence of the Cu(II)-phthalocyanines both on the initial reaction rate and on the mineralization

process was provided by taking into account intrinsic electronic and physico-chemical properties<sup>32</sup>.

#### References

- a). Gainsford, G.J., Kemmitt, T., Lensink, C., and Milestone, N.B. Inorg. Chem. 1995, 34, 746-748;
   b). Gainsford, J.G., Kemmitt, T., and Milestone, B.N. Inorg. Chem. 1995, 34, 5244-5251.
- Wang, D., Yu, R., Kumada N. (1999) Hydrothermal synthesis and characterization of a novel one-dimensional titanium glycolate complex single crystal: (Ti(OCH<sub>2</sub>CH<sub>2</sub>O)<sub>2</sub>, Chemistry of Materials, 11, 2008-2012.
- P. Piboonchaisit, S. Wongkasemjit and R. Laine, "A Novel Route to Tris(silatranyloxy-i-propyl)amine Directly from Silica and Triisopropanolamine", Sci. Asia, 25, 113-119 (1999).
- a). Bickmore, C.R., Waldner, K.F., Baranwal, R., Hinklin, T., Freadwell, D.R., Laine R.M. (1998) Ultrafine titania by flame spray pyrolysis of a titanatrane complex. European Ploymer Journal, 18, 287-297; b). Laine, R.M., Youngdahl, K.A., Nardi, P. Washington Research Foundation, U.S. Pat. No. 5,099,052, 1992; c). Laine, R.M., Youngdahl, K.A. Washington Research Foundation, U.S. Pat. No. 5,216,155, 1993.
- Suzuki, E., Kusano, S., Hatayama, H., Okamoto, M., and Ono, Y. J.Mater.Chem 1997, 7(10), 2049-2051.
- 6. Yi, G., Sayer, M., Ceram. Bulletin., 1991, 70, 1173.
- 7. Zhang, Y., Weidenkaff, A., Reller A. (2002) Mesoporous structure and phase transition of nanocrystalline TiO<sub>2</sub>. Materials Letters, 54, 375-381.
- 8. Wei, Y., Wu, R., Zhang Y. (1999) Preparation of monodispersed spherical TiO<sub>2</sub> powder by forced hydrolysis of Ti(SO<sub>4</sub>)<sub>2</sub> solution. Materials Letter,41, 101-103.
- 9. Sun, Y., Li, A., Qi, M., Zhang, L., Yao, X. (2001) High surface area anatase titania nanoparticles prepared by MOCVD. Material Science and Engineering: B, 86, 185-188.
- 10. Kim, E.J., Hahn, S.H. (2001) Microstructural changes of microemulsion-mediated TiO<sub>2</sub> particles during calcinations. Materials Letters, 49, 244-249.

- 11. Wu, M., Lin, G., Chen, D., Wang, G., He, D., Feng, S., Xu R. (2002) Solhydrothermal synthesis and hydrothermally structure evolution of nanocrystal titanium dioxide. Chemistry of Material, 14, 1974-1980.
- 12. Khalil, K.M.S and Zaki, M.I. (2001) Preparation and characterization of sol-gel derived mesoporous titania spheroids. Powder Technology, 120, 256-263.
- 13. Kominami, H., Kohno, M., Takada, Y., Inoue, M., Inui, T., Kera, Y. (1999) Hydrolysis od titanium alkoxide in organic solvent at high temperaturas: A new synthetic method for nanosized, thermally stable titanium (IV) oxide.Industrial and Engineering Chemistry Research, 38, 3925-3931.
- 14. Winter, H.H., Chambon, F. (1986) Analysis of linear viscoelasticity of a crosslinking polymer at the gel point. Journal of Rhelogy, 30, 367-382.
- Muthukumar M, (1989) Screening effect on viscoelasticity near the gel point.
   Macromocules, 22, 4656-4658.
- 16. M. Taramasso, G. Perego, B. Notari, US Patent 4410501 (1983).
- 17. Marra, G.L., Artioli, G., Fitch, A.N., Milanesio, M., Lamberti, C. (2000) Orthorhombic to monoclinic phase transition in high-Ti-loaded TS-1: an attempt to locate Ti in the MFI framework by low temperature XRD. Microporous and mesoporous Materials, 40, 85-94.
- 18. Grieneisen, J.L., Kessler, H., Fache, E., Le Govic, A.M. (2000) Synthesis of TS-1 in fluoride medium. A new way to a cheap and efficient catalyst for phenol hydroxylation. Microporous and Mesoporous Materials, 37, 379-386.
- 19. Khomane, R.B., Kulkarni, B.D., Paraskar, A., Sainkar, S.R. (2002) Synthesis, characterization and catalytic performance of titanium silicate-1 prepared in micellar media. Materials Chemistry and Physics, 76, 99-103.
- Xia, Q.H. and Gao, Z. (1997) Crystallization kinetics of pure TS-1 zeolite using quaternary ammonium halides as templates. Materials Chemistry and Physics, 47, 225-230.
- Newalkar, B.L., Olanrewaju, J., Komarneni, S. (2001) Direct synthesis of titanium substituted mesoporous SBA-15 molecular sieve under microwavehydrothermal conditions. Chemistry of Materials, 13, 552-557.
- Ohgushi, T., Komarneni, S., Bhalla, A.S. (2001) Mechanism of microwave heating of zeolite A. Journal of Porous Materials, 8, 23-35.

- 23. Kunii, K., Narahara, K., Yamanaka, S. (2002) Template-free synthesis of AlPO<sub>4</sub>-H1, -H2, and -H3 by microwave heating. Microporous and Mesoporous Materials, 52, 159-167.
- 24. Arafat, A., Jansen, J.C., Ebaid, A.R., Bekkum, H.V. (1993) Microwave preparation of zeolite Y and ZSM-5. Zeolites, 13, 162-165.
- 25. Li, Y.G., Lee, Y.M., Porter, J.F. (2002) The synthesis and characterization of titanium silicate-1. Journal of Materials Science, 37, 1959-1965.
- 26. Figoli, A., Sager, W., Wessling, M. (2002) Synthesis of novel nanostructured mixed matrix membranes. Desalination, 148, 401-405.
- 27. Ziegler, S., Theis, J., Fritsch, D. (2001) Palladium modified porous polymeric membranes and their performance in selective hydrogenation of propyne. Journal of Membrane Science, 187, 71-84.
- 28. Lu, Z., Liu, G., Duncan, S. (2003) Poly(2-hydroxyethyl acrylate-co-methyl acrylate)/SiO<sub>2</sub>/TiO<sub>2</sub> hybrid membranes. Journal of Membrane Science, 221, 113-122.
- 29. Pechar, T.W., Tsapatsis, M., Marand, E., Davis, R. (2002) Preparation and characterization of a glassy fluorinated polyimide zeolite-mixed matrix membrane. Desalination, 146, 3-9.
- 30. Molinari, R., Palmisano, L., Drioli, E., Schiavello, M. (2002) Studies on various reactor configueations for coupling photocatalysis and membrane processes in water purification. Journal of Membrane Science, 206, 399-415.
- 31. Karakulski, K., Morawski, W.A., Grzechulska, J. (1998) Purification of bilge water by hybrid ultrafiltration and photocatalytic processes. Separation and Purification Technology, 14, 163-173.
- 32. Mele, G., Ciccarella, G., Vasapollo, G., Garcia-Lopez, E., Palmisano, L., Schiavello, M. (2002) Photocatalytic degradation of 4-notrophenol in aqueous suspension by using polycrystalline TiO<sub>2</sub> samples impregnated with Cu(II)-phthalocyanine. Applied Catalysis B: Environmental, 38, 309-319.

# CHAPTER III OBJECTIVES

The objectives of this is work are;

- Study of a method for synthesizing and characterizing titanium glycolate and titanium triisopropanolamine precursors.
- 2. Study of the sol-gel process and viscoelastic property of titanium glycolate.
- 3. Study of the sol-gel process of mixed titanium glycolate and silatrane precursors.
- 4. Preparation of a mixed matrix membrane to study its photo-catalytic property, selectivity and permeability.

#### CHAPTER IV

# OXIDE ONE POT SYNTHESIS OF A NOVEL TITANIUM GLYCOLATE AND ITS PYROLYSIS

#### **Abstract**

A much milder, simpler and more straightforward reaction to titanium glycolate product was successfully investigated by the reaction of titanium dioxide, ethylene glycol and triethylenetetramine using the oxide one pot synthesis (OOPS) process. FT-IR spectrum demonstrates the characteristics of titanium glycolate at 619 and 1080 cm<sup>-1</sup> assigned to Ti-O stretching and C-O-Ti stretching vibration, respectively. <sup>13</sup>C-solid state NMR spectrum gives two peaks at 75.9 and 79.8 ppm due to the relaxation of the crystalline spirotitanate product. The percentage of carbon and hydrogen from elemental analysis are 28.6 and 4.8, respectively. Thermal analysis study from TGA exhibits one sharp transition at 340°C, corresponding to the decomposition transition of organic ligand, and giving a ceramic yield of 46.95% which is close to the theoretical yield of 47.5%. XRD patterns show the morphology change of its pyrolyzed product from anatase to rutile as increasing calcination temperatures from 500° to 1100°C while at 300°C the amorphous phase is formed.

Keywords: Titanium Dioxide, Titanium Glycolate, Oxide One Pot Synthesis,

Pyrolysis, Phase Transformation

#### Introduction

Titania is a very useful material and has received a great attention in recent years for its humidity- and gas-sensitive behavior, excellent dielectric property, as well as catalysis applications. The important factor to produce titania with good properties is the purity of titanium alkoxide precursor. However, the synthesis of titanium alkoxides is greatly challenging to scientists due to their extreme moisture sensitivity and very expensive starting materials. In this work a great interest in titanium glycolate, Ti(OCH<sub>2</sub>CH<sub>2</sub>O)<sub>2</sub>, is owing to its difference from most crystalline titanium alkoxides, generally having low polymeric O-dimensional molecular. Nevertheless, Ti(OCH<sub>2</sub>CH<sub>2</sub>O)<sub>2</sub> is a novel crystalline complex with infinite one-dimensional chains, and exhibits outstanding high stability not only in alcohol, but also in water.<sup>2</sup>

The method required for the synthesis of alkoxy derivatives of an element generally depends on its electronegativity. In the case of comparatively less active metals, a catalyst is generally employed for successful synthesis of metal alkoxides. Wang et al.<sup>2</sup> synthesized Ti(OCH<sub>2</sub>CH<sub>2</sub>O)<sub>2</sub> from very expensive starting material, tetraethyl orthotitanate to react with ethylene glycol using n-butylamine as a catalyst. The reaction took place under a very vigorous condition. It occurred in a Teflon-lined stainless steel autoclave at 160°-180 °C for 5 days. The alkalinity of the initial reaction mixture is a dominant factor of the product. The ethylene glycol served as both a solvent and a bidentate chelate occupying sites on titanium coordination sphere so as to bridge adjacent titanium atoms and formed the one-dimensional structure.

Gainsford et al.<sup>3-4</sup> studied the synthesis and characterization of the soluble titanium glycolate complexes obtained from the reaction of titanium dioxide or titanium isopropoxide with glycol in the presence of alkali metal hydroxides. The reaction of Ti(O-i-Pr)<sub>4</sub> with 2 equivalent of sodium or potassium hydroxides provided tris(glycolate) salts, which were highly crystalline, hygroscopic materials, crystallized as salts and solvated with varying numbers of glycol molecules.

Suzuki et al.<sup>5</sup> synthesized titanium tetraalkoxides from hydrous titanium dioxide (TiO<sub>2</sub>.nH<sub>2</sub>O) and dialkyl carbonates in an autoclave at a heating rate of 90Kh<sup>-1</sup>. The effect of reaction temperature was studied. At temperature range of 495-533 K, practically completed conversion of hydrous titanium dioxide to Ti(OEt)<sub>4</sub> could be attained. LiOH, NaOH, KOH, and CsOH were used as catalysts which NaOH gave the highest yield of Ti(OEt)<sub>4</sub>. The effect of the molar ratios of diethyl carbonate/hydrous

titanium dioxide was studied. As high molar ratio of 10 was required to obtain a high yield of Ti(OEt)<sub>4</sub>.

Related metalloglycolates formed from alkaline glycol were reported for aluminium and titanium<sup>6-11</sup>. Potassium and sodium tris(glycotitanate) complexes were obtained from the reaction of titanium dioxide or titanium tetraisopropoxide with ethylene glycol in the presence of alkali metal hydroxides.<sup>3-4</sup>

Laine et al. investigated a straightforward, low-cost reute to alkoxide precursors by direct reactions of a stoichiometric mixture of silica and group I metal hydroxide with ethylene glycol. This route, termed the 'oxide one pot synthesis' (OOPS) process, provides processable precursors, as shown in Scheme 1. 12-14

#### Scheme 1

Recently, Jitchum *et al.* synthesized neutral alkoxysilanes, tetracoordinated spirosilicates, directly from silica and ethylene glycol or ethylene glycol derivatives, using triethylenetetramine as catalyst, in the absence or presence of potassium hydroxide as co-catalyst (Scheme 2).<sup>15</sup>

## Scheme 2

The OOPS method is simple, low-cost and can produce new chemicals in only one step. Thus, the objective of this work is to use the OOPS process to synthesize titanium glycolate. The phase transformation of its pyrolyzed product is studied, as well.

# Experimental

#### Materials

UHP grade nitrogen; 99.99% purity, was obtained from Thai Industrial Gases Public Company Limited (TIG). Titanium dioxide was purchased from Sigma-Aldrich Chemical Co. Inc. (USA) and used as received. Ethylene glycol (EG), purchased from Malinckrodt Baker, Inc. (USA) was purified by fractional distillation under nitrogen at atmospheric pressure, 200°C before use. Triethylenetetramine (TETA) was purchased from Facai Polytech. Co. Ltd. (Bangkok, Thailand) and distilled under vacuum (0.1 mm/Hg) at 130°C prior to use. Acetonitrile was purchased from Lab-Scan Company Co. Ltd. and purified by standard distilling over calcium hydride powder.

#### Instrumentai

Fourier transform infrared spectra (FT-IR) were recorded on a VECOR3.0 BRUKER spectrometer with a spectral resolution of 4 cm<sup>-1</sup> using transparent KBr pellets containing 0.001 g of the sample was ground and mixed with 0.06 g of KBr. Thermal gravimetric analysis (TGA) was carried out using a Perkin Elmer thermal analysis system with a heating rate of 10 °C/min over 30°-800°C temperature range. Mass spectrum using the positive fast atom bombardment mode (FAB<sup>+</sup>-MS) was measured on a Fison Instrument (VG Autospec-ultima 707E) with VG data system using glycerol as the matrix, cesium gun as initiator, and cesium iodide (CsI) as a standard for peak calibration. <sup>13</sup>C- solid state NMR spectroscopy modeled Bruker AVANCE DPX-300 MAS-NMR was used to determine peak position of carbon containing in the product. Elemental analysis (EA) was carried out on a C/H/0 Analyser (Perkin Elmer PE2400 series II). X-ray diffraction patterns were analyzed using a D/MAX-2200H Rigaku equipped with Cu X-ray generator.

## Methodology

The titanium glycolate was synthesized by the OOPS method, see Scheme 3. A mixture of TiO<sub>2</sub> (2g, 0.025 mol) and TETA (3.65g, 0.0074 mol) was stirred vigorously in excess EG (25 cm<sup>3</sup>) and heated at the boiling point of EG under N<sub>2</sub> atmosphere. After heating for 24 h the solution was centifuged to separate the unreacted TiO<sub>2</sub> from the

solution part. The excess EG and TETA were removed by vacuum distillation to obtain crude precipitate product. The white solid product was washed with acetonitrile and dried in a vacuum desiccator.

TiO<sub>2</sub> + HOCH<sub>2</sub>CH<sub>2</sub>OH 
$$\xrightarrow{\text{TETA}}$$
  $\xrightarrow{\text{Q}}$  Ti  $\xrightarrow{\text{Q}}$  + 2 H<sub>2</sub>O Scheme 3

#### Results and Discussion

# Synthesis

The reaction of titanium dioxide, triethylenetetramine catalyst and ethylene glycol used as both solvent and reactant was achieved by heating in a simple distillation apparatus. The glycol was slowly distilled off along with water generated during the condensation reaction to drive the reaction forward. The resulting product was isolated by distilling off glycol, followed by addition of acetronitrile to remove residual glycol and TETA. The final product, titanium glycolate, was moisture-stable.

## Characterization

FT-IR spectrum of titanium glycolate is shown in Figure 1. As compared with the work done by Wang<sup>2</sup>, the result clearly shows the characteristics of titanium alkoxide at 1080 and 619 cm<sup>-1</sup> bands, corresponding to C-O-Ti and Ti-O stretching, respectively. Moreover, the band at 2927-2855 cm<sup>-1</sup> is assigned to the C-H stretching of ethylene glycol ligand.

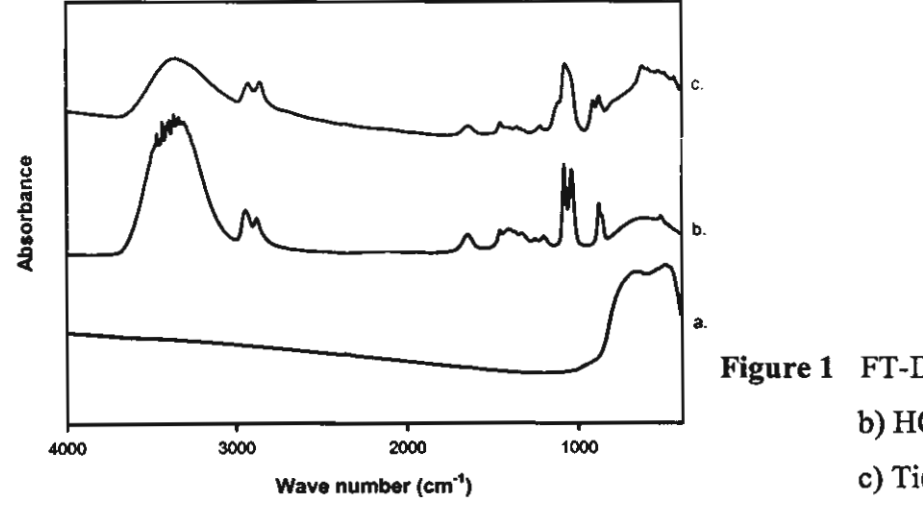


Figure 1 FT-IR spectra of a) TiO<sub>2</sub>, b) HOCH<sub>2</sub>CH<sub>2</sub>OH and c) Ti(OCH<sub>2</sub>CH<sub>2</sub>O)<sub>2</sub>

Due to the insolubility of the product in organic solvent, <sup>13</sup>C-solid state NMR was employed. The obtained spectrum, see Figure 2, gives two peaks at 74.8 and 79.2 ppm. It is due to the crystalline phase of titanium glycolate, causing the peak to split during relaxation time of nuclei, as discussed by Wang.<sup>2</sup>

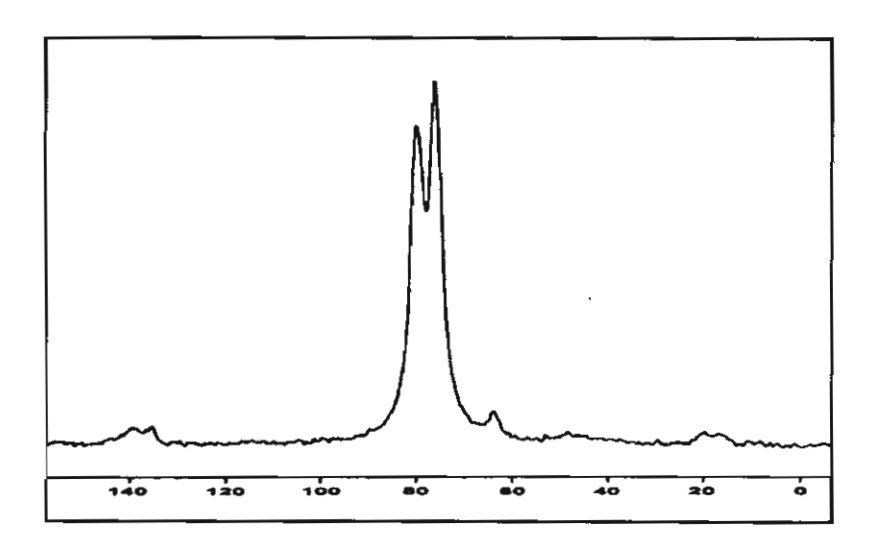


Figure 2 <sup>13</sup>C-Solid state NMR spectrum of the synthesized Ti(OCH<sub>2</sub>CH<sub>2</sub>O)<sub>2</sub>

To confirm the structure of the desired product, both elemental analysis and mass spectroscopy techniques are carried out. The results are shown in Tables 1 and 2, respectively. The obtained C/H percentages are close to those calculated theoretically. The proposed fragmentation and structures presented in Table 2 also confirms the expected structure of the titanium glycolate product.

Table1 Percentages of C and H presented in the synthesized Ti(OCH<sub>2</sub>CH<sub>2</sub>O)<sub>2</sub>

Element (%)	Theoretical	Experimental
С	27.9	28.6
H	5.6	4.8

M/e	%intensity	Proposed structure
169	8.5	Ti O + H <sup>+</sup>
94	73.5	O-Ti-OCH <sub>2</sub>
45	63.5	CH <sub>2</sub> CH <sub>2</sub> OH

Table 2 Proposed fragmentation and product structures of Ti(OCH<sub>2</sub>CH<sub>2</sub>O)<sub>2</sub>

As for its thermal stability, Figure 3 shows the same TGA thermogram as obtained by Wang<sup>2</sup>. The result exhibits one sharp transition at 340°C, corresponding to the decomposition transition of the glycol ligand. The final ceramic yield obtained is 46.95% that is close to the theoretical yield of 47.5%.

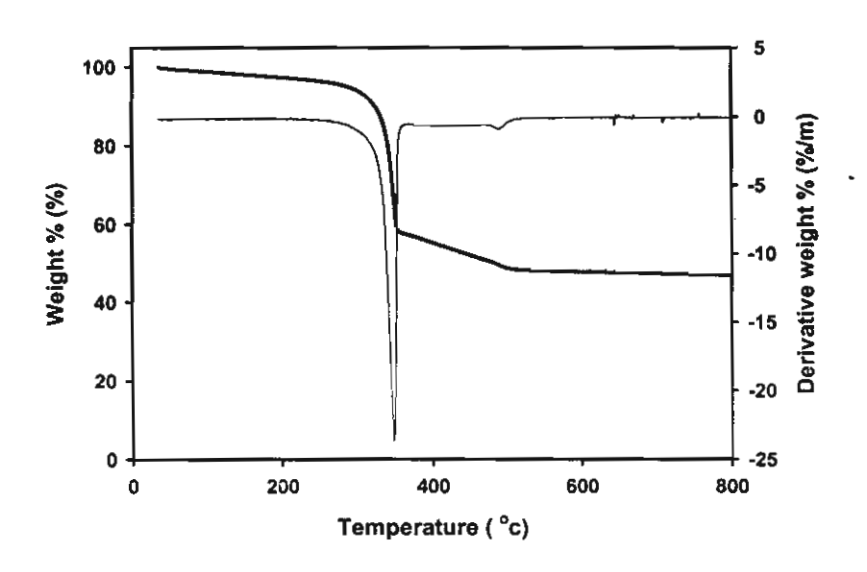


Figure 3: TGA curve of Ti(OCH<sub>2</sub>CH<sub>2</sub>O)<sub>2</sub>

#### Phase transformation

The TGA result indicats the oxidation of organic compound at 340 °C, and the crystallization at 500 °C. Study of the phase transformation was conducted at the calcinations temperature ranging from 300° to 1100°C. The crystalline titanium glycolate decomposed and changed to amorphous phase at 300 °C (Figure 4). As

increasing the calcination temperature, the XRD pattern gives anatase phase at 500 °C to 900 °C and completely changes to rutile phase at 1100°C.

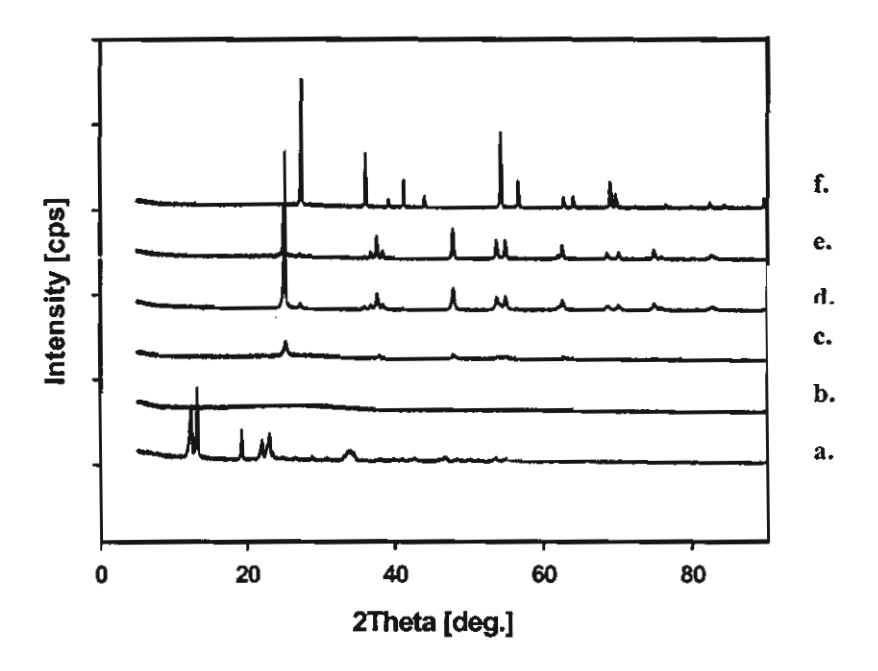


Figure 4 XRD patterns of Ti(OCH<sub>2</sub>CH<sub>2</sub>O)<sub>2</sub> at different temperatures: a) ambient, b) 300°, c) 500°, d) 700°, e) 900° and f) 1100°C.

#### **Conclusions**

Titanium glycolate is successfully synthesized using low cost starting materials, and a much simpler and milder reaction condition. The product shows good property in moisture stability. The results from spectroscopy, namely, FT-IR, EA, Solid state NMR, and TGA, confirm the product structure. The transformation from anatase to rutile phase indicates the anatase stability up to 900°C. The stability of the synthesized product remarkably provides researchers to make use in many applications.

### References

- Ding, X.Z., and Liu, X.H. Materials Science and Engineering A224. 1997, 210-215
- 2. Wang, D., Yu, R., Kumada, N. Chem. Mater. 1999, 11, 2008-2012.
- 3. Gainsford, G.J., Kemmitt, T., Lensink, C., and Milestone, N.B. Inorg. Chem. 1995, 34, 746-748.

- Gainsford, J.G., Kemmitt, T., and Milestone, B.N. Inorg. Chem. 1995, 34, 5244-5251.
- Suzuki, E., Kusano, S., Hatayama, H., Okamoto, M., and Ono, Y. J.Mater.Chem 1997, 7(10), 2049-2051.
- 6. Bickmore, C.R., Waldner, K.F., Baranwal, R., Hinklin, T., Freadwell, D.R., and Laine, R.M. Journal of the European ceramic Society. 1998, 18, 287-297.
- Yang, J., MEI, S., and Ferreira, J.M.F. Materials Science and Engineering C 2001, 15, 183-185.
- 8. Laine, R.M.; Youngdahl, K.A.; Nardi, P. Washington Research Foundation, U.S. Pat. No. 5,099,052, 1992.
- 9. Laine, R.M.; Youngdahl, K.A. Washington Research Foundation, U.S. Pat. No. 5,216,155, 1993.
- 10. Day, V.W., Eberspacher, .A., Frey, M.H., Klemperer, W.G., Liang, S. and Payne, D.A. Chem Mater 1996, 8, 330-332.
- 11. Duan, Z., Thomas, L.M., and Verkade, J.G. Polyhedran 1997, 16, 635-641.
- 12. Laine, R.M.; Blohowiak, K.Y.; Robinson, T.R.; Hoppe, M.L.; Nardi, P.; Kampf, J.: Uhm, J. Nature **1991**, 353, 642.
- Blohowiak, K.Y.; Laine, R.M.; Robinson, T.R.; Hope, M,L.; Kampf, J.I. Inorganic and Organometallic Polymers with Special Properites; ACS: Netherland, 1992.
- Bickmore, C.; Hoppe, M.L.; Laine, R.M. Mat.Res.Soc.Symp.Proc. 1992, 249, 81.
- 15. Jitchum, V.; Chivin, S.; Wongkasemjit S.; Ishida, H. Tetrahedron 2001, 57, 3997.

## **CHAPTER V**

# STRUCTURAL AND RHEOLOGICAL ASPECT OF MESOPOROUS NANOCRYSTALLINE TiO<sub>2</sub> SYNTHESIZED VIA SOL-GEL PROCESS

#### **Abstract**

Mesoporous nanocrystalline titanium dioxide was prepared via 'he sol-gel technique using titanium glycolate as precursor in 1M HCl solution at various HCl:H<sub>2</sub>O ratios. XRD analysis indicates the anatase phase forms at calcination temperatures in the range 600°-800°C. From the average grain sizes, we deduce that the nucleation rate dominates the kinetics at lower temperature, and growth rate becomes the controlling factor at higher temperature for materials prepared at HCl:H<sub>2</sub>O ratios of 0.28 and 0.33. At higher volume ratios, the growth rate appears to be the dominant factor at all temperatures. The highest specific surface area (BET) obtained was 125 m<sup>2</sup>/g at the HCl:H<sub>2</sub>O ratio of 0.28. A small decrease of specific surface area was observed from low to high acid ratio and a substantial decrease from lower to higher temperature. The material calcined at 800°C was found to consist primarily of spherical particles with diameters smaller than 1 \mu. Application of the Winter rheological criteria for the gel point indicates that the gelation time increases with increase of the HCl:H2O volume ratio. The fractal dimension of the critical gel cluster decreases with acid ratio, whereas the gel strength increases with acid ratio. Thus increase of acidity leads to a less dense but stronger network structure.

**Keywords**: Titanium glycolate, Titania, Rheology, Sol-gel process and Viscoelastic properties

#### Introduction

Titanium dioxide or titania, TiO<sub>2</sub>, is widely used in the field of catalysis, as filters, adsorbents, and catalyst supports<sup>1-2</sup>. The porous anatase form, as compared to the rutile phase, is of greater importance and interest due to its better catalytic properties. Therefore, a key goal is to prepare anatase nanoparticles, with high surface area, uniform particle size and pore structure, and a high anatase-rutile transformation temperature<sup>3</sup>.

Sol-gel processing has become one of the most successful techniques for preparing nanocrystalline metallic oxide materials. In general, this method involves the hydrolysis and polycondensation of a metal alkoxide, to ultimately yield hydroxide or oxide under well-specified reaction conditions<sup>4</sup>. The key advantage of preparing metallic oxides by the sol-gel method is the possibility to control their microstructure and homogeneity. To obtain homogeneous nanoscale macromolecular oxide networks via sol-gel processing, control of hydrolysis is essential. The properties and nature of the product are controlled by the particular alkoxide used, the presence of acidic or basic additives, the solvent, and various other processing conditions (e.g. temperature). The calcination temperature is also a key factor, especially for titania preparation. Too low a temperature results in incomplete combustion and too high a temperature causes phase transformation.

Many studies have been directed to prepare titania powder with increased textural and structural stability. For example, Zhang et al.<sup>5</sup> prepared and studied mesoporous nanocrystalline TiO<sub>2</sub> by a sol-gel technique using butanediol mixed with tetrapropylorthotitanate. A surface area of 97 m<sup>2</sup>/g was obtained after calcination at 400°C for 2h. Wei et al.<sup>6</sup> prepared nanodisperse spherical TiO<sub>2</sub> particles by forced hydrolysis using boiling reflux Ti(SO<sub>4</sub>)<sub>2</sub> solution in the presence of H<sub>2</sub>SO<sub>4</sub>. The particle size distribution was in the range 70-100 nm. Sun et al.<sup>7</sup> prepared nanosized anatase titania with average grain sizes ranging from 7.4 to 15.2 nm using MOCVD technology to pyrolyze titanium tetrabutoxide in an oxygen containing atmosphere. The smallest average grain size and the highest surface area were obtained at 700°C. Kim et al.<sup>8</sup> synthesized ultrafine titania particles by hydrolysis of titanium tetraisopropoxide (TTIP) in the aqueous cores of water/NP-5/cyclohexane microemulsions with increasing calcination temperature from 300° to 700°C, the specific surface area of the TiO<sub>2</sub> particles decreased from 325.6 to 5.9 m<sup>2</sup>/g, whereas the average pore radius increased

from 1.4 to 25.1 nm. Wu et al.<sup>9</sup> synthesized nanocrystalline titanium dioxide using the sol-hydrothermal method with titanium n-butoxide (TNB) as precursor, in various acidic media (HCl, HNO<sub>3</sub>, H<sub>2</sub>SO<sub>4</sub>, and CH<sub>3</sub>COOH). Nanocrystals of pure rutile with size < 10 nm were obtained at higher HCl concentrations under mild conditions. The propensity of acidic medium for rutile formation is shown as follows: HCl > HNO<sub>3</sub> > H<sub>2</sub>SO<sub>4</sub> > HAc.

Knowledge of the evolution in rheological properties during sol-gel processing is a useful guide to the manufacturer when formulating dispersions to optimize the physical properties required in the final product<sup>10</sup>. Thus, in this work, our aims are to synthesize high surface area anatase TiO<sub>2</sub> and to study the rheological properties of titanium glycolate synthesized directly from inexpensive and widely available TiO<sub>2</sub> and ethylene glycol via the Oxide One Pot Synthesis (OOPS) method<sup>11</sup>. We also investigate the influence of the acid concentration used in acid-catalyzed hydrolysis, the effect of calcination temperature on morphology and phase transformation, and gain some insight into the gel mechanism.

## **Experimental**

#### Materials

Titanium dioxide (surface area 12 m²/g) was purchased from Sigma-Aldrich Chemical Co. Inc. (USA) and used as received. Ethylene glycol (EG) was purchased from Malinckrodt Baker, Inc. (USA) and purified by fractional distillation at 200°C under nitrogen at atmospheric pressure, before use. Triethylenetetramine (TETA) was purchased from Facai Polytech. Co. Ltd. (Bangkok, Thailand) and distilled under vacuum (0.1 mm/Hg) at 130°C prior to use. Acetonitrile was purchased from Lab-Scan Company Co. Ltd. and purified by distilling over calcium hydride powder.

## Instrumental

Fourier transform infrared spectra (FT-IR) were recorded on a VECOR3.0 BRUKER spectrometer with a spectral resolution of 4 cm<sup>-1</sup> using transparent KBr pellets containing 0.001 g of sample mixed with 0.06 g of KBr. Thermal gravimetric analysis (TGA) was carried out using a Perkin Elmer thermal analysis system with a heating rate of 10°C/min over 30°-800°C temperature range. The mass spectrum was obtained on a Fison Instrument (VG Autospec-ultima 707E) with VG data system, using

the positive fast atomic bombardment mode (FAB<sup>+</sup>-MS) with glycerol as the matrix, cesium gun as initiator, and cesium iodide (CsI) as a standard for peak calibration. <sup>13</sup>C-solid state NMR spectroscopy was performed using a Bruker ADVANCE DPX-300 MAS-NMR. Elemental analysis (EA) was carried out on a C/H/N Analyser (Perkin Elmer PE2400 series II).

# Preparation of titanium glycolate

The procedure adopted followed previous work<sup>11</sup>. A mixture of TiO<sub>2</sub> (2g, 0.025 mol) and TETA (3.65g, 0.0074 mol) was stirred vigorously in excess EG (25 cm<sup>3</sup>) and heated to 200°C for 24 h. The resulting solution was centrifuged to separate the unreacted TiO<sub>2</sub>. The excess EG and TETA were removed by vacuum distillation to obtain a crude precipitate. The white solid product was washed with acetonitrile, dried in a vacuum desiccator and characterized using FTIR, <sup>13</sup>C-solid state NMR, EA, FAB<sup>+</sup>-MS, and TGA.

FTIR: 2927-2855 cm<sup>-1</sup> (vC-H), 1080 cm<sup>-1</sup> (vC-O-Ti bond), and 619 cm<sup>-1</sup> (vTi-O bond). <sup>13</sup>C-solid state NMR: two peaks at 74.8 and 79.2 ppm. EA: 28.6% C and 4.8% H. FAB<sup>+</sup>-MS: approximately 8.5% of the highest m/e at 169 of [Ti(OCH<sub>2</sub>CH<sub>2</sub>O)<sub>2</sub>]H<sup>+</sup>, 73% intensity at 94 of [OTiOCH<sub>2</sub>] and 63.5% intensity at m/e 45 of [CH<sub>2</sub>CH<sub>2</sub>OH]. TGA: one sharp transition at 340°C and 46.95% ceramic yield corresponding to Ti(OCH<sub>2</sub>CH<sub>2</sub>O)<sub>2</sub>.

# Sol-gel processing of titanium glycolate

The hydrolysis of titanium glycolate (0.026 g) was carried out via addition of  $\mu$ L of 1M HCl mixed with distilled water in volume ratios of HCl:H<sub>2</sub>O 0.45, 0.39, 0.33, and 0.28. The mixtures were magnetically stirred and heated in a water bath at 50°C until a clear gel was obtained. The gels were calcined for 2 h at 600°, 700°, and 800°C.

## Rheological study of titanium glycolate

Gelation occurs when aggregation of particles or molecules takes place in a liquid, under the action of Van der Waals forces or via the formation of covalent or noncovalent bonds<sup>12</sup>. The process can be conveniently monitored using rheological measurement techniques<sup>13</sup>. The rheometric measurements were conducted using an ARES rheometer with parallel plate geometry, 25 mm in diameter. The storage (G') and loss (G") moduli were determined using oscillatory shear at frequencies in the range 0.2-6.4 rad/s. The strain amplitude was small enough to ensure that all experiments

were conducted within the linear viscoelastic region, where G' and G" are independent of the strain amplitude. Titanium glycolate 0.026 g was hydrolyzed at different HCl:H<sub>2</sub>O volume ratios of 0.45, 0.39, 0.33 or 0.28. The hydrolysis temperature was selected to be 30°C. The mixtures were stirred until homogeneous before being transferred to the rheometer.

## Characterization of calcined materials

Crystallinity and average grain sizes were characterized using a D/MAX-2200H Rigaku diffractometer with CuKα radiation on specimens prepared by packing sample powder into a glass holder. The diffracted intensity was measured by step scanning in the 2θ range between 5° to 90°. Specific surface area, nitrogen adsorption-desorption, and pore size distribution were determined using an Autosorp-1 gas sorption system (Quantachrome Corporation) via the Brunauer-Emmett-Teller (BET) method. A gaseous mixture of nitrogen and helium was allowed to flow through the analyzer at a constant rate of 30 cc/min. Nitrogen was used to calibrate the analyzer, and also as the adsorbate at liquid nitrogen temperature. The samples were throughly outgassed for 2h at 150°C, prior to exposure to the adsorbent gas. Material morphology was observed using a JEOL 5200-2AE(MP 15152001) scanning electron microscope. Samples were prepared for SEM analysis by attachment to aluminum stubs, after pyrolysis at 800°C. Prior to analysis, the specimens were dried in a vacuum oven at 70°C for 5 h followed by coating with gold via vapor deposition. Micrographs of the pyrolyzed sample surfaces were obtained at x10,000 magnification.

# Results and discussion

The investigation of the hydrolysis reaction of titanium glycolate precursor using FTIR is illustrated in figure 1. The spectra show an increase in the peak intensity of Ti-O-Ti stretching at approximately 500-800 cm<sup>-1</sup> due to hydrolysis of the precursor. The peak at 1000-1100 cm<sup>-1</sup>, corresponding to C-O stretching of ethylene glycol also increases, reflecting the production of ethylene glycol during the hydrolysis reaction. In the case of higher acid ratio (0.45), the degree of crosslinking is greater than those obtained from the hydrolysis in lower acid ratios. The acid can act as a catalyst to hydrolyze the alkoxide by protonating the ethoxy ligands during hydrolysis. Thus, the

elimination of the protonated ethoxy ligand leaving group is no longer the rate limiting step, and, as a result, the hydrolysis occurs more rapidly.

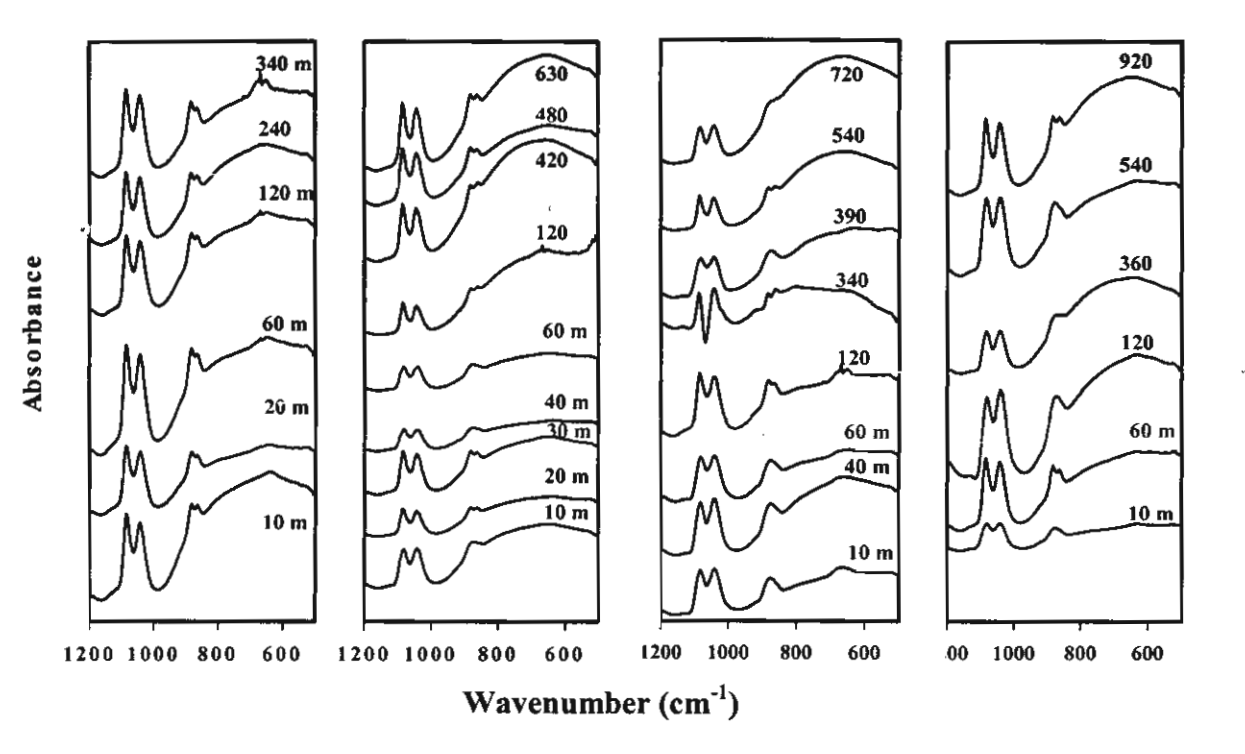


Figure 1 FT-IR spectra of titania gel at HCl:H<sub>2</sub>O volume ratios of a) 0.28, b) 0.33, c) 0.39 and d) 0.45

Calcination is a treatment commonly used to improve the crystallinity of TiO<sub>2</sub> powder. When TiO<sub>2</sub> is calcined at higher temperature, a transformation to rutile phase usually occurs<sup>13</sup> and comprises anatase, rutile, and brookite. XRD patterns (Fig. 2) show the phase transformations encountered when titanium glycolate precursor is calcined at temperatures in the range 390°-1100°C. Amorphous material is obtained at the lowest temperature (300°C) whereas at 500°C broader anatase peaks appear. As the calcination temperature increases, the intensity of anatase peaks becomes stronger and well resolved. However, if the calcination temperature is increased to 900°C, small rutile peaks are found, indicating the onset of the transformation to rutile.

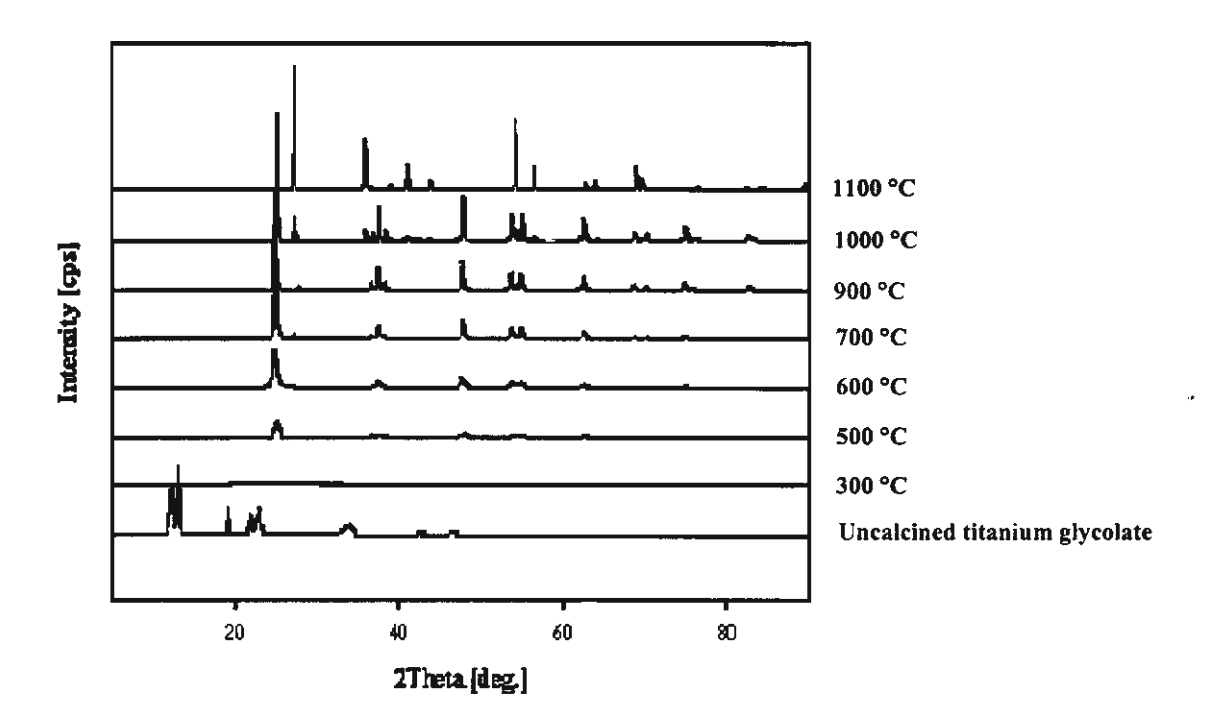


Figure 2 XRD patterns of uncalcined and calcined titanium glycolate precursor at different temperatures.

The synthesis procedure was changed to obtain porous anatase for better catalytic properties. Specimens obtained via the sol-gel process at different volume ratios of HCl:H<sub>2</sub>O, viz. 0.45, 0.39, 0.33, and 0.28, were subjected to calcination at 600°, 700°, and 800°C, to obtain porous anatase titania<sup>3</sup>. Fig. 3 shows the XRD patterns of anatase formation in a specimen at the HCl:H<sub>2</sub>O volume ratio of 0.28. Our results indicate that the synthesized anatase is stable up to calcination temperatures of 800°C, which is a little higher than previous studies, which report the transformation of anatase to rutile in the range of 600°-700°C<sup>7, 13-14</sup>.

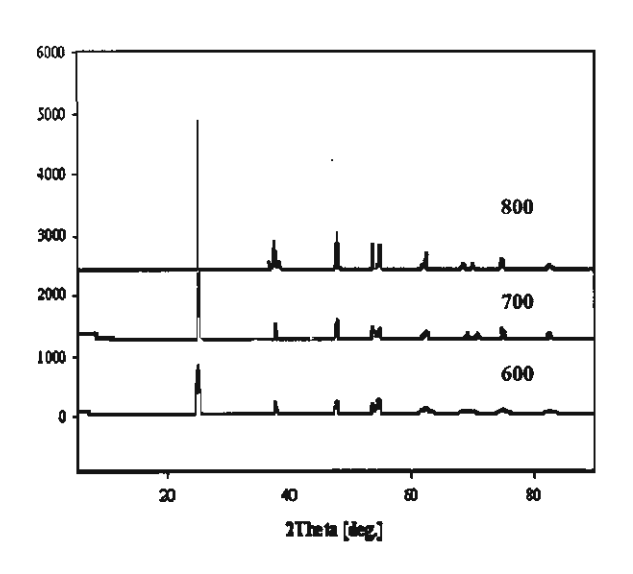


Figure 3 XRD patterns of titania gel using the HCl:H<sub>2</sub>O volume ratio of 0.28 and calcined at a) 600°, b) 700° and c) 800°C.

As can be seen in Fig. 4, at 0.28 and 0.33 ratios, the average grain size decreases significantly from 600°C (18.8 and 17.1 nm) to 700°C (13.9 and 14.2 nm) and then increases substantially again at 800°C (31.3 and 29.8 nm). These results are reminiscent of observations by Sun et al<sup>7</sup> of the temperature dependence of grain sizes of anatase produced by the MOCVD method. The size variation was interpreted in terms of the rate of particle growth relative to the rate of particle nucleation. Use of elevated temperatures accelerates not only the nucleation rate but also the particle growth rate. For acid:water ratios of 0.28 and 0.33, at lower temperatures, the nucleation rate is dominant, whereas the growth rate becomes the controlling factor at higher temperature. Acid:water ratios of 0.39 and 0.45 ratios show a slightly different pattern, in which grain size increases mildly between 600° and 700°C, and then more dramatically at 800°C, suggest that the growth rate is dominant at all temperatures.

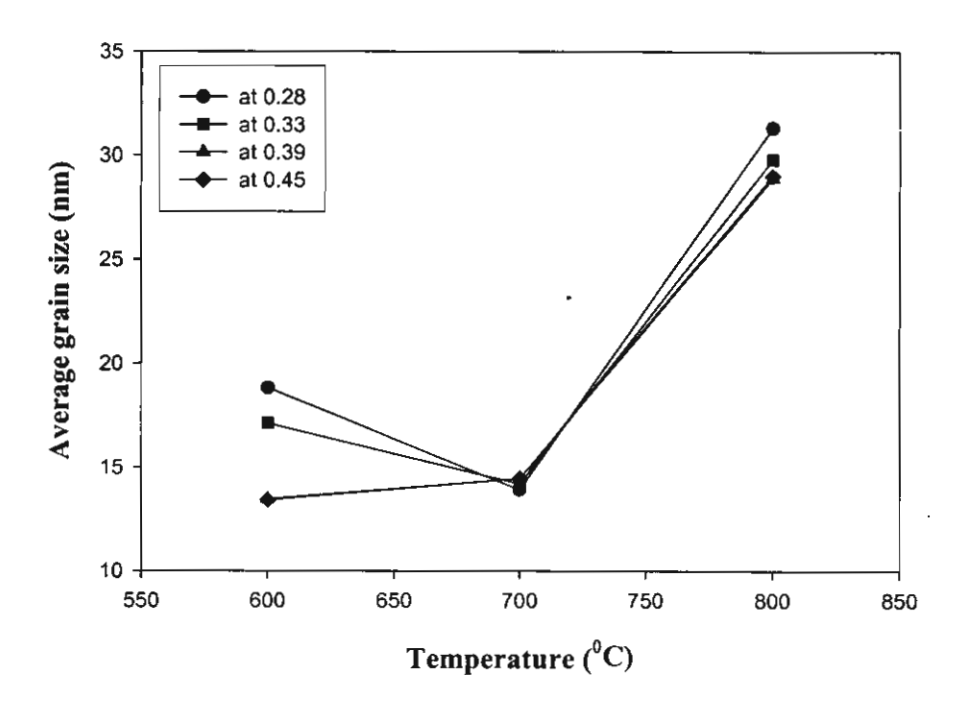


Figure 4 The average grain sizes of the particles prepared at different volume ratios of HCl:H<sub>2</sub>O (0.28, 0.33, 0.39, 0.45, respectively) and different calcination temperatures (600°, 700° and 800°C).

Coincidentally, the nitrogen adsorption-desorption isotherm of the material obtained at 0.28 HCl:H<sub>2</sub>O volume ratio and calcined at 600°C for 2h indicates a mesoporous structure, as seen in figure 5(a). The isotherm is of type IV, characteristic

of mesoporous material. The hysteresis loop exhibited by the specimen is mainly of type H2. The pore size distribution in figure 5(b) shows a major porosity in the range of 4-18 nm. To confirm an increase in crystallinity as temperature increases, specific surface area measurements were carried out and, as expected, we find that the higher the calcined temperature, the lower the specific surface area. The powders become dense and predominantly nonporous when the precursor is calcined at  $800^{\circ}$ C. It is known that a lower acid concentration results in a higher specific surface area due to an increasing in the cross-linking level<sup>3</sup>. This is consistent with our observation that the specific surface area decreases in the following order; 0.28 > 0.33 > 0.39 > 0.45 (Table 1). It can be concluded that sol-gel processing indeed provides a larger specific surface area which decreases with increasing calcinations temperature and acid concentration.

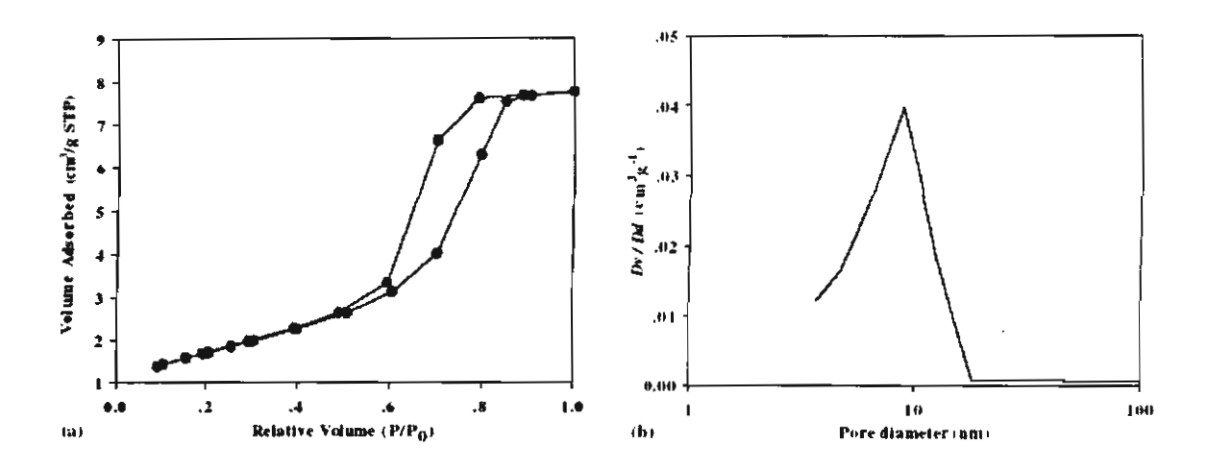


Figure 5 The nitrogen adsorption-desorption isoterm for mesoporous titania (a.) and Pore size distribution (b.) for the material obtained from 0.28 HCl:H<sub>2</sub>O volume ratio and calcined at 600°C

**Table 1** BET surface area (S<sub>BET</sub>, m<sup>2</sup>/g) of titania at various HCl:H<sub>2</sub>O volume ratios and calcinations temperatures.

Town or other (9C)	Surface area (m <sup>2</sup> /g)/ HCl:H <sub>2</sub> O			
Temperature (°C)	0.28	0.33	0.39	0.45
600	125	111	107	105
700	60	59	55	50
800	20	18	17	15

<sup>\*</sup> Surface area of the starting material  $TiO_2 = 20 \text{ m}^2/\text{g}$ 

The particle morphology of the samples obtained using a  $HCl:H_2O$  ratio of 0.33, when calcined at temperatures in the range 600°-800°C, is shown in Fig. 6. At the lowest two temperatures, Figs. 6(a) and 6(b), the material consists of particles of large size, whereas the micrograph (Fig. 6c) of the material calcined at 800°C shows a finely-divided morphology in the anatase form consisting of spherical particles approximately 1  $\mu$ m in size.

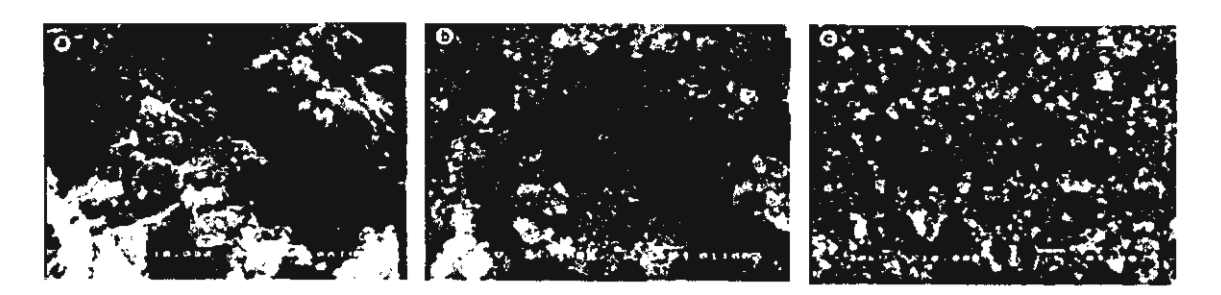


Figure 6 SEM micrographs of titania powder prepared at 0.33 volume ratio of HCl:H<sub>2</sub>O and calcined at a.) 600°, b.) 700° and c.) 800°C

Viscoelastic studies of the four different gelling systems (volume ratios of 0.28, 0.33, 0.39, and 0.45 of HCl:H<sub>2</sub>O, respectively) were carried out using the criteria proposed by Winter and Chambon<sup>15</sup> to determine the gel point, as the gelation time where a frequency-independent value of tan $\delta$  in observed. The variation in the frequency-dependence of tan $\delta$  with gelation time is shown in fig. 7, and indeed indicates tan $\delta$  become frequency independent at a particular gelation time. The shortest gelation time was observed for the system at 0.28 volume ratio (365 s) and the longest gelation time for the system of 0.45 volume ratio (870 s). An alternative method<sup>16</sup> to determine the gel point is to plot the time evolution of the apparent viscoelastic exponents n' and n'' obtained from the frequency-dependence of the modulus (G'  $\propto \omega^{n'}$ , G''  $\propto \omega^{n'}$ ), as shown in fig. 8 for the system at 0.45 volume ratio. The gel point is identified as the time where a crossover n'=n'=n is observed. The points of intersection (t<sub>gel</sub>) are found to be the same as those deduced from the plot of tan $\delta$  versus time.

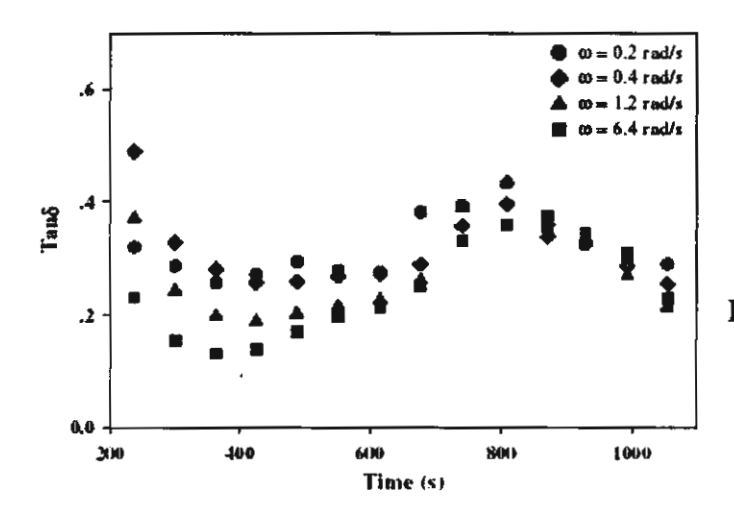
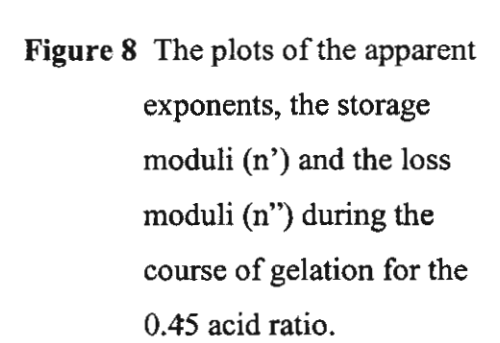
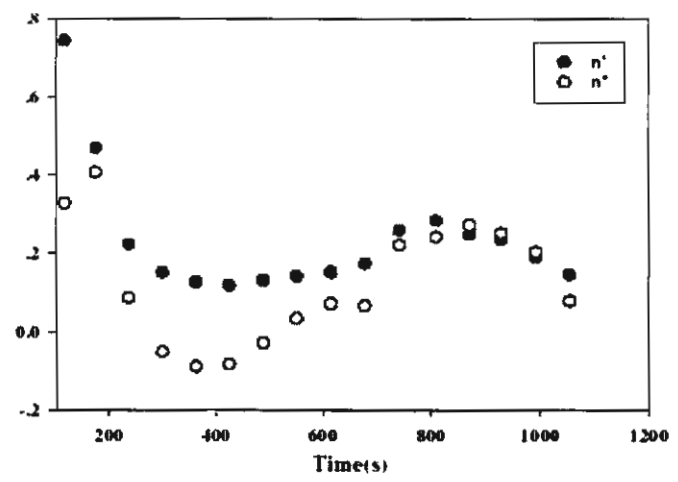


Figure 7 The plots of tanδ with time(s) at HCl:H<sub>2</sub>O volume ratio of 0.45





It is important to note that these gelling systems are highly elastic even well before the gel point, as evidenced by the fact that  $\tan \delta << 1$ . Also, the system rheology evolves relatively slowly in the vicinity of the gel point, as seen by plotting the frequency dependence of G' (Pa), G" (Pa) at pregel .stage, gel point, and postgel stage, shown in fig. 9. The data are shifted horizontally by a factor B. A similar trend is observed for all systems in that G' is higher than G", i.e. elastic behavior predominates before as well as after the gel point. We attribute this behavior to the fact that we are dealing with a concentrated colloidal dispersion, which is converted to a gel by hydrolysis from the outer surfaces of the colloidal particles. Despite this heterogeneous structure, at the gel point, the systems fulfill the Winter criteria that n'=n''=n<sub>gel</sub>, and  $\tan \delta = \tan(n_{gel}\pi/2)$  are superimposed<sup>15-19</sup>. The viscoelastic exponent  $n_{gel}$  of the system as shown in table 2 has its highest value at 0.45 volume acid ratio and the value decreases as the volume acid ratio decreases. Figure 10 shows the effect of HCl:H<sub>2</sub>O volume ratio

on the gel strength parameter, S, evaluated from the relationship<sup>16-19</sup> G'( $\omega$ ) =  $\Gamma$ (1-n)cos(n $\pi$ /2)S $\omega$ <sup>n</sup> where  $\Gamma$ (1-n) is the Legendre  $\Gamma$  function. It is evident that the gel strength increases with increasing acid ratio and reaches its highest value acid ratio = 0.39, then decreases slightly. Thus, at low acid ratio, the critical gel cluster is relatively weak, at high acid ratio it is stronger.

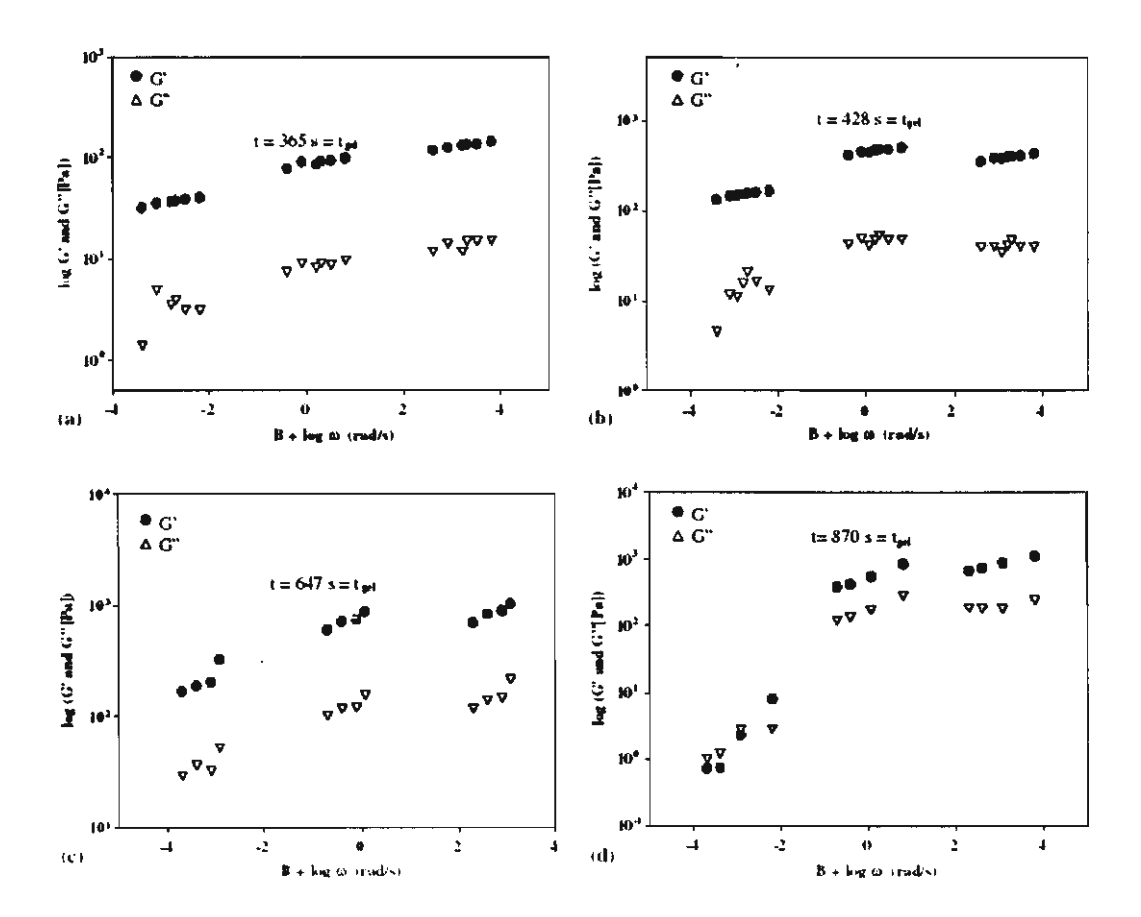
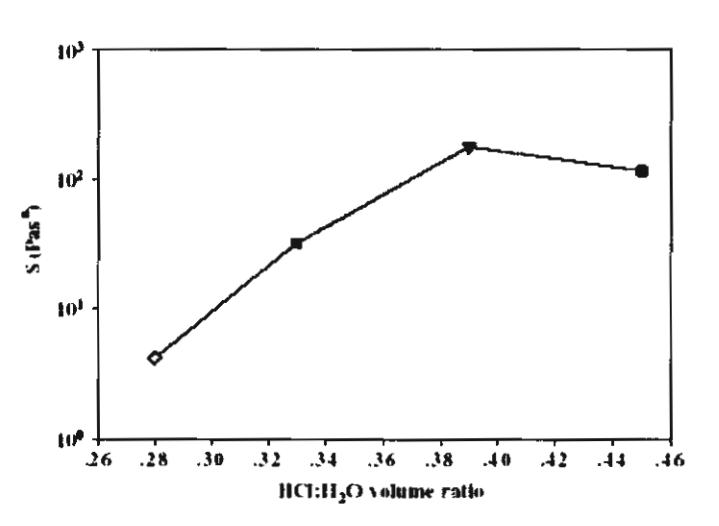


Figure 9 The frequency dependence curves of G' ( $\omega$ ) and G'' ( $\omega$ ) at ( $\bullet$ ) pregel stage(B = -3),( $\blacksquare$ ) gel point,and (B = 0),and ( $\triangle$ ) postgel stage (B = 3) of a.) 0.28, b.) 0.33, c.) 0.39 and d.) 0.45 HCl:H<sub>2</sub>O ratios.

Figure 10 The plot of gel strength parameter S at the gel point as a function of HCl:H<sub>2</sub>O volume ratio: 0.28 (♠), 0.33 (■), 0.39(♠) and 0.45 (♠).



According to the model of Muthukumar<sup>20</sup> the fractal dimension of the critical gel cluster can be obtained from the viscoelastic exponent n as  $n = d(d+2-2d_f)/2(d+2-d_f)$  where d = spatial dimension = 3. The effect of acid ratio on the fractal dimension of incipient gel is shown in fig. 11 and table 2. The fractal dimension decreases with increasing the acid ratio. A lower fractal dimension mean that the molecular weight grows slower with radius, i.e.  $M \sim R^{d_f}$ . Thus the critical gel at high acid ratio has a more open structure than at low acid ratio. This is somewhat surprising since we expect the cross-link density to be higher at higher acid ratio. Again we attribute this result to the heterogeneous character of the system\_at the gel point. The particles which comprise the gel network at low acid ratio are less hydrated and hence more dense than those at higher acid ratio.

Figure 11 The plot of fractal dimension of the critical gel ccluster as a function of acid ratio

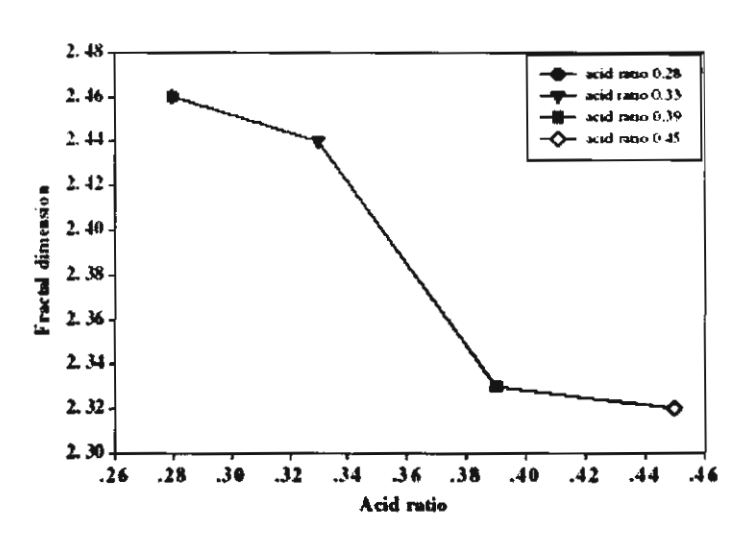


Table 2 Summary of viscoelastic exponent, fractal dimension, and gelation time(s) at various HCl:H<sub>2</sub>O volume ratios.

Acid ratio	n	df	Gelation time (s)
0.28	0.05	2.46	365
0.33	0.07	2.44	428
0.39	0.19	2.33	647
0.45	0.20	2.32	870

Figure 1? shows the frequency dependence of the dynamic viscosity at pregel stage, gel point, and postgel stage. Consistent with the highly elastic behavior evident in figure 9, at all stages  $\eta^*(\omega)$  exhibits power law frequency dependence with an exponent at the gel point of n-1. The time dependence of the complex viscosity at low frequency  $(\omega=0.4 \text{ rad/s})$  is illustrated in fig. 13. The location of the gel point for each system as determined by the Winter criteria 16-19 are indicated by arrows. At low acid ratio, the viscosity is initially high but approaches an asymptotic value which is relatively low. At high acid ratio, the viscosity is initially low but reaches a high asymptotic value. Thus, the gel strength and asymptotic complex viscosity are self-consistent and indicate that the gel becomes stronger under high acidity conditions. We interpret these results as indicating that at low acid, the precursor particles are poorly hydrated and form a more heterogeneous weak gel structure. At high acid, the particles are well solvated and form a less heterogeneous (more open) yet stronger network.

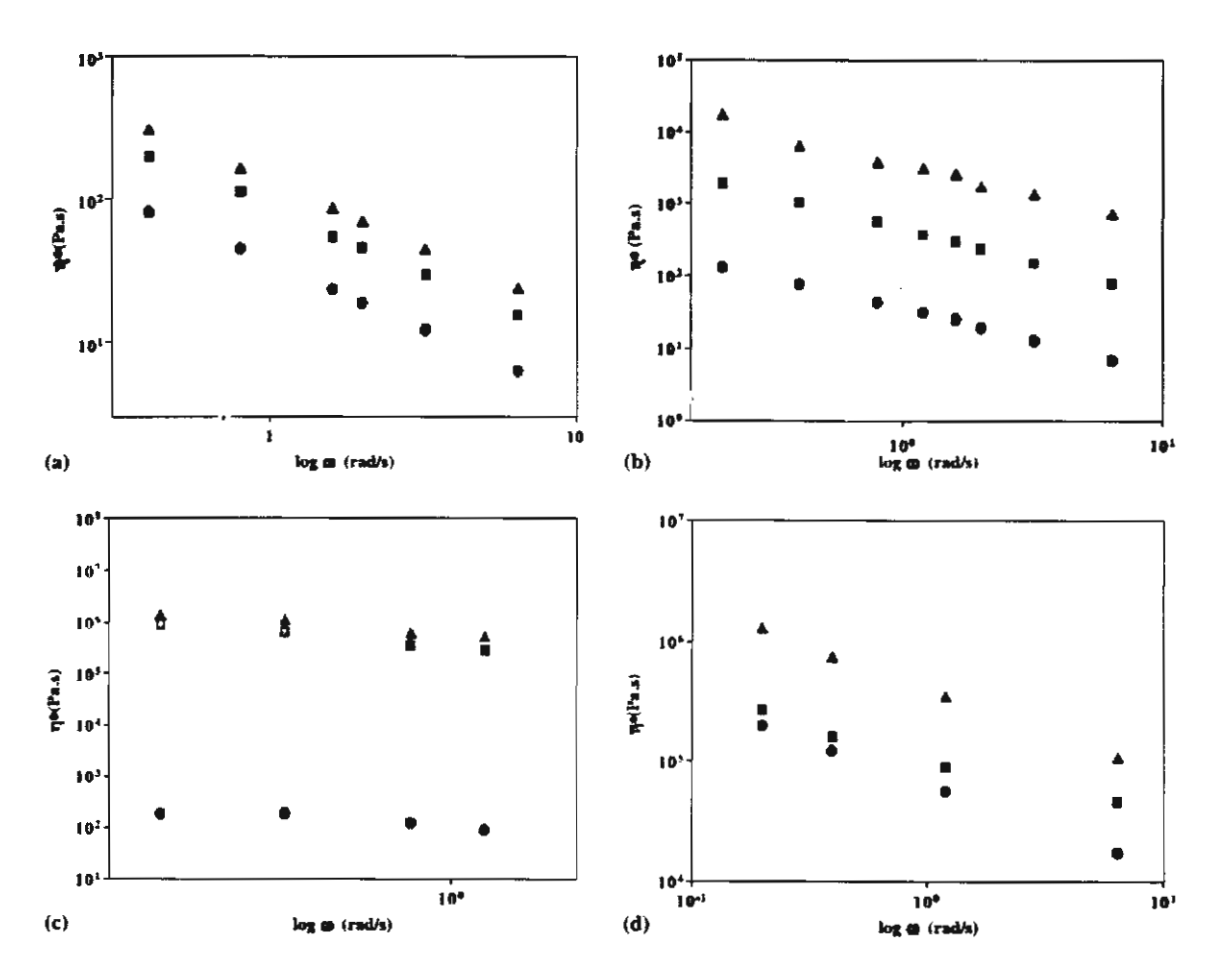


Figure 12 The effect of frequency on the complex viscosity at pregel stage, gel point, and postgel stage of a.) 0.28, b.) 0.33, c.) 0.39 and d.) 0.45 HCl:H<sub>2</sub>O volume ratios

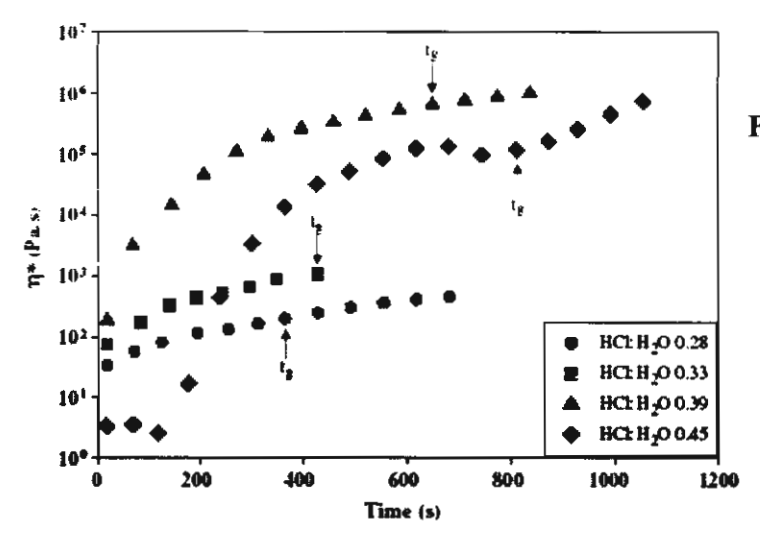


Figure 13 The time evolution of the complex viscosity (at fixed frequency of 0.4 rad/s) of a) 0.28, b) 0.33, c) 0.39 and d) 0.45 HCl:H<sub>2</sub>O volume ratio

#### Conclusions

Anatase TiO<sub>2</sub> nanoparticles were successfully prepared by sol-gel technology, using inexpensive and moisture-stable titanium glycolate as precursor in 1M HCl solution. The calcination temperature and the HCl:H<sub>2</sub>O volume ratio has a substantial influence on the surface area, phase transformation, and morphology of the products. Anatase titania is produced at calcination temperatures in the range 600° to 800°C, above which transformation to rutile occurs. Increase of temperature results in anatase of higher crystallinity but lower specific surface area, and induces a morphological change from large irregular agglomerates to more homogeneous particles of spherical shape. From XRD measurements of average grain sizes, we deduce that nucleation rate dominates the kinetics at low temperatures, and growth rate becomes the controlling factor at high temperature and low HCl:H2O ratios. Increase of HCl:H2O ratio results in a small but significant decrease in porosity. The highest specific surface area 125 m<sup>2</sup>/g is obtained at lowest HCl:H<sub>2</sub>O ratio 0.28 and lowest calcination temperature (600°C). From rheological analysis, as evaluated by the Winter criteria, the gelation time increases with increase of HCl:H2O volume ratio. The fractal dimension determined from the frequency scaling exponent of the modulus at the gel point indicates a denses critical gel structure at low acid ratio. However the complex viscosity and gel strength increase as a function of acid ratio. We interpret this behavior as indicative that, at low acidity, the gel is composed of poorly hydrated particles forming a dense but weak structure. Increased acidity increases hydration and cross-link density leading to a more open and stronger gel network.

#### References

- 1. J. Yang, S. Mei, J.M. Ferriera, Mat. Sci. Eng. C-Biomim 15 (2001) 183.
- 2. H. kominami, M. kohno, Y. Takada, M. Inoue, T. Inui, Y. Kera, Ind. Eng. Chem. Res. 38 (1999) 3931.
- K.M.S. Khalil, T. Baird, M.I. Zaki, A.A. El-Samahy, A.M. Awad, Colloid Surface A 132 (1998) 31.
- 4. K.M.S. Khalil, M.I. Zaki, Powder Technol. 120 (2001) 256.
- 5. Y. Zhang, A. Weidenkaff, A. Reller, Mater. Lett. 54 (2002) 375.
- 6. Y. Wei, R. Wu, Y. Zhang, Mater. Lett. 41 (1999) 101.
- 7. Y. Sun, A. Li, M. Qi, L. Zhang, X. Yao, Mat. Sci. Eng. B86 (2001) 185.

- 8. E.J. Kim, S.H. Hahn, Mater. Lett. 49 (2001) 244.
- M. Wu, G. Lin, D. Chen, G. Wang, D. He, S. Feng, R. Xu, Chem. Mater. 14 (2002) 1974.
- 10. Kao, S.N. Bhattacharya, J. Rheol. 42 (1998) 493.
- 11.N. Phonthammachai, T. Chairassameewong, E. Gulari, A.M. Jamieson, S. Wongkasemjit, J. Met. Mat. Min. 12 (2002) 23.
- 12. Q. Zhang, L. Gao, J. Gac, Appl. Catal. B-Solid 26 (2000) 207.
- 13. Y. Zhang, A. Weidenkaff, A. Reller, Mater. Lett. 54 (2002) 375.
- 14. J. Zhao, Z. Wang, L. Wang, H. Yang, M. Zhao, Mater. Chem. Phys. 63 (2000) 9.
- 15. H.H. Winter, F. Chambon, J. Rheol. 30 (1986) 367.
- 16. A.L. Kjoniksen, B. Nystrom, Macromolecules 29 (1996) 5215.
- 17. M. Jokinen, E. Gyorvary, J.B. Rosenholm, Colloid Surface A 141 (1998) 205.
- 18. B. Nystrom, A.L. Kjonoksen, B. Lindman, Langmuir 12 (1996) 3233.
- W. Charoenpanijkarn, M. Suwankruhasn, B. Kesapabutr, S. Wongkasemjit,
   A.M. Jamieson, Eur. Ploym. J 37 (2001) 1441.
- 20. Muthukumar, M, Macromocules 22 (1989) 4656.

#### **CHAPTER VI**

# STRUCTURAL AND CRYSTALLIZATION OF HIGH Ti LOADED TS-1 ZEOLITE

#### Abstract

The TS-1 with high Ti loading was successfully synthesized using low cost and moisture-stable precursors, titanium glycolate and silatrane. The microwave instrument was used as a heating source for synthesis. The effects of the compositions (TPA<sup>+</sup>, NaOH, H<sub>2</sub>O) and conditions (aging time, reaction temperature, reaction time) were studied. The Si:Ti molar ratios were varied from 100.00-5.00 and the ability of Ti incorporated into the zeolite framework was studied. The XRD, FT-IR, SEM and DR-UV were used to characterize the TS-1 samples and all samples showed the characteristic of MFI type. The small amount of extra-framework titanium dioxide was also identified at 5.0 Si:Ti molar ratio. The photocatalytic decomposition of 4-NP was used to test the activity of TS-1 samples and the results of all samples showed high efficiency in photocatalytic decomposition (PCD).

#### Introduction

Titanium silicate-1 (TS-1), a Ti-containing zeolite with the MFI structure, is a highly selective and active crystalline microporous heterogeneous oxidation catalyst employing H<sub>2</sub>O<sub>2</sub> under mild conditions. The titanium in TS-1 isomorphously replaces silicon in a tetrahedral site of the MFI silicate lattice. It combines the advantages of the high coordination ability of Ti<sup>4+</sup> ions with the hydrophobicity of the siliate framework, while retaining the spatial selectivity and specific local geometry of the active sites of the molecular sieve structure<sup>1</sup>. The catalytic properties of titanosilicate are unique with a variety of liquid-phase oxidation, such as phenol hydroxylation, olefin epoxidation, cyclohexanone ammoximation and the oxidation of saturated hydrocarbons and alcohol<sup>2-3</sup>. With H<sub>2</sub>O<sub>2</sub>, solvolysis produces TiOOH and SiOH with the former giving rise to the active catalytic oxidation center.

After year 1983 which Taramasso et al <sup>4</sup> reported the hydrothermal synthesis of TS-1 for the first time, there are many researches tried to increase the amount of Ti<sup>IV</sup> in the zeolite framework. A major problem often encountered the synthesis of TS-1 molecular sieve is the precipitation of oxide of the titanium outside the lattice framework, leading to samples, inactivity for oxidation reactions<sup>5</sup>. The synthesis of materials containing isolated tetrahedral Ti is rather difficult, given its strong tendency to polymerize in aqueous systems which often resulting in the formation of separate titanium dioxide phase<sup>1</sup>. Two methods to synthesize were described in the original patent using different Si sources, tetraethylorthosilicate (TEOS) and Ludox colloidal silica. TS-1 is usually synthesized using tetrapropylammonium hydroxide (TPAOH) solution, which acts as the structure directing agent and provides the alkalinity necessary for the crystallization of the zeolite<sup>6</sup>. From many previous works, maximum amount of Ti<sup>IV</sup> that can incorporated in the zeolite framework is at Si:Ti less than 35<sup>1,3,6</sup>.

Microwave-assisted-hydrothermal synthesis is the process has been used for the rapid synthesis of numerous ceramic oxides and porous materials. It offers many advantages over conventional synthesis, including the increase of temperature of the reactant to a desired range quickly in a few minutes, homogeneous nucleation, fast supersaturation by the rapid dissolution of precipitated gels and shorter crystallization time. The heat is supposedly induced by the friction of molecular rotation enhanced by microwave irradiation, thus, it is possible to heat the reactants selectively and homogeneously from inside. Furthermore, It is energy efficient and economical<sup>7-8</sup>.

In this work, we synthesized the TS-1 zeolite from moisture stable and low cost starting materials, silatrane and titanium glycolate, used for silica and titanium dioxide sources, and TPABr as a template. The hydrothermal treatment by microwave heating and various amounts of Ti incorporated in the zeolite framework were studied. The samples were characterized using XRD, SEM, FT-IR and DR-UV. The photocatalytic decomposition of 4-NP was used to test the activity of TS-1 samples.

# **Experimental**

#### Materials

Titanium dioxide (surface area 12 m²/g) was purchased from Sigma-Aldrich Chemical Co. Inc. (USA) and used as received. Ethylene glycol (EG) was purchased from Malinckrodt Baker, Inc. (USA) and purified by fractional distillation at 200°C under nitrogen atmosphere, before use. Triethylenetetramine (TETA) was purchased from Facai Polytech. Co. Ltd. (Bangkok, Thailand) and distilled under vacuum (0.1 mm/Hg) at 130°C prior to use. Acetonitrile was purchased from Lab-Scan Company Co. Ltd. and purified by distilling over calcium hydride powder. 4-Nitrophenol was purchased from Sigma-Aldrich Chemical Co. Inc. (USA).

#### Instrumental

Fourier transform infrared spectra (FT-IR) were recorded on a VECOR3.0 BRUKER spectrometer with a spectral resolution of 4 cm<sup>-1</sup> using transparent KBr pellets containing 0.001 g of sample mixed with 0.06 g of KBr. Thermal gravimetric analysis (TGA) was carried out using a Perkin Elmer thermal analysis system with a heating rate of 10°C/min over 30°-800°C temperature range.

# Preparation of titanium glycolate

The procedure adopted followed previous work<sup>9</sup>. A mixture of TiO<sub>2</sub> (2g, 0.025 mol) and TETA (3.65g, 0.0074 mol) was stirred vigorously in excess EG (25 cm<sup>3</sup>) and heated to 200°C for 24 h. The resulting solution was centrifuged to separate the unreacted TiO<sub>2</sub>. The excess EG and TETA were removed by vacuum distillation to obtain a crude precipitate. The white solid product was washed with acetonitrile, dried in a vacuum desiccator and characterized using FTIR and TGA.

FTIR: 2927-2855 cm<sup>-1</sup> (vC-H), 1080 cm<sup>-1</sup> (vC-O-Ti bond), and 619 cm<sup>-1</sup> (vTi-O bond). TGA: one sharp transition at 340°C with 46.95% ceramic yield corresponding to Ti(OCH<sub>2</sub>CH<sub>2</sub>O)<sub>2</sub>.

# Preparation of silatrane<sup>9</sup>

A mixture of Si(OH)<sub>2</sub> (6g, 0.1 mol) and TEA (18.648g, 0.125 mol) was stirred vigorously in excess EG (100 cm<sup>3</sup>) and heated to 200°C for 10 h. The resulting solution was vacuumed to remove EG to obtain a crude precipitate. The white solid product was washed with acetonitrile, dried in a vacuum desiccator and characterized using FTIR and TGA.

Fi-IR: 3422 cm-1 ( $\nu$  O-H), 2986-2861 cm-1 ( $\nu$  C-H), 2697 cm-1 ( $\nu$  N-Si), 1459-1445 cm-1 ( $\delta$  C-H), 1351 cm-1 ( $\delta$  C-N), 1082 cm-1 ( $\delta$  Si-O-C), 579 cm-1 ( $\nu$  N-Si). TGA: one sharp transition at 380°C with 21.6% ceramic yield corresponding to N[CH<sub>2</sub>CH<sub>2</sub>O]<sub>3</sub>SiOCH<sub>2</sub>CH<sub>2</sub>N(CH<sub>2</sub>CH<sub>2</sub>OH)<sub>2</sub>.

# Preparation of TS-1 zeolite

Hydrothermal syntheses were carried out using microwave irradiation. The TS-1 initial solution molar composition of gel SiO<sub>2</sub>:0.1TiO<sub>2</sub>:0.1TPA<sup>+</sup>:0.4NaOH:114H<sub>2</sub>O. The effects of conditions were studied by varying the aging time (20, 60, 70, 90, 110, 130, 150, 170h), reaction time (5, 10, 15, 20h) and reaction temperature (120, 150, 180°C), amounts of TPA<sup>+</sup>, NaOH and H<sub>2</sub>O. study of the Ti incorporated in the zeolite framework,  $SiO_2:xTiO_2:0.3TPA^+:0.4NaOH:114H_2O$  ( x = 0.1, 0.3, 0.5, 0.7, 1.0, 1.3, 1.7,2.0) was used. The solution was then aged at room temperature for 110h. After aging, the solution was transferred into Teflon vessel and heated under microwave irradiation at 150°C for various reaction times. The obtained TS-1 zeolite was washed several times with distilled water, dried at 60°C overnight and calcined at 550°C for 2h (0.5°C/min).

### Photocatalytic decomposition of 4-nitrophenol

Photocatalytic reactions were carried out in a 250 ml batch reactor with a gas inlet and outlet at the flow rate of O<sub>2</sub> gas 20 ml/min. The cooling water jacket was used to control the temperature at 30°C. The suspensions were illuminated by using a Hg Philip UV lamp. The concentration of 4-NP was 40 ppm and the solution was continuous magnetically stirred. The TS-1 zeolite prepared at Si/Ti molar ratios of 100.00, 14.29, 7.69 and 5.00 was added in the solution with 0.8 g/l of catalyst, 10

mmol/l H<sub>2</sub>O<sub>2</sub> was then slowly dropped. The samples were taken out and analyzed the concentration of 4-NP using Shimadzu UV-240 spectrophotometer.

#### TS-1 characterization

TS-1 samples were characterized by various techniques. XRD patterns were characterized using a D/MAX-2200H Rigaku diffractometer with CuKα radiation on specimens prepared by packing sample powder into a glass holder. The diffracted intensity was measured by step scanning in the 2θ range between 5° to 50°. Fourier transform infrared spectra (FT-IR) were recorded on a VECOR3.0 BRUKER spectrometer with a spectral resolution of 4 cm<sup>-1</sup> using transparent KBr pellets containing 0.001 g of sample mixed with 0.06 g of KBr. Samples were prepared for SEM analysis by attachment to aluminum stubs, after pyrolysis at 550°C. Prior to analysis, the specimens were dried in a vacuum oven at 70°C for 5 h followed by coating with gold via vapor deposition. Micrographs of the pyrolyzed sample surfaces were obtained at x7,500 magnification. Diffuse reflectance ultraviolet-visible (DR-UV) spectra were analyzed

# **Results and Discussion**

## Synthesis of TS-1

TS-1 is successfully synthesized by microwave hydrothermal treatment using silatrane and titanium glycolate as precursors in the condition with NaOH and TPABr. The XRD pattern (figure 1) shows the characteristic of MFI structure as reported by many literatures  $^{1,3,10-11}$ . The single peaks at  $2\theta = 24.4^{\circ}$  indicate a change from monoclinic symmetry (silicate) to orthorhombic symmetry (TS-1) $^{1,12}$ . The FT-IR spectra of TS-1 in the framework Ti-O-Si bond stretching region shows an absorption band located at 960 cm $^{-1}$  (figure 2). This band has been also observed in Ti-containing zeolites, being mainly assigned to the stretching mode of [SiO<sub>4</sub>] tetrahedral bond with Ti atoms  $^{13-14}$ . However, such assignment has been interpreted in term of Si-OH groups with many defect structures  $^{15}$ . The bands at 550 and 800 cm $^{-1}$  are assigned to  $\delta$ (Si-O-Si) and  $\upsilon$ (Si-O-Si), respectively. The diffuse reflectance spectra as figure 3 shows only one absorption band with a maximum at 210 nm, attribute to tetra-coordinated titanium, and there is no peak at 330 nm which is the peak of titanium dioxide extra-framework.

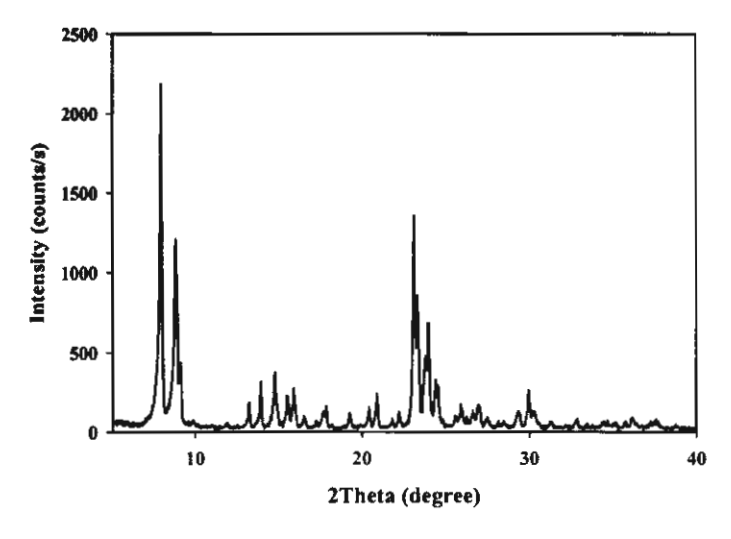


Figure 1 The XRD pattern of calcined TS-1 sample.

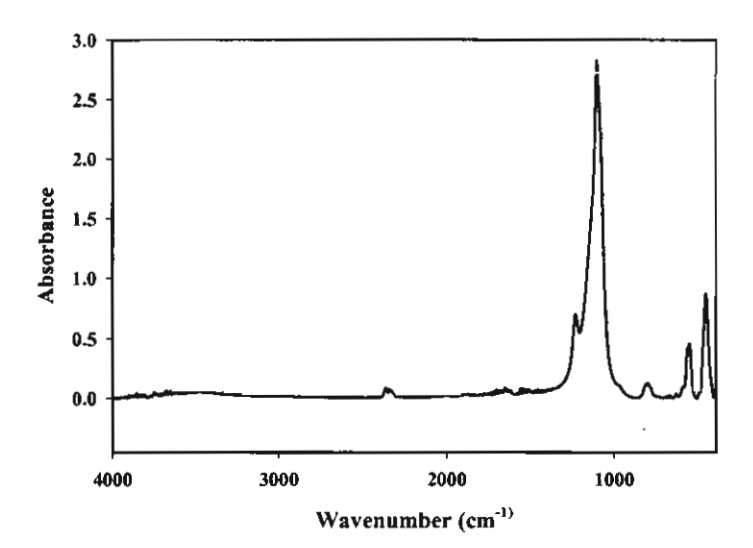


Figure 2 The FT-IR spectra of calcined TS-1 sample.

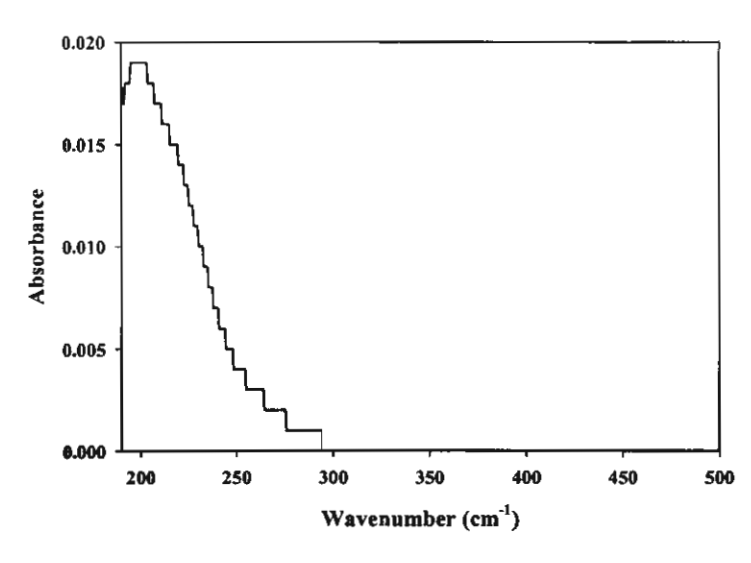


Figure 3 The DR-UV spectra of calcined TS-1 sample.

Effect of crystallization conditions and compositions of TS-1

1 Effect of reaction temperature

The effect of reaction temperature is studied by varying the temperature at 120°, 150° and 180°C. The synthesis formula is Si:0.1Ti:0.4NaOH: 0.1TPA:114H<sub>2</sub>O. Figure 4 shows the XRD patterns of all samples, the intensity of peak increases as the reaction temperature. Its mean that when increasing the reaction temperature lead to the higher rate of crystallization. From the SEM micrograph of calcined samples, the crystal size increases with the reaction temperature. At 120°C (figure 5.1), the crystals have round shape and not uniform (0.5-2.5µm). As increasing the temperature to 150°C (figure 5.2), the crystals are uniform with cubic structure (1.µm). The largest crystal size (4µm) is observed at 180°C (figure 5.3) and indicates larger growth in c direction with hexagonal shape. When rising the temperature to 180°C, the degradation of the organic template is occurred. From the result, the suitable reaction temperature for a smallest and uniformly crystal is at 150°C.

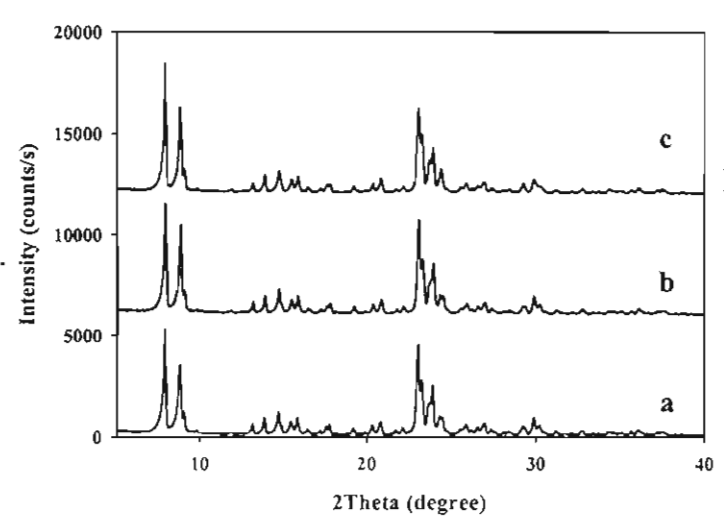


Figure 4 The XRD pattern of TS-1 samples at various reaction temperatures of a) 120°, b) 150° and c) 170°C.

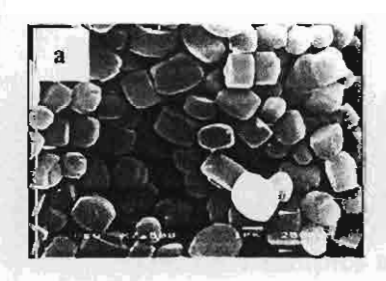






Figure 5. The SEM micrograph of TS-1 sample at various reaction temperatures of a) 120°, b) 150° and c) 170°C.

The Si:0.1Ti:0.4NaOH:0.1TPA:114H<sub>2</sub>O formula is used to study the effect of reaction time to the crystallization of TS-1 zeolite. The reaction times are varies from 5, 10, 15 and 20 h at reaction temperature 150°C. The results show that at low reaction time the amorphous phase occurs and the conversion to TS-1 zeolite is lower than at higher time. It is mean that increasing the reaction time causes the increasing of the rate of crystallization. The SEM micrograph (figure 6) shows the large crystal size (5µm) at 5h and the size decreases dramatically to 1.3µm at 15h, the crystals have uniformly cubic shape. Increasing the reaction time to 20 h causes the larger crystal size and has a higher growth in b direction.

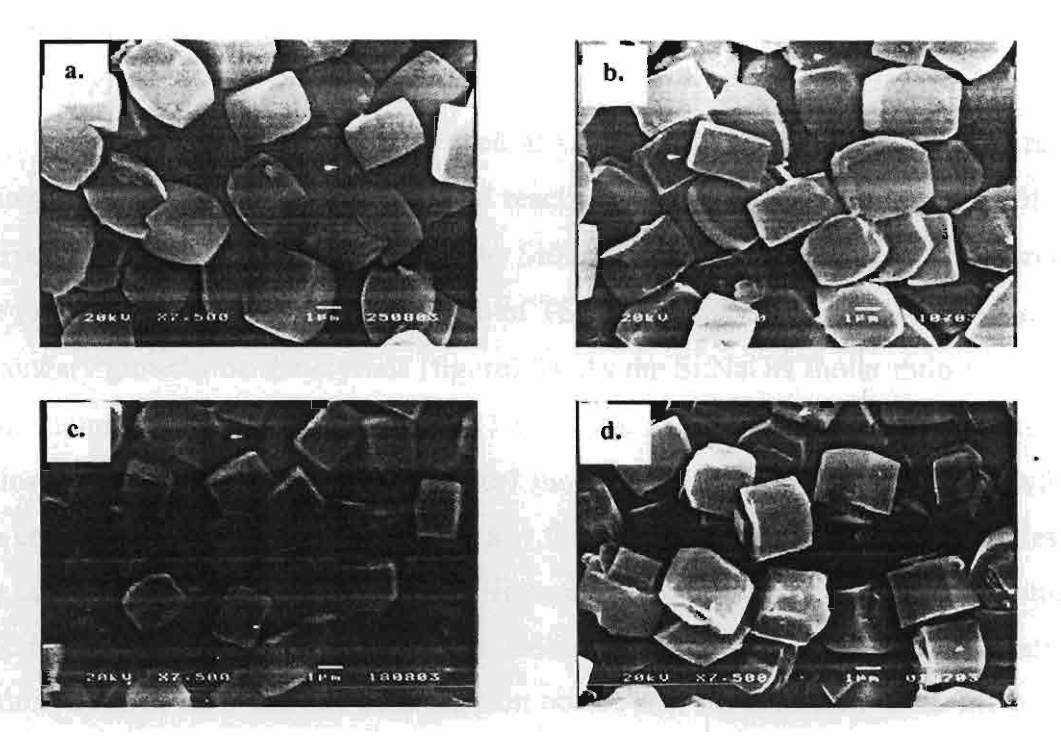


Figure 6. The SEM micrograph of TS-1 samples at various reaction times of a) 5, b) 10, c) 15 and d) 20h.

#### 3 Effect of Aging time

The TS-1 samples at varies aging times (20, 60, 70, 90, 110, 130, 150 and 170h) are carried out at Si:0.1Ti:0.4NaOH:0.1TPA:114H<sub>2</sub>O, reaction temperature 150°C and reaction time 15h. From the SEM micrographs in figure 7, at lower aging time, the large crystal sizes are formed with lower conversion to the TS-1 zeolite and present the large amount of amorphous phase. When the time increases, the crystal size becomes smaller until at aging time 130h the size increases again. The hydrolysis and condensation

reactions of silatrane and titanium precursors cause the polymerization to form the network and initially at low aging time the hydrolysis of precursor does not involve all the alkyl ligand, therefore, some organic ligands still present in the solution. The remaining organic ligand can participate with the organic template and form a primary unit, then the primary units are agglomerate and the nucleation occurs. At longer aging time, the large amount of primary particles occurs and results in the higher agglomeration and crystallization rate caused the smaller size with higher formation of zeolite after hydrothermal synthesis, which the growth rate is dominant. At longer aging time (130h), the limit of the primary unit formation occurs, therefore, the agglomeration occurs at the former nuclei.

## 4 Effect of NaOH:Si

The effect of NaOH:Si is studied at varying ratio from 0.1 to 1.0 mol ratio at aging time 110h, reaction time 15h and reaction temperature 150°C. At 0.1 mol ratio, the product is amorphous as shown in the SEM micrograph (figure 8). When increasing the ratio to 0.3, a very large crystal size of TS-1 zeolite is occurred (10µm) with many secondary growths on the crystals (figure 7.2). As the Si:NaOH molar ratio increases to 0.4, the uniform and smaller crystals (1.3 µm) are formed (figure 7.3). Increasing the ratios to 0.5 causes the larger size and 0.7 molar ratio has many secondary growths on the crystals (figures 7.4 and 7.5). Until at 1.0 molar ratio (figure 7.6), the particles loss the cubic shape. The increasing of NaOH causes the increasing in the concentration of reactive species available in solution for zeolite nucleation which NaOH accelerates the hydrolysis rate, after that the condensation occurs and starts to form a zeolite network with greater numbers of nuclei are generated and smaller particle size products are formed (0.3 molar ratio). At large amount of NaOH, the hydrolysis increases and the large crystals with secondary growths are formed (0.5 and 0.7 molar ratios). When increasing to a very high amount of NaOH, the sodium will efficiently occupy the surface of the silica gel particles cause the retardation of the nucleation because the TPA-Silica interaction is greatly reduced. A large part of the silica is in the core of the gel bodies and not accessible for nucleation formation 16.

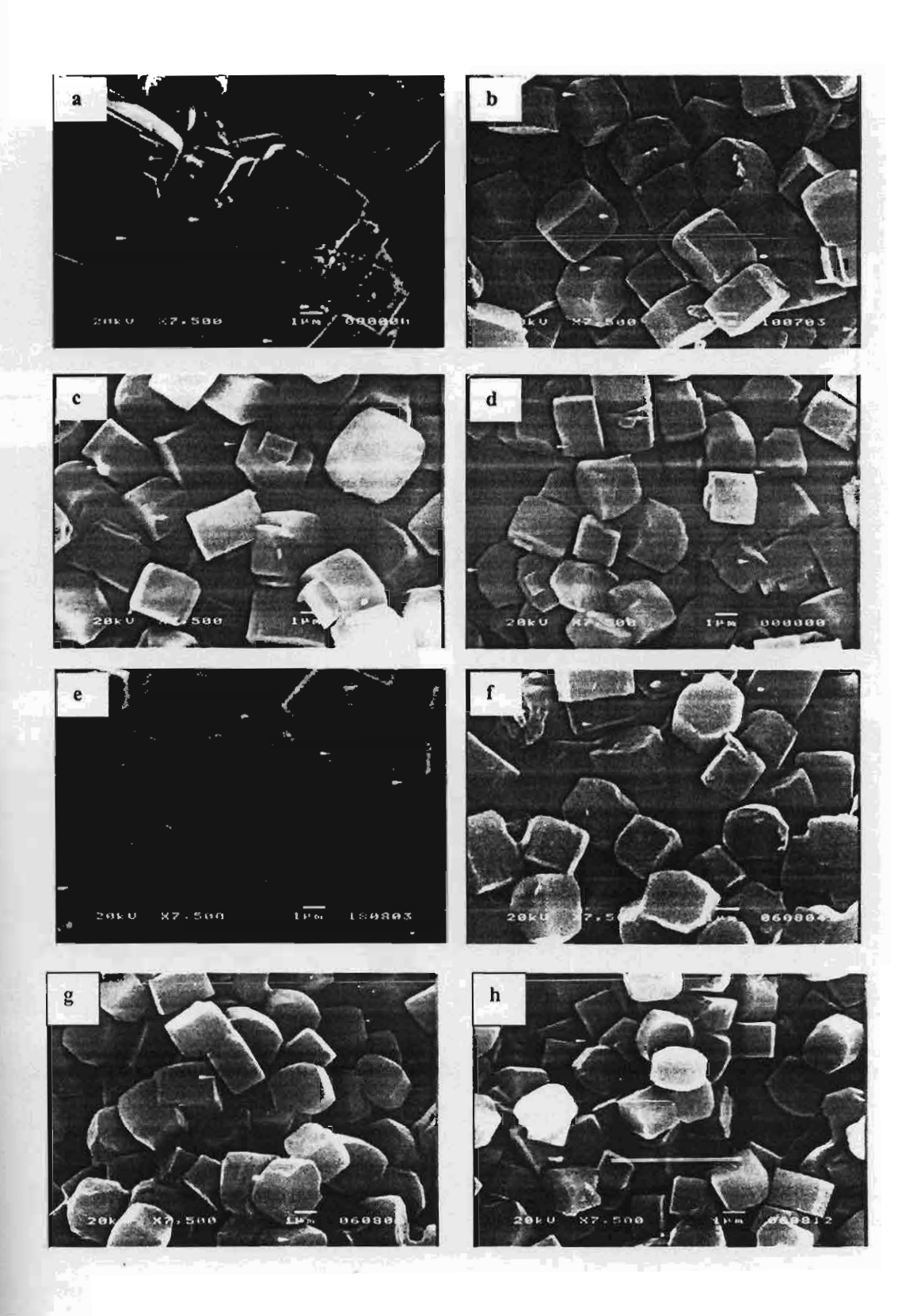


Figure 7. The SEM micrograph of TS-1 samples at various aging times of a) 20, b) 60, c) 70, d) 90, e) 110, f) 130, g) 150 and h) 170h.

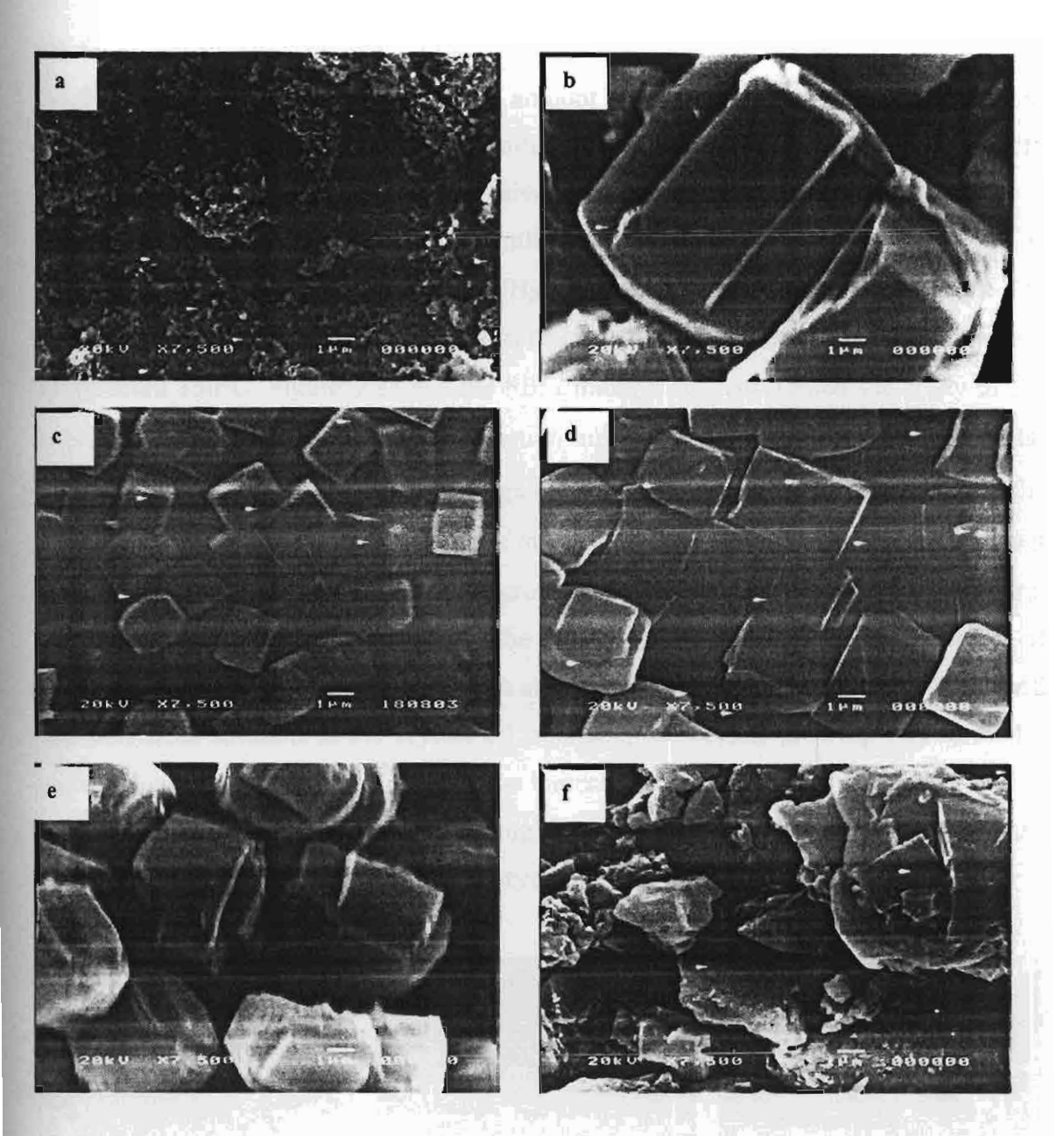


Figure 8. The SEM micrographs of TS-1 samples at various NaOH:Si molar ratios of a) 0.1, b) 0.3, c)0.4, d) 0.5, e) 0.7 and f) 1.0.

# 5 Effect of TPA:Si

The steric stabilization of nuclear-sized entities, is also critically dependent on the cation balance. The TPA<sup>+</sup> cation is widely used in the synthesizing of zeolite, the bulky quaternary ammonium cations adsorbed on to particle surfaces provide steric stabilization, preventing aggregation upon collision<sup>16</sup>. There are many types of template use for synthesize the zeolite such as TPAOH, TBABr, 1,6-hexanediamine and TPABr. Wang et al.<sup>6</sup> found that the synthesis by using TBABr will produce a favorable effect on

the formation of ZSM-11 and synthesize by 1,6-hexanediamine can use only for low titanium content which increasing the amount of titanium leads to a decrease of crystallinity. To decrease the cost of synthesis, TPAOH is replaced by TPABr. From many works TPABr showed a good selective oxidation reaction<sup>6,12</sup>.

In our work, TPABr is used to synthesize TS-1 zeolite and the effect of TPA<sup>+</sup> is studied at Si:0.1Ti:0.4NaOH: xTPA<sup>+</sup>:114H<sub>2</sub>O (x = 0.05, 0.1, 0.2, 0.3, 0.4 and 0.5). The crystallization conditions are at aging time 110 h, reaction time 15h and reaction temperature 150°C. Figure 9 shows the SEM micrograph represented the study of the effect of TPA<sup>+</sup>:Si at aging time 110h, reaction time 15h, 150°C and 0.4 Si:NaOH molar ratio. At low molar ratio (3.05), the large crystals are formed (10μm). Increasing the amount of TPA<sup>+</sup> causes the decreasing of the crystal size (1.2μm at 0.3 molar ratio) but at large amount of TPA<sup>+</sup>, the secondary growths occur (0.4 and 0.5 molar ratios). From the explanation of the Koegler *et al.*<sup>17</sup>, the nucleation starts to occur on the surface of the large gel sphere; both TPA<sup>+</sup> and silica are abundance, into the gel sphere. TPA<sup>+</sup> will transport from solution to the crystal/gel interface, the crystal growing and formed a perfected cubic shape. Its mean that if we increase the amount of TPA<sup>+</sup>, it will lead to the higher nucleation as shown here. At higher TPA<sup>+</sup>, the dendritic growth occurs at the surface of zeolite. This is indicative of very high supersaturation.

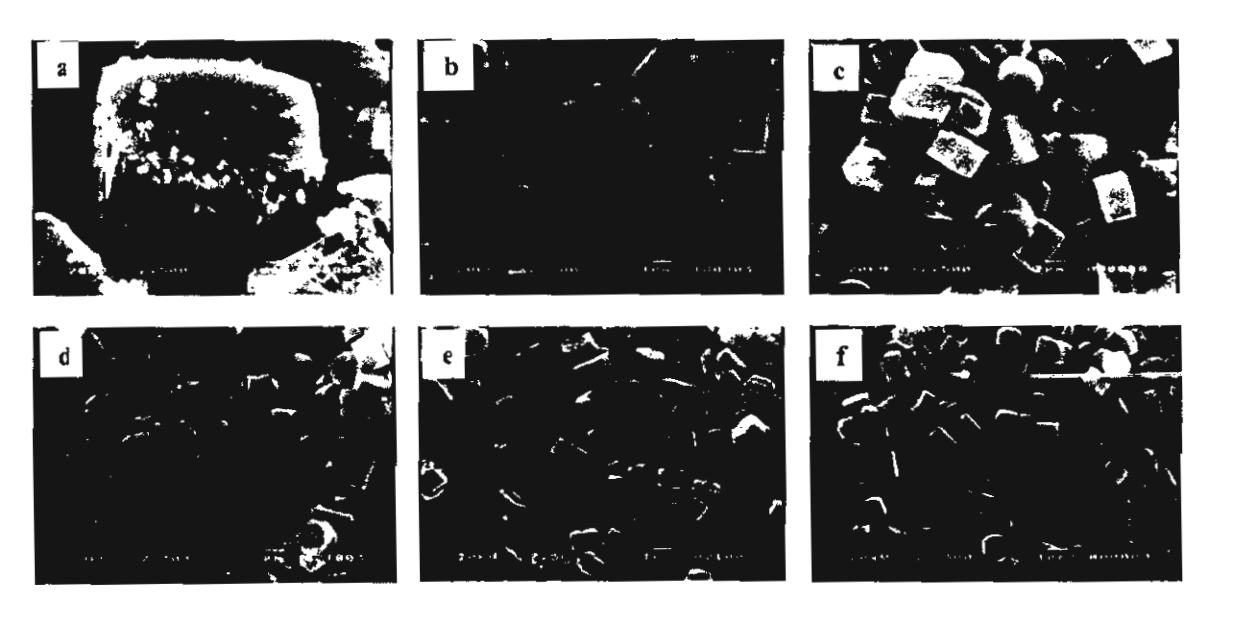


Figure 9. The SEM micrographs of TS-1 samples at various TPA:Si molar ratios of a) 0.05, b) 0.1, c) 0.2, d) 0.3, e) 0.4 and f) 0.5.

# 6 Effect of H<sub>2</sub>O:Si ratio

The dilution is studied at Si:0.1Ti:0.4NaOH:0.3TPA:xH<sub>2</sub>O (x = 80, 114, 140, 170 and 200). The reaction time is 15h, 150°C and aging time 110h. From the SEM micrograph as figure 10, at lower  $H_2O:Si$  shows a non-uniform crystal structure. As increasing the ratio to 114, the uniform and completely cubic structures are formed but when further increasing to higher ratio the crystal size are larger and have many defects.

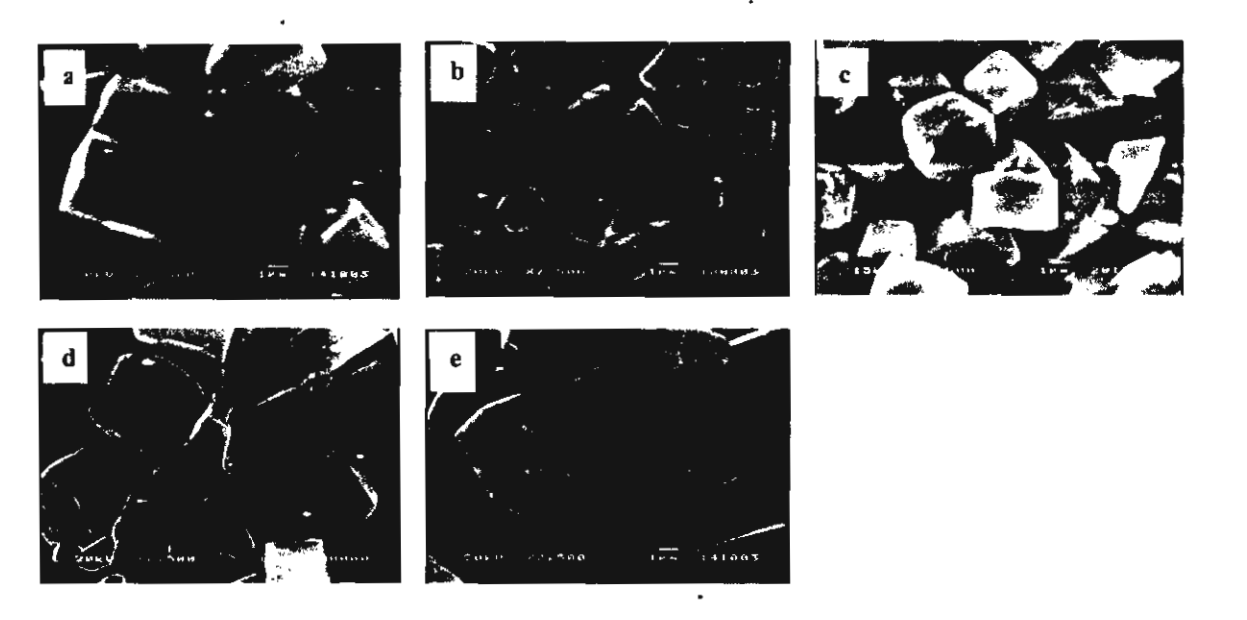


Figure 10. The SEM micrographsof TS-1 samples at various H<sub>2</sub>O:Si molar ratios of a) 80, b) 114, c) 140, d) 170 and e) 200.

# 7 Effect of Si:Ti ratio

The effect of Si:Ti on the crystallization of TS-1 is carry out at Si:xTi:0.4NaOH:0.3TPA:114H<sub>2</sub>O (x = 100.00, 33.33, 20.00, 14.29, 10.00, 7.69, 5.88 and 5.0). The reaction temperature is 150°C, aging time 110h and reaction times are varied from 15 to 35 h depending on the Ti loading (Table 1). We find that at high Ti loading, increasing the reaction time leads to the higher Ti incorporation. Figure 11 illustrates the FT-IR spectra of TS-1 samples A-H. The peak at 960 cm<sup>-1</sup> attributes to a stretching mode of an [SiO<sub>4</sub>] unit bonded to a Ti<sup>4+</sup> ion. (O<sub>3</sub>SiOTi)<sup>12</sup> represents the incorporation of titanium in the MFI framework. A strong band at 550cm<sup>-1</sup> is the characteristic of MFI structure<sup>8</sup>. The DR-UV spectra of the samples A-H are shown in figure 12. The strong peak at 210 nm has been assigned to the tetra-coordinate of titanium in the zeolite framework. The broad band peak at 280 nm indicates the partially

polymerized hexa-coordinated Ti species, which contain Ti-O-Ti and belong to a silicon-rich amorphous phase<sup>19</sup>. The band at 330 nm, which assigns to the extra-framework anatase phase, is shown as a little peak in sample H. The peaks at both 210 and 280 nm are increase from sample A to H as higher titanium content and the band shift to higher wavelengths at sample with lower Si/Ti ratio because of the higher proportion of hexa-coordinate species. The peak at 280 nm increases stronger than 210 nm at sample F that means the hexa-coordinated Ti species will form at higher titanium loaded. The SEM micrograph and XRD of TS-1 samples A-H are shown in figures 13 and 14, all of the samples show the characteristic of TS-1 zeolite with the MFI structure.

**Table1** The TS-1 samples at varies Si:Ti molar ratios and reaction time (h).

Sample	Si/Ti molar ratio	Reaction time (h)
a	100.00	15
b	33.33	15
c	20.00	20
d	14.29	25
e	10.00	- 25
f	7.69	35
g	5.88	35
h	5.00	35

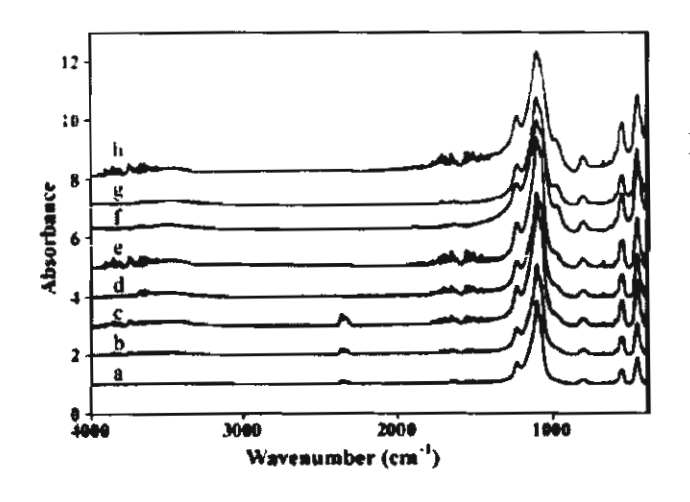


Figure 11 The FT-IR spectra of TS-1 sample at various Si:Ti molar ratios of a) 100.00, b) 33.33, c) 20.00, d) 14.29, e) 10.00, f) 7.69, g) 5.88 and h) 5.00.

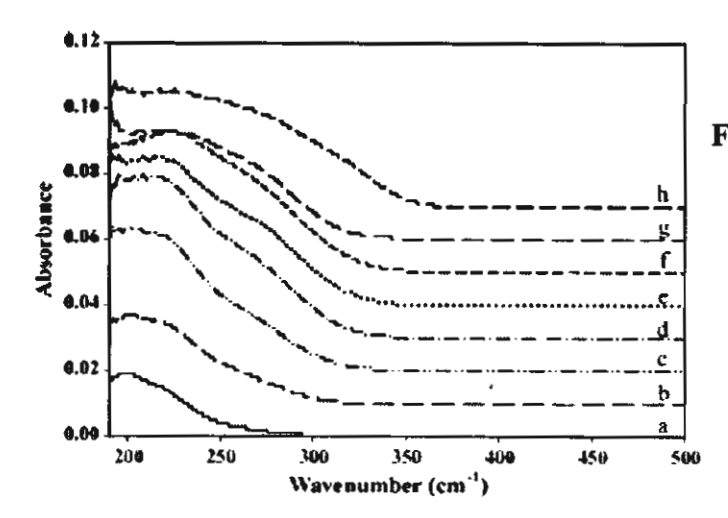


Figure 12 The DR-UV spectra of TS-1 sample at various Si:Ti molar ratios of a) 100.00, b) 33.33, c) 20.00, d) 14.29, e) 10.00, f) 7.69, g) 5.88 and h)

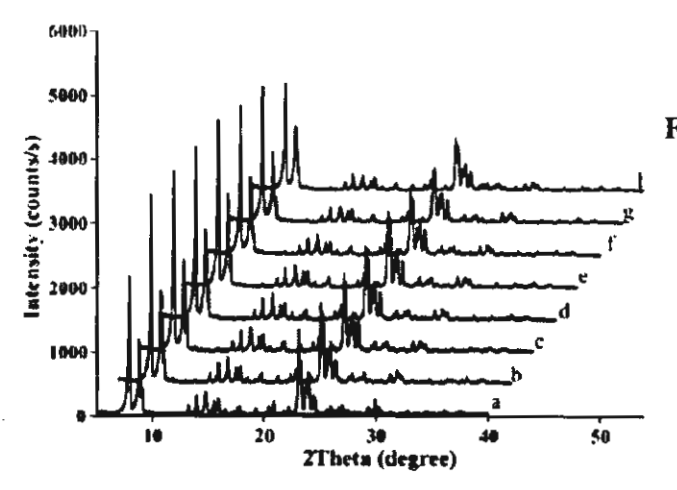


Figure 13 The XRD pattern of TS-1 sample at various Si:Ti molar ratios of a) 100.00, b) 33.33, c) 20.00, d) 14.29, e) 10.00, f) 7.69, g) 5:88 and h) 5.00.

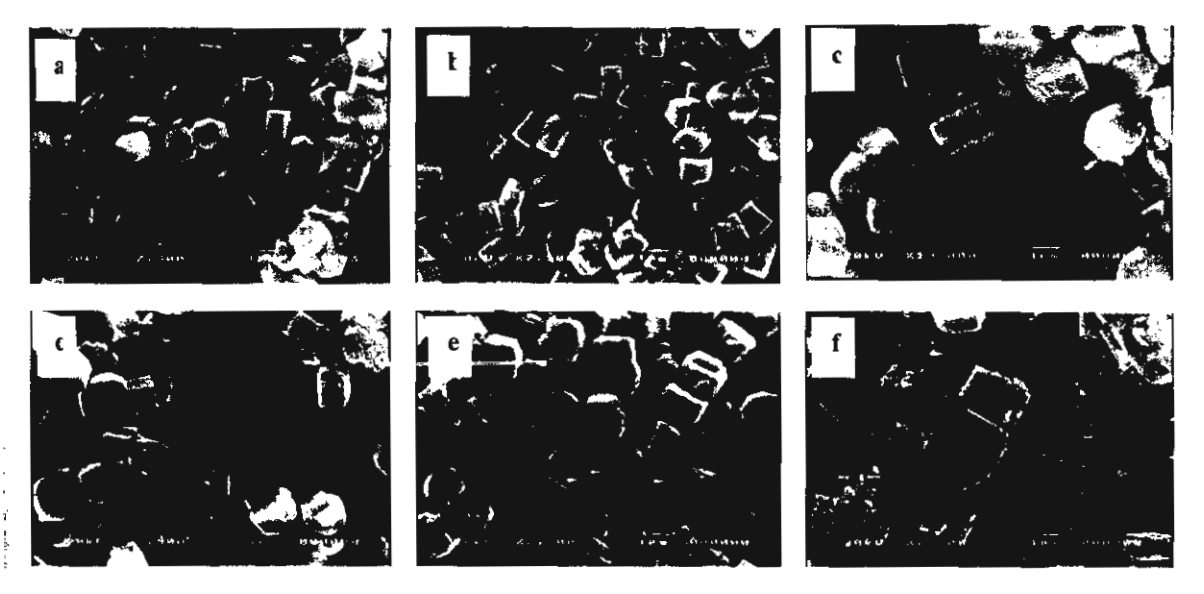


Figure 14 The SEM micrograph of TS-1 sample at various Si:Ti molar ratios of a) 100.00, b) 33.33, c) 20.00, d) 14.29, e) 10.00, f) 7.69, g) 5.88 and h) 5.00.

## Photocatalytic decomposition of 4-nitrophenol

From the discussion of Lee *et al* and Lea *et al*.<sup>20-21</sup>, the photocatalytic decomposition of 4-NP was completely in the presence of H<sub>2</sub>O<sub>2</sub> and UV irradiation. The photodecomposition of 4-NP is governed by \*OH radical reactions. The \*OH can be easily to formed from titanium-hydroperoxide species. Thus, in our work we carried out the PCD of 4-NP at 1.0 mmol/l of H<sub>2</sub>O<sub>2</sub> under UV irradiate. Table 2 shows the results from PCD of 4-NP with TS-1 zeolite at various Si/Ti molar ratios. The PCD increases with the amount of titanium incorporated in the zeolite and the fastest complete decomposition is at 5.0 Si:Ti molar ratio.

Table2 Photocatalytic degradation of 4-nitrophenol

Si/Ti (molar	Time for completely photocatalytic decomposition of 4-NP (h)	
ratio)		
100.00	4.00	
14.29	2.00	
7.69	1.30	
5.00	1.00	

# Conclusions

The TS-1 with highly titanium incorporated in the zeolite framework was synthesized from low cost and moisture-stable precursors, silatrane and titanium glycolate, under microwave instrument. The effect of the compositions (TPA<sup>+</sup>, NaOH and H<sub>2</sub>O) and conditions (aging time, reaction time and reaction temperature) were studied. The suitable condition for synthesizing TS-1 Si:0.1Ti:0.4NaOH:0.3TPA:114H<sub>2</sub>O at aging time 110h, reaction time 15h and reaction temperature 150°C. The Si:Ti molar ratio 100.00-5.00 was studied and the results from XRD, FT-IR, SEM and DR-UV indicated that from this route highly crystalline and the Ti atoms are occupying in the zeolite framework. The reaction times were varied at different Ti loaded, which at higher titanium loading the higher reaction time was an important factor. The photocatalytic decomposition of 4-NP was used to test the activity

of prepared TS-1 samples. The samples showed high efficiency in PCD of 4-NP and the PCD increased with amount of titanium loading.

#### References

- Y.G. Li, Y.M. Lee, J.F. Porter, Journal of materials science 37 (2002) 1959-1965.
- 2. R.J. Davis, Z. Liu, Chemistry of Material 9 (1997) 2311-2324.
- 3. R.B. Khomane, B.D. Kulkarni, A. Paraskar, S.R. Sainkar, *Materials Chemistry and Physics* 76 (2002) 99-103.
- 4. M. Taramasso, G. Perego, B. Notari, US Patent 4410501 (1983).
- M.R. Prasad, G. Kamalakar, S.J. Kulkarni, K.V. Raghavan, K.N. Rao, P.S. Sai Prasad, S.S. Madhavendra, Catalysis Communication 3 (2002) 399-404.
- 6. X-S. Wang, X-W. Guo, Catalysis today 51 (1999) 177-180.
- K. Kunii, K. Narahara, S. Yamanaka, Microporous and Mesoporous Materials 52 (2002) 159-167.
- 8. S. Komarneni, A.S. Bhalla, Journal of Porous Materials 8 (2001) 23-35.
- a) P. Piboonchaisit, S. Wongkasemjit and R. Laine, "A Novel Route to Tris(silatranyloxy-i-propyl)amine Directly from Silica and Triisopropanolamine", Sci. Asia, 25, 113-119 (1999); b) N. Phonthammachai, T. Chairassameewong, E. Gulari, A.M. Jamieson, S. Wongkasemjit, J. Met. Mat. Min. 12 (2002) 23.
- 10. Q.H. Xia, Z. Gao, Materials Chemistry and Physics 47 (1997) 225-230.
- 11. G.L. Marra, G. Artioli, A.N. Fitch, M. Milanesio, C. Lamberti, *Microporous and mesoporous Materials* 40 (2000) 85-94.
- 12. J.L. Grieneisen, H. Kessler, E. Fache, A.M. Le Govic, *Microporous and Mesoporous Materials* 37 (2000) 379-386.
- 13. D.P. Serrano, M.A. Uguina, G.Ovejero, R.V. Grieken, M. Camacho, *Microporous Materials* 4 (1995) 273-282.
- M.R. Boccuti, K.M. Rao, A. Zecchina, G. Leofanti, G. Petrini, Structure and Reactivity of Surfaces 48 (1989) 133-144.
- B.L. Newalkar, J. Olanrewaju, S. Komarneni, Chemistry of Materials 13 (2001) 552-557.

- C.S. Cundy, J.O. Forrest, R.J. Plaisted, Microporous and Mesoporous Materials 66 (2003) 143-156.
- 17. J.H. Koegler, H.V. Bekkum, J.C. Jansen, Zeolites 19 (1997) 262-269.
- M.A. Uguina, D.P. Serrano, G. Ovejero, R.V. Grieken, M. Camacho, Applied Catalysis A 124 (1995) 391-408.
- T. Blasco, M.A. Camblor, A. Corma, J. Perez-Pariente, Journal of American Chemical Society 115 (1995) 11806-11813.
- G.D. Lee, S.K. Jung, Y.J. Jeong, J.H. Park, K.T. Lim, B.H. Ahn, S.S. Hong, Applied Catalysis A 239 (2003) 197-268.
- 21. J. lea, A.A. Adesina, Journal of Techol Biotechnol 76 (2003) 803-810.

#### **CHAPTER VII**

## PHOTOCATALYTIC MEMBRANE REACTOR OF A NOVEL HIGH SURFACE AREA TiO<sub>2</sub>

#### Abstract

Photocatalytic membranes were successfully prepared using an efficient TiO<sub>2</sub> catalyst with high surface area, dispersed into different polymeric matrices, viz. cellulose acetate, polyacrylonitrile and polyvinyl acetate. The catalyst was directly synthesized using titanium triisopropanolamine as precursor. The membranes were characterized using FT-IR, SEM and their photocatalytic performance was tested, viz. stability, permeate flux and photocatalytic degradation of 4-nitrophenol (4-NP). We find that polyacrylonitrile provides the most effective matrix, showing the highest stability and the lowest permeate flux. The amount of TiO<sub>2</sub> loaded in the membrane was varied between 1, 3 and 5 wt% to explore the activity and stability of membranes in the photocatalytic reaction of 4-NP. As expected, the higher the loading of TiO<sub>2</sub> loaded, the higher the resulting catalytic activity.

#### Introduction

Purification of industrial wastewater has become an increasingly important issue, and many researchers are engaged in developing methodology to obtain efficient, low cost wastewater treatment to render harmless of all toxic species present without leaving hazardous residues. Many technologies developed for wastewater treatment, including air stripping, the use of granular activated carbon, biological degradation<sup>1</sup>, chemical oxidation and heterogeneous photocatalysis2-3, have been demonstrated to be effective for complete mineralization of many toxic, bacteria and bio-resistant organic compounds in wastewater under mild experimental conditions<sup>4-7</sup>. The heterogeneous photocatalysis process harnesses radiant energy from natural or artificial light sources to degrade organic pollutants into their mineral components8. TiO2 is a well-established catalyst for photocatalytic degradation due to its combination of high activity, chemical stability and non-toxic properties. Photocatalytic degradation generally occurs via production of OH° radicals. When semiconductive TiO2 is illuminated by radiation of appropriate energy, electrons and holes are generated within the TiO2 structure. In the presence of O2, OH radicals are formed by reaction between the valence band holes and activated OH groups, e.g from adsorbed H2O on the TiO2 surface. To accelerate the oxidation reaction, efficient scavenging of e by O2 is necessary. The organic pollutant is attacked by hydroxyl radicals and generates organic radicals or intermediates 9-12. The main drawback to practical implementation of the photocatalysis method arises from the need for an expensive liquid-solid separation process, due to the formation of milky dispersions upon mixing the catalyst powder with water<sup>13</sup>.

Currently, this drawback is solved by the use of a  $TiO_2$  membrane, consisting of fine  $TiO_2$  particles dispersed in a porous matrix. Such titania membranes have attracted a great deal of attention in recent years due to their unique characteristics, including high water flux, semiconducting properties, efficient photocatalysis and chemical resistance relative to other membrane materials, such as silica and  $\gamma$ -alumina<sup>14</sup>.

Many techniques have been explored for the fixation of titania powder, including sputtering on glass, silicon or alumina<sup>15</sup>, coating via sol-gel processing on porous stainless steel plate, α-Al<sub>2</sub>O<sub>3</sub> or zeolites<sup>16-19</sup> were studied. However, the use of mixed matrix membranes (MMM), i.e. membranes containing microencapsulated TiO<sub>2</sub>, becomes of increasing interest because of their high selectivity combined with outstanding separation performance, processing capabilities, and low cost, when

polymers are used as the matrix. Many researchers<sup>20-27</sup> have explored ways to develop and facilitate the separation process, using very thin microencapsulated membranes to allow for high fluxes. Such a membrane must have a high volume fraction of homogeneously distributed encapsulated particles in a defect- and void-free polymer matrix<sup>28</sup>. Polymeric membranes are not appropriate for use in membrane reactor applications where high temperatures are needed for reaction. Thus, application of MMM for catalysis of low temperature reactions has become a main topic for many researchers, for examples, hydrogenation of propyne<sup>29</sup>, photomineralization of nalkanoic acids<sup>30</sup>, wet air oxidation of dyeing wastewater, and photocatalytic oxidations<sup>31-34</sup>.

To obtain a high photocatalytic activity, the surface area of catalyst is very important. Thus, in our work, thermally stable TiO<sub>2</sub> with high surface area is synthesized from moisture-stable titanium triisopropanolamine. The performance of this material as a component of an MMM was evaluated in a photocatalytic membrane reactor, using 4-nitrophenol as a model substrate, with regard to stability tests, effect of membrane type (PAN, PVac, CA), and TiO<sub>2</sub> loading. A comparison is made between as-prepared and commercial TiO<sub>2</sub>.

#### **Experimental**

#### Materials

Titanium dioxide (surface area 12 m²/g) was purchased from Sigma-Aldrich Chemical Co. Inc. (USA) and used as received. Ethylene glycol (EG) was purchased from Malinckrodt Baker, Inc. (USA) and purified by fractional distillation at 200°C under nitrogen atmosphere before use. Triethylenetetramine (TETA) was purchased from Facai Polytech. Co. Ltd. (Bangkok, Thailand) and distilled under vacuum (0.1 mm/Hg) at 130°C prior to use. Triisopropanolamine (TIS) and 4-nitrophenoi were purchased from Sigma-Aldrich Chemical Co. Inc. (USA).

#### Titanium tri-isopropanolamine precursor preparation

A mixture of TiO<sub>2</sub> (2g, 0.025 mol), TIS (9.55g, 0.05 mol) and TETA (3.65g, 0.0074 mol) was stirred vigorously in excess EG (25 cm<sup>3</sup>) and heated to 200°C for 24 h. The resulting solution was centrifuged to separate the unreacted TiO<sub>2</sub>. The excess EG and TETA were removed by vacuum distillation at 150°C to obtain a crude precipitate.

The product was characterized using FTIR, FAB<sup>+</sup>-MS and TGA. Fourier transform infrared spectra (FT-IR) were recorded on a VECOR3.0 BRUKER spectrometer with a spectral resolution of 4 cm<sup>-1</sup>. Thermal gravimetric analysis (TGA) was carried out using a Perkin Elmer thermal analysis system with a heating rate of 10°C/min over 30°-800°C temperature range. The mass spectrum was obtained on a Fison Instrument (VG Autospec-ultima 707E) using the positive fast atomic bombardment mode (FAB<sup>+</sup>-MS) with glycerol as the matrix, cesium gun as initiator, and cesium iodide (CsI) as a standard for peak calibration.

#### High surface area TiO2 preparation

After removal of any excess solvent from titanium triisopropanolamine precursor, the precursor was transferred to a crucible and calcined at 600°C for 2h at heating rate of 0.25°C/min. The white powder was ground and stored in a desiccator for further use.

#### Membrane preparation

#### Polyacrylonitrile membrane

A 10 wt% mixture of polyacrylonitrile powder in dimethyl formamide (DMF) was vigorously stirred at 50°C until homogeneous. A specified amount of TiO<sub>2</sub> was added to the stirred polymer solution. Partial vacuum was applied for a brief duration to ensure the removal of air bubbles. The mixture was then coated on a clean glass plate using a casting knife. The resulting membrane was allowed to set for 2 min before being dried in a vacuum oven at 40°C overnight following by 60°C for 2h and 80°C for 2h. The prepared membrane was cut into a circular shape with a diameter of 6 cm and thickness of 15 μm.

#### Cellulose acetate membrane

The membrane preparation was followed Kunprathippanja's method<sup>32</sup>. To a suspension of TiO<sub>2</sub>, cellulose acetate was added. A partial vacuum was applied for a brief duration to ensure the removal of air bubbles, while the suspension was stirred to obtain a homogeneous suspension. The solution was then coated on the surface of a clean glass plate. The membrane was allowed to set for 2 min, followed by submersion in an ice water bath for 2 min. The membrane was then soaked in a hot water bath at 90°C for 1h before being dried. The obtained membrane was cut into a circular shape with a diameter of 6 cm and thickness of 15 μm.

#### Polyvinyl acetate membrane

The polymer was dissolved at 50°C in tetrahydrofuran (THF) and stirred until all the polymer had dissolved in the solvent. TiO<sub>2</sub> was then added to the stirring polymer solution, followed by degassing to remove air bubbles. The mixture was transferred to a teflon flat sheet and cast to the desired thickness. The prepared membrane was left overnight at room temperature to slowly evaporate solvent and then dried in a vacuum oven at 40°C for 2h. The membrane was cut into a circular shape with a diameter of 6 cm and thickness of 15 µm.

#### Stability test of prepared membranes

The prepared polymeric membranes (PAN, CA and PVAc) were placed in the membrane reactor and irradiated under UV irradiation for 15 h. The concentration of 4-NP used was 140 ppm. The samples were withdrawn and analyzed for total organic carbon (TOC) to verify that the organic components were released from the prepared membrane. SEM was used to investigate the presence of defects in membranes before and after the stability test.

#### Photocatalytic decomposition of 4-nitrophenol

The photocatalytic reactions were carried out in a 500 ml continuous batch glass reactor, figure 1, with a gas inlet and outlet at an O<sub>2</sub> flow rate of 20 ml/min. A cooling water jacket was used to maintain the temperature at 30°C. The suspensions and membrane were illuminated using a 100 Watt Hg Philip UV lamp. The concentration of 4-NP used was 140 ppm and the solution was continuously stirred. The obtained permeate was removed at 1h intervals and analyzed to determine the concentration of 4-NP using a Shimadzu UV-240 spectrophotometer.

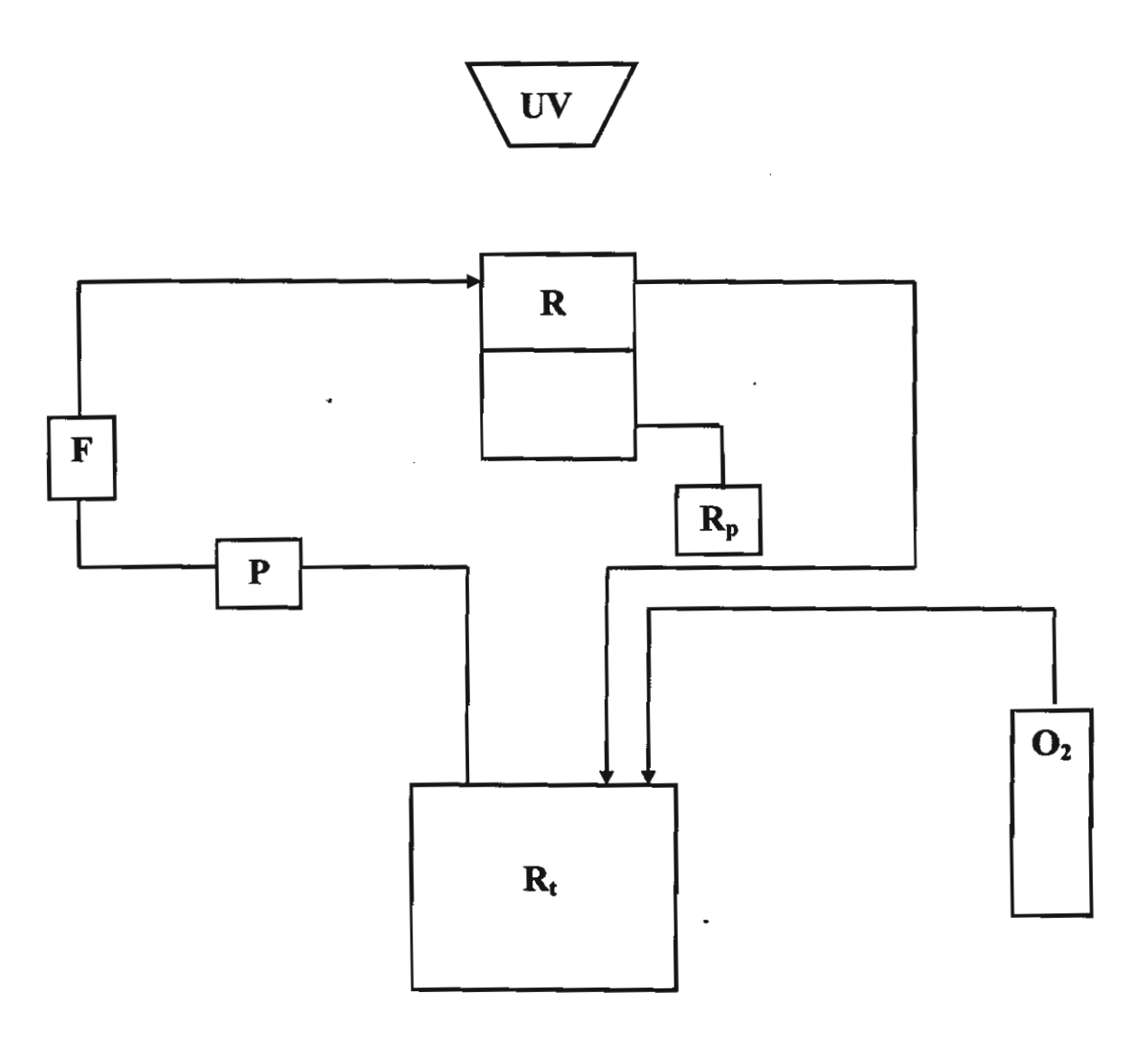


Figure 1 The schematic diagram of photocatalytic membrane reactor (F, flowmeter; R, reactor; R<sub>p</sub>, permeate reservoir; R<sub>t</sub>, recirculating tank and P, peristaltic pump).

#### Titanium triisopropanolamine and TiO2 catalyst characterization

High surface area TiO<sub>2</sub> was characterized by various techniques. The XRD pattern was obtained using a D/MAX-2200H Rigaku diffractometer with CuKα radiation on specimens prepared by packing sample powder into a glass holder. The diffracted intensity was measured by step scanning in the 2θ range of 5° to 90°. Fourier transform infrared spectra (FT-IR) were recorded on a VECOR3.0 BRUKER spectrometer with a spectral resolution of 4 cm<sup>-1</sup>. Samples pyrolyzed at 600°C were analyzed using SEM by attachment onto aluminum stubs after coating with gold via vapor deposition. Micrographs of the pyrolyzed sample surfaces were obtained at

x7,500 magnification. Specific surface area and nitrogen adsorption-desorption were determined using an Autosorp-1 gas sorption system (Quantachrome Corporation) via the Brunauer-Emmett-Teller (BET) method. A gaseous mixture of nitrogen and helium was allowed to flow through the analyzer at a constant rate of 30 cc/min. Nitrogen was used to calibrate the analyzer, and also as the adsorbate at liquid nitrogen temperature. The samples were thoroughly outgassed for 2h at 150°C, prior to exposure to the adsorbent gas.

#### Membrane characterization

Three different types of membranes made from PAN, CA and PVAc were characterized using SEM, FT-IR and DR-UV. The morphology of membranes was analyzed by attachment onto aluminum stubs and coated with gold via vapor deposition. The membranes were frozen in liquid nitrogen and fractured to examine the cross-sectional areas. The samples were characterized on a JEOL 5200-2AE(MP 15152001) scanning electron microscope. Fourier transform infrared spectra (FT-IR) were recorded on a VECOR3.0 BRUKER spectrometer with a spectral resolution of 4 cm<sup>-1</sup> using transparent KBr pellets containing 0.001 g of sample mixed with 0.06 g of KBr. The samples were also analyzed to determine the amount of TiO<sub>2</sub> using a Shimadzu UV-240 spectrophotometer.

#### Results and discussion

#### Titanium triisopropanolamine precursor characterization

The synthesized titanium triisopropanolamine was characterized using FT-IR, TGA, MS and SEM. The IR spectrum (fig 2.) of the product shows bands at 3400 cm<sup>-1</sup> (OH group), 2927-2855 cm<sup>-1</sup> (C-H stretching), 1460 cm<sup>-1</sup> (C-H bending of CH<sub>2</sub> group), 1379 cm<sup>-1</sup> (C-H bending of CH<sub>3</sub> group), 1085 cm<sup>-1</sup> (C-O-Ti stretching), 1020 cm<sup>-1</sup> (C-N bending) and 554 cm<sup>-1</sup> (Ti-O stretching). The TGA thermogram, as seen in figure 3, shows two transitions, at 280° and 365°C, corresponding to the decomposition of unreacted triisopropanolamine and the triisopropanolamine ligand, respectively, reflecting the use of excess triisopropanolamine in the reaction and no purification of the obtained product. The final ceramic yield of the product was calculated from the starting point of the second decomposition transition, and was found to be 16.60%, close to the theoretical ceramic yield of 18.65%. The results of mass spectral analysis, summarized in table1, confirm the prepared sample has the desired structure.

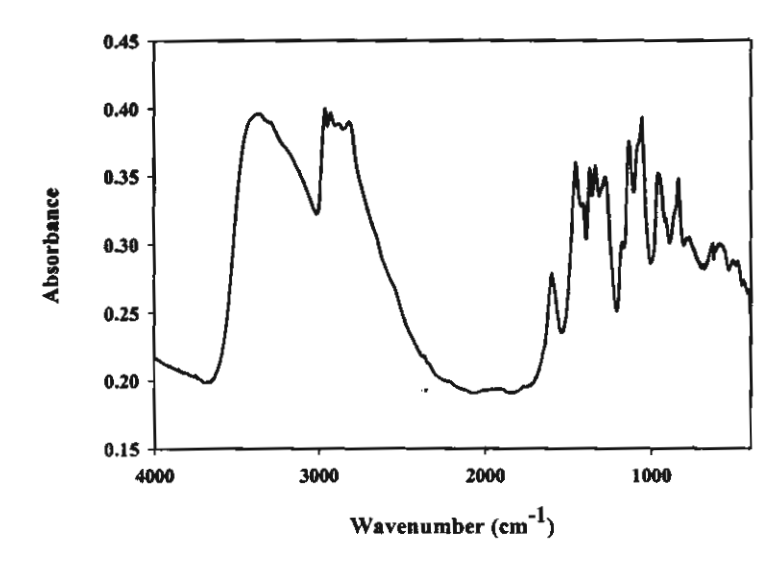


Figure 2 FT-IR spectrum of titanium triisopropanolamine.

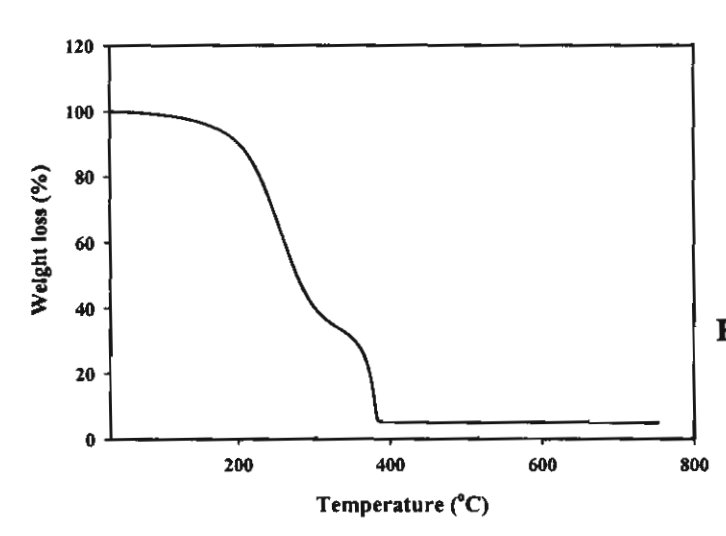


Figure 3 TGA thermogram
of titanium
triisopropanolamine.

Table 1 The proposed structure and fragments of the synthesized titanium triisopropanolamine.

M/e	%intensity	Proposed structure		
428	10	H <sup>+</sup> [HOCH <sub>3</sub> CHCH <sub>2</sub> ]N[CH <sub>2</sub> CH <sub>3</sub> CHO] <sub>2</sub> Ti[OCHCH <sub>3</sub> CH <sub>2</sub> ] <sub>2</sub> N[CH <sub>2</sub> CHCH <sub>3</sub> OH]H <sup>+</sup>		
410	5	[CH <sub>3</sub> CH <sub>2</sub> CH <sub>2</sub> ]N[CH <sub>2</sub> CHCH <sub>3</sub> O] <sub>2</sub> Ti[OCHCH <sub>3</sub> CH <sub>2</sub> ] <sub>2</sub> N [CH <sub>2</sub> CHCH <sub>3</sub> OH]		
214	58	[H <sub>2</sub> NCHCH <sub>3</sub> CH <sub>2</sub> O] <sub>2</sub> Ti[OH]		
192	100	H+N[CH <sub>2</sub> CHCH <sub>3</sub> OH] <sub>3</sub>		

#### TiO<sub>2</sub> catalyst characterization

The calcined product was characterized using XRD, BET surface area and SEM to confirm the presence of the active anatase phase of  $TiO_2$ . The XRD pattern shown in fig. 4, exhibits diffraction peaks at  $2\theta = 25.28$ , 37.66, 47.90, 54.64, 62.58, 69.76, 75.26 and 82.72, and the particle morphology (fig. 5) shows irregularly-shaped particles, characteristic of the anatase phase of  $TiO_2$ , as previously reported<sup>35</sup>. The surface area measurement of a sample calcined at 600°C for 2h shows a high surface area of 163 m<sup>2</sup>/g. Also, the nitrogen adsorption-desorption isotherm of this material exhibits type IV character (fig. 6.) indicative of a mesoporous structure.

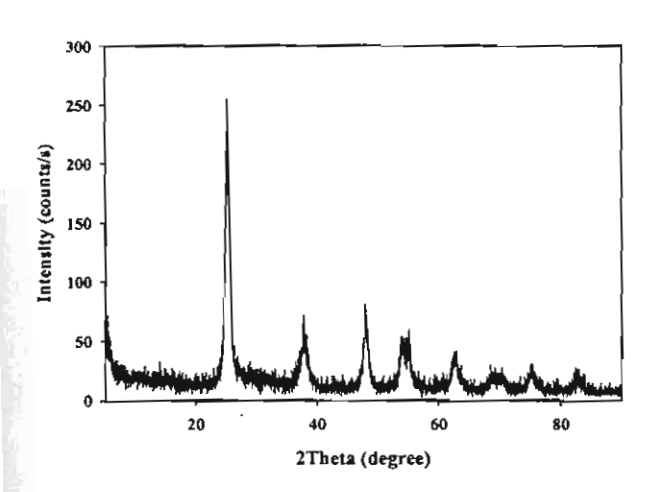


Figure 4 XRD pattern of the anatase phase of the prepared TiO<sub>2</sub> catalyst calcined at 600°C for 2h.



Figure 5 SEM micrograph of the anatase phase of the prepared

TiO<sub>2</sub> catalyst calcined at 600°C for 2h.

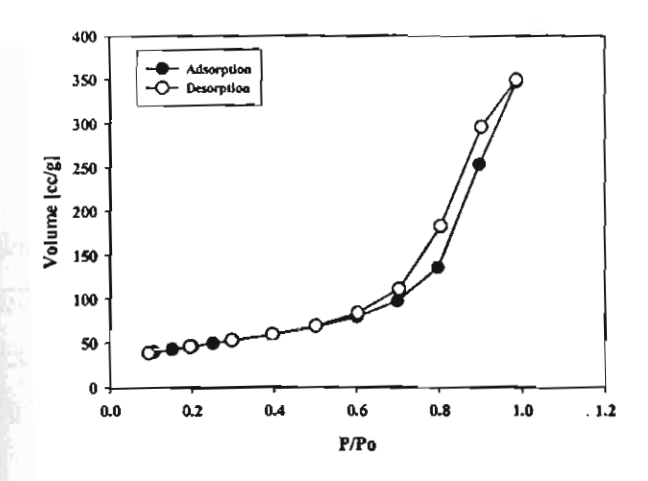


Figure 6 Nitrogen adsorption

desorption isoterm for the

prepared mesoporous titania

calcined at 600°C

#### Membranes characterization

The prepared mixed matrix membranes were characterized with respect to their functional groups using FT-IR, their morphology using scanning electron microscopy (SEM) and the amount of TiO<sub>2</sub> loaded in the membrane using diffuse reflectance UV. The membrane stability test was also carried out to demonstrate that the obtained material is suitable for use as a membrane.

The FT-IR spectrum of CA (fig. 7a) shows the characteristic abscrption bands of C=O, C-O-C and C-C bonds at 1780, 1174 and 1020 cm<sup>-1</sup>, respectively. The peak in the region of 800-500 cm<sup>-1</sup> is associated with the vibration of the Ti-O bond<sup>25</sup>. For the PAN membrane (fig 7b), the band at 2260 cm<sup>-1</sup> is characteristic of the CN bond while the spectrum of PVAc in fig. 7c shows bands at 1780 and 1200 cm<sup>-1</sup> representing the C=O and C-C bonds, respectively.

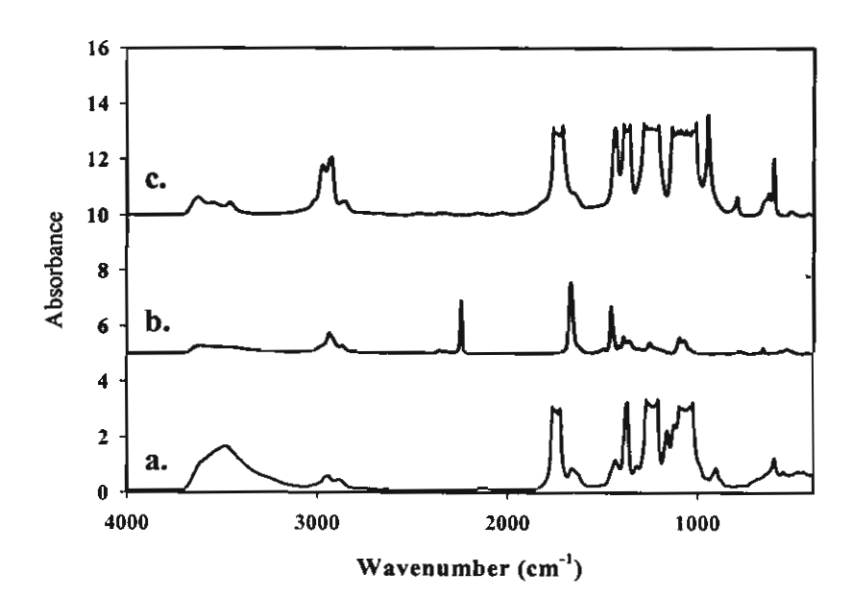


Figure 7 FT-IR spectra of the prepared membranes using 1wt%TiO<sub>2</sub> mixed in a). cellulose acetate, b), polyacrylonitrile and c), polyvinyl acetate.

SEM micrographs of the fracture surfaces of all three types of membranes are shown in figure 8. The CA membrane (fig. 8a.) presents a porous surface distinctly different from the surfaces of PAN and PVAc (fig.8b. and 8c.). The TiO<sub>2</sub> particles are immobilized within the polymeric matrix. No significant loss of particles was observed during the membrane formation process on the glass plate. The micrographs reveal no

evidence for the presence of voids between the polymer and TiO<sub>2</sub>. TiO<sub>2</sub> particles are well distributed across the surface and do not agglomerate.

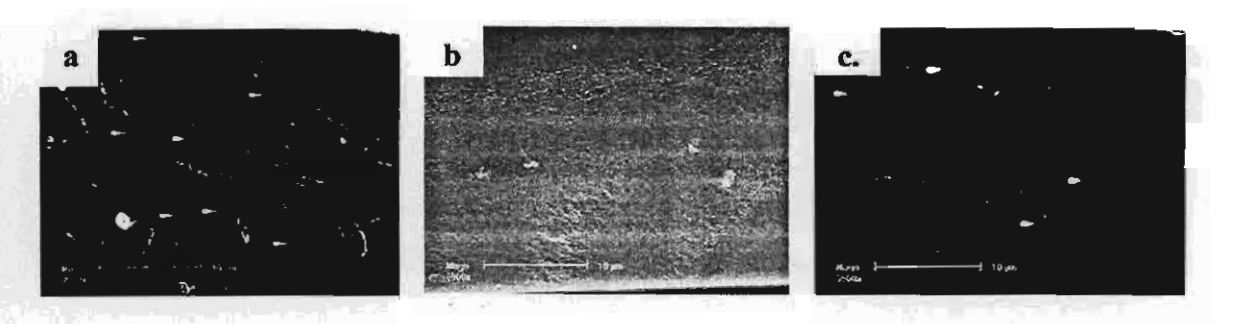


Figure 8 SEM micrographs of mixed matrix membranes using a.) cellulose acetate, b.) polyacrylonitrile and c.) polyvinyl acetate.

The PAN membrane type was selected to study the effect of TiO<sub>2</sub> loading, varying the percentage of TiO<sub>2</sub> between 1, 3 and 5 wt%. Figure 9 shows the DR-UV spectra of the prepared membranes. As expected, the absorbance at 320 nm, which is characteristic of TiO<sub>2</sub>, increases with the amount of TiO<sub>2</sub>. Morphological analysis by SEM, shown in fig. 10, indicates that TiO<sub>2</sub> particles are well dispersed throughout the PAN matrix at all loadings.

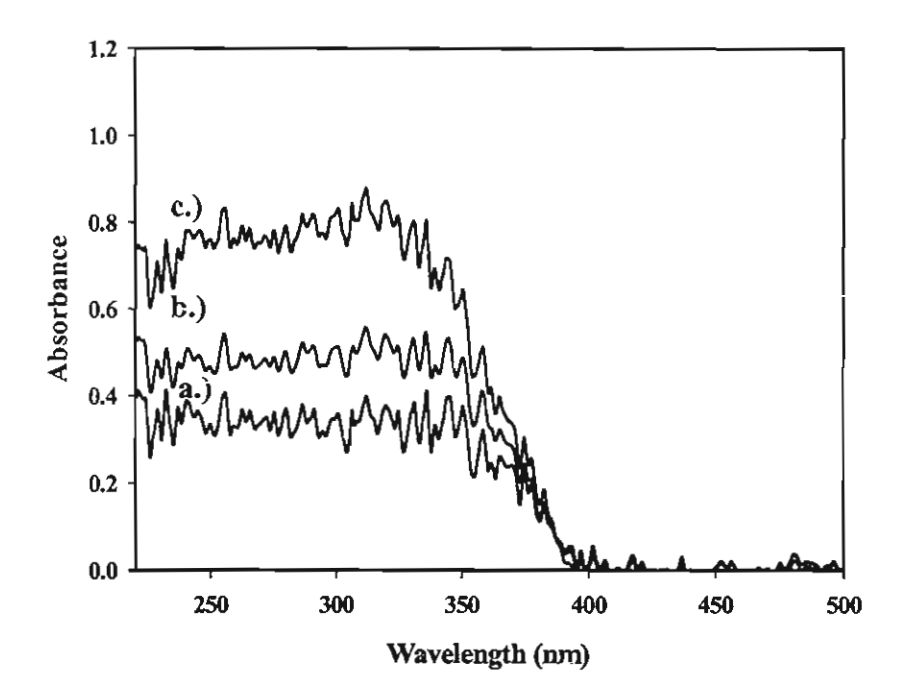


Figure 9 DR-UV spectra of polyacrylonitrile membranes at various percentages of TiO<sub>2</sub>; a) 1, b) 3 and c) 5wt%.



Figure 10 SEM micrographs of polyacrylonitrile membranes at various percentages of TiO<sub>2</sub>; a) 1, b) 3 and c) 5wt%

The stability of the prepared membranes was tested using UV illumination and exposure to 4-NP for 15h, and evaluation by TOC, as summarized in table 2. The PAN and CA membranes were stable under these conditions, as indicated by essentially no change in TOC values. However, the PVAc membrane showed a higher TOC value, indicative that the PVAc membrane was not stable and undergoes decomposition.

 Table 2
 The stability tests of the prepared membranes.

Membrane type	TOC (at initial)	TOC (after 15h)
PAN	22.39	22.68
CA	22.63	22.57
PVAc	22.35	32.22

### Photocatalytic degradation of 4-nitrophenol

The photocatalytic activities of the three membrane types were assessed using the photoreactor shown in fig. 1, employing 1 wt% immobilized photocatalyst TiO<sub>2</sub>, oxygen flow rate of 20 ml/min. 4-NP flow rate of 30 ml/min and 4-NP concentration of 140 ppm. The permeation flux data (fig. 11) shows that CA and PAN membranes have constant low permeate flux levels, 12.38 and 5.31 l/h m<sup>2</sup>, respectively, whereas the PVAc membrane shows a steep increase in permeate flux from 10.62 to 120 l/h m<sup>2</sup> as reaction time increases from 1 to 2h. The higher permeate flux of CA membrane than PAN is consistent with the SEM observation in fig. 8, that the CA membrane is more porous than the PAN membrane. The dramatic increase in permeate flux of the PVAc membrane occurs because of the decomposition of this membrane, which generates

defects during the reaction, as confirmed by the SEM micrograph in figure 12. The holes generated in the polymer matrix cause an increase in the flux and a decrease in the photodegradation activity. The efficiencies of the PAN and CA membranes for photocatalytic degradation of 4-NP are illustrated in fig. 13, which indicates, at 1 wt% Ti loading, no substantive differences in the rate of degradation of 4-NP between the PAN and CA membranes. During the first hour of UV illumination, the concentration of 4-NP permeating through the PAN membrane is higher than through the CA membrane. This is unexpected and may reflect experimental uncertainty, since, in view of the higher permeate flux of the CA membrane, more 4-NP molecules should penetrate through the CA membrane. However, after 7hr of illumination, each membrane shows similar activity, as expected at such low TiO<sub>2</sub> loadings. For the PVAc membrane, the reaction could not be monitored through 7hr because the defects produced by degradation causing an extremely high flux, as discussed above.

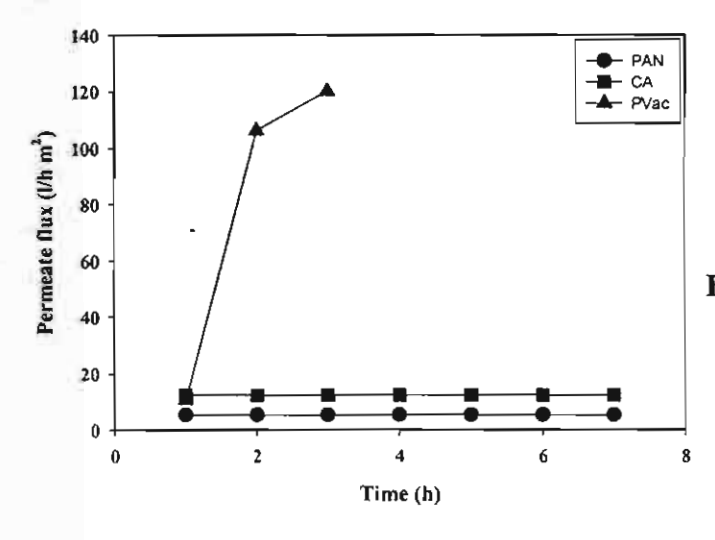


Figure 11 The permeate flux versus reaction time of all three types of the prepared membranes.



Figure 12 SEM micrograph
showing the defect of
polyvinyl acetate membrane
after the reaction.

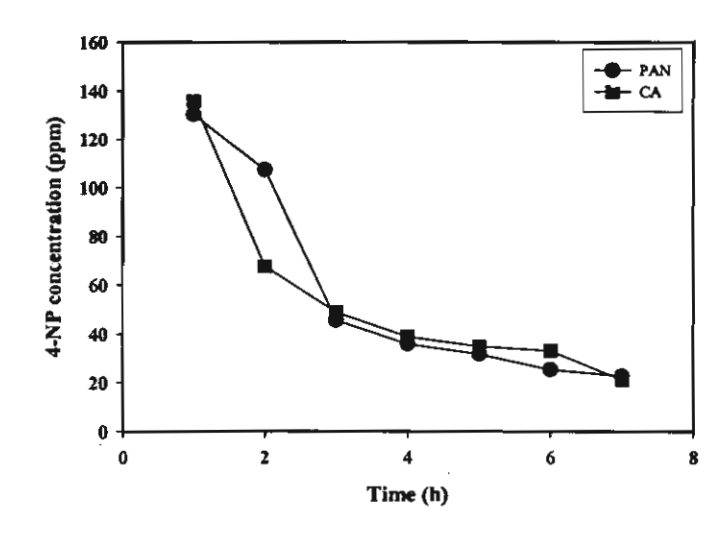


Figure 13 The degradation of 4
NP with the reaction time of polyacrylonitrile and cellulose acetate membranes.

# Effect of various amounts of $TiO_2$ in PAN membrane on the photocatalytic degradation of 4-nitrophenol

The PAN membrane was selected to investigate the effect of TiO<sub>2</sub> loading on the efficiency of photocatalytic degradation because of its stability and the fact that it exhibits the lowest permeant flux. Figure 14 shows the permeant flux of PAN membranes at the three loading levels, 1, 3 and 5 wt% of TiO<sub>2</sub>. We find that the flux is constant for all three samples, and increases with the amount of TiO<sub>2</sub> from 5.31, to 8.13 to 12.73 l/h m<sup>2</sup>, respectively. In fig. 15, the efficiency of degradation of 4-NP at the three loading levels of TiO<sub>2</sub> is reported. Initially, the decrease of 4-NP at 3 and 5% loadings appears to be faster than at 1%. As for Fig. 13, however, this may be experimental error. At long times, there appears to be no significant differences in the concentrations of 4-NP measured. The reason may be that the percentage of TiO<sub>2</sub> is too low to see any differences in the degree of degradation of 4-NP. However, when compared with literature results<sup>34</sup>, performed at much higher loading levels of TiO<sub>2</sub>, it appears that these membranes show a higher level of catalytic activity.

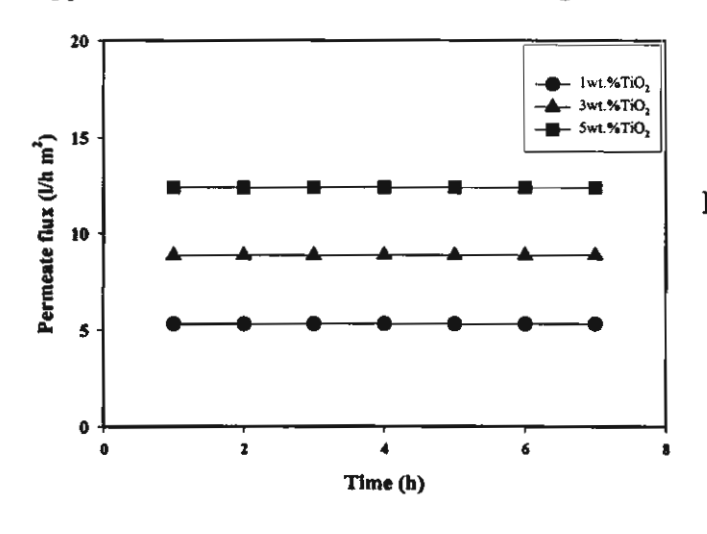


Figure 14 The permeate flux versus reaction time of polyacrylonitrile membranes at various percentages of TiO<sub>2</sub>.

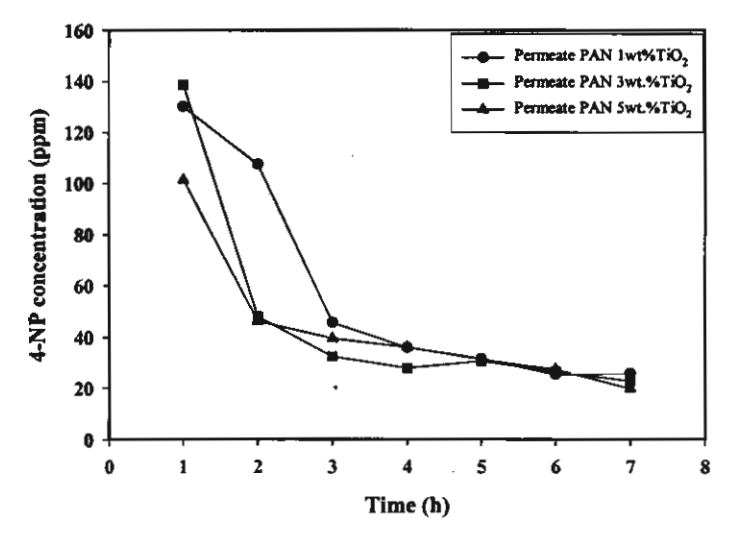


Figure 15 The degradation of 4-NP with the reaction time of polyacrylonitrile membranes at various percentages of TiO<sub>2</sub>.

Commercial TiO<sub>2</sub> (Degussa P25) is also studied to compare with our TiO<sub>2</sub> at loading level of 3wt%. The result, see fig. 16, indicates no permeation of 4-NP through membrane prepared using commercial TiO<sub>2</sub> and the efficiency of degradation of 4-NP measured from the retentate of two membranes shows that the degradation of 4-NP in the membrane prepared using our TiO<sub>2</sub> is distinguishably lower.

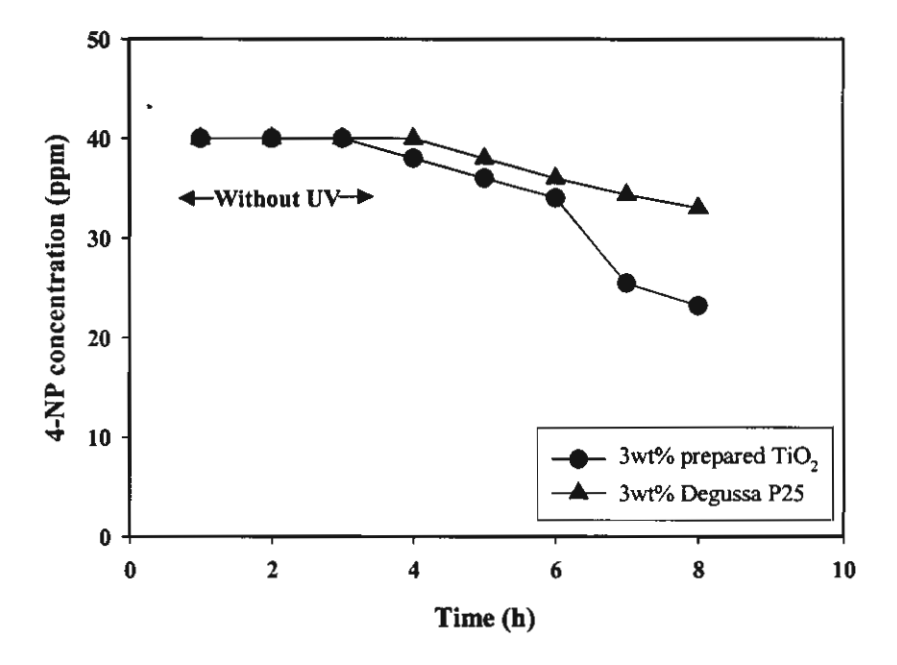


Figure 16 Effect of TiO<sub>2</sub> type mixed in the polyacrylonitrile membrane on the degradation of 4-NP.

#### Conclusions

The titanium triisopropanolamine precursor can be prepared by a very simple method (the oxide one pot synthesis) from low cost starting materials, and yields a TiO<sub>2</sub> catalyst with high surface area was obtained after calcinations of the precursor at 600°C for 2h. Polymeric membranes loaded with the as-prepared TiO<sub>2</sub> catalyst show an impressively high efficiency for the photocatalytic degradation of 4-NP. Examination of the properties of three different types of membrane (PAN, CA and PVAc) indicates that the highest stability and lowest permeate flux is observed with the PAN membrane and the poor stability occurs with the PVAc membrane. The photocatalytic degradation of 4-NP increases with increased percentage of TiO<sub>2</sub> loaded in the PAN membrane.

#### References

- Razo-Flores, M. Iniestra-Gonzalez, J.A. Field, P. Olguin- Lora, L. Puig-Grajales, Journal of Environmental Engineering (2003) 999-1006.
- 2. S. Zhou, A.K. Ray, Ind. Eng. Chem. Res. 42 (2003) 6020-6033.
- H. Chun, W. Yizhong, T. Hongxiao, Applied Catalysis B: Environmental 35 (2001) 95-105.
- 4. V. Loddo, G. Marci, C. Martin, L. Palmisano, V. Rives, A. Sclafani, Applied Catalysis B: Environmental 20 (1999) 29-45.
- B. Barni, A. Cavicchioli, E. Riva, L. Zanoni, F. Bignoli, I.R. Bellobono, Chemosphere 30 (1995) 1847-1860.
- P-C. Maness, S. Smolinski, D.M. Blake, Z. Huang, E.J. Wolfrum, W.A. Jacoby, Applied and Environmental Microbiology 65 (1999) 4094-4098.
- 7. A.J. Maira, W.N. Lau, C.Y. Lee, P.L. Yue, C.K. Chan, K.L. yeung, Chemical Engineering Science 58 (2003) 959-962.
- 8. D. Chen, A.K. Ray, Applied Catalysis B: Environmental 23 (1999) 143-157.
- 9. R. Villacres, S. Ikeda, T. Torimoto, B. Ohtani, Journal of Photochemistry and Photobiology A: Chemistry 160 (2003) 121-126.
- A.G. Rincon, C. Pulgarin, N. Adler, P. Peringer, Journal of Photochemistry and Photobiology A: Chemistry 139 (2001) 233-241.
- 11. A. Makowski, W. Wardas, Current topics in Biophysics 25 (2001) 19-25.
- 12. S. Liu, K. Li, Journal of Membrane Science 218 (2003) 269-277.

- D. Dumitriu, A.R. Bally, C. Ballif, P. Hones, P.E. Schmid, R. Sanjines, F. Levy,
   V.I. Parvulescu, Applied Catalysis B: Environmental 25 (2000) 83-92.
- L. Zhang, T. Kanki, N. Sano, A. Toyoda, Separation and Purification Technology 31 (2003) 105-110.
- T.V. Gestel, C. Vandecasteele, A. Buekenhoudt, C. Cotremont, J. Luyten, R. Leysen, B.V.D. Bruggen, G. Maes, Journal of Membrane Science 209 (2002) 379-389.
- P. PuhlfurB, A. Voigt, R. Weber, M. Morbe, Journal of Membrane Science 174 (2000) 123-133.
- 17. Y.S.S. Wan, J.L.H. Chau, A. Gavriilidis, K.L. Yeung, Microporous and Mesoporous Materials 42 (2001) 157-175.
- 18. J. Chen, L. Eberlein, C.H. Langford, Journal of Photochemistry and Photobiology A: Chemistry 148 (2002) 183-189.
- 19. I. Ortiz, P. Alonso, A. Urtiaga, Desalination 149 (2002) 67-72.
- K. Karakulski, W.A. Morawski, J. Grzechulska, Separation and Purification Technology 14 (1998) 163-173.
- 21. C.M. Zimmerman, A. Singh, W.J. Koros, Journal of Membrane Science 137 (1997) 145-154.
- M-E. Avramescu, Z. Borneman, M. Wessling, Journal of Chromatography A 1006 (2003) 171-183.
- 23. M. M. Clark, P. Lucas, Journal of Membrane Science 143 (1998) 13-25.
- 24. Z. Lu, G. Liu, S. Duncan, Journal of Membrane Science 221 (2003) 113-122.
- Q. Hu, E. Marand, S. Dhingra, D. Fritsch, J. Wen, G. Wilkes, Journal of Membrane Science 135 (1997) 65-79.
- S.B. Tantekin-Ersolmaz, L. Senorkyan, N. Kalaonra, M. Tather, A. Erdem-Senatalar, Journal of Membrane Science 189 (2001) 59-67.
- 27. A. Figoli, W. Sager, M. Wessling, Desalination 148 (2002) 401-405.
- 28. S. Ziegler, J. Theis, D. Fritsch, Journal of Membrane Science 187 (2001) 71-84.
- 29. L. Rivas, I. R. Bellobono, F. Ascari, Chemosphere 37 (1998) 1033-1044.
- 30. L. Lei, X. Hu, P.-L. Yue, Water Research 32 (1998) 2753-2759.
- 31. R. Molinari, M. Mungari, E. Drioli, A.D. Paola, V. Loddo, L. Palmisano, M. Schiavello, Catalysis Today 55 (2000) 71-78.

- 32. W. Rattanawong, S. Osuwam, T. Risksomboon, S. Kulprathipanja, American Chemical Society, Div. Pet. Chem. 46 (2001) 166-167.
- 33. M.E. Zorn, Proceeding of the 13<sup>th</sup> Annual Wisconsin Space Conference August 14-15, 2003. Green Bay, WI. Wisconsin Space Grant Consortium: 2003.
- 34. R. Molinari, L. Palmisano, E. Drioli, M. Schiavello, Journal of Membrane Science 206 (2002) 399-415.
- 35. N. Phonthammachai, T. Chairassameewong, E. Gulari, A. M. Jamieson, S. Wongkasemjit, Microporous and Mesoporous Materials 66 (2003) 261-271.

## CHAPTER VIII CONCLUSIONS

Titanium glycolate and titanium triisopropanolamine are successfully synthesized using low cost starting materials, and a much simpler and milder reaction condition. The products show good property in moisture stability. The results from spectroscopy, namely, FT-IR, EA, Solid state NMR, and TGA, confirm the product structure. The transformation from anatase to rutile phases of calcined titanium glycolate indicates the anatase stability up to 900°C. The stability of the synthesized product remarkably provides researchers to make use in many applications. Anatase TiO<sub>2</sub> nanoparticles were successfully prepared by the sol-gel technology, using moisture-stable titanium glycolate as precursor in 1M HCl solution. The calcination temperature and the HCl:H<sub>2</sub>O volume ratio have a substantial influence on the surface area, phase transformation and morphology of the products. Anatase titania is produced at calcination temperatures in the range of 600° to 800°C, above which transformation to rutile occurs. Increase of temperature results in anatase of higher crystallinity but lower specific surface area, and induces a morphological change from large irregular agglomerates to more homogeneous particles of spherical shape. From XRD measurements of average grain sizes, we deduce that nucleation rate dominates the kinetics at low temperatures, and growth rate becomes the controlling factor at high temperature and low HCl:H2O ratios. Increase of HCl:H2O ratio results in a small but significant decrease in porosity. The highest specific surface area 125 m<sup>2</sup>/g is obtained at the lowest HCl:H<sub>2</sub>O ratio of 0.28 and the lowest calcination temperature (600°C). From rheological analysis, as evaluated by the Winter criteria, the gelation time increases with increase of HCl:H2O volume ratio. The fractal dimension determined from the frequency scaling exponent of the modulus at the gel point indicates a denses critical gel structure at low acid ratio. However, the complex viscosity and gel strength increase as a function of acid ratio. We interpret this behavior as indicative that, at low acidity, the gel is composed of poorly hydrated particles forming a dense but weak structure. Increase in acidity increases hydration and cross-link density leading to a more open and stronger gel network. From the rheological study of different ceria gelling system using HCl:alkoxide molar ratio of 0.8, 0.9, 1.0 and 1.1, as evaluated by Winter et al., the gelation time increases as increasing HCl:alkoxide molar ratio. The gel strength increases as a function of acid ratio and the fractal dimension determined from the frequency scaling exponent of the modulus at the gel point indicate a tight structure at low acid ratio. The TS-1 with highly titanium incorporated in the zeolite framework was synthesized from moisture-stable precursors, silatrane and titanium glycolate, under microwave treatment. The effects of the compositions (TPA<sup>+</sup>, NaOH and H<sub>2</sub>O) and conditions (aging time, reaction time and reaction temperature) showed that the suitable condition for synthesizing TS-1 was Si:0.1Ti:0.4NaOH:0.3TPA:114H<sub>2</sub>O at aging time 110h, 15h reaction time and reaction temperature of 150°C. As for the Si:Ti molar ratio, from XRD, FT-IR, SEM and DR-UV results, it is indicated that high crystallinity and the Ti atoms are occupying in the zeolite framework. Moreover, at higher titanium loading the higher reaction time was an important factor. It is also important to the photocatalytic decomposition of 4-NP. The samples showed high efficiency in PCD of 4-NP and the PCD increased with amount of titanium loading.

The titanium triisopropanolamine precursor was successfully prepared using the same method, and yields a TiO<sub>2</sub> catalyst with high surface area after calcinations of the crude precursor at 600°C for 2h. Polymeric membranes loaded with the as-prepared TiO<sub>2</sub> catalyst show an impressively high efficiency for the photocatalytic degradation of 4-NP. Examination of the properties of three different types of membrane (PAN, CA and PVAc) indicates that the highest stability and the lowest permeate flux are observed with the PAN membrane and the poor stability occurs with the PVAc membrane. The photocatalytic degradation of 4-NP increases with increasing percentage of TiO<sub>2</sub> loaded in the PAN membrane.

**APPENDIX: Project Outputs** 

A. National Patent

## ព្យាព្រ

แบบ สป/สผ/อสป/003-ก หน้า 1 ของจำนวน 3 หน้า

for A rel	สำหรับเจ้าหน้าที่				
	วันรับคำขอ 19 ถึ:	เลขที่กำขอ			
	วันชิ้นคำขอ	103423			
คำขอรับสิทธิบัศร/อนุสิทธิบัศร	สัญลักษณ์ร่ามนกการประดิษฐ์ระหว่างประเทศ				
🖾 การประดิษฐ์	ใช้กับแบบผลิดภัณฑ์				
🗖 การออกแบบผลิตภัณฑ์	ประเภทผลิตภัณฑ์				
🔲 อนุสิทธิบัตร	วันประกาศใจษณา	เลขที่ประกาศโพษณา			
ซ้าพเข้าผู้ถงถายมือชื่อในคำขอรับสิทธิบัตร/อนุสิทธิบัตรนี้	วันออกสิทธิบัตร/อนุสิทธิบัตร	เลขที่สิทธิบัตร/อนุสิทธิบัตร			
ขอรับสิทธิบัคร/อนุสิทธิบัคร ตามพระราชบัญญัติสิทธิบัคร พ.ศ. 2522		4 9 9 4			
แก้ไขเพิ่มเดิม โดยพระราชบัญญัติสิทธิบัตร (ฉบับที่ 2) พ.ศ 2535 และ พระราชบัญญัติสิทธิบัตร (ฉบับที่ 3) พ.ศ 2542	ลายมือชื่อเจ้าหน้าที่				
<ol> <li>เรื่อที่แสดงถึงการประดิษฐ์/การออกแบบผลิตภัณฑ์</li> </ol>	<u> </u>				
เชื่อแผ่นสำหรับย่อยสถายสารพิษและเชื้อโรคด้วยแสง					
2.คำขอรับสิทธิบัตรการออกแบบผลิตภัณฑ์นี้เป็นคำขอสำหรับแบบผลิ	คภัณฑ์อย่ามดีควกับและเป็นดำ <b>ขอ</b> ลำ	<u> </u>			
ในงำนวน คำพอ ที่อื่นในคราวเคียรกัน					
<ol> <li>ลู้ขอรับสิทธิบัคร/อนุสิทธิบัคร และที่อยู่ (เลขที่ ถนน ประเทศ)</li> </ol>	3.1 สัญชาติ				
ดูที่หน้า 3	3.2 โทรศัพท์				
	3.3 โทรสาร				
	3.4 อีเมล์				
4.สิทธิในการขอรับสิทธิบัตร/อนุสิทธิบัตร	<u> </u>				
🔲 ผู้ประดิษฐ์หู้ออกแบบ 🗹 ผู้รับโอน 🔲 ผู้ขอรับสิทธิ	โดยเหตุอื่น				
5.คัวแทน(ถ้าปี)ที่อยู่ (เลขที่ อนน จังหวัด รหัสไปรษณีย์) 5.1 ด้วแทนเลขที่ 1453					
นายบงคล แก้วบหา	5.2 โทรศัพท์ 0-2218-2895-6				
สถาบันทรัพธ์สินทางปัญญาแห่งจุฬาลงกรณ์มหาวิทยาลัย รั้น 9 ห้อ อาคารเทพทวาราวดี คณะนิติศาสคร์ จุฬาลงกรณ์มหาวิทยาลัย	4 904 5.3 โทรสาร 0-2215-0	5.3 โทรสาร 0-2215-0115			
อ พารเทพทราร เวพ พณะนพทากพร ชุพ เถจารอนมหารทธากอ ถนนพญาไท แขวจวังใหม่ เขตปทุมวัน กรุงเทพฯ 10330	5.4 อีเมล์	5.4 อีเมล์			
6.ผู้ประดิษฐ์/ผู้ออกแบบผลิตภัณฑ์ และที่อยู่ ( เลขที่ ถนน ประเทศ )					
รองศาสตราจารย์ คร.สุจิตรา วงศ์เกษบจิตต์ และ นางสาวนพวรระ	น พระรรมชัช				
วิทธาลัยปีโดรเลียมและปีโดรเคมี จุฬาลงกรณ์มหาวิทธาลัย แขวงวัง	ใหม่ เขตปทุมวัน กรุงเทพฯ 10330				
7. คำขอรับสิทธิบัตร/อนุสิทธิบัตรนี้แอกจากหรือเกี่ยวข้องกับคำขอเดิม					
ผู้ขอรับสิทธิบัตร/อนุสิทธิบัตร ขอให้ถือว่าได้อื่นคำขอรับสิทธิบัตร/อนุสิทธิบัตรนี้ ในวันเดียวกับคำขอรับสิทธิบัตร					
***	ริบัตรนี้แยกจากหรือเกี่ยวจ๊องกับคำระ				
🔲 คำขอเดิมมีการประดิษฐ์หลายอย่าง 🔲 ถูกคัดค้านเนื่องจากผู้ขอใน่มีสิทธิ์ 🗀 ขอเปลี่ยนแปลงประเภทของสิทธิ์					

<u>พมายมหตุ</u> ในกรณีที่ไม่อาจระบุราชละเอ็จลได้ครบด้วน ให้จัดทำเป็นเอกสารแบบท้ายแบบทีมที่นี้โดยระบุทมายเลขกำกับข้อและทัวข้อที่แสดงราชละเอ็จด เพิ่มเดิมดังกล่าวด้วย

## แบบ สป/สผ/อสป๋/001-ก หน้า 2 ของจำนวน 3 หน้า

<ol> <li>การขึ้นกำขอนอกราชอาณารัก</li> </ol>	13						
วันชื่นคำขอ	เถขที่คำขอ	ประเทศ	สัญลักษณ์จันเนกการ ประดิษฐ์ระหว่างประเทศ	สถานะคำขอ			
8.1		-					
8.2							
ເນ							
8.4 🔲 ผู้ขอรับสิทธิบัคร/อนุสิทธิบัครขอสิทธิให้ถือว่าได้อื่นคำขอนี้ในวันที่ได้อื่นคำขอรับสิทธิบัคร/อนุสิทธิบัครในค่างประเทศเป็นครั้งแรกโดย							
🔲 ได้ชื่นเอกสารหลักฐานหรือมคำขอนี้ 🔲 ขอชื่นเอกสารหลักฐานหลังจากวันชื่นคำขอนี้							
9.การแสดงการประดิษฐ์ หรือการออกแบบผถิตภัณฑ์ ผู้ขอรับสิทธิบัตร/อนุสิทธิบัตร ได้แสดงการประดิษฐ์ที่หน่วยงานของรัฐเป็นผู้จัด							
วันแสดง	วันเปิดงานแสดง	ผู้รัก					
10.การประดิษฐ์เกี่ยวกับจุลรีพ							
10.1 เลขทะเบียนผ่ากเก็บ	10.2 วัน	ที่ฝากเก็บ	10.3 สถาบันฝากเก็บ	Missine.			
				-			
•			และจะจัดอื่นคำขอรับสิทธิบัด	ร/อนุสิทธิบัตรนีที่จัดทำ			
เป็นภาษาไทยภายใน 90 วัน นัก							
🗆 อังกฤษ 🗆 ฝรั่งเศ							
12.ผู้ของบลทรบคร/อนุลทรบเ หลังจากวันที่	เด็ดน เด็ดน		รับจดทะเบียน และประกาศใจเ	ผญาอนุสทธบครน			
กลงจมามหา ☐ ผู้ขอรับสิทธิบัตร/อนุสิทธิบั		ท.ศ แลง ในการประ	กาสโคเนคเว	·			
13.คำขอรับสิทธิบัตร/อนุสิทธิบั			ระกอบคำขอ				
ก. แบบพิมพ์คำขอ	2 หน้า		☑ เอกสารแสดงสิทธิในการขอรับสิทธิบัตร/อนุสิทธิบัตร				
<ol> <li>รายละเอียดการประดิษฐ์</li> </ol>			□ หนังสือรับรองการแสดงการประดิษฐ์/การออกแบบ				
หรือคำพรรณนาแบบผลิต	เภัณฑ์ 6 หน้า		ผถิตภัณฑ์				
ค. ข้อถือสิทษี 2	หน้า	่ ชานังส์	☑ หนังสือมอบอำนาจ				
ง, รูปเขียน รูป	หน้า	□ tena	🔲 เอกสารราชละเอียดเกี่ยวกับจุลจีพ				
<ol> <li>ภาพแสดงแบบผลิตภัณฑ์</li> </ol>	•	□ reua.	🔲 เอกสารการขอนับวันอื่นคำขอในค่างประเทศเป็นวันอื่น				
🗖 รัฤเล็ฉท รัเ	ป หน้า	ค้าขอ	คำขอในประเทศไทย				
🗆 ภาพถ่าย 📑	ป หน้า	□ lana	🗆 เอกสารขอเปลี่ยนแปลงประเภทของสิทธิ				
ฉ. บทสรูปการประดิษฐ์ ! หน้า 🖾 เอกสารอื่น ๆ							
15. จ้าหเจ้าขอรับรองว่า							
	เชยื่นจะรับสิทธิบัตร/ คบสั	ัทธิ์ทัพรบาก่อน					
<ul> <li>่ การประดิษฐ์นี้ไม่เคยอื่นขอรับสิทธิบัตร/ อนุสิทธิบัตรมาก่อน</li> <li>่ การประดิษฐ์นี้ได้พัฒนาปรับปรุงมาจาก</li></ul>							
			***************************************	***************************************			
16.ถายมือชื่อ ( 🔲 ผู้ขอรับสิทธิบัตร /อนุสิทธิบัตร; 🗹 ด้วแทน )							
אואלאין אם כוא דיאינבחוו מחפעטרע							

<u>หมายเทพ</u> บุคคลใดอื่นขอวับสิทธิบัตรการประดิษฐ์หรือการออกแบบหอิตภัณฑ์ หรืออนุสิทธิบัตร โดยการแฮพงร้อความอันเป็นเท็จแก่พนักงานเข้าหน้าที่ เพื่อให้ ได้ไปซึ่งสิทธิบัตรหรืออนุสิทธิบัตร ต้องระวางไทมชำลุกไม่เกินทกเดือน หรือปรับไม่เกินทำทันบาท หรือทั้งปรับ

แบบ สป/สม/อสป/ก01-ก หนัว 3 ของร้านวน 3 หนัว

3.ผู้ขอรับสิทธิบัคร/อนุสิทธิบัคร และที่อยู่ (เลขที่ ถนน บ่าะเทศ) จูทาลงกรณ์มหาวิทยาลัย อยู่ที่ จุฬาลงกรณ์มหาวิทยาลัย ถนนพญาไห แขวงวังใหม่ เขตปทุมวัน กรุงเทพฯ 10330 3.1 สัญหาติ ไทย 3.2 โทรศัพท์ 0-2218-2895-6 3.3 โทรสาร 0-2215-0115 สำนักงานกองทุนสนับสนุนการวิจัฮ อยู่ที่ ขั้น 14 อาการ เอส เอ็ม ทาวเวอร์ 979/17-21 ถนนพหลโตริน แขวงสามเสนใน เขคพญาไท กรุงเทพฯ 10400 3.1 ลัญชาติ ใหย 3.2 โทรศัพท์ 0-2298-0455 3.3 โทรสาร 0-2298-0476

#### หน้าที่ 1 ของจำนวน 6 หน้า

### รายละเชียดการประดิษฐ์

## ชื่อที่แสดงถึงการประดิษฐ์

5

10

15

20

25

30

เยื่อแผ่นสำหรับย่อยสลายสารพิษและเชื้อโรคด้วยแสง

ลักษณะและความมุ่งหมายของการประติษฐ์

การประดิษฐ์นี้เกี่ยวร้องกับเยื่อแผ่นลำหรับกระบวนการย่อยสลายสารพิษและเชื้อโรคด้วย แสง (Polymeric Membranes for Photocatalytic Degradation) ซึ่งประกอบด้วย โพลีอะคลิโลใน ไตรล์, ไดเมธิลฟอร์มามายด์ และ ไททาเนียมไดออกไซด์

ในอีกรูปแบบหนึ่งของการประดิษฐ์ เยื่อแผ่น ซึ่งประกอบด้วย โพลีไวนิลอะซิเตด, เตตระ ไฮโดรฟูแรน และ โททาเนียมไดออกไซด์

ในอีกรูปแบบหนึ่งของการประดิษฐ์ เยื่อแผ่น ซึ่งประกอบด้วย เซลลูโลสอะซิเตด, อะซีโตน และ ไททาเบียมไดออกไซด์

ความมุ่งหมายของการประดิษฐ์นี้ เพื่อนำไปใช้สลายสารอินทรีย์จำพวกเบนซีนและอนุ พันธ์ของเบนซีน ซึ่งเป็นสารก่อโรคมะเร็งภายในร่างกายมนุษย์ และยังใช้ย่อยสลายเชื้อโรคและ แบคทีเรีย เยื่อเลือกผ่านนี้มีส่วนผสมของสารไททาเนียมไดออกไซด์ที่มีพื้นที่ผิวสูงสำหรับ กระบวนการสลายสารอินทรีย์ด้วยแสง

## สาขาวิทยาการที่เกี่ยวข้องกับการบ่ระดิษฐ์

การประดิษฐ์นี้เกี่ยวร้องกับวิทยาการต่างๆ ได้แก่ การกำจัดน้ำเสียจากอุตสาหกรรมปิโตร เคมี โดยใช้กระบวนการแตกสลายสารอินทรีย์ด้วยแสง (Photocatalysis) กระบวนการเพิ่ม ไฮโดรเจนอะตอมแก้โมเลกุลของสารโพรไพร์ (Hydrogenation of propyne) กระบวนการเพิ่ม ออกซิเจนอะตอมแก่สารอินทรีย์ (Oxidation of organic compound) กระบวนการแยกแก็ส (Gas separation) และกระบวนการกำจัดแบคทีเรียด้วยแสง (Bactericidol activity of photocatalyst)

## ภูมิหลังของศิลปะหรือวิทยาการที่เกี่ยวข้อง

กระบวนการย่อยสลายสารอินทรีย์และสารอนินทรีย์ที่เป็นองค์ประกอบในน้ำทิ้งจากโรง งานอุตสาหกรรมจัดว่าเป็นประเด็นสำคัญมากในปัจจุบัน ดังนั้น จึงได้รับความสนใจจาก นักวิทยาศาสตร์มากมายในการศึกษาและวิจัย เพื่อจุดมุ่งหมายในการเพิ่มประสิทธิภาพของการ กำจัดน้ำเสีย รวมถึงการกำจัดน้ำเสียด้วยกระบวนการที่ใช้ต้นทุนต่ำ และย่อยสลายสารโดยไม่ เหลือสารพิษตกต้างในน้ำ นอกจากนี้ ในปัจจุบันมลภาวะจากสิ่งแวดล้อมเป็นปัญหาที่ต้องแก้ไข

#### หน้าที่ 2 ของจำนวน 6 หน้า

โดยเร็ว ซึ่งมลภาวะเหล่านี้ ได้แก่ อนุภาคสิ่งมีชีวิตชนาดเล็กที่พบในน้ำ และอากาศ การกำจัดเชื้อ โรคต่างๆ ในน้ำนั้นมีประโยชน์โดยตรงต่อการอุปโภค บริโภคของมนุษย์ อีกทั้งยังมีผลต่อการผลิต ผลิตภัณฑ์ต่างๆ ที่ใช้ในคน และลัตว์ กระบวนการการกำจัดเชื้อโรคในอากาศนั้นมีความสำคัญ มากในทางการแพทย์ ซึ่งต้องการความระมัดระวังเป็นอย่างสูงในเรื่องการปนเปื้อนของสารทาง ชีวภาพต่างๆ เนื่องจากในกระบวนการทดลองเกี่ยวกับสัตว์ พืช และคนนั้นมีโอกาสที่จะติดเชื้อได้ ง่าย กระบวนการกำจัดที่ใช้กันอย่างแพร่หลายในประเทศพัฒนาแล้วคือ วิธีการเพิ่มคลอรีน (Chlorination) การเติมโอโซน (Ozonation) และกระบวนการย่อยสลายด้วยแลง (Photocatalytic degradation) ซึ่งเป็นวิธีที่มีประสิทธิภาพและใช้ในระดับใหญ่

กระบวนการย่อยสลายสารด้วยแลงเป็นกระบวนการที่มีประสิทธิภาพสูงซึ่งใช้พลังงานแลง จากธรรมชาติและแลงที่ประสิษฐ์ชื่นเป็นแหล่งพลังงานที่ใช้ในกระบวนการย่อยสลายสารโดยใช้ สารไททาเนียมไดออกไซด์เป็นตัวเร่งปฏิกิริยา ซึ่งสารไททาเนียมไดออกไซด์นี้มีประสิทธิภาพสูงและ ใช้กันอย่างแพร่หลาย นอกจากนั้น ยังมีความเสถียรต่อสารเคมีสูง และที่ลำคัญมากกว่านั้น คือ เป็นสารที่ไม่เป็นพิษต่อสิ่งแวดล้อมอีกด้วย ในปัจจุบันกระบวนการย่อยสลายด้วยแลงที่มีสารไททา เนียมไดออกไซด์เป็นองค์ประกอบนั้นเป็นที่ยอมรับและใช้กันอย่างแพร่หลายรวมทั้งมีการศึกษา วิจัยและพัฒนาเพื่อใช้กับการใช้งานในรูปแบบใหม่ๆ เช่น หน้ากากกำจัดแบคทีเรีย (Environmental safety mask and respirator) ระบบกรองอากาศด้วยกระบวนการย่อยสลายสาร ด้วยแลง (Photocatalytic air filtration system) ระบบการกำจัดเชื้อรา จุลินทรีย์ เชื้อใจรัส และ แบคทีเรียในน้ำ (Deactivation of fungi, microorganisms, viruses and bacteria in water) นอกจากนี้ยังมีการใช้ปฏิกิริยาการย่อยสลายด้วยแลงที่มีสารไททาเนียมไดออกไซด์เป็นองค์ประ กอบในการสลายเซลล์มะเร็ง และเนื้องอก อีกทั้งยังใช้ในทางทันตกรรม คือ เป็นวัสดุจุดพัน เพื่อ ป้องกันการเจริญเติบโตของแบคทีเรียในช่องปาก และใช้เป็นองค์ประกอบในแปรงสีพันที่มีการ กระตุ้นด้วยแสง (Light activated tooth brush)

10

15

20

25

30

ข้อเสียของกระบวนการย่อยสลายสารด้วยแสงในน้ำเกิดขึ้น เนื่องจากต้องใช้กระบวนการ แยกของเหลวออกจากของแข็งที่เกิดจากการกระจายตัวของสารไททาเนียมไดออกไรด์ในน้ำ หลังจากเสร็จสิ้นกระบวนการย่อยสลายซึ่งกระบวนการนี้มีราคาแพง และใช้เวลานาน ในปัจจุบัน ได้มีการแก้ไขข้อเสียดังกล่าวโดยการใช้เยื่อแผ่นที่มีสารไททาเนียมไดออกไขด์กระจายตัวผังอยู่ใน เยื่อแผ่น ดังนั้น เยื่อแผ่นที่ประกอบด้วยสารไททาเนียมไดออกไขด์จึงเป็นที่สนใจและใช้กันอย่าง แพร่หลายเนื่องจากเยื่อแผ่นนี้มีลักษณะเฉพาะคือ มีปริมาณการไหลผ่านของน้ำสูง มีคุณสมบัติใน การเป็นสารกึ่งตัวนำ มีประสิทธิภาพในการย่อยสลายสารอินทรีย์ และมีความเสถียรต่อสารเคมีสูง อีกทั้งยังลดกระบวนการในการแยกสารไททาเนียมไดออกไขด์ออกจากสารผสมอีกด้วย

#### หน้าที่ 3 ของจำนวน 6 หน้า

กระบวนการยึดอนุภาคของสารไททาเนียมไดออกไซด์ลงบนวัสดุรองรับนั้นสามารถทำได้ หลายวิธี เช่น การพ่นอนุภาคไททาเนียมไดออกไซด์ลงบนแก้ว ซิลิกอน หรืออะลูมินา การเคลือบลง บนผิวของสารชีโอไลด์ หรือแผ่นสแตนเลสที่มีรูพรุนด้วยกระบวนการโซล-เจล แต่อย่างไรก็ตาม การ ใช้เยื่อแผ่นที่มีการเชื่อมกันระหว่างของผสม (Mixed Matrix Membrane) ซึ่งเป็นเยื่อแผ่นที่มีสารไท ทาเนียมไดออกไซด์เป็นองค์ประกอบนั้นกำลังเป็นที่สนใจในปัจจุบัน เนื่องจากมีความโดดเด่นคือ ความสามารถในการเลือกผ่านโมเลกุลสาร มีราคาถูก และมีวิธีการเตรียมที่ไม่ขับข้อน

## การเปิดเผยการประดิษฐ์โดยสมบูรณ์

10

15

20

25

30

การประดิษฐ์นี้เกี่ยวร้องกับเยื่อแผ่นลำหรับกระบวนการย่อยสลายสารพิษและเชื้อโรคด้วย แสง (Polymeric Membranes for Photocatalytic Degradation) ซึ่งประกอบด้วย โพลีอะคลิโลไน ไตรล์ 1-2 กรัม โดเมธิลฟอร์มามายด์ 8-10 กรัม และ ไททาเนียมไดออกไซด์ 0.1-0.2 กรัม

วิธีการเตรียมประกอบด้วย การผสมสารโพลีอะคลีโลในไตรดีในสารไดเมธิลพ่อร์มามายด์
คนสารผสมอย่างต่อเนื่องรวมทั้งให้ความร้อนแก่สารผสมที่อุณหภูมิ 50 องศาเซลเซียส จนกระทั่ง
โพลีอะคลิโลในไตรค์ละลายในไดเมททิลพ่อร์มามายด์อย่างสมบูรณ์ ตั้งสารทิ้งไว้จนเย็น จากนั้นจึง
ผสมสารไททาเนียมไดออกไซด์ที่มีพื้นที่ผิวสูงลงไป คนสารผสมอย่างต่อเนื่องจนกระทั้งสารไททา
เนียมไดออกไซด์กระจายตัวอย่างสม่ำเสมอในสารละลายของโพลีอะคลีโลในไตรค์ จากนั้นจึงเท
สารผสมลงบนกระจกผิวเรียบและใช้มีคล้ำหรับหล่อแบบปาคสารผสมให้เป็นแผ่น ตั้งสารไว้ที่
อุณหภูมิห้อง เป็นเวลา 30-60 นาที เพื่อให้เยื่อแผ่นคงรูป นำเยื่อแผ่นไปอบในตู้อบแบบสุญญากาศ
โดยปรับอุณหภูมิของตู้อบเป็น 40 องศาเซลเซียส เป็นเวลา 15-20 ชั่วโมง ต่อจากนั้นปรับอุณหภูมิ
เป็น 60 องศาเซลเซียส เป็นเวลา 2-3 ชั่วโมง ตามด้วยการเพิ่มอุณหภูมิเป็น 80 องศาเซลเซียส เป็น เวลา 2-3 ชั่วโมง

ในอีกรูปแบบหนึ่งของการประดิษฐ์ เยื่อแผ่นลำหรับกระบวนการย่อยสลายสารพิษและเชื้อ โรคด้วยแสง (Polymeric Membranes for Photocatalytic Degradation) ซึ่งประกอบด้วย โพลีไว นิลอะซิเตด 1-2 กรัม เตตระไฮโดรฟูแรน 8-10 กรัม และ ไททาเนียมไดออกไซด์ 0.1-0.2 กรัม

วิธีการเตรียมประกอบด้วย การผสมสารโพลีไวนิลอะริเตดในตัวทำละลายเตตระไฮโดรฟิว แรน คนสารผสมอย่างต่อเนื่องรวมทั้งให้ความร้อนแก่สารผสมที่อุณหภูมิ 50 องศาเซลเซียส จนกระทั่งสารทั้งสองละลายเร้าด้วยกันอย่างสมบูรณ์ ตั้งสารทิ้งไว้รอจบเย็นจากนั้นจึงผสมสาร ไททาเนียมโดออกไซด์ที่มีพื้นที่ผิวสูงลงไป คนสารผสมอย่างต่อเนื่องจนกระทั้งสารไททาเนียมได ออกไซด์กระจายตัวอย่างสม่ำเสมอในสารละลายของโพลีไวนิลอะริเตด เทสารผสมลงบนแผ่น เทฟลอนผิวเรียบและใช้มีดสำหรับหล่อแบบปาดสารผสมให้เป็นแผ่น ตั้งเยื่อแผ่นไว้ที่อุณหภูมิห้อง

#### หน้าที่ 4 ของจำนวน 6 หน้า

เป็นเวลา 15-20 ชั่วโมง น้ำเยื่อแผ่นไปอบในคู้อบแบบสุญญากาศโดยปรับอุณหภูมิของคู้อบเป็น 40-50 องศาเรลเรียล เป็นเวลา 2-3 ชั่วโมง

ในอีกรูปแบบหนึ่ง องการประดิษฐ์ เยื่อแผ่นสำหรับกระบวนการย่อยสลายสารพิษและเชื้อ โรคด้วยแสง (Polymeric Membranes for Photocatalytic Degradation) ซึ่งประกอบด้วย เซลลูโลสอะริเศด 1-2 กรัม อะรีโตน 8-10 กรัม และ ไททาเนียมไดออกไซด์ 0.1-0.2 กรัม

5

10

15

20

25

วิธีการเครียมประกอบด้วย การละลายเซลลูโลสอะซิเตดในตัวทำละลายอะซิโตน คนสาร ผสมอย่างต่อเนื่องจนกระทั่งสารทั้งสองละลายเข้าด้วยกันอย่างสมบูรณ์ ผสมสารไททาเนียมได ออกไซด์ที่มีพื้นที่ผิวสูงลงในสารละลายดังกล่าวพร้อมทั้งคนสารผสมอย่างต่อเนื่องจนกระทั้งสารไท ทาเนียมไดออกไซด์กระจายตัวอย่างสม่ำเสมอในสารละลายของเซลลูโลสอะซิเตด เทสารผสมลง บนกระจกผิวเรียบและใช้มีดสำหรับหล่อแบบปาดสารผสมให้เป็นแผ่น ตั้งสารไว้ที่อุณหภูมิห้องเป็น เวลา 2-5 นาที เพื่อให้เยื่อแผ่นคงรูป นำเยื่อแผ่นไปแข่ในน้ำเย็นเป็นเวลา 2-5 นาที จากนั้นจึงนำ เยื่อแผ่นแข่ในน้ำร้อน 90 องศาเซลเซียสเป็นเวลา 1-2 ชั่วโมง

สารไททาเนียมไดออกไซด์ เป็นสารซึ่งสังเคราะห์จากสารตั้งต้นไททาเนียมไตไอโรโพล พาโนลามีน

สารไททาเนียมไดออกไซด์ที่มีพื้นที่ผิวสูงเตรียมได้จากสารไททาเนียมไตไอโซโพลพาโน ลามีน ซึ่งประกอบด้วยขั้นตอนของการเผาสารละลายขันหนึดของไททาเนียมไตไอโซโพลพาโนลา มีนด้วยเตาเผาที่อุณหภูมิ 600 องศาเซลเซียส เป็นเวลา 2 ชั่วโมงด้วยอัตราเร็วของการเพิ่ม อุณหภูมิ 0.1-0.5 องศาเซลเซียสต่อนาที นำสารที่ได้มาบด

สารไททาเนียมไตรไอโชโพลพาโนลามีนได้จากการลังเคราะห์สารไททาเนียมไดออกไซด์
และไตรไอโชโพลพาโนลามีน ซึ่งประกอบด้วยขั้นตอนของการผสมสารประกอบไททาเนียมได
ออกไซด์ 2-2.5 กรัม ไตรไอโชโพลพาโนลามีน 9-10 กรัม ไตรเอธิลีนเตตระมีน 3-4 กรัม และเอธิลีน ไกลคอล 20-25 มิลลิลิตร คนสารละลายผสมพร้อมทั้งให้ความร้อน กลั่นสารละลายที่อุณหภูมิ ประมาณ 200 องศาเซลเซียส เป็นเวลา 1 วัน จากนั้นจึงทำการกลั่นเพื่อกำจัดเอธิลีนไกลคอล และ ไตรเอธิลีนเตตระมีนที่มีมากเกินพอที่อุณหภูมิ 150 องศาเซลเซียส

สมบัติในการทนต่อสาร 4-ในโดรพีนอล และรังสียูวีของเยื่อแผ่นทั้งสามชนิด สรุปไว้ใน ตารางดังต่อไปนี้

#### หน้าที่ 5 ของจำนวน 6 หน้า

- \* ปริมาณสารชินทรีย์ทั้งหมด (Total Organic Carbon)
- \*\* 4-ในโตรฟีนอล (4-nitrophenol)

ชนิดของเยื่อแผ่น และสภาวะในการ ทดสอบ	ค่า TOC" เริ่มต้น (มิลลิกรัมต่อลิตร)	ค่า TOC หลังจากทคสอบเป็นเวลา 6 ชั่วโมง (มิลลิกรัมต่อลิตร)
โพลีอะคลิโลในไตรล์+น้ำ+รังสียูวี	0	0
เขลลูโลสอะชิเตด+น้ำ+รังสียูรี	0	0
โพลีไวนิลอะซิเตด+น้ำ+รังสียูวี	o	11.79
โพลีอะคลิโลไนไตรล์+4-NP**+รังสียูวี	22.35	22.34
เชลดูโลสอะชิเคต+4-NP+รังสียูวี	22.35	22.35
โพลีใวนิลอะซิเตด+4-NP+รังสียูวี	22.35	32.22
โพลีอะคลิโลไนไ <b>ตรล์+</b> 4-NP	22.35	22.36
เรลลูโลสอะริเภค+4-NP	22.35	22.35
โพลีโวนิลอะริเศด+4-NP	22.35	36.44

#### 5 ตัวอย่าง

10

15

ตัวอย่างที่จะกล่าวถึงต่อไปนี้ มีวัตถุประสงค์เพื่อที่จะให้เกิดความเข้าใจในการประดิษฐ์ให้ มากขึ้น ตัวอย่างถูกตั้งใจที่จะให้เป็นแบบแสดงให้เห็นเพื่ออธิบายเท่านั้น และไม่สามารถถือเป็น การจำกัดขอบเขตการประดิษฐ์

ตัวอย่างที่ 1 การเตรียมเยื่อแผ่นจากสารผสมสูตร ! รวมถึงการทดสอบการทนต่อสาร 4-ในโตร ฟินอล และรังสียูวี

รั้นแรก:1.<u>การสังเคราะห์สารไททาเนียมไตรไอโซโพลพาโนลามีนจากไททาเนียมได</u> ออกไซต์ และไตรไอโซโพลพาโนลามีน

ผสมสารประกอบไททาเนียมโดออกไซด์ 2-2.5 กรัม โตรไอโซโพลพาโนลามีน 9-10 กรัม โตรเอธิลีนเตตระมีน 3-4 กรัม และเอธิลีนไกลคอล 20-25 มิลลิลิตร คนสารละลายผสมพร้อมทั้งให้ ความร้อน กลั่นสารละลายที่อุณหภูมิประมาณ 200 องศาเซลเซียสเป็นเวลา 1 วัน จากนั้นจึงทำ

#### หน้าที่ 6 ของจำนวน 6 หน้า

การกลั่นเพื่อกำจัดเอธิลีนไกลดอล และไตรเอธิลีนเตตระมีนที่มีมากเกินพอที่อุณหภูมิ 150 องศา เขตเขียส

ตรวจสอบสารละลายข้นหนืดที่มีองค์ประกอบของสารผลิตภัณฑ์รวมกับสารไตรไอโซโพล พาโนลามีนที่มากเกินพอ ด้วยเครื่อง FT-IR, TGA และ FAB<sup>\*</sup>-MS

2. การเตรียมสารไททาเนียมที่มีพื้นที่ผิวสูงจากสารไททาเนียมไดไอโซโพลพาโนลามีน เผาสารละลายรับหนีดของไททาเนียมไดไอโซโพลพาโนลามีนด้วยเดาเผาที่อุณหภูมิ 600 องศาเซลเชียสเป็นเวลา 2 ชั่วโมงด้วยอัตาเร็วของการเพิ่มอุณหภูมิ 0.1-0.5 องศาเซลเซียสต่อนาที นำสารที่ได้มาบด ตรวจสอบผลิตภัณฑ์ด้วยเครื่อง XRD, SEM และ TGA

ขั้นที่สอง: การเตรียมเยื่อแผ่นโพลีอะคลิโลโนไตรด์

ผสมสารโพลีอะคลีโลในไตรด์ (1-2 กรัม) ในสารไดเมธิลพ่อร์มามายด์ (8-10 กรัม) คนสาร ผสมอย่างต่อเนื่องรวมทั้งให้ความร้อนแก่สารผสมที่อุณหภูมิ 50 องศาเซลเซียสจนกระทั่งโพลีอะคลีโลในไตรด์ละสายในไดเมททิลพ่อร์มามายด์อย่างสมบูรณ์ ตั้งสารทิ้งไว้จนเย็นจากนั้นจึงผสมสาร ไททาเนียมไดออกไซด์ที่มีพื้นที่ผิวสูงประมาณ 0.1-0.2 กรัม ลงไป คนสารผสมอย่างต่อเนื่องจนกระ ทั้งสารไททาเนียมไดออกไซด์กระจายตัวอย่างสม่ำเสมอในสารละลายของโพลีอะคลีโลในไตรด์ จากนั้นจึงเทสารผสมลงบนกระจกผิวเรียบและใช้มีดสำหรับหล่อแบบปาดสารผสมให้เป็นแผ่น ตั้ง สารไว้ที่อุณหภูมิห้องเป็นเวลา 30-60 นาทีเพื่อให้เยื่อแผ่นคงรูป นำเยื่อแผ่นไปอบในตู้อบแบบ สุญญากาศโดยปรับอุณหภูมิของตู้อบเป็น 40 องศาเซลเซียสเป็นเวลา 15-20 ชั่วโมง ต่อจากนั้น ปรับอุณหภูมิเป็น 60 องศาเซลเซียสเป็นเวลา 2-3 ชั่วโมง ตามด้วยการเพิ่มอุณหภูมิเป็น 80 องศา เซลเซียสเป็นเวลา 2-3 ชั่วโมง

ขึ้นที่สาม: <u>การทดสอบความทนต่อสาร 4-ในโตรฟินอล และรังสียูวี</u>

แข่เยื่อแผ่นโพลีอะคลีโลไนโตรด์ลงในสารละลาย 4-ไนโตรฟินอลที่มีความเข้มข้น 40-60 มิลลิกรัมต่อลิตร หรือน้ำกลั่น เปรียบเทียบระหว่างผลที่เกิดจากการฉายและไม่ฉายรังสียูวี ดูดสาร ออกมาทดสอบการเปลี่ยนแปลงค่า TOC หลังจากทำการทดลองเป็นเวลา 3-6 ชั่วโมงเพื่อ ตรวจสอบปริมาณสารอินทรีย์ที่หลุดออกมาจากเยื่อแผ่นโพลีอะคลิโลไนไตรด์

วิธีการในการประดิษฐ์ที่ดีที่สุด

เหมือนกับที่ได้กล่าวไว้แล้วในหัวร้อการเปิดเผยการประดิษฐ์โดยสมบูรณ์

25

5

10

15

20

#### หน้าที่ 1 ของจำนวน 2 หน้า

#### ช้อถือสิทธิ

 เยื่อแผ่นสำหรับกระบวนการย่อยสลายสารพิษและเชื้อโรคด้วยแสง ซึ่งประกอบด้วย โพลีอะคลิโลไนไตรส์ 1-2 กรัม ไดเมธิลฟอร์มามายด์ 8-10 กรัม และ ไททาเนียมไดออกไรด์ 0.1-0.2 กรับ

5

10

15

 เยื่อแผ่นสำหรับกระบวนการย่อยสลายสารพิษและเชื้อโรคด้วยแลง ซึ่งประกอบด้วย โพลีไว นิลอะซิเตด 1-2 กรัม เตตระไฮโดรฟูแรน 8-10 กรัม และ ไททาเนียมไดออกไซด์ 0.1-0.2 กรัม

20

25

4. วิธีการเตรียมเยื่อแผ่นตามข้อถือสิทธิ 3 ซึ่งประกอบด้วย การผลมสารโพลีไวนิลอะซิเตดใน ตัวทำละลายเตตระไฮโดรฟิวแรน คนสารผสมอย่างต่อเนื่องรวมทั้งให้ความร้อนแก่สารผสม ที่อุณหภูมิ 50 องศาเซลเซียสจนกระทั่งสารทั้งสองละลายเข้าด้วยกันอย่างสมบูรณ์ ตั้งสาร ทิ้งไว้รอจนเย็นจากนั้นจึงผสมสารไททาเนียมไดออกไซด์ที่มีพื้นที่ผิวสูงลงไป คนสารผสม อย่างต่อเนื่องจนกระทั้งสารไททาเนียมไดออกไซด์กระจายตัวอย่างสม่ำเสมอในสารละลาย ของโพลีไวนิลอะซิเตด เทสารผสมลงบนแผ่นเทพ่ลอนผิวเรียบและใช้มีดสำหรับหล่อแบบ ปาดสารผสมให้เป็นแผ่น ตั้งเยื่อแผ่นไว้ที่อุณหภูมิห้องเป็นเวลา 15-20 ชั่วโมง นำเยื่อแผ่นไป อบในต้อบแบบสุญญากาศโดยปรับอุณหภูมิของต้อบเป็น 40-50 องศาเซลเซียส เป็นเวลา 2-3 ชั่วโมง

#### หน้าที่ 2 ของจำนวน 2 หน้า

- เยื่อแผ่นสำหรับกระบวนการย่อยสลายสารพิษและเรื้อโรคด้วยแสง ซึ่งประกอบด้วย
   เชลลูโลสอะซิเตด 1-2 กรัม อะซีโตน 8-10 กรัม และ ไททาเนียมไดออกไรด์ 0.1-0.2 กรัม
- 6. วิธีการเตรียมเยื่อแผ่นตามข้อถือสิทธิ 5 ซึ่งประกอบด้วย การละลายเซลลูโลสอะซิเตดในตัว ทำละลายอะซิโตน คนสารผสมอย่างต่อเนื่องจนกระทั่งสารทั้งสองละลายเข้าด้วยกันอย่าง สมบูรณ์ ผสมสารไททาเนียมไดออกไซด์ที่มีพื้นที่ผิวสูงลงในสารละลายดังกล่าวพร้อมทั้งคน สารผสมอย่างต่อเนื่องจนกระทั้งสารไททาเนียมไดออกไซด์กระจายตัวอย่างสม่ำเสมอใน สารละลายของเซลลูโลสอะซิเตด เทสารผสมลงบนกระจกผิวเรียบและใช้มีดลำหรับหล่อ แบบปาดสารผสมให้เป็นแผ่น ตั้งสารไว้ที่อุณหภูมิห้องเป็นเวลา 2-5 นาที เพื่อให้เยื่อแผ่นคง รูป นำเยื่อแผ่นไปแช่ในน้ำเย็นเป็นเวลา 2-5 นาที จากนั้นจึงนำเยื่อแผ่นแช่ในน้ำร้อน 90 องศาเซลเซียสเป็นเวลา 1-2 ชั่วโมง
  - 7. เยื่อแผ่นตามข้อถือสิทธิ 1 หรือ 3 หรือ 5 ที่ซึ่งไททาเนียมโดออกไซด์เป็นสารซึ่งสังเคราะห์ จากสารตั้งต้นไททาเนียมไตไอโซโพลพาโนลามีน
  - 8. วิธีการตามชื่อถือสิทธิ 2 หรือ 4 หรือ 6 ที่ซึ่งสารไททาเนียมไดออกไซด์ที่มีพื้นที่ผิวสูงเตรียมได้ จากสารไททาเนียมไตไอโซโพลพาโนลามีน ซึ่งประกอบด้วยขั้นตอนของการเผาสารละลาย ขันหนืดของไททาเนียมไตไอโซโพลพาโนลามีนด้วยเตาเผาที่อุณหภูมิ 600 องศาเซลเขียส เป็นเวลา 2 ขั่วโมงด้วยอัตราเร็วของการเพิ่มอุณหภูมิ 0.1-0.5 องศาเซลเขียสต่อนาที นำสาร ที่ได้มาบด
- 9. วิธีการตามข้อถือสิทธิ 7 ที่ซึ่งสารไททาเนียมไตรไอโซโพลพาโนลามีนได้จากการลังเคราะห์ สารไททาเนียมไดออกไซด์ และไตรไอโซโพลพาโนลามีน ซึ่งประกอบด้วยขั้นตอนของการ ผสมสารประกอบไททาเนียมไดออกไซด์ 2-2.5 กรัม ไตรไอโซโพลพาโนลามีน 9-10 กรัม ไตร เอธิลีนเตตระมีน 3-4 กรัม และเอธิลีนไกลคอล 20-25 มิลลิลิตร คนสารละลายผสมพร้อมทั้ง ให้ความร้อน กลั่นสารละลายที่อุณหภูมิประมาณ 200 องศาเซลเซียส เป็นเวลา 1 วัน จากนั้นจึงทำการกลั่นเพื่อกำจัดเอธิลีนไกลคอล และไตรเอธิลีนเตตระมีนที่มีมากเกินพอที่ อุณหภูมิ 150 องศาเซลเซียส

5

10

15

20

25

## หน้าที่ 1 ของจำนวน 1 หน้า

กมสร์กุบเลกุระษศสั

การประดิษฐ์นี้เกี่ยวร้องกับเยื่อแผ่นสำหรับกระบวนการย่อยสลายสารพิษและเชื้อโรคด้วย แสงที่ใช้ไททาเนียมไดอถูกไซด์เป็นตัวเร่งปฏิกิริยา B. Photocatalytic Membrane of a Novel High Surface Area TiO<sub>2</sub> Synthesized from Titanium Triisopropanolamine Precursor

AOC1108

APPLIED ORGANOMETALLIC CHEMISTRY Appl. Organisacial. Chem. 2006; 20: 000-000 Published online in Wiley InterScience (www.interscience.wiley.com) DOI:10.1002/acc.1108

Materials, Nanoscience and Catalysis



## Photocatalytic membrane of a novel high surface area TiO<sub>2</sub> synthesized from titanium triisopropanolamine precursor

N. Phonthammachai<sup>1</sup>, E. Gulari<sup>2</sup>, A. M. Jamieson<sup>3</sup> and S. Wongkasemjit<sup>1</sup>\*

<sup>1</sup>The Petroleum and Petrochemical College, Chulalongkorn University, Bangkok, Thailand

<sup>2</sup>Department of Chemical Engineering, University of Michigan, Ann Arbor, Michigan, USA

Received 4 October 2005: Revised 25 October 2005; Accepted 10 April 2006

Photocatalytic membrane was successfully prepared using an efficiently high surface area TiO2 catalyst, dispersed into polyacrylonitrile matrix. The catalyst was directly synthesized using titanium triisopropanolamine as a precursor. The membranes were characterized using FT-IR, TGA, SEM and their photocatalytic performance tested, viz. stability, permeate flux and photocatalytic degradation of 4-NP. We find that polyacrylonitrile is an effective matrix, showing high stability and low permeate flux. The amount of  $TiO_2$  loaded in the membrane was varied between 1, 3 and 5 wt% to explore the activity and stability of membranes in the photocatalytic reaction of 4-NP. As expected, the higher the loading of TiO2 loaded, the higher the resulting catalytic activity. Copyright @ 2006 John Wiley & Sons, Ltd.

KEYWORDS: mixed matrix membrane; photocatalysis; 4-nitrophenol; titanium triisopropanolamine

### 1 INTRODUCTION

3

10

11

12

14

15

17

18

The use of mixed matrix membranes (MMM), i.e. membranes containing microencapsulated TiO2, is of increasing interest because of their high selectivity combined with outstanding separation performance, processing capabilities and low cost, when polymers are used as the matrix. Many researchers 1-4 have explored ways to develop and facilitate the separation process, using very thin microencapsulated membranes to allow for high fluxes. Such a membrane must have a high volume fraction of homogeneously distributed encapsulated particles in a defect- and void-free polymer matrix.5 Polymeric membraries are not appropriate for use in membrane reactor applications where high temperatures are needed for reaction. Thus, application of MMM for catalysis of low temperature reactions has become a main topic for many researchers, examples being hydrogenation

\*Correspondence to: S. Wongkasemjit, The Petroleum and Petro-chemical College, Chulalongkorn University, Bangkok, Thailand. E-mail: dnujitra@chula.ac.th 19 20

Contract/grant sponsor: Postgraduate Education and Research Program in Petroleum and Petrochemical Technology Fund. Contract/grant sponsor: Ratchadapisale Sompote Fund. Contract/grant sponsor: Chulalongkorn University. Contract/grant sponsor: Thailand Research Fund. 21 22

23

of propyne,6 photomineralization of n-alkanoic acids,7 wet 25 air oxidation of dyeing wastewater, and photocatalytic oxidations.8-11

The heterogeneous photocatalysis process harnesses radiant energy from natural or artificial light sources to degrade organic pollutants into their mineral components.12 TiO2 is a well-established catalyst for photocatalytic degradation due to its combination of high activity, chemical stability and non-toxic properties. Photocatalytic degradation generally occurs via production of OH° radicals. The organic pollutant is attacked by hydroxyl radicals and generates organic radicals or intermediates. 13-16 The main drawback to practical implementation of the photocatalysis method arises from the need for an expensive liquid-solid separation process due to the formation of milky dispersions upon mixing the catalyst powder with water.17

Currently, this drawback is solved by the use of a TiO2 membrane, consisting of fine TiO2 particles dispersed in a porous matrix. Such titania membranes have attracted a great deal of attention in recent years due to their unique characteristics, including high water flux, semiconducting properties, efficient photocatalysis and chemical resistance relative to other membrane materials, such as silica and y-alumina.#



30

30

44

<sup>&</sup>lt;sup>3</sup>Department of Macromolecular Science, Case Western Reserve University, Cleveland, Ohio, USA



76

77

78

79

80

81

90

91

102

103

104

105

N. Phonthammachai et al.

To obtain a high photocatalytic activity, the surface area of catalyst is very important. Thus, in our work, thermally stable TiO<sub>2</sub> with high surface area is synthesized from moisturestable titanium triisopropanolamine. The performance of this material as a component of an MMM was evaluated in a photocatalytic membrane reactor, using 4-nitrophenol as a model substrate, with regard to stability tests and TiO2 loading.

12

14

15

16

17

18

21

23

25

26

27

28

29

30

31

32

33

34

35

36

37

38

39

40

41

12 43

44

45

46

17

48

49

50

51

52

3

5

### **EXPERIMENTAL**

### **Materials**

13 Titarium dioxide (surface area 12 m²/g) was purchased from Sigma-Aldrich Chemical Co. Inc. (USA) and used as received. Ethylene glycol (EG) was purchased from Malinckrodt Baker Inc. (USA) and purified by fractional distillation at 200°C under nitrogen atmosphere before use. Triethylenetetramine 19 (TETA) was purchased from Facai Polytech. Co. Ltd. 20 (Bangkok, Thailand) and distilled under vacuum (0.1 mmHg) at 130°C prior to use. Triisopropanolamine (TIS) was purchased from Sigma-Aldrich Chemical Co. Inc. (USA). 4 22 Nitrophenol was purchased from Sigma-Aldrich Chemical 24 Co. Inc. (USA).

### Titanium tri-isopropanolamine precursor preparation and characterization

A mixture of TiO2 (2 g. 0.025 mol), triisopropanolamine (9.55 g, 0.05 mol) and triethylenetetramine (3.65 g, 0.0074 mol) was stirred vigorously in excess ethylene glycol (25 cm<sup>3</sup>) and heated to 200°C for 24 h. The resulting solution was centrifuged to separate the unreacted TiO2. The excess EG and TETA were removed by vacuum distillation at 150 °C to obtain a crude precipitate. The product was characterized using FIIR, FAB+-MS and TGA. Fourier transform infrared spectra (FT-IR) were recorded on a VECOR3.0 Bruker spectrometer with a spectral resolution of 4/cm. Thermal gravimetric analysis (TGA) was carried out using a Perkin Elmer thermal analysis system with a heating rate of 10°C/min over a 30-800°C temperature range. The mass spectrum was obtained on a Fison Instrument (VG Autospec-ultima 707E) using the positive fast atomic bombardment mode (FAB+-MS) with glycerol as the matrix, cesium gun as initiator and cestum todide (CsI) as a standard for peak calibration.

FT-IR: 3400 (\(\sqrt{OH}\), 2927-2855 (\(\sqrt{C-H}\), 1460 (\(\delta C-H\) of CH2 group), 1379 (&C-H of CH3 group), 1085 (JC-O-Ti), 1020 (&C-N) and 554/cm (JTi-O); TGA: decomposition transition at 365°C with 16.60% ceramic yield (theoretical ceramic yield of 18.65%); FAB+-MS: Ti([OCHCH3CH2]2N[CH2CHCH3OH])22H+ at m/e 428.

### High surface area TiO2 preparation and characterization

53 After removal of any excess solvent from titanium tritsopropanolamine precursor, the precursor was transferred to 55 a crucible and calcined at 600°C for 2 h at heating rate of 0.25°C/min. TiO<sub>2</sub> was characterized by various techniques. The XRD pattern was obtained using a D/MAX-2200H 58 Rigaku diffractometer with CuKer radiation on specimens 59 prepared by packing sample powder into a glass holder. The 60 diffracted intensity was measured by step scanning in the 61 20 range of 5° to 90°. Thermal stability was characterized on a Perkin Emer thermal analysis system with a heating rate 63 of 10°C/min over 30-800°C temperature range. Samples 64 pyrolyzed at 600°C were analyzed using SEM by attach- 65 ment onto aluminum stubs after coating with gold via vapor deposition. Micrographs of the pyrolyzed sample surfaces were obtained at ×7500 magnification. Specific surface area and nitrogen adsorption-desorption were determined using an Autosorp-1 gas sorption system (Quantachrome Corporation) via the Brunauer-Emmett-Teller (BET) method. A gaseous mixture of nitrogen and helium was allowed to flow through the analyzer at a constant rate of 30 cm3/min. Nitrogen was used to calibrate the analyzer and also used as the adsorbate at liquid nitrogen temperature. The samples were thoroughly outgassed for 2 h at 150°C, prior to exposure to the adsorbent gas.

### Membrane preparation and characterization

A 10 wt% mixture of polyacrylonitrile powder in dimethylformamide (DMP) was vigorously stirred at 50°C until homogeneous. A specified amount of TiO2 was added to 83 the stirred polymer solution. Partial vacuum was applied 84 for a brief duration to ensure the removal of air bubbles. 85 The mixture was then coated on a clean glass plate using a 86 casting knife. The resulting membrane was allowed to set for 2 min before being dried in a vacuum oven at 40°C overnight following by 60°C for 2 h and 80°C for 2 h. The prepared membrane with thickness of 15 µm was cut into a circular shape with a diameter of 6 cm.

The membrane made was characterized using SEM and 92 TGA. The morphology of membranes was analyzed by attachment onto aluminum stubs and coated with gold via vapor deposition. The membranes were frozen in liquid nitrogen and fractured to examine the cross-sectional areas. The samples were characterized on a Jeol 5200-2AE (MP 97 15152001) scanning electron microscope. The samples were 98 also analyzed using Perkin Elmer thermal analysis system with a heating rate of 10°C/min over 30-500°C temperature 100 range to determine the organic residue in the prepared 101 membranes

### Stability tests of prepared membranes

The experiment was carried out to check the stability 106 of prepared polymeric membrane (PAN) by placing the 107 prepared membranes in a Petri dish containing either distilled 108 water or 40 ppm 4-NP solution with and without irradiation 109 for 6 h. The solutions were then withdrawn and analyzed for  $_{110}$ total organic carbon (TOC) to verify the organic components  $\frac{1}{111}$ released from the membrane.

Copyright © 2006 John Wiley & Sons, Ltd.

Appl. Organometal. Chem. 2006; 20: 000-000 DOE 10.1002/40c

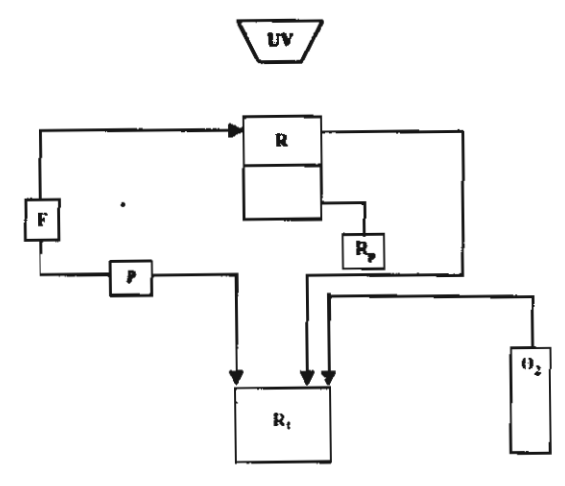


Figure 1. Schematic diagram of photocatalytic membrane reactor (F. flowmeter; R, reactor;  $R_p$ , permeate reservoir;  $R_t$ , recirculating tank; and P, peristatitic pump).

Photocatalytic decomposition of 4-nitrophenol

The photocatalytic reactions were carried out in a 1000 ml continuous batch glass reactor, Fig. 1, with gas inlet and outlet at an O<sub>2</sub> flow rate of 20 ml/min. A cooling water jacket was used to maintain the temperature at 30 °C. The suspensions and membrane were illuminated using a 100 W Hg Philip UV lamp. The concentration of 4-NP used was 40 ppm and the solution was continuously stirred. The obtained permeate was removed at 1 h intervals and analyzed to determine the concentration of 4-NP using a Shimadzu UV-240 spectrophotometer. For different pH value, H<sub>2</sub>SO<sub>4</sub> was used to adjust the pH value measured using an Ecoscan pH meter.

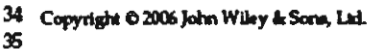
### **RESULTS AND DISCUSSION**

### TiO<sub>2</sub> catalyst preparation

Я

Ø

High surface area TiO<sub>2</sub> catalyst was characterized using XRD, TGA, BET and SEM to confirm the presence of the active anatase phase of TiO<sub>2</sub>. The TGA thermogram (not given) illustrates absence of organic species, meaning the formation of pure TiO<sub>2</sub>, while the XRD pattern shown in Fig. 2, exhibits diffraction peaks at 29 = 25.28, 37.94, 47.98, 54.64, 62.58, 69.76, 75.26 and 82.72. The average grain size of calcined TiO<sub>2</sub> calculated from Scherrer equation, is 12.42 nm. The SEM micrograph (not shown) presents similar particle morphology of the prepared anatase phase of TiO<sub>2</sub> to those in the literature. <sup>19-28</sup> The surface area measurement shows a high surface area of 163 m<sup>2</sup>/g; also, the nitrogen adsorption-desorption isotherm of this material exhibits type IV character (Fig. 3), indicative of a mesoporous structure.



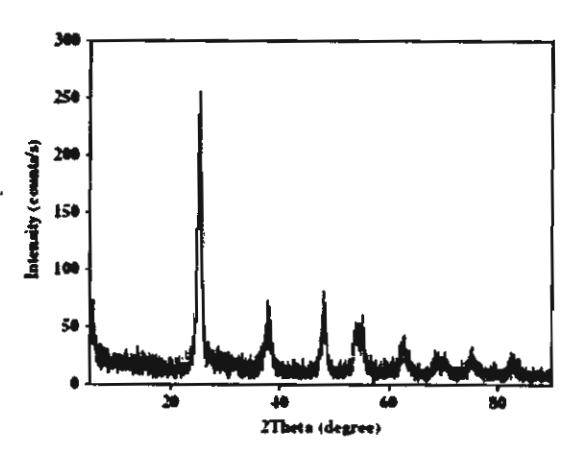


Figure 2. XRD pattern of the anatase phase of the prepared TiO<sub>2</sub> catalyst after calcinations of the precursor at 600 °C for 2 h

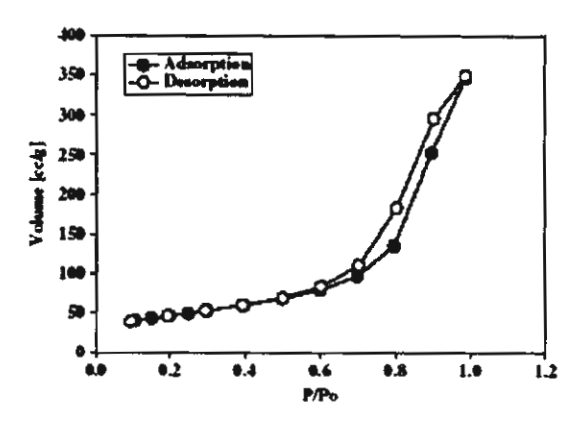


Figure 3. Ntrogen adsorption-desorption isoterm for the prepared mesoporous titania calcined at 600 °C.

### Membranes preparation

The prepared mixed matrix membranes were characterized with respect to their purity using TGA thermogram and their morphology using scanning electron microscopy (SEM). The TGA thermogram (not given) gives only one transition at around 300 °C, referring to the degradation of PAN membrane, <sup>22,23</sup> respectively. An SEM micrograph of the surface of the prepared membrane is shown in Fig. 4(a). When the TiO<sub>2</sub> particles are immobilized within the polymeric matrix, the micrographs seveal no evidence for the presence of voids between the polymer and TiO<sub>2</sub>, implying that the membranes are dense. TiO<sub>2</sub> particles are well distributed across the surface. As varying the percentage of TiO<sub>2</sub> between 1, 3 and 5 wt%, morphological analysis by SEM, as shown in

Appl. Organometal. Chem. 2006; 20: 000-000 DOI: 10.1002/aoc

Figure 4. SBM micrographs of mixed matrix membranes using (a) polyacrylonitrile (PAN), (b) PAN + 1 wt% TiO<sub>2</sub>, (c) PAN + 3 wt%  $TIO_2$  and (c) PAN + 5 wt%  $TIO_2$ .

Fig. 4(b-d), indicates, TiO2 particles are dispersed throughout the PAN matrix at all loadings.

### Stability tests of prepared membranes

3 4

8

10

11

12

13

14

15

16

17 18

19 20 21

22

23

24

25

The stability of the prepared PAN membranes is summarized in Table 1, presenting the TOC results of the tested membrane. It was found that the PAN membrane is undoubtedly stable even under irradiation conditions.

The photocatalytic degradation of 4-nitrophenol The photocatalytic activity of the PAN membrane was assessed using the photoreactor, employing 1 wt% immobilized photocatalyst TiO2, oxygen flow rate of 20 ml/min, 4-NP flow rate of 30 ml/min and 4-NP concentration of 40 ppm at pH 3.9.10,24 The permeate flux data (not shown) indicate that the prepared PAN membrane has constant low

Table 1. The stability tests of the prepared membranes

Membrane type and condition	TOC value at initial (ppm)	TOC value after 6 h (ppm)
PAN + H <sub>2</sub> O + UV	0	0
PAN +4NP+UV	22.35	22.34
PAN + 4-NP	22.35	22.36

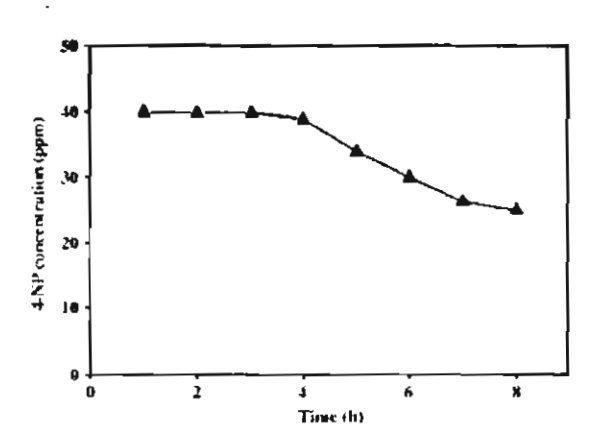


Figure 5. The degradation of 4-NP with the reaction time of the PAN membranes performed at pH 3.

permeate flux level, 5.31 1/h m2. The efficiency of the PAN 26 membrane for photocatalytic degradation of 4-NP is illus- 27 trated in Fig. 5, which indicates that, at 1 wt% Ti loading in 28 PAN membrane, the degradation of 4-NP occurs faster after 4 h irradiation.

3

5

tn

11

12

13

15

16

17

18

19

20

21

22

23

24

25 26

27

29

30

31

32

33

34

35

36

37

### Effect of various amounts of TiO2 in PAN membrane on the photocatalytic degradation of 4-nitrophenol

Materials, Nanoscience and Catalysis

4-NP auto-photolysis was first carried out without the mixed matrix membrane and showed no degradation. The experiment was thus performed to study the permeate flux of PAN membranes at the three loading levels, 1, 3 and 5 wt% of TiO2 (Fig. 6). We found that the flux is constant for all three samples, and increases with the amount of TiO2 from 5.3, to 8.1 to 12.7 1/h m2, respectively. In Fig. 7, the efficiency of degradation of 4-NP at the three loading levels of TiO2 is reported. The decrease of 4-NP at 3 and 5% loadings appears to be faster than at 1%. The reason may be that the TiO2 loading is too low to see any differences in the degree of degradation of 4-NP. However, when compared with literature results,11 performed at much higher loadings of TiO2, it appears that these membranes show a higher level of catalytic activity.

Commercial TiO2 (Degussa P25) was also studied for comparison with our TiO2 at loading level of 3 wt%. The result, see Fig. 8, indicates no permeation of 4-NP through a membrane prepared using commercial TiO2 and the efficiency of degradation of 4-NP measured from the retentate of two membranes shows that the degradation of 4-NP in the membrane prepared using our TiO2 is distinguishably lower.

### Effect of pH on degradation of 4-nitrohenol

From the literature, the rate of 4-NP decomposition at lower pH is faster and shows the highest activity at pH 3.9,16.36 Therefore, we compare the experiment of 4-NP solution at pH = 3 (adjust pH value of 4-NP solution by H2SOa) with pH = 7 (without the pH adjustment of 4-NP solution). It was found that the results indeed are the same after irradiation, see Fig. 9. The 4-NP concentration at pH = 3declines sharply when applied the UV irradiation and reaches to the complete degradation after 8 h reaction time. Only 25% degradation occurs in the solution having pH = 7. Figure 10

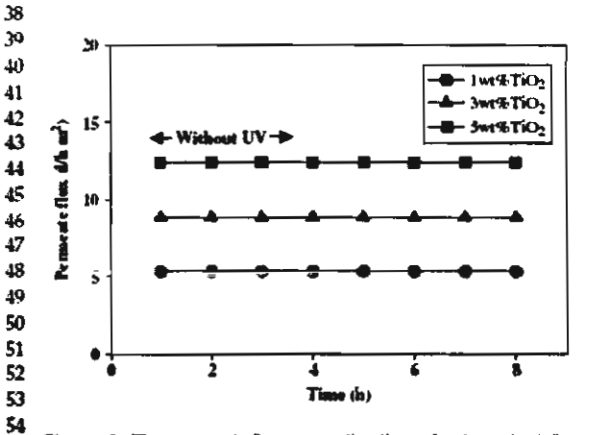


Figure 6. The permeate flux vs reaction time of polyacrylonitrie membranes at various percentages of TIO2 and pH 3.

Copyright © 2006 John Wiley & Sons, Ltd.

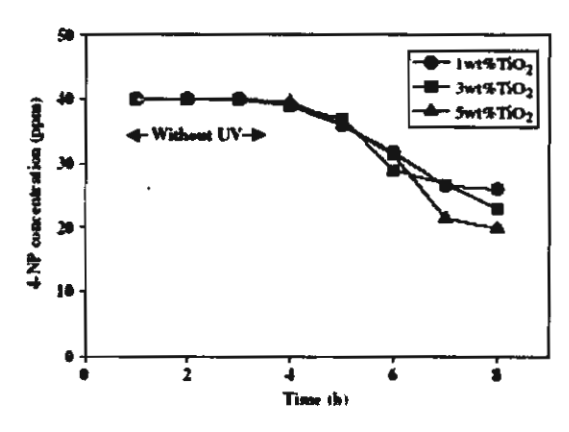


Figure 7. The degradation of 4-NP with the reaction time of polyacrylonitrile membranes at various percentages of TiO2 and pH 3.

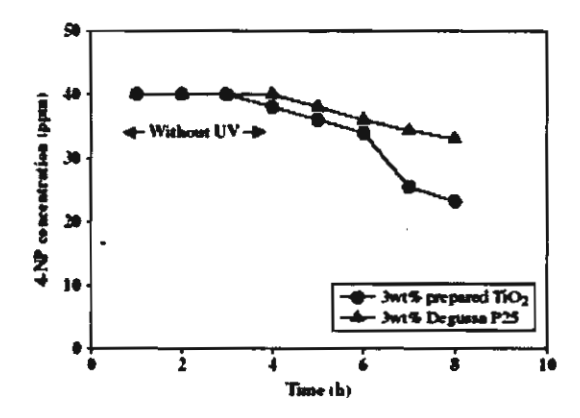


Figure 8. Effect of TiO2 type mixed in the polyacrylonitrile membrane on the degradation of 4-NP.

shows the UV spectra of 4-NP concentration at pH = 3 in 57 which the 4-NP is completely degraded. The surface of TiO2 is positively charged in acidic media, therefore, the higher H+ concentration leads to the higher OH radicals for the photodegradation of 4-NP.25

### CONCLUSIONS

The titanium triisopropanolamine precursor can be prepared by a very simple method (the oxide one pot synthesis) from low cost starting materials, and yields a TiO2 catalyst with high surface area obtained after calcinations of the precursor at 600°C for 2 h. Polymeric membranes loaded with the as-prepared TiO2 catalyst show an impressively

> Appl. Organometal. Chem. 2006; 20: 000-000 DOI: 10.1002/aoc

66 68 70

61

62

63

64

### N. Phonthammachai et al.

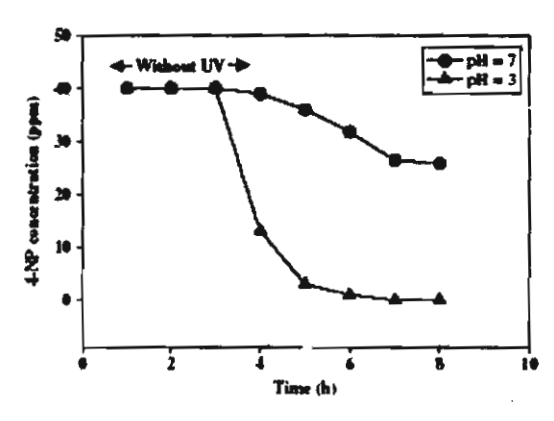


Figure 9. Effect of pH on the degradation of 4-NP using 3 wt% TIO, loaded in the polyacrylonitrile membrane.

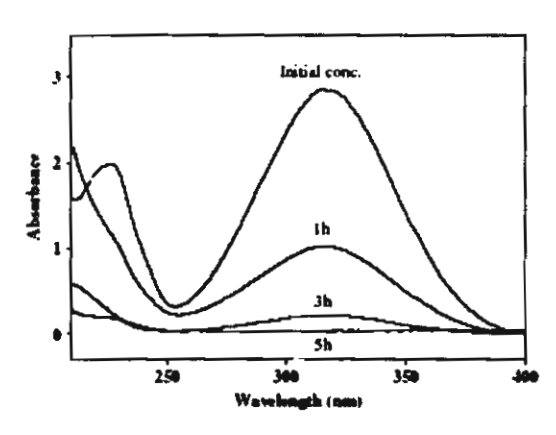


Figure 10. The UV spectra of 4-NP solution analyzed at different reaction time and pH = 3 using 1 wt% TiO2 loaded in the polyacrylonitrile membrane.

1 high efficiency for the photocatalytic degradation of 4-NP. Examination of the properties of the PAN membrane indicates that it has considerably high stability low permeate flux. The photocatalytic degradation of 4-NP increases with increasing percentage of TiO2 loaded in the PAN membrane. Higher

### Materials, Nanoscience and Catalysis



57

58

54)

60

61

62

63

64 65

66

67 68

40

70

71

72

73

74

75

76

77

78

79 80

81

82

83

84

85

86

87

88

89

90

91

92

93

94

95

96

97

98

00

100

101

102 103

104

105

106

107

108

109

110

111

112

efficiency of photocatalytic degradation of 4-NP is illustrated at lower pH value.

### Acknowledgements

This research work was supported by the Postgraduate Education and Research Program in Petroleum and Petrochemical Technology (ADB) Fund, Ratchadapisake Sompote Fund, Chulalongkorn University and the Thailand Research Fund (TRF).

### REFERENCES

- 1. Karakulaki K, Morawaki WA, Grzechulaka J. Sep. Parif. Technol. 1998: 14: 163.
- 2. Zimmerman CM, Singh A, Koros WJ. J. Membr. Sci. 1997; 137:
- 3. Avramescu M-E, Borneman Z, Wessling M. J. Chromatogr. A 2003; 1006: 171.
- 4. Clark MM, Lucas P. J. Membr. Sci. 1998; 143: 13.
- Ziegler S, Theis J, Fritsch D. J. Membr. Sci. 2001; 187: 71.
   Rivas L, Bellobono IR, Ascart F. Chemosphere 1998; 37: 1033.
- Lei L, Hu X, Yue P-L. Water Res. 1998; 32: 2753.
- Molinari R. Murgari M, Drioli E. Paola AD, Palmisano L, Schiavello M. Catal. Today 2000; 53: 71.
- Zorn ME. Photocatalytic oxidation of gas-phase compounds in confined areas: investigation of multiple component systems. In Proceedings of the 13th Annual Wisconsin Space Confern August 2003. Space Geart Consortium: Green Bay, WI, 2003. 10. Chen D, Ray AK. Water Res. 1998; 32(11): 3223.
- 11. Molinari R, Palminano L, Drioli E, Schiavello M. J. Membr. Sci. 2002: 206: 399.
- Chen D, Ray AK. Appl. Catal. B Environ. 1999; 23: 143.
   Villacres R, Reeda S, Torimoto T, Ohtani B. J. Photochem. Phot
- A 2008: 160: 121.
- Rincon AG, Pulgarin C, Adler N, Peringer P. J. Phot Photobiol. A 2001; 139: 233.
- Makowski A, Wardas W. Curr. Top. Biophys. 2001; 25: 19.
- Maurino V, Minero C, Pelizzetti E, Piccinini F Hidaka H. J. Photochem. Photobiol. A 2001; 109: 171. Minero C, Pelizzetti E, Piccinini P, Serpone N,
- 17. Dumitriu D, Bally AR, Ballif C, Hones P, Schmid PE, Se Levy F, Parvulescu VI. Appl. Cetal. B Environ. 2001; 25: 83.
  18. Zhang L, Kanki T, Sano N, Toyoda A. Sep. Purif. Technol. 2003; 31:
- 105.
- 19. Phonthammachai N, Chairassameewong T, Gulari E, Jamieson AM, Wongkasemjit S. Microporous Mesoporous Mater. 2003; 66: 261.
- Khalil KMS, Zaki Ml. Powder Technol. 2001; 120: 256.
- 21. Kirn EJ, Hahn SH. Mater Lett. 2001; 49: 244.
- Kim SJ, Shin SR, Kim Sl. High Perform. Polym. 2002; 14: 309
- 23. Wang Y, Santiago-Aviles JJ, Furlan R, Ramos ID. IEEE Tss Nanotechnol, 2003; 2: 39.
- Mano JF, Kontarova D, Reis RL. J. Mater. Sci. 2003; 14: 127.
- 25. Kartal OE, Erol M, Oguz H. Chem. Engag 2001; 24: 645.

5

7

8

٥

10

11

12

13

14

15

16

17

		,	
	M.		
C. Crystallization and ca	talytic activity of hi	gh titanium loaded TS	S-1 zeolite



## Available online at www.sciencedirect.com

PHYSICS

Materials Chemistry and Physics 97 (2006) 458-467

### Crystallization and catalytic activity of high titanium loaded TS-1 zeolite

N. Phonthammachai a, M. Krissanasaeranee a, E. Gulari b, A.M. Jamieson c, S. Wongkasemjit a,\*

\* The Petroleum and Petrochemical College, Chulalonghorn University, Soi Chula 122, Physikai Road, Bangkok 10330, Thailand
\* Department of Chemical Engineering, University of Michigan, Ann Arbor, MI, USA
\* Department of Macromolecular Science, Case Western Reserve University, Cleveland, OH, USA

Received 19 August 2004; received in revised form 15 August 2005; accepted 23 August 2005

#### Abstract

TS-1 zerolite with high Ti loading was successfully synthesized from low-cost and moisture-stable precursors, titanium glycolate and silatrane, using microwave heating. The effect of composition, viz. tetrapropylammonium ion (TPA\*), NaOH, H<sub>2</sub>O, and reaction conditions, viz. aging time, reaction temperature, and reaction time, was studied. The Si:Ti mole ratios were varied from 100.00 to 5.00 and the extent to which Ti is incorporated into the zerolite framework was evaluated. The TS-1 samples were characterized by XRD, FT-IR, S.E.M. and DR-UV, and confirmed the fingerprint of MFI type zerolite. A small amount of extra-framework titanium dioxide was also identified at a Si:Ti mole ratio of 5.0. Photocatalytic decomposition of 4-nitrophenol (4-NP) was used to test the catalytic activity of the TS-1 samples. All samples showed high catalytic efficiency, which increased with Ti loading.

© 2005 Elsevier B.V. All rights reserved.

Keywords: Photocatalytic decomposition: Silatrane; Titanium glycolate; TS-1 zeolite

### 1. Introduction

Titanium silicate-1 (TS-1), a Ti-containing zeolite with the MFI structure, is a microporous crystalline material, used as a highly-selective heterogeneous oxidative catalyst, employing H<sub>2</sub>O<sub>2</sub> under mild conditions. The titanium isomorphously replaces silicon in a tetrahedral side of the MFI silicate lattice. TS-1 combines the advantages of having the high coordination ability of Ti<sup>44</sup> ions with the hydrophobicity of the silicate framework, while retaining the spatial selectivity and specific local geometry of the active sites of the molecular sieve structure [1]. The catalytic properties of titanosilicate are unique, encompassing a variety of liquid-phase oxidations, such as phenot hydroxylation, olefin epoxidation, cyclohexanone ammoximation and the oxidation of saturated hydrocarbons and alcohols [2,3]. With H<sub>2</sub>O<sub>2</sub>, solvolysis produces TiOOH and SiOH, the former giving rise to the active catalytic oxidation center.

Since 1983, when Taramasso et al. [4] reported the hydrothermal synthesis of TS-1 for the first time, many attempts have been made to increase the amount of Ti(IV) in the zeolite framework. A major problem often encountered in the synthesis of TS-1 molecular sieves is the precipitation of titanium oxide outside the lattice framework, leading to materials which are inactive for oxidative catalysis [5]. The synthesis of materials containing isolated tetrahedral Ti is challenging due to the strong tendency of Ti to polymerize under aqueous conditions, often forming a separate titanium dioxide phase [1]. Two methods to synthesize TS-1 were described in the original patent using different Si sources, tetraethylorthosilicate (TEOS) and Ludox colloidal silica, and typically employing tetrapropylammonium hydroxide (TPAOH) as the structure directing agent and to provide the alkalinity necessary for the crystallization of the zeolite [6]. From previous work, the maximum amount of Ti(IV) incorporated in the zeolite framework corresponds to a Si:Ti ratio of approximately 33-35 [1,3,6]. Furthermore, attempts to achieve a higher degree of substitution (Si/Ti = 10, 15 and 30) have not been successful with Ti fully incorporated into the lattice framework.

Microwave-assisted-hydrothermal synthesis is a process which has been used for the rapid synthesis of numerous ceramic oxides and porous materials [7–9]. It offers many advantages over conventional synthesis including quick and homogeneous heating in a few minutes, homogeneous nucleation, fast supersaturation through rapid dissolution of precipitated gels and shorter crystallization times. Heating is induced via the friction of molecular motion enhanced by microwave irradiation, thus it

0254-0584/\$ -- see front matter © 2005 Elsevier B.V. All rights reserved. doi:10.1016/j.matchemphys.2005.08.047

Corresponding author. Tel.: +66 2 218 4133; fax: +66 2 215 4459.
 E-mail addresses: daujitra@chula.ac.th, Sujitra.D@chula.ac.th
 (S. Wongkasemjit).

is possible to heat the reactants selectively and homogeneously throughout the material. Furthermore, microwave heating is energy efficient and economical [10,11].

In this work, we synthesized TS-1 zeolite from moisturestable, low-cost starting materials, silatrane and titanium glycolate, as sources of silica and titanium dioxide, respectively, and using tetrapropylammonium bromide (TPABr) as a template and microwave heating. Various amounts of Ti were incorporated in the zeolite framework. The samples were characterized using XRD, S.E.M., FT-IR and DR-UV. Photocatalytic decomposition of 4-NP was carried out to test the activity of the TS-1 samples.

### 2. Experimental

### 2.1. Materials

Titasiura dioxide (surface area 12 m<sup>2</sup>g<sup>-1</sup>) was purchased from Sigma-Aldrich Chemical Inc. (USA) and used as received. Ethylene glycel (EG) was purchased from Malinckrodt Baker Inc. (USA) and purified by fractional distillation at 200°C under nitrogen at atmospheric pressure before use. Triethylenetetraraine (TETA) was purchased from Facal Polytech Co. Ltd. (Bangkok, Thailand) and distilled under vacuum (0.1 mmHg) at 130°C prior to use. Acctonitrile was purchased from Lab-Scan Company Co. Ltd. and purified by distilling over calcium hydride powder. 4-Nitrophenol was purchased from Sigma-Aldrich Chemical Co. Inc. (USA).

### 2.2. Instrumental

Fourier transform-infrared spectra (FT-IR) were recorded on a VECOR3.0 BRUKER spectrometer with a spectral resolution of 4 cm<sup>-1</sup> using transparent KBr pellets containing 0.001 g of sample mixed with 0.06 g of KBr. Thermogravimetric analysis (TGA) was carried out using a Perkin-Elmer thermal analysis system with a heating rate of 10 °C min<sup>-1</sup> over 30–800 °C temperature range. The mass spectrum was obtained on a Pison Instrument (VG Autospoultima 707E) with VG data system, using the positive fast atomic bombardment mode (FAB\*-MS) with glycerol as the matrix, cesium gam as inkintor, and cesium iodide (CsI) as a standard for peak calibration. <sup>13</sup>C-solid-state NMR spectroscopy was performed using a Bruker AVANCE DPX-300 MAS-NMR. Elemental analysis (EA) was carried out on a C/H/N Analyser (Perkin-Elmer PE2400 series II).

### 2.3. Preparation of titanium glycolate

The procedure adopted followed previous work [12]. A mixture of TiO<sub>2</sub> (2.g., 0.025 mol) and TETA (3.65 g. 0.0074 mol) was stirred vigorously in excess BG (25 cm<sup>2</sup>) and heated to 200 °C for 24 h. The resulting solution was centrifuged to separate the unreacted TiO<sub>2</sub>. The excess BG and TETA were removed by vacuum distillation to obtain a crude precipitate. The white solid product was washed with acotonitrile, dried in a vacuum desiccator and characterized using FT-IR. <sup>13</sup>C-solid-state NMR, EA, FAB\*-MS, and TGA.

FFIR: 2927-2855cm<sup>-1</sup> ( $\nu$ C-H<sub>3</sub>, 1080cm<sup>-1</sup> ( $\nu$ C-O-Ti bond), and 619cm<sup>-1</sup> ( $\nu$ Ti-O bond). <sup>13</sup>C-solid-state NMR: two peaks at 74.8 and 79.2 ppm. EA: 28.6% C and 48.5 H. FAB\*-MS: approximately 8.5% of the highest *mle* at 169 of [Ti(OCH<sub>2</sub>CH<sub>2</sub>O)<sub>2</sub>]H\*, 7.3% intensity at 94 of [OTIOCH<sub>2</sub>] and 63.5% intensity at *mle* 45 of [CH<sub>2</sub>CH<sub>2</sub>OH<sub>3</sub>]. TGA: a single sharp transition at 340°C and 46.95% ceramic yield corresponding to Ti(OCH<sub>2</sub>CH<sub>2</sub>O)<sub>2</sub>.

### 2.4. Preparation of silatrane

The procedure adopted followed Wongkanemit's work [13]. A mixture of Si(OH)2 (6 g. 0.1 mol) and TEA (18.648 g. 0.125 mol) was stirred vigorously in excess EG (100 cm<sup>3</sup>) and heated to 200 °C for 10h. The resulting solution was placed under vacuum to remove EG and obtain a crude precipitate. The white

solid product was washed with acctoniztile, dried in a vacuum desicemer and characterized using PT-IR, FAB\*-MS, and TGA.

PT-IR: 3422 cm<sup>-1</sup> (vO—H), 2986–2861 cm<sup>-1</sup> (vC—H). 2697 cm<sup>-1</sup> (vN—Si), 1459–1445 cm<sup>-1</sup> (δC—H), 1351 cm<sup>-1</sup> (δC—N), 1082 cm<sup>-1</sup> (δS—O—C), 579 cm<sup>-1</sup> (vN—Si), PAB\*-MS: approximately 100% of the met at 174 of N[CH<sub>2</sub>CH<sub>2</sub>O]si\*, 11.3% intensity at 236 of H\*OCH<sub>2</sub>CH<sub>2</sub>OSi [OCH<sub>2</sub>CH<sub>2</sub>D<sub>1</sub>N, 2.6% intensity at 323 of H\*[HOCH<sub>2</sub>CH<sub>2</sub>D<sub>1</sub>CH<sub>2</sub>CH<sub>2</sub>D<sub>3</sub>N+2CH<sub>2</sub>D<sub>3</sub>N+2CH<sub>2</sub>D<sub>3</sub>N+2CH<sub>2</sub>D<sub>3</sub>N+2CH<sub>2</sub>D<sub>3</sub>N+2CH<sub>2</sub>D<sub>3</sub>N+2CH<sub>2</sub>D<sub>3</sub>N+2CH<sub>2</sub>D<sub>3</sub>N+2CH<sub>2</sub>D<sub>3</sub>N+2CH<sub>2</sub>D<sub>3</sub>N+2CH<sub>2</sub>D<sub>3</sub>N+2CH<sub>2</sub>D<sub>3</sub>N+2CH<sub>2</sub>D<sub>3</sub>N+2CH<sub>2</sub>D<sub>3</sub>N+2CH<sub>2</sub>D<sub>3</sub>N+2CH<sub>2</sub>D<sub>3</sub>N+2CH<sub>2</sub>D<sub>3</sub>N+2CH<sub>2</sub>D<sub>3</sub>N+2CH<sub>2</sub>D<sub>3</sub>N+2CH<sub>2</sub>D<sub>3</sub>N+2CH<sub>2</sub>D<sub>3</sub>N+2CH<sub>2</sub>D<sub>3</sub>N+2CH<sub>2</sub>D<sub>3</sub>N+2CH<sub>2</sub>D<sub>3</sub>N+2CH<sub>2</sub>D<sub>3</sub>N+2CH<sub>2</sub>D<sub>3</sub>N+2CH<sub>2</sub>D<sub>3</sub>N+2CH<sub>2</sub>D<sub>3</sub>N+2CH<sub>2</sub>D<sub>3</sub>N+2CH<sub>2</sub>D<sub>3</sub>N+2CH<sub>2</sub>D<sub>3</sub>N+2CH<sub>2</sub>D<sub>3</sub>N+2CH<sub>2</sub>D<sub>3</sub>N+2CH<sub>2</sub>D<sub>3</sub>N+2CH<sub>2</sub>D<sub>3</sub>N+2CH<sub>2</sub>D<sub>3</sub>N+2CH<sub>2</sub>D<sub>3</sub>N+2CH<sub>2</sub>D<sub>3</sub>N+2CH<sub>2</sub>D<sub>3</sub>N+2CH<sub>2</sub>D<sub>3</sub>N+2CH<sub>2</sub>D<sub>3</sub>N+2CH<sub>2</sub>D<sub>3</sub>N+2CH<sub>2</sub>D<sub>3</sub>N+2CH<sub>2</sub>D<sub>3</sub>N+2CH<sub>2</sub>D<sub>3</sub>N+2CH<sub>2</sub>D<sub>3</sub>N+2CH<sub>2</sub>D<sub>3</sub>N+2CH<sub>2</sub>D<sub>3</sub>N+2CH<sub>2</sub>D<sub>3</sub>N+2CH<sub>2</sub>D<sub>3</sub>N+2CH<sub>2</sub>D<sub>3</sub>N+2CH<sub>2</sub>D<sub>3</sub>N+2CH<sub>2</sub>D<sub>3</sub>N+2CH<sub>2</sub>D<sub>3</sub>N+2CH<sub>2</sub>D<sub>3</sub>N+2CH<sub>2</sub>D<sub>3</sub>N+2CH<sub>2</sub>D<sub>3</sub>N+2CH<sub>2</sub>D<sub>3</sub>N+2CH<sub>2</sub>D<sub>3</sub>N+2CH<sub>2</sub>D<sub>3</sub>N+2CH<sub>2</sub>D<sub>3</sub>N+2CH<sub>2</sub>D<sub>3</sub>N+2CH<sub>2</sub>D<sub>3</sub>N+2CH<sub>2</sub>D<sub>3</sub>N+2CH<sub>2</sub>D<sub>3</sub>N+2CH<sub>2</sub>D<sub>3</sub>N+2CH<sub>2</sub>D<sub>3</sub>N+2CH<sub>2</sub>D<sub>3</sub>N+2CH<sub>2</sub>D<sub>3</sub>N+2CH<sub>2</sub>D<sub>3</sub>N+2CH<sub>2</sub>D<sub>3</sub>N+2CH<sub>2</sub>D<sub>3</sub>N+2CH<sub>2</sub>D<sub>3</sub>N+2CH<sub>2</sub>D<sub>3</sub>N+2CH<sub>2</sub>D<sub>3</sub>N+2CH<sub>2</sub>D<sub>3</sub>N+2CH<sub>2</sub>D<sub>3</sub>N+2CH<sub>2</sub>D<sub>3</sub>N+2CH<sub>2</sub>D<sub>3</sub>N+2CH<sub>2</sub>D<sub>3</sub>N+2CH<sub>2</sub>D<sub>3</sub>N+2CH<sub>2</sub>D<sub>3</sub>N+2CH<sub>2</sub>D<sub>3</sub>N+2CH<sub>2</sub>D<sub>3</sub>N+2CH<sub>2</sub>D<sub>3</sub>N+2CH<sub>2</sub>D<sub>3</sub>N+2CH<sub>2</sub>D<sub>3</sub>N+2CH<sub>2</sub>D<sub>3</sub>N+2CH<sub>2</sub>D<sub>3</sub>N+2CH<sub>2</sub>D<sub>3</sub>N+2CH<sub>2</sub>D<sub>3</sub>N+2CH<sub>2</sub>D<sub>3</sub>N+2CH<sub>2</sub>D<sub>3</sub>N+2CH<sub>2</sub>D<sub>3</sub>N+2CH<sub>2</sub>D<sub>3</sub>N+2CH<sub>2</sub>D<sub>3</sub>N+2CH<sub>2</sub>D<sub>3</sub>N+2CH<sub>2</sub>D<sub>3</sub>N+2CH<sub>2</sub>D<sub>3</sub>N+2CH<sub>2</sub>D<sub>3</sub>N+2CH<sub>2</sub>D<sub>3</sub>N+2CH<sub>2</sub>D<sub>3</sub>N+2CH<sub>2</sub>D<sub>3</sub>N+2CH<sub>2</sub>D<sub>3</sub>N+2CH<sub>2</sub>D<sub>3</sub>N+2CH<sub>2</sub>D<sub>3</sub>N+2CH<sub>2</sub>D<sub>3</sub>N+2CH<sub>2</sub>D<sub>3</sub>N+2CH<sub>2</sub>D<sub>3</sub>N+2CH<sub>2</sub>D<sub>3</sub>N+2CH<sub>2</sub>D<sub>3</sub>N+2CH<sub>2</sub>D<sub>3</sub>N+2CH<sub>2</sub>D<sub>3</sub>N+2CH<sub>2</sub>D<sub>3</sub>N+2CH<sub>2</sub>D<sub>3</sub>N+2CH<sub>2</sub>D<sub>3</sub>N+2CH<sub>2</sub>D<sub>3</sub>N+2CH<sub>2</sub>D<sub>3</sub>N+2CH<sub>2</sub>D<sub>3</sub>N+2CH<sub>2</sub>D<sub>3</sub>N+2CH<sub>2</sub>D<sub>3</sub>N+2CH<sub>2</sub>D<sub>3</sub>N+2CH<sub>2</sub>D<sub>3</sub>N+2CH<sub>2</sub>D<sub>3</sub>N+2CH<sub>2</sub>D<sub>3</sub>N+2CH<sub>2</sub>D<sub>3</sub>N+2CH<sub>2</sub>D<sub>3</sub>N+2CH<sub>2</sub>D<sub>3</sub>N+2CH<sub>2</sub>D<sub>3</sub>D<sub>3</sub>N+2CH<sub>2</sub>D<sub>3</sub>D<sub>3</sub>N+2CH<sub>2</sub>D<sub>3</sub>D<sub>3</sub>N+2CH<sub>2</sub>D<sub>3</sub>D<sub>3</sub>N+2CH<sub>2</sub>D<sub>3</sub>D<sub>3</sub>N+2CH<sub>2</sub>D<sub>3</sub>D<sub>3</sub>N+2CH<sub>2</sub>D<sub>3</sub>D<sub>3</sub>D<sub>3</sub>N+2CH<sub>2</sub>D<sub>3</sub>D<sub>3</sub>N+2CH<sub>2</sub>D<sub>3</sub>D<sub>3</sub>D<sub>3</sub>D<sub>3</sub>D<sub>3</sub>D<sub>3</sub>D<sub>3</sub>D<sub>3</sub>D<sub></sub>

### 2.5. Preparation of TS-1 zeolite

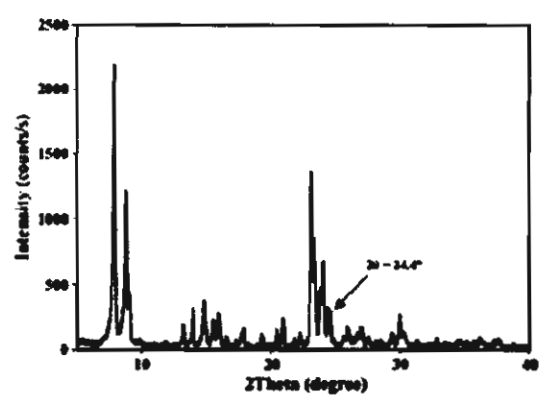
The hydrothernaal syntheses were carried out using microwave irradiation and a sample mixture with initial molar composition equal to SiO<sub>2</sub>:0.01TiO<sub>2</sub>:0.1TPA\*:0.4NaOH:114H<sub>2</sub>O. The effect of reaction conditions was studied by varying the aging time (20, 60, 70, 90, 110, 130, 150 and 170 h, reaction time (5, 10, 15 and 20 h) and reaction temperature (120, 150 and 180 °C). The effect of composition was studied by varying the concentration of TPA\*. NaOH and H<sub>2</sub>O. To investigate the Ti amount incorporated into the zeolite framework, compositions with the formula SiO<sub>2</sub>:/TRO<sub>2</sub>:0.3TPA\*:0.4NaOH:114H<sub>2</sub>O (r =0.01, 0.03, 0.05, 0.07, 0.1, 0.13, 0.17 and 0.2) were used. The solutions were aged at room temperature for 110 h and heated in a microwave at 150°C for various reaction times. The TS-1 zeolite product was washed several times with distilled water, dried at 60°C overnight and calcined at 550°C for 2h at a heating rate of 0.5 °C min<sup>-1</sup>.

### 2.6. Photocaralytic decomposition of 4-nitrophenol

The photocatalytic reactions were carried out in a 250 ml batch reactor with a g.s inlet and outlet at an O<sub>2</sub> flow rate of 20 ml min<sup>-1</sup>. A cooling water jacket was used to control the temperature at 30 °C. The issepassions were illuminated using a 100 W Hg Philip UV lamp. The concentration of 4-NP used was 40 ppm and the solution was continuously, magnetically stirred. The TS-1 zeolite at Si/Ti molar ratios of 100.00, 14.3, 7.7 and 5.0 was added into the solution. The concentration of catalyst was fixed at 0.8 g  $\Gamma^{-1}$ . Ten millimoles per litre  $H_2O_2$  was then dropped into the mixture. The samples were taken out and analyzed to determine the concentration of 4-NP using a Shimadzu UV-240 spectroobnometer.

### 2.7. TS-1 characterization

The TS-1 samples were characterized by various techniques, XRD patterns were characterized using a D/MAX-2200H Rigaku diffractometer with



Pig. 1. The XRD pattern of a calcinod TS-1 sample prepared from a reaction mixture of composition SiO<sub>2</sub>:0.01 TiO<sub>2</sub>:0.1TPA\*:0.4NaOH:114H<sub>2</sub>O: arrow indicates location of peak at 29=24.4\*.

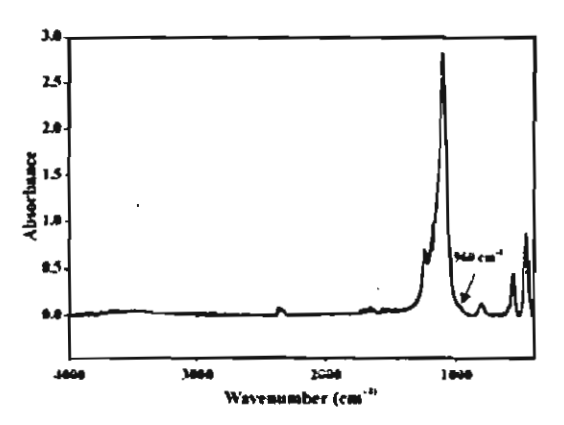


Fig. 2. The FT-IR spectra of a calcined TS-1 sample prepared from a reaction mixture of composition SiO<sub>2</sub>:0.017iO<sub>2</sub>:0.17PA\*:0.4NaOH:114H<sub>2</sub>O: arrow indicates location of shoulder at 960 cm<sup>-1</sup>.

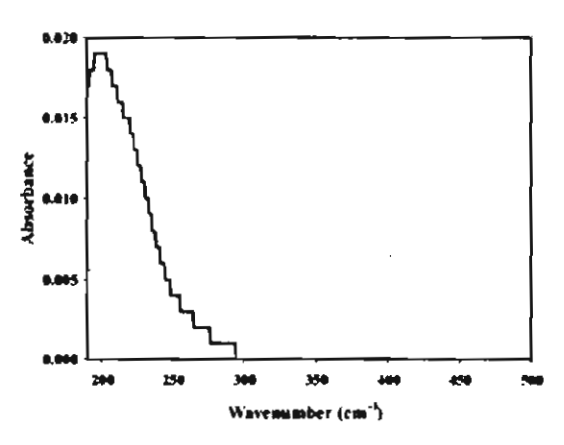


Fig. 3. DR-UV spectra of a calcined TS-1 sample prepared from a reaction mixture of composition SiO<sub>2</sub>:0.01TIO<sub>2</sub>:0.1TPA\*:0.4NaOH:114H<sub>2</sub>O.

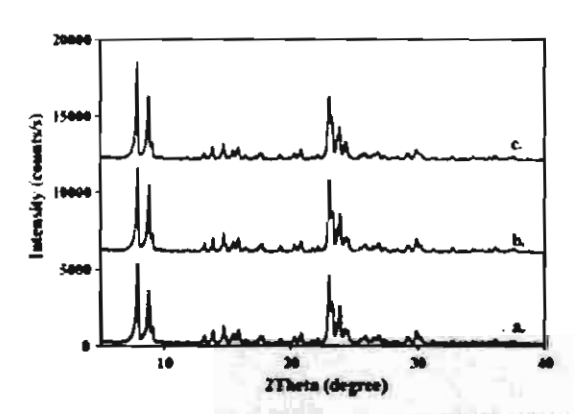


Fig. 4. XRD patterns of TS-1 samples prepared from reaction mixtures of composition SiO<sub>2</sub>:0.01TiO<sub>2</sub>:0.1TPA\*:0.4NsOH:114H<sub>2</sub>O at reaction temperatures of (a) 120°C, (b) 150°C and (c) 170°C.

Ca Ka radiation on specimens prepared by packing sample powder into a glass holder. The diffracted intensity was measured by step scanning in the 20 range between 5 and 50°. Fourier transform-infrared spectra (FT-IR) were corried on a VECOR3.0 BRUKER spectrometer with a spectral resolution of 4 cm<sup>-1</sup> using transparent KBr pellets containing 0.001 g of sample mixed with 0.06 g of KBr. The morphology of samples attached to aluminum stubs was analyzed using S.E.M., after pyrolysis at 550°C. Prior to analysis, the specimens were dried in a vacuum oven at 70°C for 5 h followed by coating with gold via vapor deposition. Micrographs of the pyrolyzed sample surfaces were obtained at 7,500× magnification. Diffuse reflectance ultraviolet-visible (DR-UV) spectra were analyzed using Shimadzu UV-240 spectrophotometer.

### 3. Results and discussion

### 3.1. Synthesis of TS-1

Our results indicate that TS-! is successfully synthesized by microwave hydrothermal treatment using silatrane and titanium

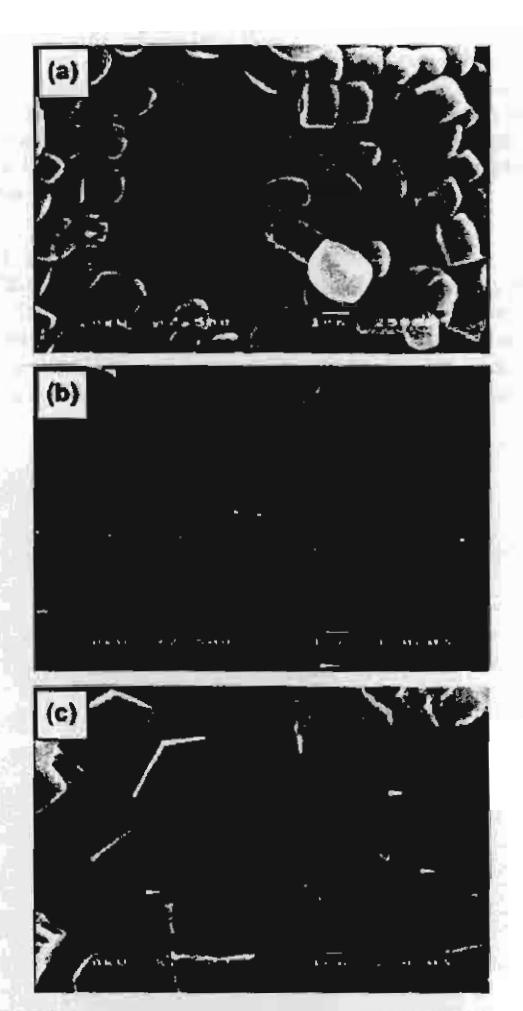


Fig. 5. S.E.M. micrographs of TS-1 samples prepared from reaction mixtures of composition SiO<sub>2</sub>:0.01TiO<sub>2</sub>:0.1TPA\*:0.4NaOH:114H<sub>2</sub>O at the reaction temperature of (a) 120°C, (b) 150°C and (c) 170°C.

glycolate as precursors, NaOH as a catalyst and TPABr as a template. The XRD pattern (Fig. 1) shows the characteristics of the MFI structure as widely reported in the literature [1,3,14,15]. The single peak at  $2\theta = 24.4^{\circ}$  indicates a change from monoclinic symmetry (silicate) to orthorhombic symmetry (TS-1) [1,16]. The FT-IR spectrum of TS-1 in the Ti-O-Si stretching region shows an absorption band at 960 cm<sup>-1</sup> (Fig. 2), which is observed in Ti-containing zeolites, and is typically assigned to the stretching mode of the [SiO4] tetrahedral bond with Ti atoms [17,18]. However, such assignment has also been interpreted in term of Si-OH groups with many defect structures [19]. The bands at 550 and 800 cm<sup>-1</sup> are assigned to 5(Si-O-Si) and v(Si-O-Si), respectively. The diffuse reflectance spectrum in Fig. 3 shows one weak absorption band with a maximum at 210 nm, attributed to tetra-coordinated titanium. No peak is observed at 330 nm, which is characteristic of extra-framework titanium dioxide.

### 3.2. Effect of crystallization conditions and compositions of TS-1

### 3.2.1. Effect of reaction temperature

The effect of reaction temperature was studied by varying the temperature at 120, 150 and 180 °C. The composition used was Si:0.01Ti:0.4NaOH:0.1TPA:114H<sub>2</sub>O. Fig. 4 shows the XRD patterns of all samples investigated. The peak intensities slightly increase with temperature, implying that increase of temperature leads to a higher rate of crystallization. From the S.E.M. micrographs of the calcined samples (Fig. 5), the crystal size increases with reaction temperature. At 120 °C (Fig. 5a), the crystals have rounded shapes and are not uniform in size

 $(0.5-2.5 \,\mu m)$ . On increasing the temperature to  $150\,^{\circ}$ C (Fig. Sb), the crystals become larger and more uniform, and have a cubic shape  $(1-2\,\mu m)$ . The largest crystal sizes ( $\sim 4\,\mu m$ ) are observed at  $180\,^{\circ}$ C (Fig. 5c), and the shape becomes hexagonal, indicating increased growth in the c-direction. Additionally, at  $180\,^{\circ}$ C, degradation of the organic template also occurs. Thus, the most suitable reaction temperature to obtain the smallest and most uniform crystal: is at  $150\,^{\circ}$ C.

### 3.2.2. Effect of reaction time

A composition of Si:0.01Ti:0.4NaOH:0.1TPA:114H<sub>2</sub>O was used to investigate the effect of reaction time on the crystallization of TS-1 zeolite. The reaction times were varied from 5, 10, 15 to 20 h at a reaction temperature of 150°C. The results show that, at reaction times shorter than 5 h, amorphous phase occurs and the conversion to TS-1 zeolite is low. It was found that the longer the reaction time, the higher is the crystallization rate. The S.E.M. micrographs (Fig. 6) show a large crystal size (5  $\mu$ m) after 5 h reaction time, and the size decreases dramatically to 1.3  $\mu$ m after 15 h. These crystals have a uniform cubic shape. Further increase of the reaction time to 20 h results in a larger crystal size and more extensive growth in the b-direction. Thus, 15 h reaction time is optimum to obtain uniform crystals for the specified composition.

### 3.2.3. Effect of aging time

TS-1 samples at various aging times (20, 60, 70, 90, 110, 130, 150 and 170 h) were prepared with composition Si:0.01Ti:0.4NaOH:0.1TPA:114H<sub>2</sub>O formula at a reaction temperature of 150°C and reaction time of 15 h. From the S.E.M. micrographs in Fig. 7, at the shortest aging time, large crys-

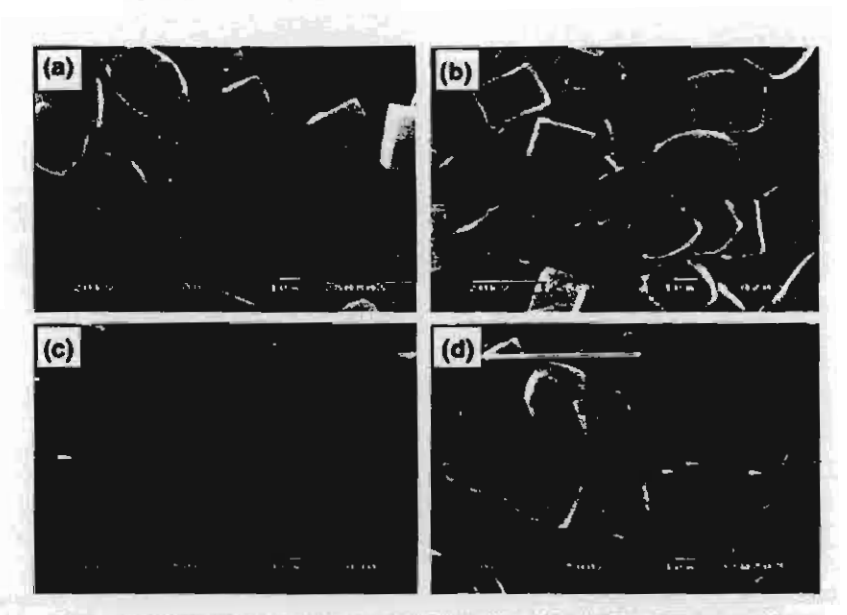


Fig. 6. S.E.M. micrographs of TS-1 samples prepared from reaction mixtures of composition SiO<sub>2</sub>:0.01TiO<sub>2</sub>:0.1TPA\*:0.4NnOH:114H<sub>2</sub>O at reaction times of (a) 5h, (b) 10h, (c) 15h and (d) 20h.

tals of TS-1 are observed, which coexist with a large amount of amorphous phase (not shown). On increasing the aging time, the crystal size becomes smaller. However, at an aging time of 130 h the size increases again. During the aging process, the hydrolysis and condensation reactions of silatrane and titanium precursors induce polymerization to form a network. Initially, only partial hydrolysis of the precursors occurs. Therefore, some organic ligand remains and interacts with the organic template to form a primary unit. The primary units then agglomerate and

nucleation occurs [20]. At longer aging times, large numbers of primary particles are created, resulting in higher agglomeration and crystallization rates, which, in turn, results in formation of larger amounts of zeolite but with crystals of smaller size. During hydrothermal synthesis, using microwave heating, the crystal growth rate becomes dominant. At the longest aging time of 130 h, a limit is reached in the formation of primary units, and therefore further agglomeration occurs at the existing nuclei, leading to more rounded crystals.

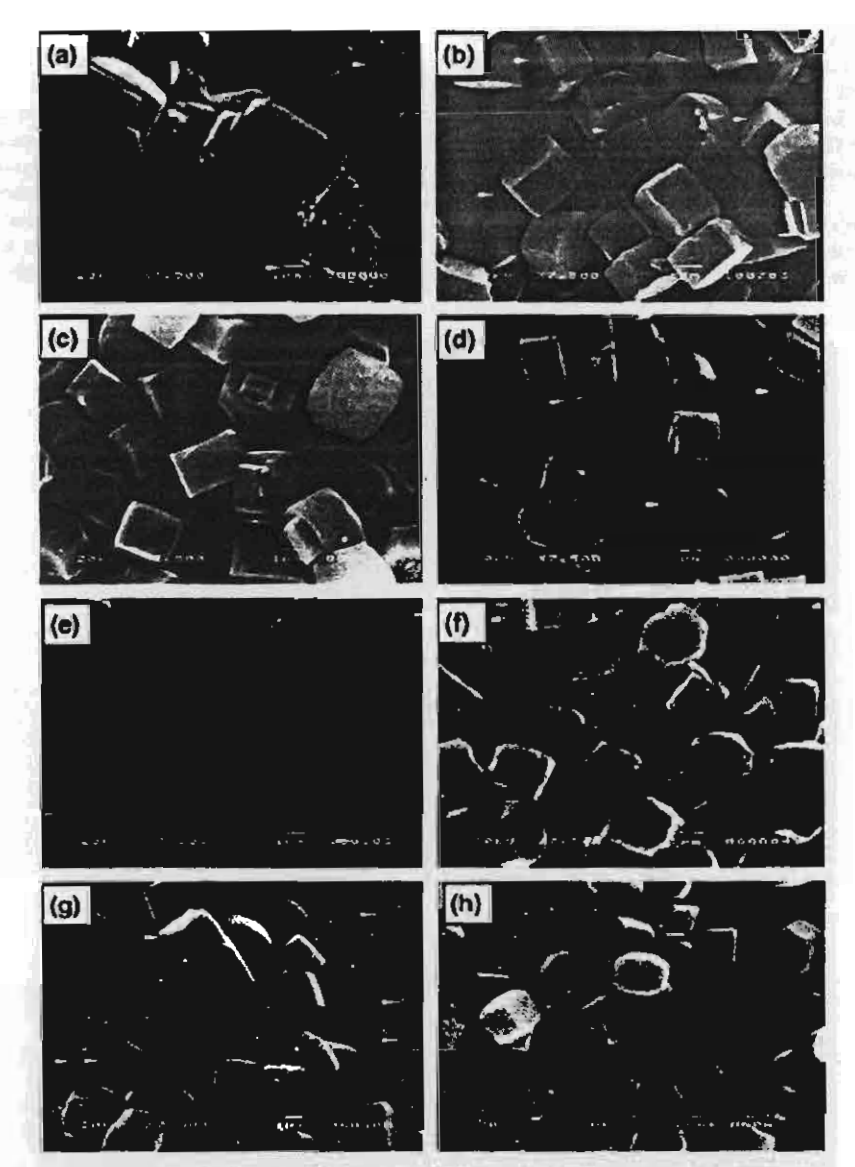


Fig. 7. S.E.M. micrographs of TS-1 surspice prepared from reaction mixtures of composition SiO2:0.01TiO2:0.1TPA\*:0.4NnOH:114H2O at aging times of (a) 20 h. (b) 60 h. (c) 70 h. (d) 90 h. (e) 110 h. (f) 130 h. (g) 150 h and (h) 170 h.

### 3.2.4. Effect of the NaOH:Si ratio

The NaOH:Si ratio was varied from 0.1 to 1.0 mole ratio at 110h aging time, 15 h reaction time and 150 °C reaction temperature. At 0.1 mole ratio, the product is clearly amorphous, as evident in the S.E.M. micrograph (Fig. 8a). On increasing the ratio to 0.3, very large crystals (10 µm) of TS-1 zeolite were formed, with many secondary growths on the crystals (Fig. 8b). When the NaOH:Si ratio increases to 0.4, more uniform and smaller crystals (1-2 µm) are formed (Fig. 8c). Further increase in the ratio to 0.5 produces crystals of larger size and at a ratio of 0.7, many secondary growths occur on the crystals (Fig. 8d and e, respectively). At the highest NaOH:Si ratio, 1.0 (Fig. 8f), the cubic shape of the particles is damaged. Higher concentrations of NaOH accelerate the hydrolysis rate, resulting in an increase in reactive species for zeolite nucleation. This leads to the formation of smaller crystals on initially increasing the NaOH:Si ratio to 0.3 mole ratio. However, at too high a NaOH concentration, the hydrolysis and condensation reaction rates become too rapid which generates larger crystals with secondary growths (at 0.5 and 0.7 mole ratios). At the highest concentration of NaOH (1.0 mole ratio) it appears sufficient sodium ions are present to saturate the surface of the silica particles, causing retardation of nucleation due to a reduction in the TPA-Si interaction [21].

### 3.2.5. Effect of the TPA:Si ratio

The steric stabilization of nuclear-sized entities is also critically dependent on the cation balance. The TPA+ cation widely used in the synthesis of zeolite contains bulky quaternary ammonium cations, which adsorb to particle surfaces, and provide steric stabilization, preventing aggregation upon collision [20]. Many types of templates have been used to synthesize TS-1 zeolites, including TPAOH, TPABr, TBABr and 1,6-hexanediamine. However, Wang and Guo [6] found that use of TBABr increase formation of unwanted ZSM-11, and that use of 1,6-hexanediamine led to a decrease in crystallinity when the amount of Ti was increased. To reduce the cost of the synthesis. TPAOH may be replaced by TPABr. In fact, much previous work indicates use of TPABr as template for TS-1 generates product with high selective catalytic efficiency [6,15].

In our work, TPABr was used to synthesize TS-1 zeolite and the effect of TPA+ concentration was studied by investigating the behavior of systems with the composition

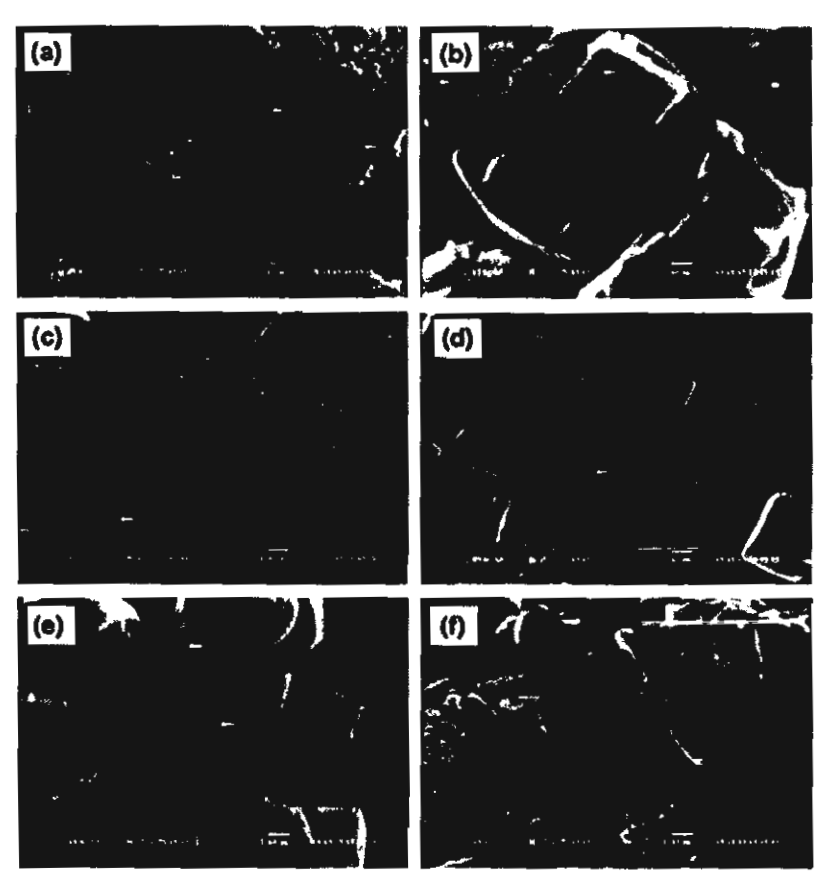


Fig. 8. S.E.M. micrographs of T3-1 samples at NnOH:Si mole ratios of (a) 0.1, (b) 0.3, (c) 0.4, (d) 0.5, (e) 0.7 and (f) 1.0.

Si:0.01Ti:0.4NaOH:xTPA\*:114H<sub>2</sub>O (x=0.05, 0.1, 0.2, 0.3, 0.4 and 0.5). The crystallization conditions were set at 110 h aging time, 15 h reaction time and the 150 °C reaction temperature. Fig. 9 shows S.E.M. micrographs describing the effect of TPA\*:Si ratio with a Si:NaOH mole ratio of 0.4. At low TPA\*:Si ratio (0.05), large crystals are formed (10 µm), and with increasing level of TPA\* the crystal size decreases (1-2 µm at 0.3 mole ratio). However, at too high a concentration of TPA\* (0.4 and 0.5 mole ratios), secondary growths occur. Following the interpretation of Koegler et al. [21], when both TPA\* and silica are abundant, nucleation occurs at the surfaces of the gel particles created by hydrolysis and condensation reaction. TPA\* diffuses from solution to the crystal/gel interface, resulting in new crystal growth, as seen here.

### 3.2.6. Effect of the H2O:Si ratio

The effect of dilution was studied using systems with the composition Si:0.1Ti:0.4NaOH:0.3TPA: $xH_2O$  (x=80, 114, 140, 170 and 200). The reaction time and temperature were set at 15 h, 150 °C, respectively, and the aging time at 110 h. From the S.E.M. micrographs in Fig. 10, the lowest  $H_2O:Si$  ratio shows a non-uniform crystal structure. On increasing the ratio to 114, more uniform and completely cubic structures are

Table 1
The TS-1 samples at various Si:TI molar ratios and reaction times (b)

Samples SI/TI molar ratio	Reaction time (h)		
A 100.0	15		
33.3	1.5		
20.0	20		
C 20.0 D 14.3 E 10.0	25		
10.0	25		
7.7	35		
5.9	35		
H 5.0	35		
3.0			

obtained, but further increase generates larger crystals with many defects.

### 3.2.7. Effect of the Si:Ti ratio

The effect of the Si:Ti ratio on the crystallization of TS-1 was carried out by investigating systems with the composition Si:xTi:0.4NaOH:0.3TPA:114H<sub>2</sub>O formula (x=0.01, 0.03, 0.05, 0.07, 0.1, 0.13, 0.17 and 0.2). The reaction temperature and the aging time were fixed at 150°C and 110 h, respectively. The reaction times were varied from 15 to 35 h depending on the Ti loading (samples labeled A-H in Table 1). Longer reaction

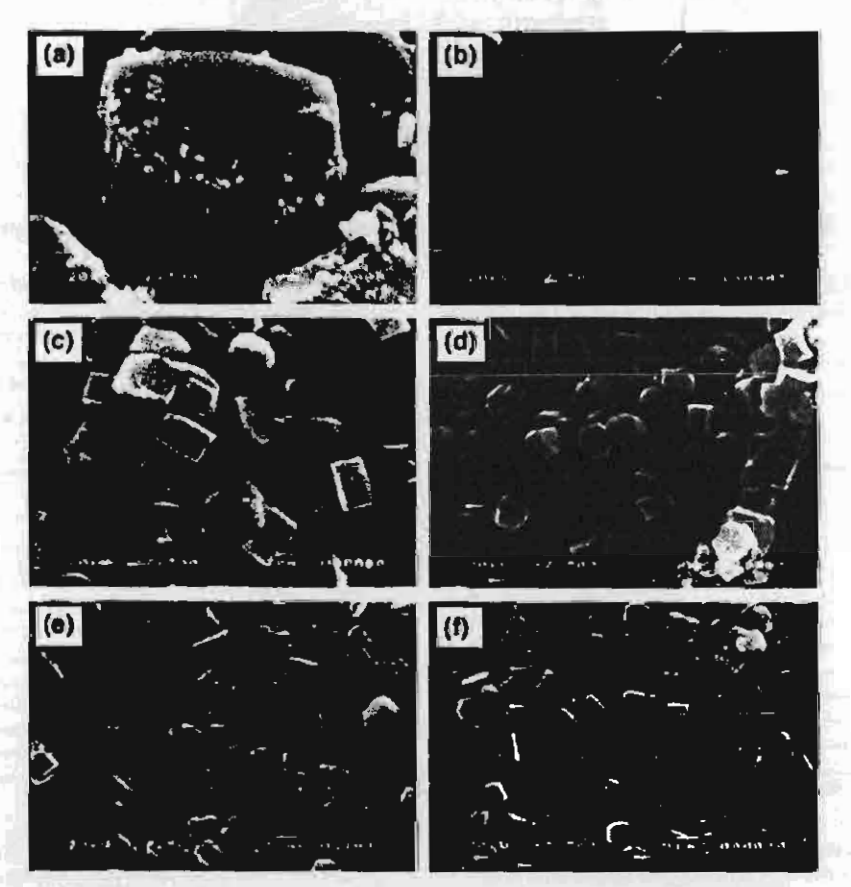


Fig. 9. S.E.M. micrographs of TS-1 samples at TPA:St mole ratios of (a) 0.05, (b) 0.1, (c) 0.2, (d) 0.3, (e) 0.4 and (f) 0.5.

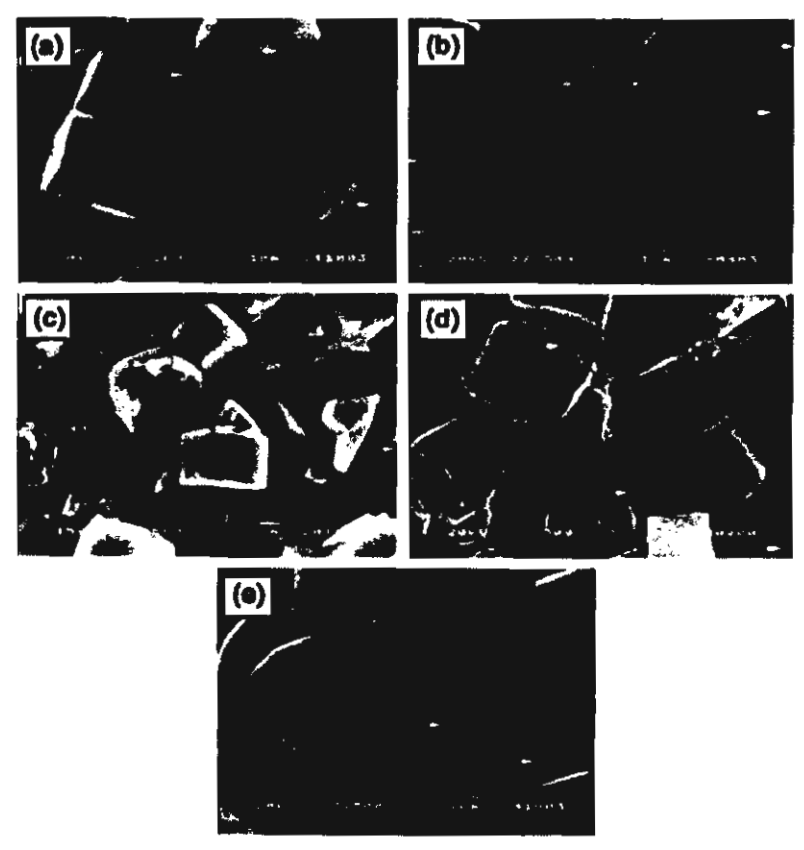


Fig. 10. S.E.M. micrographs of T3-1 samples at H2O:Si mole ratios of (a) 80, (b) 114. (c) 140, (d) 170 and (e) 200.

times were found to be necessary at higher Ti loadings to ensure complete incorporation of Ti in the zeolite framework. Fig. 11 exhibits the corresponding FT-IR spectra of TS-1 samples. The peak at 960 cm<sup>-1</sup> is attributed to the stretching mode of [SiO<sub>4</sub>] units bonded to a Ti<sup>4+</sup> ion (O<sub>3</sub>SiOTi) [15] and indicates increasing incorporation of titanium in the MFI framework. A strong

band at 550 cm<sup>-1</sup> is characteristic of the MFI structure [22]. The DR-UV spectra of these samples are shown in Fig. 12. The strong peak at 210 nm is assigned to tetra-coordinated titanium in the zeolite framework. A broad shoulder at 280 nm indicates partially polymerized hexa-coordinated Ti species, containing

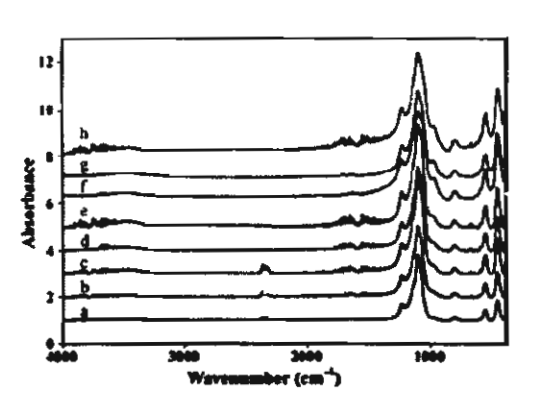


Fig. 11. FT-IR spectra of TS-1 samples at Si:Ti mole ratios of (a) 100.0, (b) 33.3, (c) 20.0, (d) 14.3, (e) 10.0, (f) 7.7, (g) 5.9 and (h) 5.0.

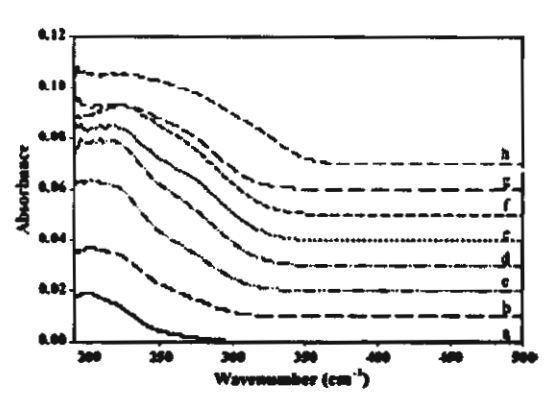


Fig. 12. DR-UV spectra of TS-1 samples at St-Ti mole ratios of (a) 100.0, (b) 33.3, (c) 20.0, (d) 14.3, (e) 10.0, (f) 7.7, (g) 5.9 and (h) 5.0.

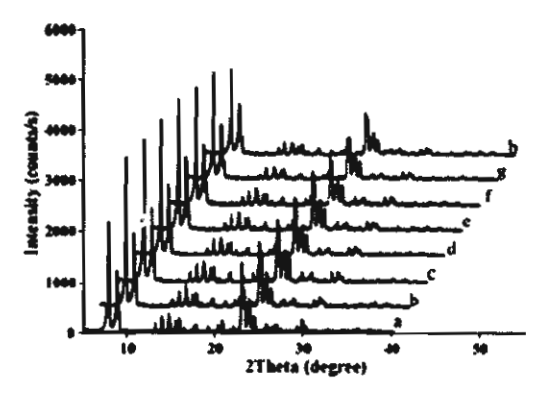


Fig. 13. XRD patterns of TS-1 samples at Si:Ti mole ratios of (a) 100.0, (b) 33.3, (c) 20.0, (d) 14.3, (e) 10.0, (f) 7.7, (g) 5.9 and (h) 5.0.

Ti-O-Ti. We deduce that these species are present in the zeolite framework rather than a silicon-rich amorphous phase [23], on the basis of XRD and S.E.M. results, which show no evidence of an amorphous phase. Moreover, absorbance at 330 nm is assigned to the extra-framework anatase phase, and is observed as a small contribution only in sample H. Peaks at 210 and 280 nm increase from sample A to H reflecting increasing titanium content and there is an apparent shift of the 210 nm band to higher wavelength because of the increased proportion of hexacoordinate species. The intensity of the 280 nm peak of samples F-H increases more strongly than that at 210 nm, indicating that hexa-coordinated Ti species are preferentially formed at higher titanium loadings. The S.E.M. micrographs and XRD patterns of TS-1 samples A-H are shown in Figs. 13 and 14. All samples show the characteristics of TS-1 zeolite with the MFI structure.

### 3.3. Photocatalytic decomposition of 4-nitrophenol

From the reports of Lee et al. [24] and Lea and Adesina [25], the photocatalytic decomposition (PCD) of 4-NP goes to completion in the presence of  $\rm H_2O_2$  under UV irradiation. The photodecomposition of 4-NP is initiated by \*OH radicals, which are easily formed via formation of titanium-hydroperoxide complexes. Thus, we investigated the catalytic activity of our Ticontaining TS-1 zeolites on the PCD of 4-NP in the presence of 1.0 mmol  $\rm I^{-1}$  of  $\rm H_2O_2$  under UV irradiation. Table 2 summarizes the results as a function of Si/Ti mole ratio. The rate of PCD increases uniformly with the amount of titanium incorporated in the zeolite, the fastest complete decomposition occurring with the 5.0 Si:Ti molar ratio.

Table 2 The photocatalytic degradation of 4-aitrophenol

Si/Ti molar ratio	Time for completely photocatalytic decoraposition of 4-NP (h)
100,0	4.0
14.3	2.0
7.7	1.3
5.0	1.0

#### 4. Conclusions

TS-1 zeolites with high titanium content incorporated in the zeolite framework were synthesized using low cost and moisture-stable precursors, silatrane and titanium glycolate, under microwave heating. The effect of the reactant composition (TPA+, NaOH and H2O) and conditions (aging time, reaction time and reaction temperature) were studied and we found that the optimum condition for synthesizing TS-1 is at a composition of Si:0.01Ti:0.4NaOH:0.3TPA:114H2O, with 110 h aging time, 15 h reaction time and at 150 °C reaction temperature. Si:Ti molar ratios in the range 100.0-5.0 were studied and the results from XRD, FT-IR, S.E.M. and DR-UV indicate that via this novel route highly crystalline materials, having high content of Ti atoms incorporated in the zeolite framework are obtained. The reaction times were varied at different Tilloadings, and show that at higher titanium loadings, longer reaction times are necessary. Photocatalytic decomposition of 4-NP was used as an assay for the catalytic activity of the prepared TS-1 samples, and demonstrated increased efficiency with increasing level of titanium loading.

### Acknowledgements

This research work was supported by the Postgraduate Education and Research Program in Petroleum and Petrochemical Technology (ADB) Fund, Ratchadapisake Sompote Fund, Chulalongkorn University and the Thailand Research Fund (TRF).

### References

- [1] Y.G. Li, Y.M. Lee, J.F. Porter, J. Mater. Sci. 37 (2002) 1959-1965.
- [2] R.J. Davis, Z. Liu, Chem. Mater. 9 (1997) 2311-2324.
- [3] R.B. Khomane, B.D. Kulkarni, A. Paraskar, S.R. Sainkar, Matez. Chem. Phys. 76 (2002) 99–103.
- [4] M. Taramasso, G. Perego, B. Notari, US Patent 4,410,501 (1983).
- [5] M.R. Prasad, G. Karnalakar, S.J. Kulkami, K.V. Raghavan, K.N. Rao, P.S. Sai Prasad, S.S. Madhavendra, Catal. Commun. 3 (2002) 399-404.
- [6] X.-S. Wang, X.-W. Guo, Catal. Today 51 (1999) 177–180.
- [7] M. Sathupanya, E. Gulari, S. Wongkasemjit, Mesopor, Micropor, Mater. 83 (1) (2004) 174.
- [8] M. Sathupanya, E. Gulari, S. Wongkasemjit, J. Bar. Ceram. Soc. 23 (8) (2003) 1293–1303.
   [9] P. Phiriyawirut, R. Magaraphan, A.M. Jamieson, S. Wongkasemjit,
- Mesopor, Micropor, Mater, 64 (1-3) (2003) 83-93. [10] K. Kunii, K. Narahara, S. Yamanaka, Micropor, Mesopor, Mater, 52
- [10] K. Kunil, K. Narahara, S. Yamanaka, Micropor. Mesopor. Mater. 52 (2002) 159-167.
- [14] S. Komarnesi, A.S. Bhalla, J. Por. Mater. 8 (2001) 23-35.
- [12] N. Phonthamanachai, T. Chuirassameewong, E. Gulari, A.M. Jamieson, S. Wongkasemjit, J. Mot. Mater. Min. 12 (2002) 23.
- [13] P. Piboonchaisit, S. Wongkanemjit, R. Laine, Science-Asia, J. Sci. Soc. Thailand 25 (1999) 113-119.
- [14] Q.H. Xia, Z. Gao, Mater. Chem. Phys. 47 (1997) 225-230.
- [15] G.L. Marra, G. Astioli, A.N. Pitch, M. Milanesio, C. Lamberti, Micropor, Mesopor, Mater. 40 (2000) 25–94.
- [16] J.L. Grieneisen, H. Kessler, E. Fache, A.M. Le Govic, Micropor. Mesopor. Mater. 37 (2000) 379–386.
- [17] D.P. Serrano, M.A. Uguina, G. Ovejoro, R.V. Orioken, M. Carascho, Micropos, Mater. 4 (1995) 273-282.

- [18] M.R. Boccuti, K.M. Rao, A. Zetchina, G. Luofanti, G. Petrini, Struct. React, Surf. 48 (1989) 133-144.
  [19] B.L. Newalker, J. Otanewaju, S. Komerneni, Chem. Mater. 13 (2001)
- 552-557.
- [20] C.S. Cundy, J.O. Forrest, R.J. Plaisted, Micropor. Mesopor. Mater. 66 (2003) 143-156.
- [21] J.H. Koegler, H.V. Bekkum, J.C. Jansen, Zeolites 19 (1997) 262-269.
- [22] M.A. Uguina, D.P. Serrano, G. Ovejero, R.V. Gricken, M. Camacho,
- Appl. Calul. A 124 (1995) 391—108.

  [23] T. Blasco, M.A. Cambios, A. Corma, J. Porca-Pariente, J. Am. Chem.
  Soc. 115 (1995) 11806—11813.
- [24] G.D. Lee, S.K. Jung, Y.J. Jeong, J.H. Park, K.T. Lim, B.H. Ahn, S.S. Hong, Appl. Catal. A 239 (2003) 197–268.
- [25] J. Lea, A.A. Adexina, J. Techol. Biotechnol. 76 (2003) 803-810.

D. Structural and Rheological Aspect of Mesoporous Nanocrystalline TiO<sub>2</sub> via Sol-Gel Process and Its Rheological Study



## Available online at www.sciencedirect.com

MICROPOROUS AND MESOPOROUS MATERIALS

Microporous and Mesoporous Materials 66 (2003) 261-271

www.elsevier.com/locate/micromeso

# Structural and rheological aspect of mesoporous nanocrystalline TiO<sub>2</sub> synthesized via sol-gel process

N. Phonthammachai <sup>a</sup>, T. Chairassameewong <sup>a</sup>, E. Gulari <sup>b</sup>, A.M. Jamicson <sup>c</sup>, S. Wongkasemjit <sup>a,\*</sup>

<sup>b</sup> The Petroleum and Petrochemical College, Chulalongkorn University, Phya Thai Road, Bangkok 10330, Thailand Department of Chemical Engineering, University of Michigan, Ann Arbor, MI 48109-2136, USA Department of Macromolecular Science, Case Western Reserve University, Cleveland, OII 44106-1712, USA Received 4 April 2003; received in revised form 30 July 2003; accepted 20 September 2003

### Abstract

Mesoporous nanocrystalline titanium dioxide was prepared via the sol-gel technique using titanium glycolate as precursor in 1 M HCl solution at various HCl:H<sub>2</sub>O ratios. XRD analysis indicates the anatase phase forms at calcination temperatures in the range 600-800 °C. From the average grain sizes, we deduce that the nucleation rate dominates the kinetics at lower temperature, and growth rate becomes the controlling factor at higher temperature for materials prepared at HCl:H<sub>2</sub>O ratios of 0.28 and 0.33. At higher volume ratios, the growth rate appears to be the dominant factor at all temperatures. The highest specific surface area (BET) obtained was 125 m²/g at the HCl:H<sub>2</sub>O ratio of 0.28. A small decrease of specific surface area was observed from low to high acid ratio and a substantial decrease from lower to higher temperature. The material calcined at 800 °C was found to consist primarily of spherical particles with diameters smaller than 1 μm. Application of the Winter rheological criteria for the gel point indicates that the gelation time increases with increase of the HCl:H<sub>2</sub>O volume ratio. The fractal dimension of the critical gel cluster decreases with acid ratio, whereas the gel strength increases with acid ratio. Thus, increase of acidity leads to a less dense but stronger network structure.

Keywords: Titanium glycolate; Titania; Rheology; Sol-gel process and viscoelastic properties

### 1. Introduction

Titanium dioxide or titania, TiO<sub>2</sub>, is widely used in the field of catalysis, as filters, adsorbents, and catalyst supports [1,2]. The porous anatase

2003 Elsevier Inc. All rights reserved.

form, as compared to the rutile phase, is of greater importance and interest due to its better catalytic properties. Therefore, a key goal is to prepare anatase nanoparticles, with high surface area, uniform particle size and pore structure, and a high anatase-rutile transformation temperature [3].

Sol-gel processing has become one of the most successful techniques for preparing nanocrystalline metallic oxide materials. In general, this method

E-mail address: dsujitra@chula.ac.th (S. Wongkascinjit).

1387-1811/\$ - see front matter © 2003 Elsevier Inc. All rights reserved. doi:10.1016j.micromeso.2003.09.017

<sup>\*</sup>Corresponding author. Tel.: +66-2-218-4133; fax: +66-2-215-4459.

involves the hydrolysis and polycondensation of a metal alkoxide, to ultimately yield hydroxide or oxide under well specified reaction conditions [4]. The key advantage of preparing metallic oxides by the sol-gel method is the possibility to control their microstructure and homogeneity. To obtain homogeneous nanoscale macromolecular oxide networks via sol-gel processing, control of hydrolysis is essential. The properties and nature of the product are controlled by the particular alkoxide used, the presence of acidic or basic additives, the solvent, and various other processing conditions (e.g. temperature). The calcination temperature is also a key factor, especially for titania preparation. Too low a temperature result in incomplete combustion and too high a temperature causes phase transformation.

Many studies have been directed to prepare titania powder with increased textural and structural stability. For example, Zhang et al. [5] prepared and studied mesoporous nanocrystalline TiO2 by a sol-gel technique using butanediol mixed with tetrapropylorthotitanate. A surface area of 97 m<sup>2</sup>/g was obtained after calcination at 400 °C for 2 h. Wei et al. [6] prepared nanodisperse spherical TiO<sub>2</sub> particles by forced hydrolysis using boiling reflux Ti(SO<sub>4</sub>)<sub>2</sub> solution in the presence of H<sub>2</sub>SO<sub>4</sub>. The particle size distribution was in the range 70-100 nm. Sun et al. [7] prepared nanosized anatase titania with average grain sizes ranging from 7.4 to 15.2 nm using MOCVD technology to pyrolyze titanium tetrabutoxide in an oxygen containing atmosphere. The smallest average grain size and the highest surface area were obtained at 700 °C. Kim et al. [8] synthesized ultrafine titania particles by hydrolysis of titanium tetraisopropoxide (TTIP) in the aqueous cores of water/NP-5/cyclohexane microemulsions. With increasing calcination temperature from 300 to 700 °C, the specific surface area of the TiO<sub>2</sub> particles decreased from 325.6 to 5.9 m<sup>2</sup>/g, whereas the average pore radius increased from 1.4 to 25.1 nm. Wu et al. [9] synthesized nanocrystalline titanium dioxide using the solhydrothermal method with titanium n-butoxide (TNB) as precursor, in various acidic media (HCl, HNO<sub>3</sub>, H<sub>2</sub>SO<sub>4</sub> and CH<sub>3</sub>COOH). Nanocrystals of pure rutile with size <10 nm were obtained at higher HCl concentrations under mild conditions.

The propensity of acidic medium for rutile formation is shown as follows: HCl>HNO<sub>3</sub>> H<sub>2</sub>SO<sub>4</sub>> HAc. Ding and Liu [14] synthesized nanocrystalline titania powders via sol-gel processing of tetrabutyltitanate in anhydrous ethanol, and showed that HCl-cataly.ed hydrolysis favors the formation of the anatase crystal phase.

Knowledge of the evolution in rheological properties during sol-gel processing is a useful guide to the manufacturer when formulating dispersions to optimize the physical properties required in the final product [10]. Thus, in this work, our aims are to synthesize high surface area anatase TiO<sub>2</sub> and to study the rheological properties of titanium glycolate synthesized directly from inexpensive and widely available TiO<sub>2</sub> and ethylene glycol via the oxide one pot synthesis (OOPS) method [11]. We also investigate the influence of the acid concentration used in acid-catalyzed hydrolysis, the effect of calcination temperature on morphology and phase transformation, and gain some insight into the gel mechanism.

### 2. Experimental

### 2.1. Materials

Titanium dioxide (surface area 12 m²/g) was purchased from Sigma-Aldrich Chemical Co. Inc. (USA) and used as received. Ethylene glycol (EG) was purchased from Malinckrodt Baker, Inc. (USA) and purified by fractional distillation at 200 °C under nitrogen at atmospheric pressure, before use. Triethylenetetramine (TETA) was purchased from Facai Polytech. Co. Ltd. (Bangkok, Thailand) and distilled under vacuum (0.1 mm/Hg) at 130 °C prior to use. Acetonitrile was purchased from Lab-Scan Company Co. Ltd. and purified by distilling over calcium hydride powder.

### 2.2. Instrumental

Fourier transform infrared spectra (FT-IR) were recorded on a VECOR3.0 BRUKER spectrometer with a spectral resolution of 4 cm<sup>-1</sup> using transparent KBr pellets containing 0.001 g of sample mixed with 0.06 g of KBr. Thermal gravi-

metric analysis (TGA) was carried out using a Perkin Elmer thermal analysis system with a heating rate of 10 °C/min over 30-800 °C temperature range. The mass spectrum was obtained on a Fison instrument (VG Autospec-ultima 707E) with VG data system, using the positive ast atomic bombardment mode (FAB\*-MS) with glycerol as the matrix, cesium gun as initiator, and cesium iodide (Csl) as a standard for peak calibration. <sup>13</sup>C-solid state NMR spectroscopy was performed using a Bruker AVANCE DPX-300 MAS-NMR. Elemental analysis (EA) was carried out on a C/H/N analyser (Perkin Elmer PE2400 series II).

### 2.3. Preparation of titanium glycolate

The procedure adopted followed previous work [11]. A mixture of TiO<sub>2</sub> (2 g, 0.025 mol) and TETA (3.65 g, 0.0074 mol) was stirred vigorously in excess EG (25 cm<sup>3</sup>) and heated to 200 °C for 24 h. The resulting solution was centrifuged to separate the unreacted TiO<sub>2</sub>. The excess EG and TETA were removed by vacuum distillation to obtain a crude precipitate. The white solid product was washed with acetonitrile, dried in a vacuum desiccator and characterized using FT-IR, <sup>13</sup>C-solid state NMR, EA, FAB+-MS, and TGA.

FT-IR: 2927-2855 cm<sup>-1</sup> (vC-H), 1080 cm<sup>-1</sup> (vC-O-Ti bond), and 619 cm<sup>-1</sup> (vTi-O bond). <sup>13</sup>C-solid state NMR: two peaks at 74.8 and 79.2 ppm. EA: 28.6% C and 4.8% H. FAB<sup>+</sup>-MS: approximately 8.5% of the highest *mle* at 169 of [Ti(OCH<sub>2</sub>CH<sub>2</sub>O)<sub>2</sub>]H<sup>+</sup>, 73% intensity at 94 of [OTiOCH<sub>2</sub>] and 63.5% intensity at *mle* 45 of [CH<sub>2</sub>CH<sub>2</sub>OH]. TGA: one sharp transition at 340 °C and 46.95% ceramic yield corresponding to Ti(OCH<sub>2</sub>CH<sub>2</sub>O)<sub>2</sub>.

### 2.4. Sol-gel processing of titanium glycolate

The hydrolysis of titanium glycolate (0.026 g) was carried out via addition of  $160 \mu\text{L}$  of 1 M HCl mixed with distilled water in volume ratios of HCl:H<sub>2</sub>O 0.45, 0.39, 0.33 and 0.28. The mixtures were magnetically stirred and heated in a water bath at 50 °C until a clear gel was obtained. The gels were calcined for 2 h at 600, 700 and 800 °C.

### 2.5. Rheological study of titanium glycolate

Gelation occurs when aggregation of particles or molecules takes place in a liquid, under the action of Van der Waals forces or via the formation of covalent or noncovalent bonds. The process can be conveniently monitored using rheological measurement technique [5]. The rheometric measurements were conducted using an ARES rheometer with parallel plate geometry, 25 mm in diameter. The storage (G') and loss (G') moduli were determined using oscillatory shear at frequencies in the range 0.2 6.4 rad/s. The strain amplitude was small enough to ensure that all experiments were conducted within the linear viscoelastic region, where G and G' are independent of the strain amplitude. Titanium glycolate 0.026 g was hydrolyzed at different HCl:H<sub>2</sub>O volume ratios of 0.45, 0.39, 0.33 or 0.28. The hydrolysis temperature was selected to be 30 °C. The mixtures were stirred until homogeneous before being transferred to the rheometer.

### 2.6. Characterization of calcined materials

Crystallinity and average grain sizes were characterized using a D/MAX-2200H Rigaku diffractometer with Cu Ka radiation on specimens prepared by packing sample powder into a glass holder. The diffracted intensity was measured by step scanning in the  $2\theta$  range between 5° and 90°. Specific surface area, nitrogen adsorption desorption, and pore size distribution were determined using an Autosorp-1 gas sorption system (Quantachrome Corporation) via the Brunauer-Emmett-Teller (BET) method. A gaseous mixture of nitrogen and helium was allowed to flow through the analyzer at a constant rate of 30 cc/ min. Nitrogen was used to calibrate the analyzer, and also as the adsorbate at liquid nitrogen temperature. The samples were thoroughly out-gassed for 2 h at 150 °C, prior to exposure to the adsorbent gas. Material morphology was observed using a JEOL 5200-2AE(MP 15152001) scanning electron microscope. Samples were prepared for SEM analysis by attachment to aluminum stubs, after pyrolysis at 800 °C. Prior to analysis, the

specimens were dried in a vacuum oven at 70 °C for 5 h followed by coating with gold via vapor deposition. Micrographs of the pyrolyzed sample surfaces were obtained at 10,000x magnification.

### 3. Results and discussion

The investigation of the hydrolysis reaction of titanium glycolate precursor using FT-IR is illustrated in Fig. 1. The spectra show an increase in the peak intensity of Ti-O-Ti stretching at approximately 500-800 cm<sup>-1</sup> due to hydrolysis of the precursor. The peak at 1000 1100 cm<sup>-1</sup>. corresponding to C-O stretching of ethylene glycol also increases, reflecting the production of ethylene glycol during the hydrolysis reaction. In the case of higher acid ratio (0.45), the degree of cross-linking is greater than those obtained from the hydrolysis in lower acid ratios. The acid can act as a catalyst to hydrolyze the alkoxide by protonating the ethoxy ligands during hydrolysis. Thus, the elimination of the protonated ethoxy ligand leaving group is no longer the rate limiting step, and, as a result, the hydrolysis occurs more rapidly.

Calcination is a treatment commonly used to improve the crystallinity of TiO2 powder. When TiO<sub>2</sub> is calcined at higher temperature, a transformation to rutile phase usually occurs [13] and comprises anatase, rutile, and brookite. XRD patterns (Fig. 2) show the phase transformations encountered when titanium glycolate recursor is calcined at temperatures in the range 300-1100 °C. Amorphous material is obtained at the lowest temperature (300 °C) whereas at 500 °C broader anatase peaks appear. As the calcination temperature increases, the intensity of anatase peaks becomes stronger and well resolved. However, if the calcination temperature is increased to 900 °C, small rutile peaks are found, indicating the onset of the transformation to rutile.

The synthesis procedure was changed to obtain porous anatase for better catalytic properties. Specimens obtained via the sol-gel process at different volume ratios of HCl:H<sub>2</sub>O, viz. 0.45, 0.39, 0.33 and 0.28, were subjected to calcination at 600, 700 and 800 °C, to obtain porous anatase titania [3]. Fig. 3 shows the XRD patterns of anatase formation in a specimen at the HCl:H<sub>2</sub>O volume ratio of 0.28. Our results indicate that the synthesized anatase is stable up to calcination tem-

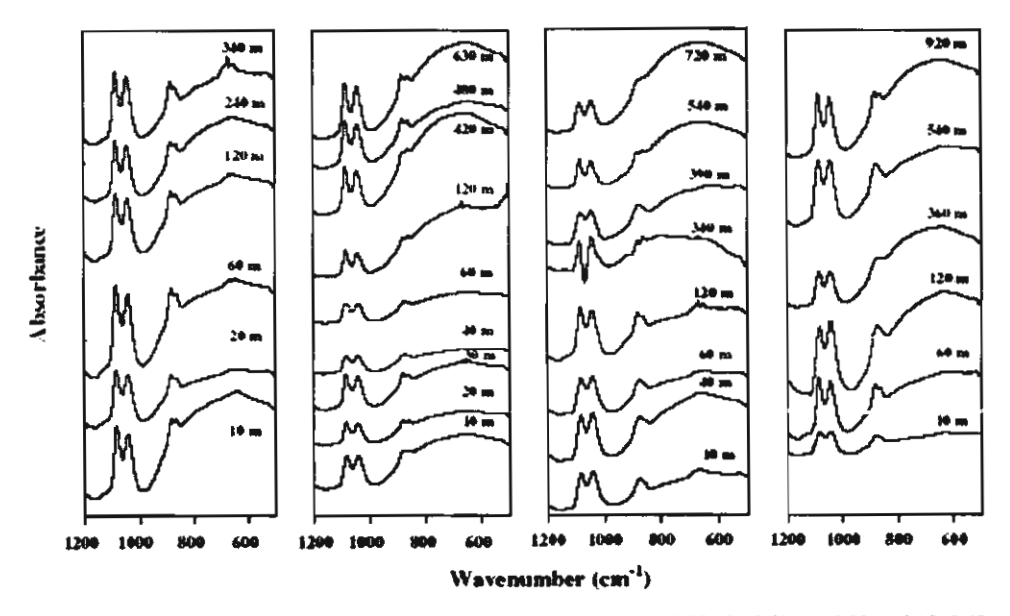


Fig. 1. The FT-IR spectra of titania get at HCl:H<sub>2</sub>O volume ratio of (a) 0.28, (b) 0.33, (c) 0.39 and (d) 0.45.

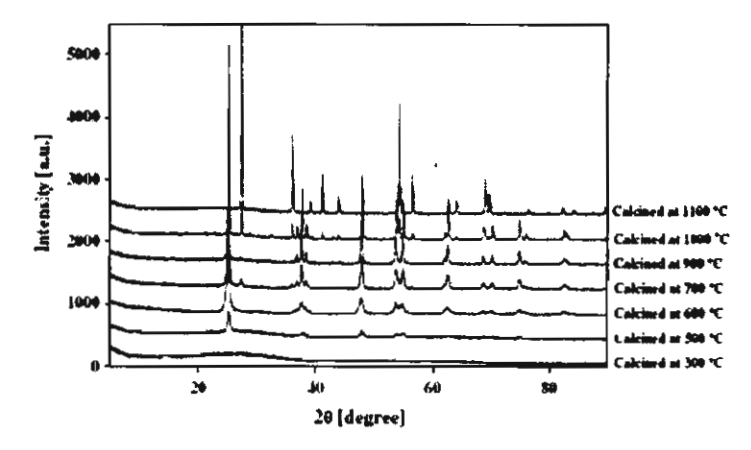


Fig. 2. XRD patterns of uncalcined and calcined titanium glycolate precursor at different temperatures.

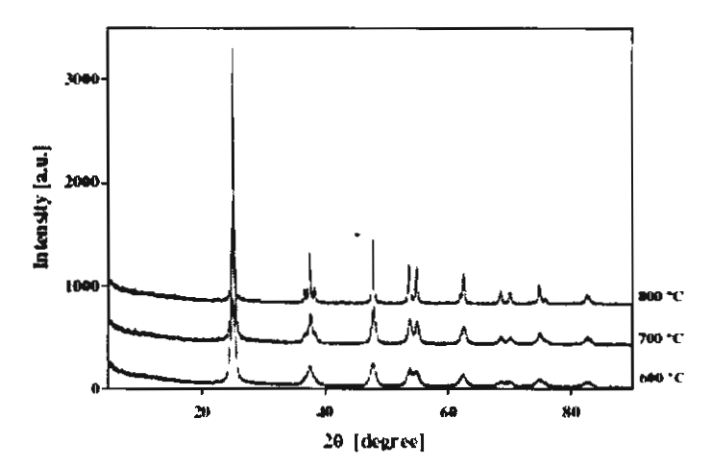


Fig. 3. XRD pattern of titania gel using the HCi:H2O volume ratio of 0.28 calcined at (a) 600 °C, (b) 700 °C and (c) 800 °C.

peratures of 800 °C, which is a little higher than previous studies, which report the transformation of anatase to rutile in the range of 600 700 °C [5,7,12,13].

As can be seen in Fig. 4, at 0.28 and 0.33 ratios, the average grain size decreases significantly from 600 °C (18.8 and 17.1 nm) to 700 °C (13.9 and 14.2 nm) and then increases substantially again at 800 °C (31.3 and 29.8 nm). These results are reminiscent of observations by Sun et al. [7] of the temperature dependence of grain sizes of anatase produced by the MOCVD method. The size variation was interpreted in

terms of the rate of particle growth relative to the rate of particle nucleation. Use of elevated temperatures accelerates not only the nucleation rate but also the particle growth rate. For acid:water ratios of 0.28 and 0.33, at lower temperatures, the nucleation rate is dominant, whereas the growth rate becomes the controlling factor at higher temperature. Acid:water ratios of 0.39 and 0.45 show a slightly different pattern, in which grain size increases mildly between 600 and 700 °C, and then more dramatically at 800 °C, suggesting that the growth rate is dominant at all temperatures.

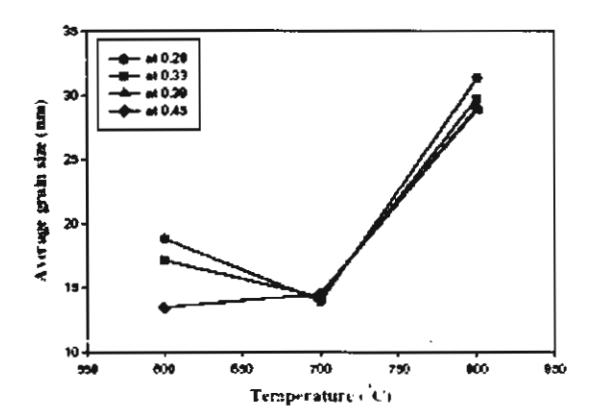
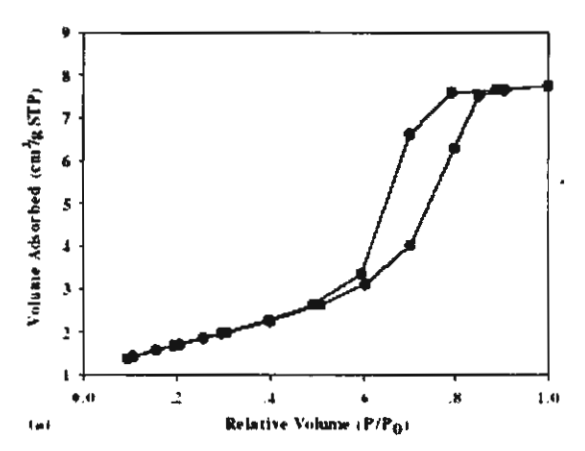


Fig. 4. The average grain sizes of the particles prepared at different volume ratios of HCl:H<sub>2</sub>O (0.28, 0.33, 0.39, 0.45, respectively) and different calcination temperatures (600, 700 and 800 °C).

Coincidentally, the nitrogen adsorption desorption isotherm of the material obtained at 0.28 HCl:H2O volume ratio and calcined at 600 °C for 2 h indicates a mesoporous structure, as seen in Fig. 5(a). The isotherm is of type IV, characteristic of mesoporous material. The hysteresis loop exhibited by the specimen is mainly of type H2. The pore size distribution in Fig. 5(b) shows a major porosity in the range of 4-18 nm. To confirm an increase in crystallinity as temperature increases, specific surface area measurements were carried out and, as expected, we find that the higher the calcination temperature, the lower the specific surface area. The powders become dense and predominantly nonporous when the precursor is calcined at 800 °C. It is known [3] that a lower acid concentration results in a higher specific surface area due to an increase in the cross-linking level. This is consistent with our observation that the specific surface area decreases in the following order; 0.28 > 0.33 > 0.39 > 0.45 (Table 1). It can be concluded that sol gel processing indeed provides a larger specific surface area which decreases with increasing calcination temperature and acid concentration.

The particle morphology of the samples obtained using a HCtH<sub>2</sub>O ratio of 0.33, when calcined at temperatures in the range 600-800 °C, is shown in Fig. 6. At the two lowest temperatures,



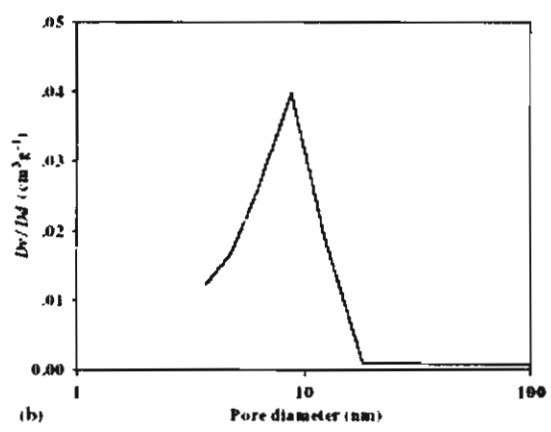


Fig. 5. The nitrogen adsorption-desorption isolerm for mesoporous titania (a) and pore size distribution (b) for the material obtained from 0.28 HCl:H<sub>2</sub>O volume ratio and calcined at 600 °C.

Table 1
BET surface area (S<sub>B-T</sub>, m<sup>2</sup>/g) of titania at various HCl:H<sub>2</sub>O volume ratios and calcination temperature

Tempera-	Surface	area (m²/g	1	
ture (°C)	0.28	0.33	0,39	0.45
600	125	111	107	105
700	60	59	55	50
800	20	18	17	15

Surface area of the starting material  $TiO_2 = 20 \text{ m}^2/\text{g}$ .

Fig. 6(a) and (b), the material consists of particles of large size, whereas the micrograph (Fig. 6(c)) of the material calcined at 800 °C shows a finely-

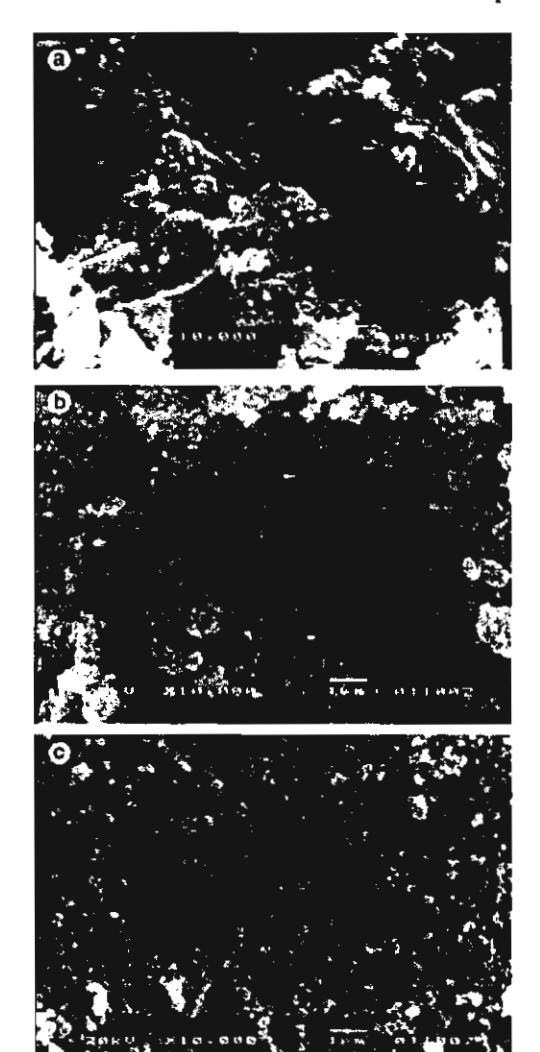


Fig. 6. SEM micrograph for titania powder at volume ratio 0.33 of HCl:H<sub>2</sub>O calcined at (a) 600 °C, (b) 700 °C and (c) 800 °C.

divided morphology in the anatase form consisting of spherical particles approximately 1 µm in size.

Viscoelastic studies of the four different gelling systems (volume ratio 0.28, 0.33, 0.39 and 0.45 of HCl:H<sub>2</sub>O, respectively) were carried out using the criteria proposed by Winter and Chambon [14] to determine the gel point, as the gelation time where a frequency independent value of  $\tan \delta$  in observed. The variation in the frequency dependence

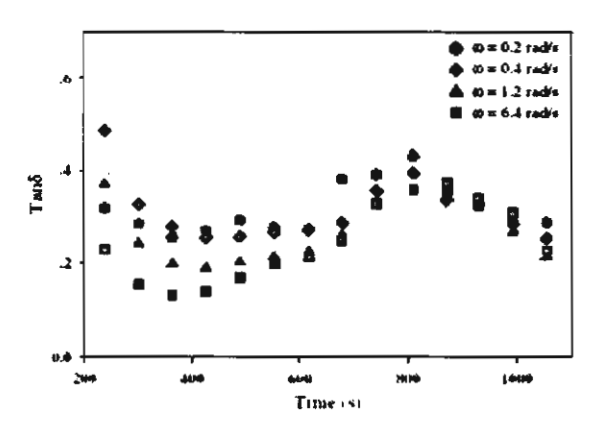


Fig. 7. The plots of  $\tan \delta$  with time(s) at HCl:H<sub>2</sub>O volume ratio of 0.45.

of  $\tan \delta$  with gelation time is shown in Fig. 7, and indeed indicates that  $\tan \delta$  becomes frequency independent at a particular gelation time. The shortest gelation time was observed for the system at 0.28 volume ratio (365 s) and the longest gelation time for the system of 0.45 volume ratio (870 s). An alternative method [15] to determine the gel point is to plot the time evolution of the apparent viscoelastic exponents n' and n'' obtained from the frequency dependence of the modulus ( $G' \propto \omega^{n'}$ ,  $G'' \propto \omega^{n''}$ ), as shown in Fig. 8 for the system at 0.45 volume ratio. The gel point is identified as the time where a cross-over n' = n'' = n is observed. The

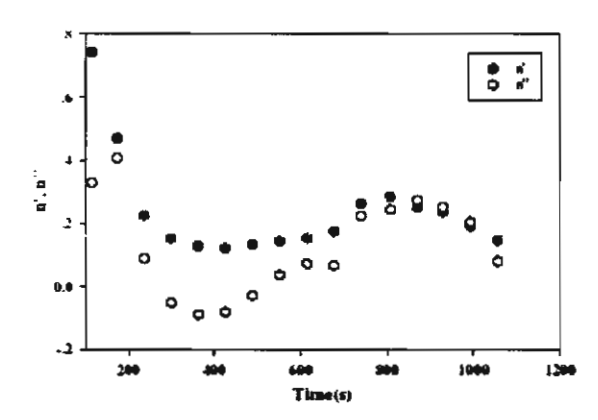


Fig. 8. The plot of the apparent exponents, the storage moduli (n') and the loss moduli (n'') during the course of gelation for the 0.45 acid ratio,

points of intersection  $(t_{gel})$  are found to be the same as those deduced from the plot of  $\tan \delta$  versus time.

It is important to note that these gelling systems are highly elastic even well before the gel point, as evidenced by the fact that  $\tan \delta \ll 1$ . Also, the system rheology evolves relatively slowly in the vicinity of the gel point, as seen by plotting the frequency dependence of G (Pa), G' (Pa) at pregel stage, gel point, and postgel stage, shown in Fig. 9. The data are shifted horizontally by a factor B. A similar trend is observed for all systems in that G is higher than G', i.e. elastic behavior predominates before as well as after the gel point. We attribute this behavior to the fact that we are dealing with a concentrated colloidal dispersion, which is

converted to a gel by hydrolysis from the outer surfaces of the colloidal particles. Despite this heterogeneous structure, at the gel point, the systems fulfil the Winter criteria that  $n' = n'' = n_{\rm gel}$ , and  $\tan \delta = \tan(n_{\rm gel}\pi/2)$  are superimposed [14-18]. The viscoelastic exponent  $n_{\rm gel}$  of the system, as shown in Table 2, has its highest value at 0.45

Table 2 Summary of viscoelastic exponent, fractal dimension, and gelation time(s) at various HCl:H<sub>2</sub>O volume ratios

Acid ratio	n	d;	Gelation time (s)
0.28	0.05	2.46	365
0.33	0.07	2.44	428
0.39	0.19	2.33	647
0.45	0.20	2.32	870

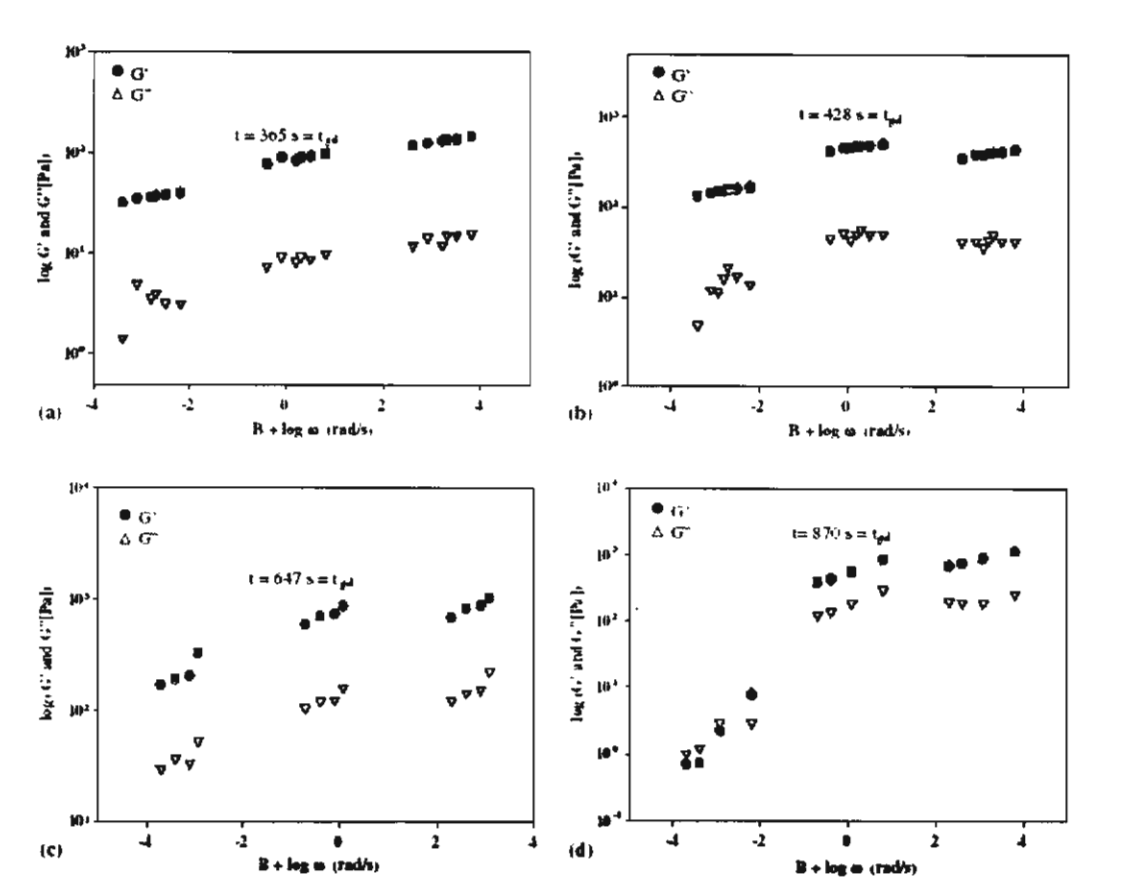


Fig. 9. The frequency dependence curves of  $G'(\omega)$  and  $G''(\omega)$  at  $(\Phi)$  pregel stage (B=-3),  $(\blacksquare)$  gel point (B=0), and  $(\Delta)$  postgel stage (B=3) of (a) 0.28, (b) 0.33, (c) 0.39 and (d) 0.45 HCl:H<sub>2</sub>O ratio.

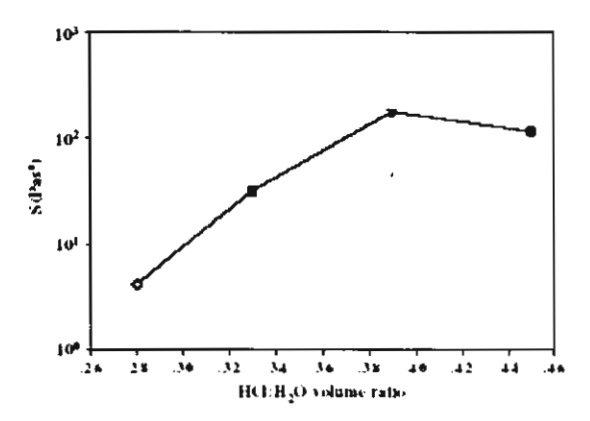


Fig. 10. The plot of gel strength parameter S at the gel point as a function of HCl:H<sub>2</sub>O volume ratio: 0.28 (\$\dag{\dag}\$), 0.33 (\$\frac{\text{m}}{2}\$), 0.39 (\$\dag{\dag}\$) and 0.45 (\$\dag{\dag}\$).

volume acid ratio and the value decreases as the volume acid ratio decreases. Fig. 10 shows the effect of HCl:H<sub>2</sub>O volume ratio on the gel strength parameter. S, evaluated from the relationship [15-18]  $G'(\omega) = \Gamma(1-n)\cos(n\pi/2)S\omega^n$  where  $\Gamma(1-n)$  is the Legendre  $\Gamma$  function. It is evident that the gel strength increases with increasing acid ratio and reaches its highest value acid ratio = 0.39, then decreases slightly. Thus at low acid ratio, the critical gel cluster is relatively weak, at high acid ratio it is stronger.

According to the model of Muthukumar [19] the fractal dimension of the critical gel cluster can be obtained from the viscoelastic exponent n as  $n = d(d + 2 - 2d_f)/2(d + 2 - d_f)$  where d spatial dimension = 3. The effect of acid ratio on the fractal dimension of incipient gel is shown in Fig. 11 and Table 2. The fractal dimension decreases with increasing the acid ratio. A lower fractal dimension means that the molecular weight grows slower with radius, i.e.  $M \sim R^{4}$ . Thus the critical gel at high acid ratio has a more open structure than at low acid ratio. This is somewhat surprising since we expect the cross-link density to be higher at higher acid ratio. Again we attribute this result to the heterogeneous character of the system at the gel point. The particles which comprise the gel network at low acid ratio are less hydrated and hence more dense than those at higher acid ratio.

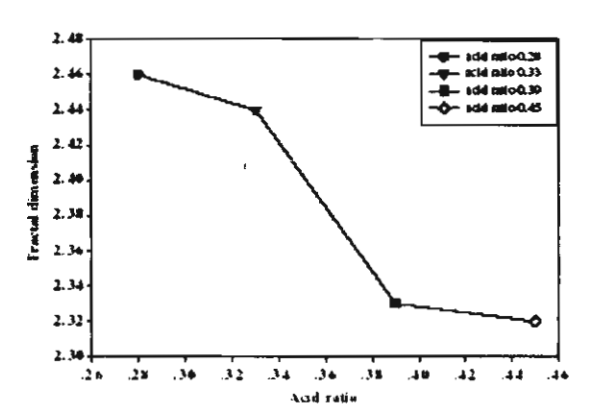


Fig. 11. The plot of fractal dimension of the critical gel cluster as a function of acid ratio.

Fig. 12 shows the frequency dependence of the dynamic viscosity at pregel stage, gel point and postgel stage. Consistent with the highly elastic behavior evident in Fig. 9, at all stages  $\eta^*(\omega)$  exhibits power law frequency dependence with an exponent at the gel point of n-1. The time dependence of the complex viscosity at low frequency ( $\omega = 0.4 \text{ rad/s}$ ) is illustrated in Fig. 13. The location of the gel point for each system as determined by the Winter criteria (16-19) are indicated by arrows. At low acid ratio, the viscosity is initially high but approaches an asymptotic value which is relatively low. At high acid ratio, the viscosity is initially low but reaches a high asymptotic value. Thus, the gel strength and asymptotic complex viscosity are self-consistent and indicate that the gel becomes stronger under high acidity conditions. We interpret these results as indicating that at low acid, the precursor particles are poorly hydrated and form a more heterogeneous weak gel structure. At high acid, the particles are well solvated and form a less beterogeneous (more open) yet stronger net-

### 4. Conclusions

Anatase TiO<sub>2</sub> nanoparticles were successfully prepared by sol-gel technology, using inexpensive

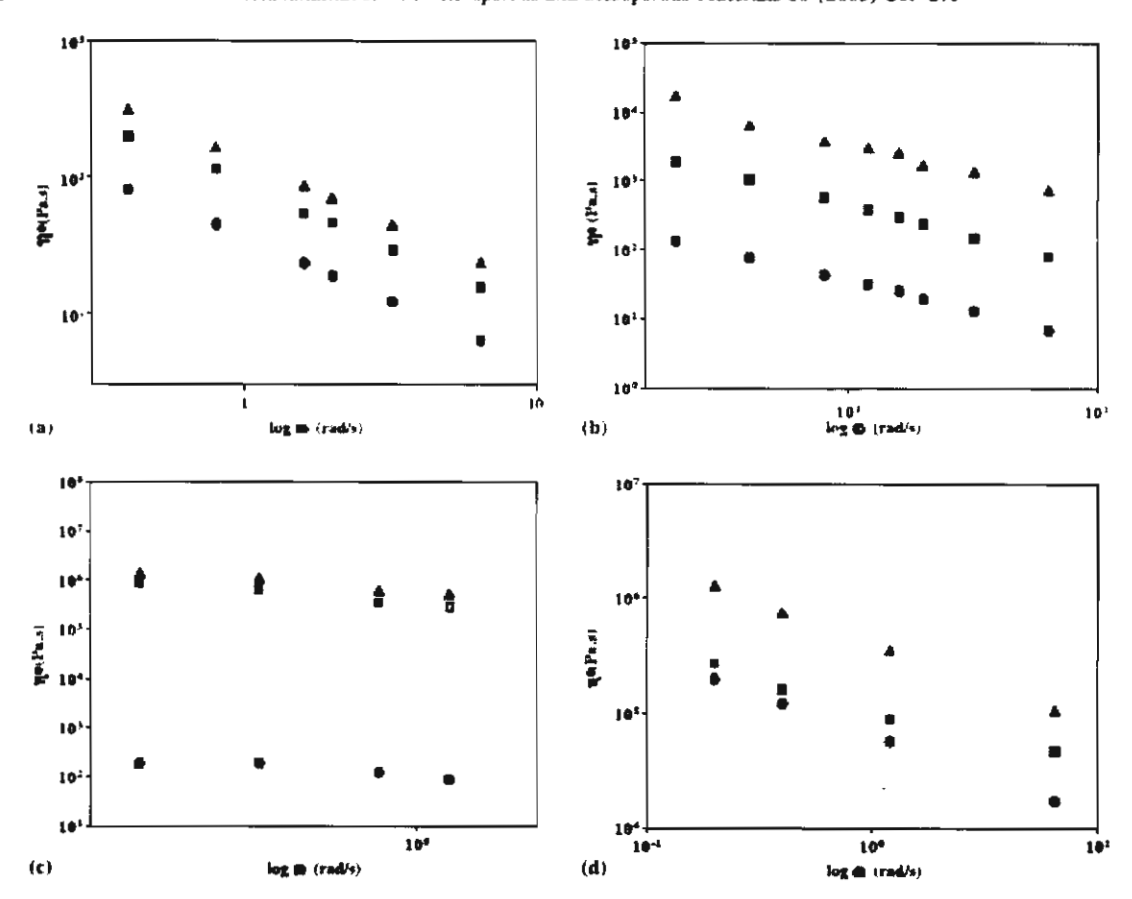


Fig. 12. The effect of frequency on the complex viscosity at pregel stage, gel point, and postgel stage of (a) 0.28, (b) 0.33, (c) 0.39 and (d) 0.45 HCl:H<sub>2</sub>O volume ratio.

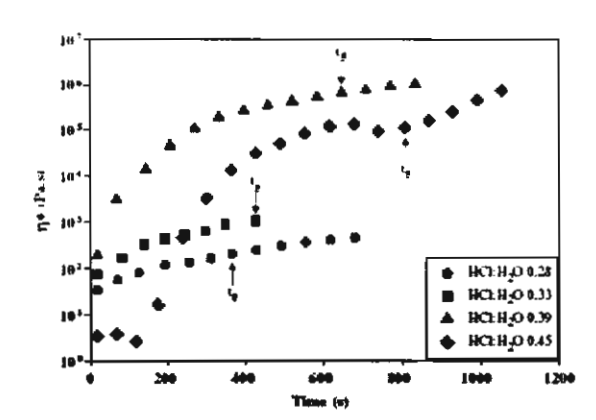


Fig. 13. The time evolution of the complex viscosity (at fixed frequency of 0.4 rad/s) of (a) 0.28, (b) 0.33, (c) 0.39 and (d) 0.45 HCl:H<sub>2</sub>O volume ratio.

and moisture-stable titanium glycolate as precursor in 1 M HCl solution. The calcination temperature and the HCl:H2O volume ratio has a substantial influence on the surface area, phase transformation, and morphology of the products. Anatase titania is produced at calcination temperatures in the range 600 800 °C, above which transformation to rutile occurs. Increase of temperature results in anatase of higher crystallinity but lower specific surface area, and induces a morphological change from large irregular agglomerates to more homogeneous particles of spherical shape. From XRD measurements of average grain sizes, we deduce that nucleation rate dominates the kinetics at low temperatures, and growth rate becomes the controlling factor at high temperature and low HCl:H2O ratios. Increase of HCl:H2O ratio results in a small but significant decrease in porosity. The highest specific surface area 125 m<sup>2</sup>/g is obtained at the lowest HCl:H<sub>2</sub>O ratio 0.28 and the lowest calcination temperature (600 °C). From rheological analysis, as evaluated by the Winter criteria. the gelation time increases with increase of HCl:H<sub>2</sub>O volume ratio. The fractal dimension is determined from the frequency scaling exponent of the modulus at the gel point indicates a dense critical gel structure at low acid ratio. However, the complex viscosity and gel strength increase as a function of acid ratio. We interpret this behavior as indicative that, at low acidity, the gel is composed of poorly hydrated particles forming a dense but weak structure. Increased acidity increases hydration and cross-link density leading to a more open and stronger gel network.

### Acknowledgements

This research work is supported by the Postgraduate Education and Research Program in Petroleum and Petrochemical Technology (ADB) Fund, Ratchadapisek Sompot Fund, Chulalongkorn University and the Thailand Research Fund (TRF).

### References

- [1] J. Yang, S. Mei, J.M. Ferriera, Mat. Sci. Eng. C-Biomim 15 (2001) 183.
- [2] H. Kominami, M. Kohno, Y. Takada, M. Inoue, T. Inui, Y. Kera, Ind. Eng. Chem. Res. 58 (1999) 3931.
- 13 K.M.S. Khalil, T. Baird, M.I. Zaki, A.A. El-Samahy, A.M. Awad, Colloid Surf. A 132 (1998) 31.
- [4] K.M.S. Khalil, M.I. Zaki, Powder Technol. 120 (2001) 256.
- [5] Y. Zhang, A. Weidenkaff, A. Reller, Mater. Lett. 54 (2002)
- [6] Y. Wei, R. Wu, Y. Zhang, Mater. Lett. 41 (1999) 101.
- [7] Y. Sun, A. Li, M. Qi, L. Zhang, X. Yao, Mat. Sci. Eng. B 86 (2001) 185.
- [8] E.J. Kim, S.H. Hahn, Mater. Lett. 49 (2001) 244.
- [9] M. Wu, G. Lin, D. Chen, G. Wang, D. He, S. Feng, R. Xu, Chem. Mater. 14 (2002) 1974.
- [10] N. Kao, S.N. Bhattacharya, J. Rheol. 42 (1998) 493.
- [11] N. Phonthammachai, T. Chairassameewong, E. Gulari, A.M. Jamieson, S. Wongkasemjit, J. Met. Mat. Min. 12 (2002) 23.
- [12] Q. Zhang, L. Gao, J. Gao, Appl. Catal. B-Solid 26 (2000) 207. [13] J. Zhao, Z. Wang, L. Wang, H. Yang, M. Zhao, Mater, Chem. Phys. 63 (2000) 9.
- [14] H.H. Winter, F. Chambon, J. Rheol. 30 (1986) 367.
- [15] A-L. Kjoniksen, B. Nystrom, Macromolecules 29 (1996) 5215.
- [16] M. Jokinen, E. Gyorvary, J.B. Rosenholm, Colloid Surf. A 141 (1998) 205.
- [17] B. Nystrom, A.-L. Kjoniksen, B. Lindman, Langmuir 12 (1996) 3233.
- [18] W. Charoenpanijkarn, M. Suwankruhasn, B. Kesapabutr, S. Wongkasemjit, A.M. Jamieson, Eur. Ploym. J 37 (2001)
- [19] M. Muthukumar, Macromolecules 22 (1989) 4656.

1	~	r

,				
E. Oxide One Po	ot Synthesis of a	n Novel Titaniu	ım Glycolate aı	nd Its Pyrolysis

Journal of Metals, Materials and Minerals. Vol. 12 No. 1 pp. 23-28, 2002.

### Oxide One Pot Synthesis of a Novel Titanium Glycolate and Its Pyrolysis

Nopphawan PHONTHAMMACHAI<sup>1</sup>, Tossaparn CHAIRASSAMEEWONG<sup>1</sup>, Erdogan GULARI<sup>2</sup>, Alexander M. JAMIESON<sup>3</sup> and Sujitra WONGKASEMJIT<sup>1</sup>\*

<sup>1</sup>The Petroleum and Petrochemical College, Chulalongkom University

<sup>2</sup>Department of Chemical Engineering, University of Michigan,

Ann Arbor, Michigan, USA

<sup>3</sup>Department of Macromolecular Science, Case Western Reserve University,

Cleveland, Ohio, USA

### Abstract

A much milder, simpler and more straightforward reaction a give to titanium glycolate product was successfully investigated by the reaction of titanium dioxide, ethylene glycol and triethylenetetramine using the oxide one pot synthesis (OOPS) process. The FT-IR spectrum demonstrates the characteristics of titanium glycolate at 619 and 1080 cm<sup>-1</sup> assigned to Ti-O stretching and C-O-Ti stretching vibrations, respectively. (Blohowiak, et al. 1992) C-solid state NMR spectrum gives two peaks at 75.9 and 79.8 ppm due to the relaxation of the crystalline spirotitanate product. The percentage of carbon and hydrogen from elemental analysis are 28.6 and 4.8, respectively. The thermal analysis study from TGA exhibits only one sharp transition at 340°C, corresponding to the decomposition transition of an organic ligand, and giving a ceramic yield, titanium glycolate, of 46.95% which is close to the theoretical yield of 47.50%. XRD patterns show the morphology change of its pyrolyzed product from anatase to rutile as increasing calcining temperatures from 500°C to 1100°C while at 300°C the amorphous phase is formed.

Keywords: Titanium Dioxide, Titanium Glycolate, Oxide One Pot Synthesis, Pyrolysis, Phase Transformation

E-mail address: dsuitra@chula.ac.th; Tel: (662) 218 4459; Fax: (662) 215 4459

<sup>\*</sup>To whom the correspondence should be addressed:

### Introduction

Titania is a very useful material and has received great attention in recent years for its humidity- and gas-sensitive behavior, excellent dielectric properties, as well as catalysis applications. (Ding and Liu, 1997). The most important factor to consider when producing titania with good properties is the purity of the titanium alkoxide precursor. However, the synthesis of titanium alkoxides is greatly challenging to scientists due to their extreme moisture sensitivity and very expensive starting materials. In this work the great interest in titanium glycolate, Ti(OCH2CH2O)2, is owing to its difference from most crystalline titanium alkoxides, generally having low polymeric O-dimensional molecules. Nevertheless, Ti(OCH<sub>2</sub>CH<sub>2</sub>O)<sub>2</sub> is a novel crystalline complex with infinite one-dimensional chains, and exhibits outstanding high stability not only in alcohol but also in water (Wang, et al. 1999).

The method required for the synthesis of alkoxy derivatives of an element generally depends on its electronegativity. In the case of comparatively less active metals, a catalyst is generally employed for successful synthesis of metal alkoxides. Wang, et al. (1999) synthesized Ti(OCH<sub>2</sub>CH<sub>2</sub>O)<sub>2</sub> from very expensive starting materials, tetraethyl orthotitanate to react with ethylene glycol using n-butylamine as a catalyst. The reaction took place under very vigorous conditions. It occurred in a Teflon-lined stainless steel autoclave at 160°-180°C for 5 days. The alkalinity of the initial reaction mixture is a dominant factor of the product. The ethylene glycol served as both a solvent and a bidentate chelate occupying sites on titanium coordination spheres so as to bridge adjacent titanium atoms and form a one-dimensional structure.

Gainsford, et al. (1995); and Gainsford, et al. (1995) studied the synthesis and characterization of the soluble titanium glycolate complexes obtained from the reaction of titanium

dioxide or titanium isopropoxide with glycol in the presence of alkali metal hydroxides. The reaction of Ti(O-i-Pr)4 with 2 equivalent amounts of sodium or potassium hydroxides provided tris(glycolate) salts, which were highly crystalline, hygroscopic materials, crystallized as salts and solvated with varying numbers of glycol molecules.

Suzuki, et al. (1997) synthesized titanium tetraalkoxides from hydrous titanium dioxide (TiO<sub>2</sub>.nH<sub>2</sub>O) and dialkyl carbonates in an autoclave at a heating rate of 90Kh<sup>-1</sup>. The effect of reaction temperature was studied. At a temperature range of 495-533 K, a practically complete conversion of hydrous titanium dioxide to Ti(OEt)<sub>4</sub> could be attained. LiOH, NaOH, KOH, and CsOH were used as catalysts of which NaOH gave the highest yield of Ti(OEt)<sub>4</sub>. The effect of the molar ratios of diethyl carbonate/hydrous titanium dioxide was studied. A high molar ratio of 10 was required to obtain a high yield of Ti(OEt)<sub>4</sub>.

Related metalloglycolates formed from alkaline glycol were reported for aluminium and titanium. (Bickmore, et al. 1998; Yang, et al. 2001; Laine, et al. 1992; Laine, et al. 1993; Day, et al. 1996; and Duan, et al. 1997). Potassium and sodium tris(glycotitanate) complexes were obtained from the reaction of titanium dioxide or titanium tetraisopropoxide with ethylene glycol in the presence of alkali metal hydroxides. (Gainsford, et al. 1995; and Gainsford, et al. 1995)

Laine, et al. (1991) investigated a straightforward, low-cost route to alkoxide precursors by direct reactions of a stoichiometric mixture of silica and group I metal hydroxide with ethylene glycol. This route, termed the 'oxide one pot synthesis' (OOPS) process, provides processable precursors, as shown in Scheme 1.(Laine, et al. 1991; Blohowiak, et al. 1992; and Bickmore, et al. 1992).

Recently Jitchum, et al. (2001) synthesized neutral alkoxysilanes, tetracoordinated spirosilicates, directly from silica and ethylene glycol or ethylene glycol

derivatives, using triethylenetetramine as a catalyst, in the absence or presence of potassium hydroxide as a co-catalyst (Scheme 2). (Jitchum, et al. 2001)

### Scheme 2.

The OOPS method is simple, low-cost and can produce new chemicals in only one step. Thus, the objective of this work is to use the OOPS process to synthesize titanium glycolate. The phase transformation of its pyrolyzed product will be studied, as well.

### Experimental

### Materials

UHP grade nitrogen; 99.99% purity was obtained from the Thai Industrial Gases Public Company Limited (TIG). Titanium dioxide was purchased from the Sigma-Aldrich Chemical Co. Inc. (USA) and used as received. Ethylene glycol (EG), was purchased from Malinckrodt Baker, Inc. (USA), and purified by fractional distillation under nitrogen at atmospheric pressure, 200°C before use. Triethylenetetramine (TETA) was purchased from Facai Polytech. Co. Ltd. (Bangkok, Thailand) and distilled under vacuum (0.1 mm/Hg) at 130°C prior to use. Acetonitrile was purchased from the Lab-Scan Company Co. Ltd.

### Instrumental

Fourier transform infrared spectra (FT-IR) were recorded on a VECOR3.0 BRUKER spectrometer with a spectral resolution of 4 cm<sup>-1</sup> using transparent KBr pellets, 0.001 g of the sample was ground and mixed with 0.06 g of KBr. Thermal gravimetric analysis (TGA) was carried out using a Perkin Elmer thermal analysis system with a heating rate of 10°C/min over

a 30°-800°C temperature range. Mass spectrum using the positive fast atom bombardment mode (FAB+MS) was measured on a Fison Instrument (VG Autospec-ultima 707E) with a VG data system using glycerol as the matrix, cesium gun as initiator, and cesium iodide (CsI) as a standard for peak calibration. (Blohowiak, et al. 1992) C-solid state NMR spectroscopy modeled Bruker AVANCE DPX-300 MAS-NMR was used to determine the peak position of carbon contained in the product. Elemental analysis (EA) was carried out on a C/H/O Analyser (Perkin Elmer PE2400 series II). X-ray diffraction patterns were analyzed using a D/MAX-2200H Rigaku equipped with Cu X-ray generator. The Carbolite model CSF 12/7 electrical muffle furnace is employed to calcine titanium glycolate with a heating rate of 10.0°C/min for 120 minutes at various temperatures of 600, 700, 800°C.

### Methodology

The titanium glycolate was synthesized by the OOPS method, see Scheme 3. A mixture of TiO<sub>2</sub> (2g, 0.025 mol) and TETA (3.65g, 0.0074 mol) was stirred vigorously in excess EG (25 cm<sup>3</sup>) and heated at the boiling point of EG under N<sub>2</sub> atmosphere. After heating for 24 h the solution was centifuged to separate the unreacted TiO<sub>2</sub> from the solution part. The excess EG and TETA were removed by vacuum distillation to obtain a crude precipitate. The white solid product was washed with acetonitrile and dried in a vacuum desiccator.

### Results and Discussion

### Synthesis

The reaction of titanium dioxide, triethylenetetramine catalyst and ethylene glycol used as both a solvent and a reactant was achieved by heating in a simple distillation apparatus. The glycol was slowly distilled off along with water generated during the condensation reaction to drive the reaction forward. The resulting product was isolated by distilling off glycol, followed by addition of acetronitrile to remove residual glycol and TETA. The final product, titanium glycolate, was moisture-stable.

### Characterization .

The FT-IR spectrum of titanium glycolate is shown in Figure 1. As compared with the work done by Wang, et al. (1999) the result clearly shows the characteristics of titanium alkoxide at the 1080 and 619 cm<sup>-1</sup> bands, corresponding to C-O-Ti and Ti-O stretching, respectively. Moreover, the band at 2927-2855 cm<sup>-1</sup> is assigned to the C-H stretching of an ethylene glycol ligand.

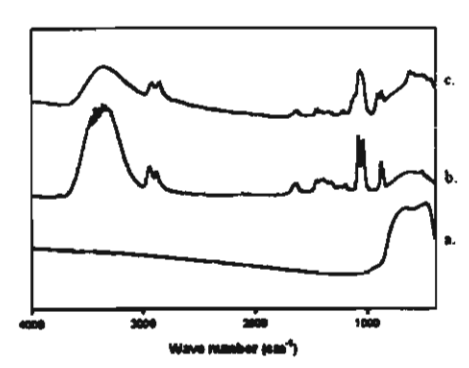


Figure 1 FT-IR spectra of (a). TiO<sub>2</sub>; (b). HOCH<sub>2</sub>CH<sub>2</sub>OH and (c). Ti(OCH<sub>2</sub>CH<sub>2</sub>O)<sub>2</sub>

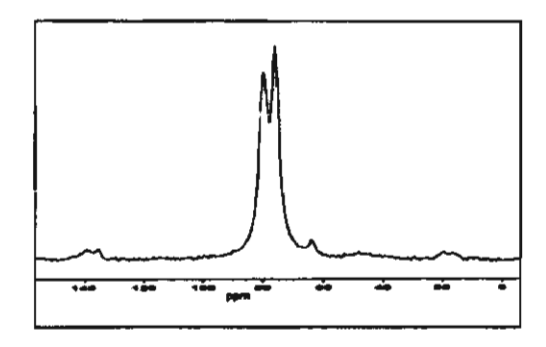


Figure 2 C-Solid state NMR spectrum of the synthesized Ti(OCH<sub>2</sub>CH<sub>2</sub>O)<sub>2</sub>

Due to the insolubility of the product in an organic solvent, (Blohowiak, et al. 1992) C-solid state NMR was employed. The obtained spectrum, see Figure 2, gives two peaks at 74.8 and 79.2 ppm. It is due to the crystalline phase of titanium glycolate, causing the peak to split during the relaxation time of the nuclei, as discussed by Wang, et al. (1999).

Table 1 Percentages of C and H present in the synthesized Ti(OCH<sub>2</sub>CH<sub>2</sub>O)<sub>2</sub>

Element (%)	Theoretical	Experimental
С	27.9	28.6
н	5.6	4.8

M/e	%intensity	Proposed structure
169	8.5	+ H+
93	100	Ti-OCH <sub>2</sub> CH <sub>2</sub> +H <sup>+</sup>
45	13	СН2СН2ОН

Table 2 The Proposed fragmentation and product structures of Ti(OCH2CH2O)2

To confirm the structure of the desired product, both elemental analysis and mass spectroscopy techniques are carried out. The results are shown in Tables 1 and 2, respectively. The obtained C/H percentages are close to those calculated theoretically. The proposed fragmentation and structures present in Table 2 also confirms the expected structure of the titanium glycolate.

As for its thermal stability, Figure 3 shows the same TGA thermogram as obtained by Wang, et al. (1999). The result exhibits one sharp transition at 340°C, corresponding to the decomposition transition of the glycol ligand. The final ceramic yield, titanium glycolate, obtained is 46.95% that is close to the theoretical yield, 47.5%.

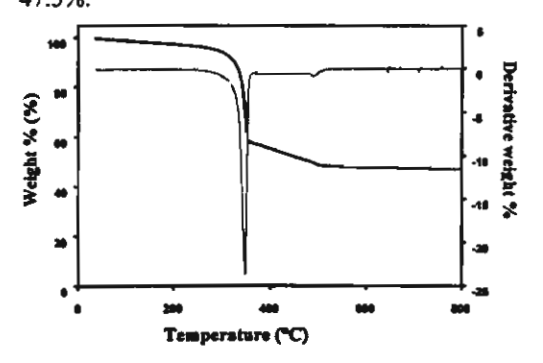


Figure 3 TGA curve of Ti(OCH<sub>2</sub>CH<sub>2</sub>O)<sub>2</sub>

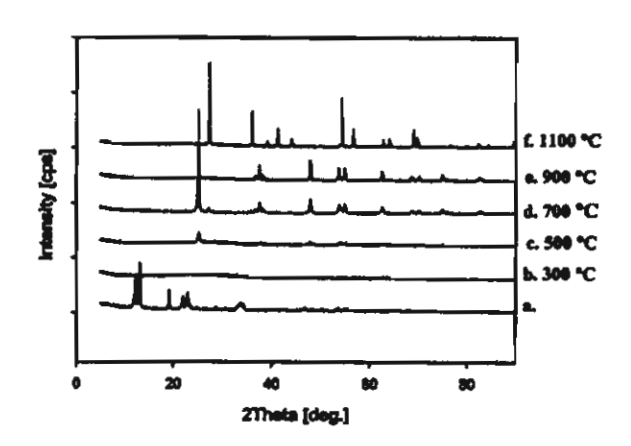


Figure 4 XRD patterns of Ti(OCH<sub>2</sub>CH<sub>2</sub>O)<sub>2</sub> at different temperatures:

- a.) titanium glycolate without calcination
- b.) 300°C, amorphous; c.) 500°C, anatase;
- d.) 700°C, anatase; e.) 900°C, anatase;
- f.) 1100°C, rutile.

### Phase transformation

The TGA result indicated the oxidation of organic compounds tables place at 340°C and the crystallisation at about 500°C. The crystalline titanium glycolate decomposed and changed to an amorphous phase at 300°C (Figure 4). As the calcination temperature, is increased the XRD pattern gives an anatase phase at 500°C to 900°C and completely changes to a rutile phase at 1100°C.

### Conclusions

Titanium glycolate is successfully synthesized using low cost starting materials, with much simpler and milder reaction conditions. The product shows the property of good moisture stability. The results from spectroscopy, namely, FT-IR, Solid state NMR, EA, and TGA, confirm the product structure. The transformation from the anatase to the rutile phase indicates anatase stability up to 900°C. The stability of the synthesized product remarkably enables researchers to make use of it in many applications.

### Acknowledgement

This research work is supported by the Thailand Research Fund (TRF).

### References

- Bickmore, C., Hoppe, M. L. and Laine, R. M. 1992. Low Temperature Route to Cordierite-Like Ceramics Using Chemical Processing Mater. Res. Soc. Symp. Proc. 249:81.
- Bickmore, C. R., Waldner, K. F., Baranwal, R., Hinklin, T., Freadwell, D. R. and Laine, R. M. 1998. Ultrafine Titania by Flame Pyrolysis of a Titanatrane Complex. J. Eur. Ceram. Soc. 18: 287-297.
- Blohowiak, K. Y., Laine, R. M., Robinson, T. R., Hoppe, M, L. and Kampf, J. I. 1992. Synthesis of penta-alkoxy and penta-aryloxy silicates directly form SiO<sub>2</sub>. In: Laine, R.M.(ed.). Inorganic and Organometallic Polymers with Special Properites. Boston, Kluwer.
- Day, V. W., Eberspacher, A., Frey, M. H., Klemperer, W. G., Liang, S. and Payne, D. A. 1996. Barium Titanium Glycolate: A New Barium Titanate Powder Precursor. Chem. Mater. 8: 330-332.
- Ding, X. Z., and Liu, X. H. 1997. Synthesis and microstructure control of nanocrystalline titania powders via a sol-gel process. *Mater. Sci. Eng.* A224.: 210-215.
- Duan, Z., Thomas, L. M. and Verkade, J. G. 1997. Synthesis of tris (dicyclohexylamido)

- titanium and zirconium chloride and the structure of (c-Hex<sub>2</sub>N)<sub>3</sub>TiCl. *Polyhedran*. 16: 635-641.
- Gainsford, G. I., Kemmitt, T., and Milestone, B. N. 1995. Ethylene Glycolate Derivatives of Aluminum: Tetra-, Penta-, and Hexacoordination. *Inorg. Chem.* 34(21): 5244-5251.
- Gainsford, G. J., Kemmitt, T., Lensink, C. and Milestone, N.B. 1995. Isolation and Characterization of Anionic Titanium Tris(glycolate) complex. *Inorg. Chem.* 34(3): 746-748.
- Jitchum, V., Chivin, S., Wongkasemjit S., and Ishida, H. 2001. Synthesis of Spirosilicates directly from silica and ethylene glycol/ethylene glycol derivatives. *Tetrahedron*. 57: 3997.
- Laine, R. M., and Youngdahl, K. A. 1993. Silicon and Aluminum Complexes. Washington Research Foundation. U.S. Patent. No. 5,216,155.
- Laine, R. M., Blohowiak, K. Y., Robinson, T. R., Hoppe, M. L., Nardi, P., Kampf, J. and UHM, J. 1991. Synthesis of Pentacoordinate Silicon Complexes from SiO<sub>2</sub>. Nature. 353(6345): 642-644.
- Laine, R. M., Youngdahl, K. A. and Nardi, P. 1992. Silicon and Aluminum Complexes. Washington Research Foundation. U.S. Patent. No. 5,099,052.
- Suzuki, E., Kusano, S., Hatayama, H., Okamoto, M., and Ono, Y. 1997. Synthesis of Titanium tetraalkoxides from hydrous titanium dioxide and dialkyl carbonates. J. Mater. Chem. 7(10): 2049-2051.
- Wang, D., Yu, R., and Kumada, N. 1999. Hydrothermal Synthesis and Characterization of a Novel One-Dimensional Titanium Glycolate Complex Single Crystal: Ti(OCH<sub>2</sub>CH<sub>2</sub>O)<sub>2</sub>. Chem. Mater. 11: 2008-2012.
- Yang, J., Mei, S. and Ferreira, J. M. F. 2001. Effect of dispersant concentration on slip casting of cordierite-based glass ceramics. *Mater. Sci. Eng.* C15: 183-185.

F. "High Surface Area and Thermally Stable TiO<sub>2</sub> Synthesized Directly from Titanium Triisopropanolamine Precursor"

### MICRO-AND MESOPOROUS MINERAL PHASES Accademia Nazionale dei Lincei, Rome, December 6-7, 2004

# HIGH SURFACE AREA AND THERMALLY STABLE TIO<sub>2</sub> SYNTHESIZED DIRECTLY FROM TITANIUM TRIISOPROPANOLAMINE PRECURSOR

Phonthammachai, N.<sup>1</sup>, Krissanasaeranee, M.<sup>1</sup>, Gulari, E.<sup>2</sup>, Jamieson, A.M.<sup>3</sup>, and Wongkasemjit, S.<sup>1</sup>

<sup>1</sup>The Petroleum and Petrochemical College, Chulalongkorn University, Bangkok, Thailand <sup>2</sup>Department of Chemical Engineering, University of Michigan, Ann Arbor, Michigan, USA <sup>3</sup>Department of Macromolecular Science, Case Western Reserve University, Cleveland, Ohio, USA

### Introduction

Titanium dioxide, TiO<sub>2</sub>, is widely used as humidity and gas sensors, dielectric ceramics, catalyst supporter, solar cell and catalyst, especially, photocatalyst. <sup>1-6</sup> Generally, most catalysts are used at high temperature, thus must present high thermal stability. Therefore, preparation of anatase nanoparticles with high surface area, uniform particle size, uniform pore structure and high anatase-rutile transformation temperature is truly desirable.

High surface area TiO<sub>2</sub> can be prepared by several methods, such as pyrolysis of titanium tetrabutoxide in oxygen containing atmosphere via the MOCVD method, hydrothermal treatment, or the most famous method, the so called sol-gel process. Although these processes are widely used, they still present two major drawbacks, viz. expensive and sensitive starting materials. The important factor to produce titania with good properties is the purity of titanium alkoxide precursor. The titanium dioxide has most often been prepared using the titanium alkoxide, however, the synthesis of metal alkoxides is greatly challenging to scientists due to their extreme moisture sensitivity because they contain an unsaturated Ti<sup>IV</sup> center which is highly reactive to air and moisture, therefore, the reaction must be carried out under inert gas. Another reason is that those titanium alkoxides are synthesized from very expensive starting materials.

On the basis of our previous work, moisture stable titanium glycolate precursor was successfully synthesized from low cost starting material, TiO<sub>2</sub>, using the Oxide One Pot Synthesis method (OOPS)<sup>13</sup> and used as precursor to produce nanocrystalline mesoporous high surface area titanium dioxide by the sol-gel process.<sup>14</sup> In this work, we demonstrate that moderately high surface area and thermally stable anatase TiO<sub>2</sub> can be obtained directly from the crude product, titanium triisopropanolamine precursor, synthesized by the reaction of TiO<sub>2</sub> and triisopropanolamine.

### Results and Discussion

### Titanium Triisopropanolamine Precursor Characterization

Titanium triisopropanolamine was synthesized by the direct reaction of titanium dioxide with triisopropanolamine in the presence of ethylene glycol and triethylenetetramine (reaction 1).

### Reaction 1.

The crude titanium triisopropanolamine was characterized using FT-IR, TGA and FAB\*-MS. The IR spectrum (figure1) shows the expected bands at 3400 cm<sup>-1</sup> (OH group), 2927-2855 cm<sup>-1</sup> (C-H stretching), 1460 cm<sup>-1</sup> (C-H bending of CH<sub>2</sub> group), 1379 cm<sup>-1</sup> (C-H bending of CH<sub>3</sub> group), 1085 cm<sup>-1</sup> (C-O-Ti stretching), 1020 cm<sup>-1</sup> (C-N bending) and 554 cm<sup>-1</sup> (Ti-O stretching). The result from TGA analysis, as can be seen in figure 2a, shows two transitions at 280° and 365°C corresponding to the decomposition of the unreacted triisopropanolamine and the triisopropanolamine ligand, respectively. The final ash yield, 16.6%, calculated from the starting point of the second decomposition transition is close to the theoretical ceramic yield of [HOCH<sub>3</sub>CHCH<sub>2</sub>]N[CH<sub>2</sub>CHO]<sub>2</sub>Ti[OCHCH<sub>3</sub>CH<sub>2</sub>]N[CH<sub>2</sub>CHCH<sub>3</sub>OH], 18.7%. The mass spectrum result (Table1) confirms the desired structure of the as-synthesized product.

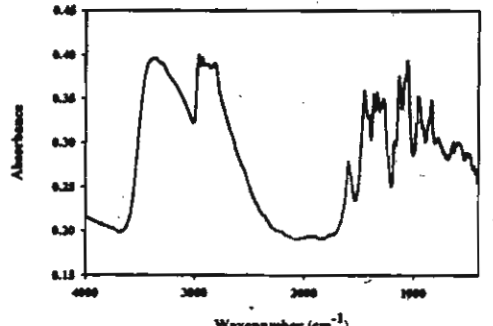


Figure 1. The FT-IR spectra of titaniumtriisopropanolamine

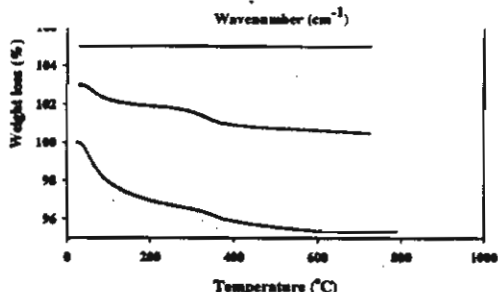


Figure 2. The TGA thermograms of a). titanium triisopropanolamine, TiO<sub>2</sub> calcined at 600°C and holding time of b). 1 h, c). 2 h, and d.) TiO<sub>2</sub> calcined at 500°C for 2 h

Table 1. The proposed structure of the synthesized titanium triisopropanolamine.

M/e	% intensity	Proposed structure
428	10	H_[HOCH2CHCH3]N[CH3CH3CH0]3L1[OCHCH3CH3]3N[CH3CHCH3OH]H,
410	5	[CH <sub>2</sub> CH <sub>2</sub> CH <sub>2</sub> ]N[CH <sub>2</sub> CHCH <sub>3</sub> O] <sub>2</sub> Ti[OCHCH <sub>3</sub> CH <sub>2</sub> ] <sub>2</sub> N [CH <sub>2</sub> CHCH <sub>3</sub> OH]
214	58	[H <sub>2</sub> NCHCH <sub>3</sub> CH <sub>2</sub> O] <sub>2</sub> Tī[OH]
192	100	H+N(CH2CHCH3OH)3

### TiO2 catalyst characterization

### Effect of calcination rate

The effect of calcination rate on the surface area is studied at 0.25, 0.5 and 1.0°C/min at calcination temperature of 600°C for 2h. The results of specific surface area summarized in table 2 show that at the lowest calcination rate (0.25°C/min) the highest surface area is observed. This is probably due to having more time for TiO<sub>2</sub> units to orderly arrange themselves.

Table 2. The specific surface area of calcined TiO<sub>2</sub> at various calcinations temperature rates.

Calcination rate (°C/min)	Specific surface area (m²/g)
0.25	163.6
0.5	86.6
1.0	67,0

### Effect of holding time

Holding time at  $600^{\circ}$ C calcination temperature also affects to the surface area. In this study, 1, 2 and 4h holding times show that using calcination rate of  $0.25^{\circ}$ C/min, the highest specific surface area,  $163.6 \text{ m}^2/\text{g}$  (table 3), was found at 2h holding time while at 1h holding time the final powder was gray in color, meaning that some organic residues remained in the sample. The TGA thermograph in figure 2b confirms that indeed there was still some organic residue, as indicated at the decomposition transition at  $365^{\circ}$ C. The TGA thermograph in figure 2c presents pure TiO<sub>2</sub> without any organic residue. As the holding time increased to 4h, the specific surface area came down to  $74 \text{ m}^2/\text{g}$ .

Table 3. The specific surface area of calcined TiO<sub>2</sub> at various holding times.

Holding time (h)	Specific surface area (m²/g)
1	65.08
2	163.64
4	74.04

From the variations of calcination rate and holding temperature, the sample with calcination rate of 0.25°C/min and holding time of 2h was selected to study the effect of calcination temperature to determine the phase transformation of TiO<sub>2</sub>. The calcined product is characterized using XRD, BET and SEM to confirm the active and thermally stable anatase phase of TiO<sub>2</sub>. The XRD patterns in figure 3 and the particle morphology in figure 4 clearly illustrate the anatase phase of TiO<sub>2</sub>, as previously studied [2]. Coincidentally, the nitrogen adsorption-desorption isotherm (figure 5) of the material calcined at 600°C for 2h indicates a mesoporous structure, having the isotherm of type IV.

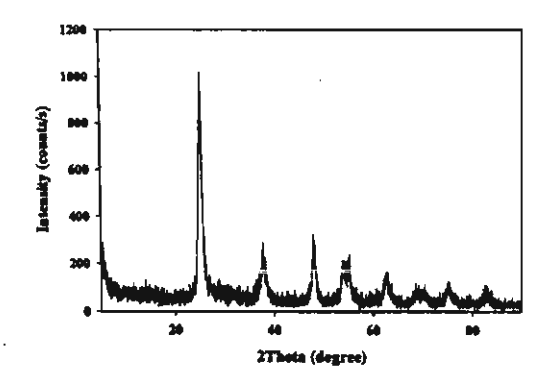


Figure 3. XRD pattern of TiO<sub>2</sub> at the 0.25°C/min calcinations rate, 2h holding time and 600°C calcination temperature.

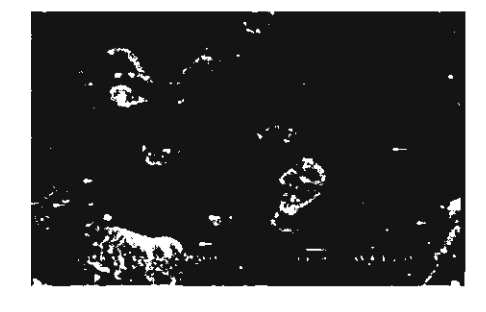


Figure 4. The SEM micrograph of TiO<sub>2</sub> at the 0.25°C/min calcinations rate, 2h holding time and 600°C calcination temperature.

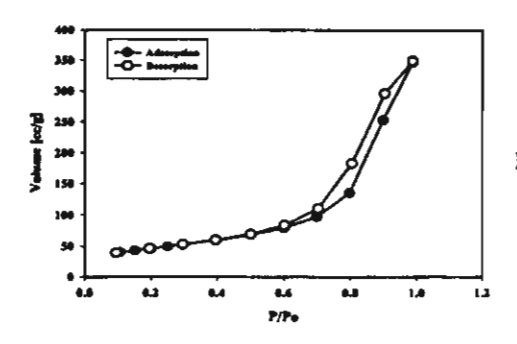


Figure 5. The nitrogen adsorption-desorption isoterm of the obtained mesoporous TiO<sub>2</sub> at 0.25°C/min calcinations rate, 2h holding time and 600°C calcination temperature.

### Effect of calcination temperature

The phase transformation of TiO<sub>2</sub> is studied at different calcination temperature, viz. 300°, 500°, 600°, 700°, 800° and 900°C using 0.25°C/min calcination rate and 2h holding time. The sample at 300°C calcination temperature has black color, indicating incomplete removal of organic compounds. The XRD pattern (figure 6a.) and SEM micrograph (figure 7a.) show the amorphous phase of sample. By increasing the temperature to 500°C, most of the sample has white color and little in gray. This is in agreement with the result of TGA (figure 2d.) showing moisture and organic residue decomposition transitions. The XRD pattern (figure 6b.) and SEM (figure 7b.) present the anatase phase of TiO<sub>2</sub>. <sup>2,10</sup> At higher calcination temperatures (600°-800°C), the anatase phase is continuously formed, see the XRD patterns in figure 6c-e, and the intensity of the peaks increases with the calcination temperature, meaning that higher cystallinity occurs as the temperature increases. The SEM micrographs of the anatase phase showed in figure 7c-e can confirm the crystalline morphology. As the temperature was increased to 900°C the XRD pattern (figure 6f) and SEM micrograph (figure 7f) indicated the rutile phase of TiO<sub>2</sub>. <sup>21-22</sup> The specific surface areas of TiO<sub>2</sub> at different calcinations temperatures are shown in table 4 in which the highest specific surface area (163.64 m<sup>2</sup>/g) is at calcinations temperature of 600°C.

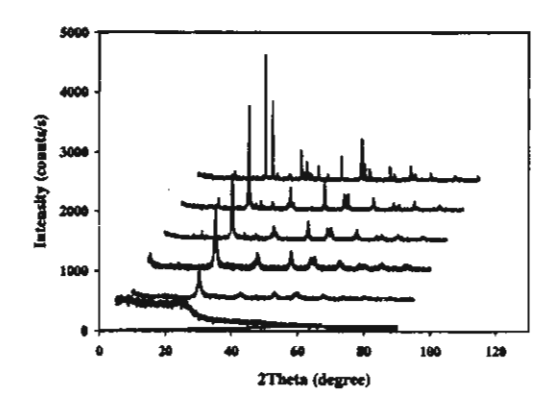


Figure 6. XRD patterns of TiO<sub>2</sub> at the temperature of a.) 300°, b.) 500°, c.) 600°, d.) 700°, e.) 800° and f.) 900°C.

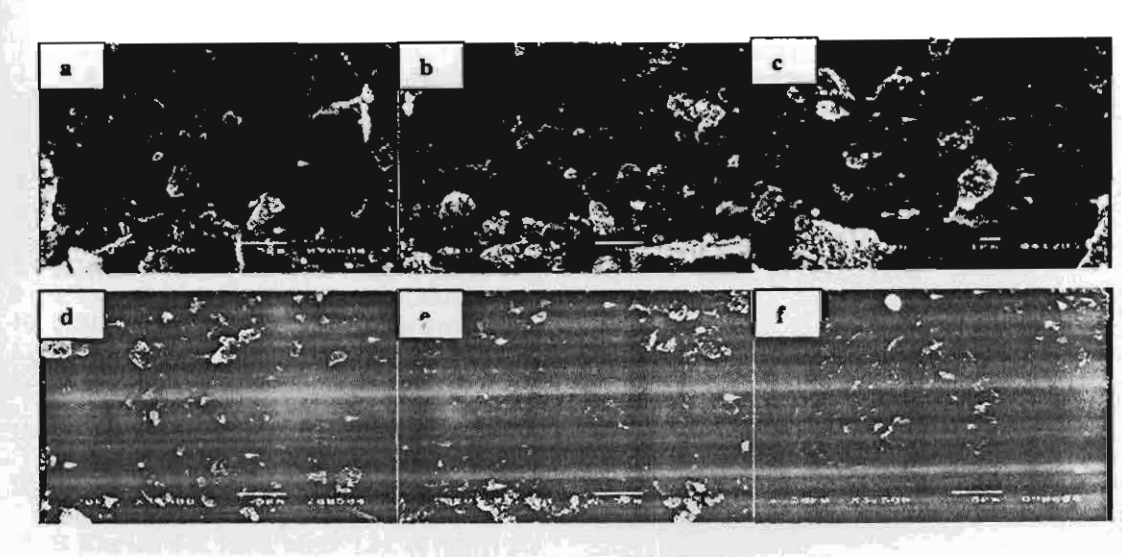


Figure 7. The SEM micrographs of TiO<sub>2</sub> at the temperature of: a.) 300°, b.) 500°, c.) 600°, d.) 700°, e.) 800° and f.) 900°C.

Table 4. The specific surface area of calcined TiO2 at various calcinations temperatures.

Calcinations temperature (°C)	Specific surface area (m²/g)
500	122.69
600	163.64
700	54.94
800	24.30
900	3.86

### References

- 1. K.M.S. Khalil, T. Baird, M.I. Zaki, A.A. El-Samahy, A.M. Awad, Colloid Surface A 132 (1998) 31.
- 2. H. kominami, M. kohno, Y. Takada, M. Inoue, T. Inui, Y. Kera, Ind. Eng. Chem. Res. 38 (1999) 3931.
- X-Z. Ding and X-H. Liu, Mat. Sci. Eng. 224 (1997) 210.
- V.G. Bessergenev, I.V. Khmelinski, R.J.F. Pereira, V.V. Krisuk, A.E. Turgambaeva, I.K. Igumenov, Vacuum 64 (2002) 275.
- P.D. Cozzoli, A. Kornowski, H. Weller, J. Am. Chem. Soc. 125 (2003) 14539.
- 5. J-G. Yu, H-G. Yu, B. Cheng, X-J. Zhao, J.C. Yu, W-K. Ho, J. Phys. Chem. B 107 (2003) 13871.
- 7. Y. Sun, A. Li, M. Qi, L. Zhang, X. Yao, Mat. Sci. Eng. 86 (2001) 185.
- 8. M. Wu, G. Lin, D. Chen, G. Wang, D. He, S. Feng, R. Xu, Chem. Mater. 14 (2002) 1974.
- 9. J. Yang, S. Mei, J.M.F. Ferreira, 15 (2001) 183.
- 10. K.M.S. Khalil and M.I. Zaki, Powder Technology 120 (2001) 256.
- 11. Y. Zhang, A. Weidenkaff, A. Reller, Mater. Lett. 54 (2002) 375.
- C.R. Bickmore, K.F. Waldner, R. Baranwal, T. Hinklin, D.R. Treadwell, R.M. Laine, J. European ceramic society 18 (1998) 287.
- N. Phonthammachai, T. Chairassameewong, E. Gulari, A.M. Jamieson, S. Wongkasemjit, J. Met. Mat. Min. 12 (2002) 23.
- N. Phonthammachai, T. Chairassameewong, E. Gulari, A. M. Jamieson, S. Wongkasemjit, Microporous Mesoporous Mater. 66 (2003) 261-271.
- 15. E. Kim and S-H. Hahn, Mater. Lett. 49 (2001) 244.
- 16. C. Suresh, V. Biju, P. Mukundan, K.G.K. Warrier, Polyhedron 17 (1998) 3131.